

**Proceedings of the  
6th International Students Conference  
“Modern Analytical Chemistry”**

Prague, 23–24 September 2010

Edited by Karel Nesměrák

*Proceedings of the  
6th International Students Conference  
“Modern Analytical Chemistry”*



**Proceedings of the  
6th International Students Conference  
“Modern Analytical Chemistry”**

Prague, 23–24 September 2010

Edited by Karel Nesměrák

Modern Analytical Chemistry (2010 : Praha, Česko)

Proceedings of the 6th International Students Conference

“Modern Analytical Chemistry” : Prague, 23–24 September 2010

/ edited by Karel Nesměrák. – 1st ed. – Prague : Charles University  
in Prague, Faculty of Science, 2010. – 126 s.

ISBN 978-80-7444-005-2 (brož.)

543

- analytical chemistry
- proceedings of conferences
- analytická chemie
- sborníky konferencí

543 – Analytical chemistry [10]

543 – Analytická chemie [10]

*The Proceedings publication was supported by research project MSM0021620857  
of the Ministry of Education of the Czech Republic.*

## Preface

Dear friends and colleagues,

We are very pleased that the number of you, the participants in the already 6th International Conference of PhD Students of Analytical Chemistry in the English Language, is so large. This Conference is aimed at supporting creativity and research activities of PhD students, helping them to develop capabilities connected with the presentation of their research results to the wide scientific public, providing the floor for discussions and exchange of experience, and laying the ground for long-term mutual cooperation. It should also contribute to mastering of the English language and possibly of some other languages.

The development of the Conference is quite impressive – from nine PhD students participating in the first meeting in 2005, to thirty of you this year, from all the participants coming merely from our Faculty of Science of Charles University in Prague in 2005, to PhD students of the Slovak University of Technology in Bratislava, the Prague Institute of Chemical Technology and of the University of Regensburg and our own students. The Conference presentations are added a further value, as they are included in the Proceedings with the appropriate ISBN code.

We would be unable to organize this Conference without the kind financial support from our sponsors. The companies AP Czech, Shimadzu, Zentiva, Quinta Analytica, HPST, and Sigma-Aldrich are cordially thanked, not only for their financial contributions on this occasion, but for their continuous cooperation and help in many of our activities.

We wish you successful presentation of your contributions, rich discussions with your colleagues from all the participating universities, pleasant social encounters and nice stay in Prague. We are happy that you have come.

Prof. RNDr. Věra Pacáková, CSc.  
the Chair of the Organizing Committee

## Sponzors

The organizing committee of 6th International Students Conference “Modern Analytical Chemistry” gratefully acknowledges the generous sponsorship of following companies:



<http://www.alsglobal.cz/>



<http://www.sigmaaldrich.com/>



<http://www.apczech.cz/>



<http://www.quinta.cz/>



<http://www.hpst.cz/>



<http://www.shimadzu.cz/>

## ZENTIVA

<http://www.zentiva.cz/>

# Programme

The conference is held at the Institute of Chemistry, Faculty of Science, Charles University in Prague (Hlavova 8, 128 43 Prague 2) in the main lecture hall (Brauner's Lecture Theater). Oral presentations are 20 minutes including discussion and speakers are asked to download their Power Point presentation on the local computer in the lecture hall before the start of the session. The coffee breaks are held in the lecture hall. The lunches are served at students' club Chladič (room 016 on the basement). The get together party will be held at Chladič club too.

## Thursday, September 23, 2010

- 9:00–9:10 **Opening**  
Prof. Věra Pacáková: *Welcoming address*
- 9:10–9:30 Dominik B. M. Grögel: *Blue to Purple Switch of Conjugated Cyanine Dyes in a Sensor for Acid-Containing Gaseous Environments* (p. 9)
- 9:30–9:50 Thomas Lang: *Luminescent ATPase Assay Using a Phosphate-sensitive Lanthanide Probe* (p. 10)
- 9:50–10:10 Stanislav Musil: *Gold Chemical Vapor Generation by Tetrahydroborate Reduction for AAS: Radiotracer Efficiency Study and Characterization of Gold Species* (p. 11)
- 10:10–10:30 Milan Svoboda: *Arsenic Speciation Analysis by Cryogenic Trapping – Hydride Generation Atomic Absorption Spectrometry; Investigation of Water Vapour Dryers* (p. 15)
- 10:30–10:40 **Coffee Break**
- 10:40–11:00 Milan Svoboda: *Arsenic Speciation Analysis by Hydride Generation Cryotrapping Atomic Fluorescence Spectrometry with Flame-in-Gas-shield Atomizer* (p. 19)
- 11:00–11:20 Mark-Steven Steiner: *Sensing Strip for Biogenic Amines Using a Chromogenic (Chameleon) Probe, a Reference Dye, and RGB Optical Readout* (p. 23)
- 11:20–11:40 Kateřina Wranová: *Determination of Platinum Group Elements (Pt, Rh and Pd) in Biological Material by Inductively Coupled Plasma Mass Spectrometry – Solving the Problem of Interferences* (p. 24)
- 11:40–12:00 Mária Andraščíková: *Determination of Pesticide Residues in Lemon Matrices by Fast Gas Chromatography and Mass Spectrometry* (p. 29)
- 12:00–13:00 **Lunch**
- 13:00–13:20 Veronika Bartáčková: *Acrylamide Analysis in Various Matrices Employing HPLC-MS/MS and UHPLC-TOF MS* (p. 35)
- 13:20–13:40 Jonas Bloedt: *Combination of Microchip Electrophoresis, Contactless Conductivity Detection and Headspace Single Drop Microextraction for the Determination of Aliphatic Amines in Seafood Samples* (p. 40)
- 13:40–14:00 Miroslava Bursová: *Development and Optimization of New Microextraction Technique for Determination of Environmental Pollutants by Gas Chromatography* (p. 41)
- 14:00–14:20 Lucie Drábová: *A New, Effective Method for Determination of Polycyclic Aromatic Hydrocarbons in Tea* (p. 45)
- 14:20–14:30 **Coffee Break**

- 14:30–14:50 Martin Franc: *The Stationary Phase Bed Compaction during the Slurry Packing of Capillary Columns* (p. 50)
- 14:50–15:10 Petra Hrádková: *Analysis of Perfluorinated Compounds: Method Validation According to the Commission Decision 2002/657/EC* (p. 53)
- 15:10–15:30 Anna Hurajová: *Comparison of DART-TOF MS, DART-Orbitrap MS and LC-MS/MS Techniques for Determination of Cyanogenic Glucosides in Flaxseed* (p. 57)
- 15:30–15:50 Lucie Janečková: *Chiral Separation of Binaphthyl Catalysts Using New Chiral Stationary Phases Based on Derivatized Cyclofructans* (p. 62)
- 15:50–16:00 **Coffee Break**
- 16:00–16:20 Štěpán Jirkal: *Comparison of Two Methods of Calculation LSER Descriptor on Retention L Data of Octenes* (p. 66)
- 16:20–16:40 Kamila Kalachová: *Implementation of GC×GC-TOF MS for the Simultaneous Determination of PCBs, PBDEs and PAHs in Environmental Samples* (p. 70)
- 16:40–17:00 Marta Kostelanská: *Determination of Mycotoxins in Infant and Baby Food Using UPLC-MS/MS Analytical Method* (p. 75)
- 17:00–17:30 **Sponsors' presentations**
- 17:30 **Get Together Party**

### Friday, September 24, 2010

- 9:00–9:20 Tomáš Křížek: *The Enzyme Kinetics Study Using Capillary Electrophoresis: Determination of Chitobiose and N-Acetylglucosamine* (p. 80)
- 9:20–9:40 Adéla Svobodová: *Monolithic Poly(styrene-divinylbenzene-methacrylic acid) Capillary Columns For Separation of Low-Molecular-Weight Compounds* (p. 84)
- 9:40–10:00 Eva Svobodová: *Micellar Electrokinetic Chromatography of Natural Organic Dyes* (p. 87)
- 10:00–10:20 Petr Žáček: *In vitro Incubation of the Labial Gland and Fat Body of the Bumblebee Males *Bombus terrestris* with [1,2-<sup>14</sup>C]acetate and Analysis of the Metabolites* (p. 92)
- 10:20–10:30 **Coffee Break**
- 10:30–10:50 Katarína Beníková: *Polymers As a Construction Part of Electrochemical Nucleic Acid Biosensors* (p. 97)
- 10:50–11:10 Aleš Daňhel: *New Types of Silver Amalgam Electrodes and Their Applications* (p. 100)
- 11:10–11:30 Dana Deýlová: *Voltammetric Determination of 2-Amino-6-Nitrobenzothiazole at Different Amalgam Electrodes* (p. 101)
- 11:30–11:50 Věra Mansfeldová: *Electrochemical Sensor: Mediator Deposition by Drop Evaporation* (p. 104)
- 11:50–12:00 **Coffee Break**
- 12:00–12:20 Lenka Němcová: *Voltammetric and HPLC Methods in the Determination of cis- and trans-Resveratrol* (p. 109)
- 12:20–12:40 Vít Novotný: *Voltammetric Determination of Aclonifen and Fluorodifen at a Silver Solid Amalgam Electrode* (p. 114)
- 12:40–13:00 Barbora Šustrová: *Modification of Gold Metal Surfaces by Thiolated Calix[4]arene and Undecanethiol: Comparative Studies* (p. 117)
- 13:00–13:10 **Closing Address**
- 13:10–14:00 **Lunch**

# Contributions



# Blue to Purple Switch of Conjugated Cyanine Dyes in a Sensor for Acid-Containing Gaseous Environments

DOMINIK B. M. GRÖGEL, AXEL DÜRKOP, OTTO S. WOLFBEIS

*Institute of Analytical Chemistry, Chemo- and Biosensors, University of Regensburg, D-93040 Regensburg, Germany, ✉ Dominik.Groegel@chemie.uni-r.de*

## Keywords

cyanine dyes  
gas sensor

Conjugated near-infrared (fluorescent) cyanine dyes are widely used as biolabels for proteins to visualize cells because their spectral characteristics (excitation around 690 nm, emission around 800 nm) prevent background emission from biological material. However, the dye is irreversibly decomposed upon protonation in aqueous media knocking off one part of the chromophoric system. This results in a blue shift of both absorbance and emission. We are presenting here a disposable sensor that uses this blue to purple switch in the presence of acid-containing gaseous environments [1–4].

Studied dye ( $\lambda_{\text{abs}} \sim 690$  nm,  $\lambda_{\text{em}} \sim 810$  nm,  $\epsilon \sim 95\,000$  M<sup>-1</sup>cm<sup>-1</sup>), depicted in Fig. 1, was mixed with a solution of a hydrogel (Hypan; 5%) and the mixture then spread on a transparent MYLAR support. Circular indicator spots of 20 mm in diameter were cut out and placed above hydrochloric acid solutions of various concentrations. The response time is 10 min and the color changes from blue to purple (Fig. 2). A control experiment with the sensor spot placed above an ammonia solution showed no change in color. The (irreversible) sensor layer is intended for use as an indicator for inappropriate

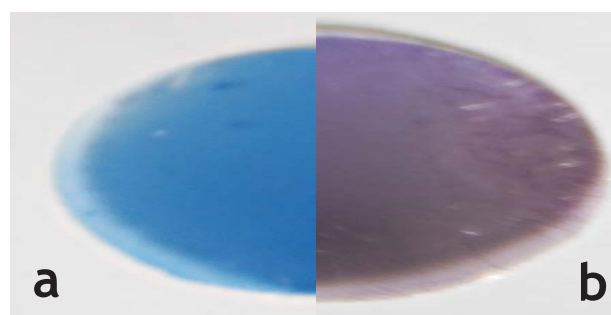


**Fig. 2.** Image of the disposable sensor before (a) and after (b) storage above a hydrochloric acid solution

storage conditions and to detect exposure to acidic gases in context with occupational health.

## References

- [1] Mishra A., Behera R.K., Behera P.K., Mishra B.K., Behera G.B.: *Chem. Rev.* **100** (2000), 1973–2011.
- [2] Oushiki D., Kojima H., Terai T., Arita M., Hanaoka K., Urano Y., Nagano T.: *J. Am. Chem. Soc.* **132** (2010), 2795–2801.
- [3] Kele P., Li X., Link M., Nagy K., Herner A., Lörincz K., Bèni S., Wolfbeis O.S.: *Org. Biomol. Chem.* **7** (2009), 3486–3490.
- [4] Descalzo A.B., Rurack K.: *Chem. Eur. J.* **15** (2009), 3173–3185.

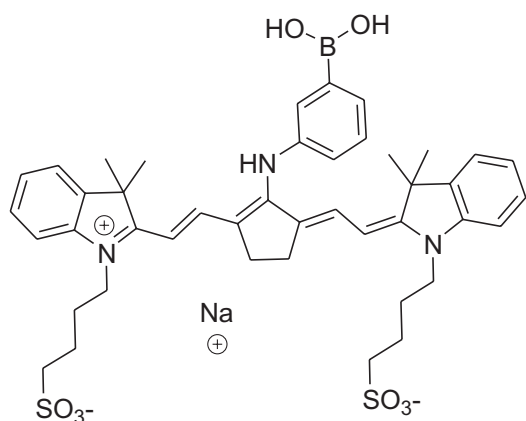


**Fig. 1.** Conjugated cyanine dye

# Luminescent ATPase Assay Using a Phosphate-sensitive Lanthanide Probe

THOMAS LANG, MICHAEL SCHÄFERLING

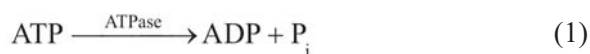
Institute of Analytical Chemistry, Chemo- and Biosensors, University of Regensburg, D-93040 Regensburg, Germany, ✉ [thomas3.lang@chemie.uni-r.de](mailto:thomas3.lang@chemie.uni-r.de)

## Keywords

ATP  
enzyme activity  
lanthanide probe  
luminescence

Recently, we have developed a method for the determination of enzyme-catalysed consumption of ATP using luminescent probes based on  $\text{Eu}^{3+}$  or  $\text{Tb}^{3+}$  complexes [1]. Many enzymes require ATP as a substrate or co-substrate as a source of chemical energy which is required for the catalysis of essential intracellular processes. Hydrolytic enzymes such as ATPases use this energy for the transport of certain ions (e.g.,  $\text{Na}^+$ ,  $\text{K}^+$ , protons) against their concentration gradient across the cell membrane. Hence, identification of regulators of these enzymes is an important task in pharmaceutical research and screening. With this new approach, enzyme activities can be directly monitored by means of fluorescent probes which indicate the turn-over of ATP in real time.

A few years ago an assay for adenylylase activity has been developed that is based on a terbium(III)-norfloxacin (Tb-Nflx) complex as the ATP-sensitive [2]. Now, this concept was adapted to monitor the activity of ATPases according to the following reaction



The assay is based on the strong quenching effect of the released phosphate anions on the lanthanide luminescence. The decrease in the luminescence intensity recorded at  $\lambda_{\text{em}} = 545 \text{ nm}$  is proportional to the concentration of ATP. The time trace of this decrease directly reflects the activity. Thus, kinetic parameters can be evaluated and enzyme regulators can be screened in microwell plate formats. This assay provides a cheap and straightforward alternative to commercially available ATPase assays which are typically based on colorimetric reactions (for example the Taussky-Shorr reagent) or the detection of ADP with specific antibodies, and are all endpoint methods.

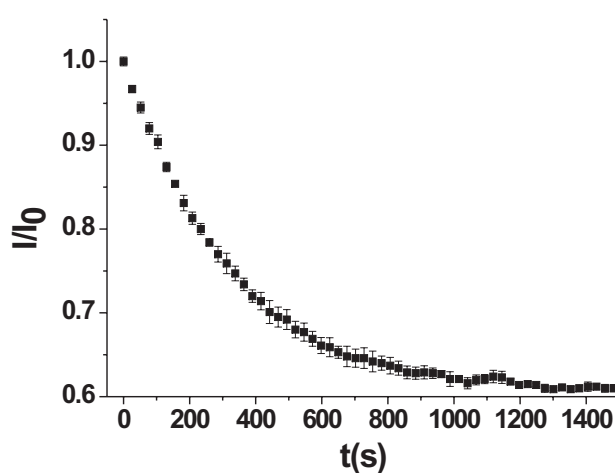


**Fig. 1.** Time response of the referenced luminescence intensity of Tb-Nflx (5:1),  $c = 25 \times 10^{-6} \text{ mol L}^{-3}$ , in the presence of 167  $\mu\text{Units}$  of adenosine 5'-triphosphatase from porcine cerebral cortex, and 1.25 nmol of ATP ( $\lambda_{\text{exc}} = 340 \text{ nm}$ ).

## References

- [1] Spangler C.M., Spangler C., Schäferling M.: *Ann. N.Y. Acad. Sci.* **1130** (2008), 138–148.
- [2] Spangler C.M., Spangler C., Göttle M., Shen Y., Tang W.-J., Seifert R., Schäferling M.: *Anal. Biochem.* **381** (2008), 86–93.
- [3] Spangler C., Schäferling M., Wolfbeis O.S.: *Microchim. Acta* **161** (2007), 1–39.

# Gold Chemical Vapor Generation by Tetrahydroborate Reduction for AAS: Radiotracer Efficiency Study and Characterization of Gold Species

STANISLAV MUSIL<sup>a, b</sup>, YASIN ARSLAN<sup>c</sup>, JAN KRATZER<sup>a</sup>, MILOSLAV VOBECKÝ<sup>a</sup>, OLDŘICH BENADA<sup>d</sup>, TOMÁŠ MATOUŠEK<sup>a</sup>, PETR RYCHLOVSKÝ<sup>b</sup>, O. YAVUZ ATAMAN<sup>c</sup>, JIŘÍ DĚDINA<sup>a</sup>

<sup>a</sup> *Institute of Analytical Chemistry of the Academy of Science of the Czech Republic, v.v.i., Veveří 97, 602 00 Brno, Czech Republic, ✉ stanomusil@biomed.cas.cz*

<sup>b</sup> *Department of Analytical Chemistry, Faculty of Science, Charles University in Prague, Albertov 6, 128 40 Prague 2, Czech Republic*

<sup>c</sup> *Chemistry Department, Faculty of Arts & Sciences, Middle East Technical University, 06531 Ankara, Turkey*

<sup>d</sup> *Institute of Microbiology of the Academy of Science of the Czech Republic, v.v.i., Videňská 1083, 142 20 Prague 4, Czech Republic*

## Keywords

<sup>198, 199</sup>Au radiotracer

chemical vapor generation

generation efficiency

transmission electron microscopy

## Abstract

For the chemical vapor generation of gold we tried to assess efficiencies of individual processes by means of <sup>198, 199</sup>Au radioactive indicator. We found that 12.9% of the analyte introduced into the reaction with tetrahydroborate was released to the gaseous phase and 11.9% reached the trapping device situated in place of the atomizer at optimized carrier gas flow rate. The remaining 88.1% of the analyte was found deposited all over the generator or in the waste. Further results also indicated that the release of volatile species to the gaseous phase could be even doubled when argon purge flow rate was increased to 600 mL min<sup>-1</sup>. We also confirmed the hypothesis that the volatile species were actually gold nanoparticles transported along with aerosol by a carrier gas to the atomizer.

## 1. Introduction

Chemical vapor generation (CVG) of transition metals for analytical atomic spectrometry appears to be a more sensitive alternative to nebulization techniques [1]. Analogously to hydride generation [2], the chemical scheme of analyte reduction by tetrahydroborate in acidic environment is utilized [3]. The practical advantage lies in analyte separation from a matrix and higher introduction efficiency. However, very little is known about the actual reaction mechanism [4]. The real identity of volatile metal species was revealed in the case of silver recently [5] when silver nanoparticles were detected in the gaseous phase by means of a transmission electron microscope. Moreover, generation efficiency [6] is still relatively low even with using various reaction modifiers. The most effective modifiers published for gold determination were diethyldithiocarbamate (DDTC) [7–9] or room temperature ionic liquids [10] with efficiencies of generation around tens of percent (compare to 100% efficiency of hydride generation). A choice of approaches to estimate the generation, release and transport efficiency is limited. The use of

a radioactive indicator appears to be the most trustworthy and effective approach which allows to quantify efficiencies in all subsequent processes of CVG in a single run.

The main objective was to determine generation efficiency in our optimized system for gold by means of the radioactive indicator. We also intended to characterize the nature of the generated „volatile“ gold species.

## 2. Experimental

### 2.1. Standards and Reagents

Deionized water (< 0.2 μS cm<sup>-1</sup>, ULTRAPURE, Watrex) was used throughout. Gold standards were prepared by dilution of 1000 mg mL<sup>-1</sup> stock solution (BDH, UK) in 0.6 mol L<sup>-1</sup> HNO<sub>3</sub> (p.p., Lach-Ner, Czech Republic) and solution of 1.0% (m/v) sodium diethyldithiocarbamate trihydrate (DDTC) (Sigma) in ethanol was added to have a final concentration 0.01% (m/v) of DDTC in the standard. A reductant solution containing 2.4% (m/v) NaBH<sub>4</sub> (FLUKA, Germany) and 133 mg L<sup>-1</sup> of Antifoam B emulsion

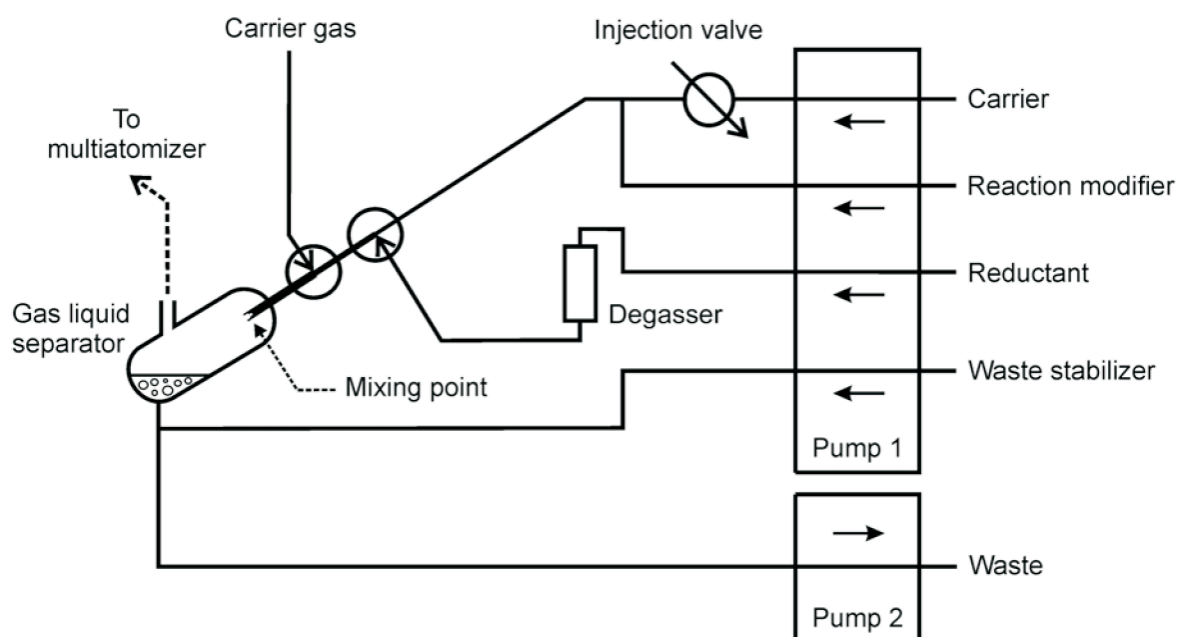


Fig. 1. The scheme of the FI generator with 0.5 mL sample loop.

(Sigma, USA) in 0.1% (m/v) KOH (p.a., Lachema, Czech Republic) was prepared daily. 20 mg L<sup>-1</sup> of Triton X-100 (Aldrich Chemical Co., USA) in 0.1 mol L<sup>-1</sup> HNO<sub>3</sub> was used as a reaction modifier. 0.5 mol L<sup>-1</sup> NaOH solution (Lach-Ner) served as a waste stabilizer.

## 2.2. System for CVG in FI Mode with AAS Detection

The detection of free Au atoms was carried out during method optimization in a quartz multiatomizer [11] with 30 mL min<sup>-1</sup> of air or 6 mL min<sup>-1</sup> of O<sub>2</sub> as outer gas by means of an atomic absorption spectrometer Perkin-Elmer 503 equipped with a Au hollow cathode lamp (242.8 nm line, slit 0.7 nm). The details of FI generator (Fig. 1) were given elsewhere [5, 12] and the optimized conditions of Au CVG are summarized in Table 1.

Table 1

Optimized CVG conditions for atomization in the multiatomizer.

Carrier (flow rate)	0.6 mol L <sup>-1</sup> HNO <sub>3</sub> (0.5 mL min <sup>-1</sup> )
Sample matrix	0.01% (m/v) DDTC in 0.6 mol L <sup>-1</sup> HNO <sub>3</sub>
Reaction modifier (flow rate)	20 mg L <sup>-1</sup> Triton X-100 in 0.1 mol L <sup>-1</sup> HNO <sub>3</sub> (0.5 mL min <sup>-1</sup> )
Reductant (flow rate)	2.4% (m/v) NaBH <sub>4</sub> , 0.1% (m/v) KOH, 133 mg L <sup>-1</sup> of Antifoam B emulsion (0.5 mL min <sup>-1</sup> )
Waste stabilizer (flow rate)	0.5 mol L <sup>-1</sup> NaOH (0.5 mL min <sup>-1</sup> )
Carrier Ar flow rate	240 mL min <sup>-1</sup>
Multiatomizer temperature	900 °C
Outer gas flow rate	30 mL min <sup>-1</sup> of air or 6 mL min <sup>-1</sup> of oxygen

## 2.3. <sup>198,199</sup>Au Radiotracer Experiments

<sup>198</sup>Au (half-life 2.7 days) of a high specific activity was prepared by bombarding target nuclide <sup>197</sup>Au (gold wire JMC 72L, Johnson Matthey Chemicals, England) in a core of a research nuclear reactor (LVR-15 Nuclear Research Institute Řež, Czech Republic) according to process <sup>197</sup>Au(n,γ)<sup>198</sup>Au that was accompanied by formation of <sup>199</sup>Au (3.14 days) due to high cross-section of neutron capture by <sup>198</sup>Au. CVG was performed for 300 s using 0.5 mL of radio-labeled solution in 0.6 mol L<sup>-1</sup> HNO<sub>3</sub> with addition of non-active (carrier) Au standard solution (1 mg L<sup>-1</sup>) with 0.01% (m/v) DDTC. The gas liquid separator outlet was not connected to the atomizer but via the transport PTFE tubing (i.d. 2.4 mm, length 84 mm) and a quartz tube (i.d. 2 mm, length 100 mm) to a trapping apparatus. It consisted of two columns, about 40 mm long, in series filled with activated charcoal granules and followed by two disc syringe filters (FP 30/0.2 CA, Whatman Schleicher & Schuell) where the analyte was removed from the gas stream. Activity in the individual parts of the system was quantified using the automatic gamma radiation counting system equipped with a scintillation NaI(Tl) well-type detector (Wizard 3, Perkin-Elmer) with 1 min counting time. Obtained count values were corrected for background and radioactive decay.

## 2.4. Electron Microscopy Investigations

In order to prepare the samples for microscopic analysis, CVG of 1 mg L<sup>-1</sup> and 10 mg L<sup>-1</sup> Au solutions was continuously performed. Volatile species were let

to adsorb onto specially prepared Cu grids [13] at the gas liquid separator outlet for 60 seconds. The samples were examined in transmission electron microscope (TEM) Philips CM100 (FEI, formerly PEO, The Netherlands) equipped with slow-scan CCD camera Mega ViewII (Olympus, Germany). Digitally recorded images were taken at magnifications of 46 k $\times$  and 130 k $\times$ , which correspond to pixel size of 1.4 nm and 0.5 nm, respectively. The Energy Dispersive X-ray Spectroscopy (EDS) micro-analysis was performed in Philips CM12/STEM electron microscope (FEI, formerly PEO, The Netherlands) equipped with EDAX DX4 X-ray analytical system (EDAX, AMETEK). The spectra from individual particles or particle clusters were recorded in Scanning Transmission Electron Microscopy (STEM) bright-field spot-mode at magnification of 50 k $\times$ , 80 kV and spot-size of 7 (10 nm) for 300 ls.

### 3. Results and Discussion

The conditions recently found as optimal for generation of volatile Ag species [5] were taken as a base for generation of volatile Au species. Before the assessment of generation efficiency was carried out, the LOD and LOQ for optimized CVG conditions (Table 1) with AAS detection in the multiatomizer had been determined as 28  $\mu\text{g L}^{-1}$  and 93  $\mu\text{g L}^{-1}$ , respectively. The linear range of calibration was 0.1–5.0  $\text{mg L}^{-1}$ .

#### 3.1. Radiotracer Examination of CVG

The Au radiotracer was employed to track analyte transfer within the apparatus and to quantify efficiency of Au volatile species generation. The results of three replicates performed in a single run for optimized generation conditions are shown in Table 2.

**Table 2**

Distribution of the radioindicator expressed as analyte fraction (in %)<sup>a</sup> determined by radiotracer counting.

Generator <sup>b</sup>	46.6 $\pm$ 0.4
Waste liquid and waste tubing	41.5 $\pm$ 0.3
Transport PTFE tubing	0.7
Quartz tube <sup>c</sup>	0.4
1. column	5.5 $\pm$ 0.1
2. column	1.5
1. filter	4.8 $\pm$ 0.1
2. filter	0.0
Total radiotracer recovery	101.0 $\pm$ 0.5

<sup>a</sup> Uncertainties below 0.05% are not shown.

<sup>b</sup> Generator components (gas liquid separator, capillaries, connections) downstream the peristaltic pump tubing.

<sup>c</sup> The simulation of the multiatomizer inlet arm

12.9% of analyte was converted to the gaseous phase and 11.9% was found in the trapping apparatus which corresponded to the overall CVG efficiency. Transport losses of 1.0% are responsible for the difference. They seem small but they are not negligible (the corresponding transport efficiency is 92%). No activity was measured on the second filter indicating a complete capturing of the „volatile“ analyte. Around 42% of <sup>198,199</sup>Au altogether was found in the waste. The rest was deposited on the walls of the apparatus, mainly in the gas liquid separator where the sample was mixed with the reductant.

In order to check the effect of increased carrier Ar flow rate, another experiment was performed with Ar flow rate of 600  $\text{mL min}^{-1}$ . Generation efficiency of 23.3  $\pm$  0.2, i.e. twice higher than for the optimized Ar flow rate, was found. This is an essential information substantiating that optimal Ar flow rate for AAS sensitivity is not compatible with a maximum generation efficiency. This is illustrated by the fact that the ratio of AAS signal for Ar flow rate of 600  $\text{mL min}^{-1}$  to that for 240  $\text{mL min}^{-1}$  was 85  $\pm$  7%.

#### 3.2. Characterization of the Nature of Au Volatile Form

In analogy to our recent finding that Ag is generated in the form of nanoparticles [5,12] we employed the TEM to test an assumption that Au was volatilized as nanoparticles as well. The glow discharge activated copper grid was situated just downstream of the GLS to collect (presumed) particles generated under optimized conditions. TEM investigation revealed the presence of nanoparticles on the grids (see Fig. 2 on next page). The detected particles were found separate or in isolated clusters of a few particles. The estimated dimension of the nanoparticles size was 10 nm. In order to verify that there are Au atoms in those nanoparticles, the EDS spectra were measured and Au atoms were clearly identified.

### 4. Conclusions

By means of the TEM we confirmed as in the case of Ag [5,12] that the volatile Au species were nanoparticles of approximately 10 nm in size transported along with aerosol by the carrier gas. Release and generation efficiencies were determined in the optimized method of chemical vapor generation of Au. The radiotracer experiments proved that nearly 13% of analyte was converted to the gaseous phase with 92% transport efficiency to the multiatomizer. Further results also indicated that generation efficiency could be significantly enhanced when Ar purge flow rate

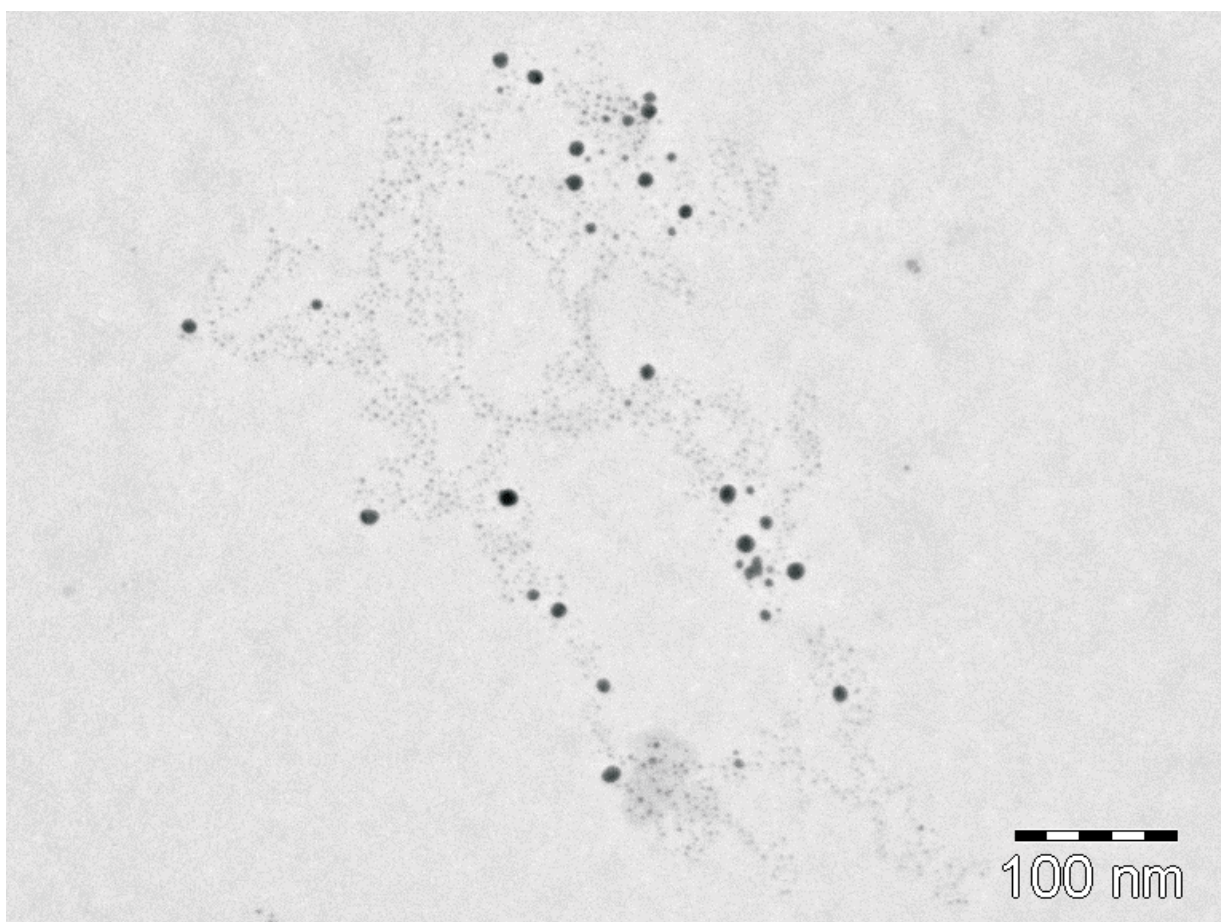


**Fig. 2.** TEM electronograms of the Au particles sampled directly at the gas liquid separator outlet.

was increased from 240 to 600 mL min<sup>-1</sup>. It could be especially beneficial when CV generator would be hyphenated with ICP-MS detector.

#### Acknowledgements

This project was supported by Czech Science Foundation (grant No. 203/09/1783); Academy of Sciences of the Czech Republic (Institutional research plan No. AV0Z40310501 and AV0Z-50200510); GA UK (project SVV 261204); the Czech Ministry of Education, Youths and Sports (project MSM 0021620857) and by ÖYP (Faculty Development Program) from the Middle East Technical University regarding the participations of Y. Arslan.

#### References

- [1] Pohl P., Prusisz B.: *Anal. Bioanal. Chem.* **388** (2007), 753–762.
- [2] Dědina J., Tsalev D. L.: *Hydride Generation Atomic Absorption Spectrometry*. Chichester, Wiley 1995.
- [3] Pohl P.: *Trends Anal. Chem.* **23** (2004), 21–27.
- [4] Feng Y. L., Sturgeon R. E., Lam J. W., D'Ulivo A.: *J. Anal. At. Spectrom.* **20** (2005), 255–265.
- [5] Musil S., Kratzer J., Vobecký M., Hovorka J., Benada O., Matoušek T.: *Spectrochim. Acta B* **64** (2009), 1240–1247.
- [6] Matoušek T.: *Anal. Bioanal. Chem.* **388** (2007), 763–767.
- [7] Xu S. K., Sturgeon R. E.: *Spectrochim. Acta B* **60** (2005), 101–107.
- [8] Ma H. B., Fan X. F., Zhou H. Y., Xu S. K.: *Spectrochim. Acta B* **58** (2003), 33–41.
- [9] Li Z. X.: *J. Anal. At. Spectrom.* **21** (2006), 435–438.
- [10] Zhang C., Li Y., Cui X. Y., Jiang Y., Yan X. P.: *J. Anal. At. Spectrom.* **23** (2008), 1372–1377.
- [11] Matoušek T., Dědina J., Selecká A.: *Spectrochim. Acta B* **57** (2002), 451–462.
- [12] Musil S., Kratzer J., Vobecký M., Benada O., Matoušek T.: *J. Anal. At. Spectrom.* (2010) DOI: 10.1039/c0ja00018c.
- [13] Benada O., Pokorný V.: *J. Electron Microsc. Techn.* **16** (1990), 235–239.

# Arsenic Speciation Analysis by Cryogenic Trapping – Hydride Generation – Atomic Absorption Spectrometry; Investigation of Water Vapour Dryers

MILAN SVOBODA<sup>a, b</sup>, PETRA TAURKOVÁ<sup>a, b</sup>, TOMÁŠ MATOUŠEK<sup>b</sup>, PETR RYCHLOVSKÝ<sup>a</sup>, JIŘÍ DĚDINA<sup>b</sup>

<sup>a</sup> Department of Analytical Chemistry, Faculty of Science, Charles University in Prague, Albertov 6, 128 40 Prague 2, Czech Republic

<sup>b</sup> Institute of Analytical Chemistry of the Academy of Science of the Czech Republic, v.v.i., Veveří 97, 602 00 Brno, Czech Republic, ✉ svoboda750@biomed.cas.cz

## Abstract

The general aim of this work was to contribute to further improvement of the method for complete speciation analysis of trivalent and pentavalent human metabolites of arsenic in complex biological matrices. The method combines selective hydride generation (based on the pre-reduction of pentavalent arsenic forms by L-cysteine) with the generation of substituted arsines followed by hydride trapping in a cryogenic trap (cooled by liquid nitrogen, packed with Chromosorb). The detection is performed by an atomic absorption spectrometer with multiatomizer.

The main target of this work was further improvement of the cryotrapping procedure. Our previous experiments showed that trap blockage by frozen water vapour presents a serious problem since ice has to be removed after each run making the analysis longer and more complicated for automatization. The amount of water vapour can be typically reduced to a tolerable extent when a nafion tube dryer with optimized flow rate of nitrogen as dryer gas is used [1]. However, methylated arsenic forms losses were observed in our experiments, probably due to sorption of analyte on nafion surface, when using the dryer. As a consequence, the nafion dryers were demonstrated to be unsuitable for drying arsenic hydrides.

Polypropylene tubes filled with potassium or sodium hydroxide were studied as alternative dryers [2]. Optimum parameters such as diameter of hydroxide beads were tested.

Advantages and disadvantages of the proposed hydroxide dryer in comparison to the conventional nafion tube dryer will be discussed including detection limits reached by atomic absorption spectrometry

## Keywords

arsenic speciation  
atomic absorption spectrometry  
cryogenic trapping  
hydride generation  
hydroxide dryer

## 1. Introduction

Inorganic As (iAs) is the prevalent form of As in the environment. Human metabolism of iAs involves reduction of As(V) to As(III) and the oxidative methylation of As(III)-species that yields methylated arsenicals containing either As (III) or As(V) [3]. Toxicity of tri- and pentavalent iAs and methylated arsenicals differ significantly [4]. Therefore, method development for oxidation state specific speciation analysis of As in biological matrices has become a key issue for As toxicology and analytical chemistry. Although the iAs(III)/iAs(V) analysis is very common, the reports on the oxidation state specific speciation analysis of methylated species – methylarsonite (MAs(III)), dimethylarsinite (DMAs(III)), methylarsonate (MAs(V)), dimethylarsinate

(DMAs(V)), and trimethylarsine oxide (TMAs(V)O) – remain very scarce [5]. The arsenic oxide (iAs(III)), disodium methylarsonate (MAs(V)), hydroxydimethylarsine oxide (DMAs(V)), trimethylarsine oxide (TMAs(V)O) were employed in this study.

One of the approaches to arsenic speciation analysis combines selective hydride generation with atomic absorption spectrometry. Whereas one aliquot is pre-reduced by L-cysteine in order to determine total arsenic as the sum of trivalent and pentavalent arsenic forms, another sample aliquot is not treated by L-cysteine. Thus, only trivalent arsenic forms are determined in the latter aliquot and content of the pentavalent forms is calculated from the difference. TRIS buffer was found to be the most suitable reaction medium yielding the highest generation efficiency for arsenic species. The pH of the buffer must be kept

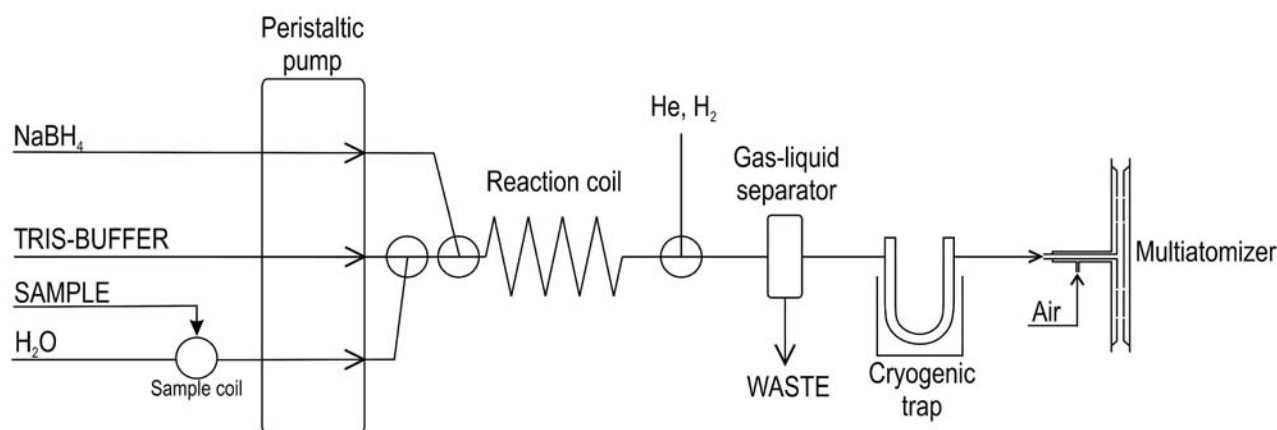


Fig. 1. Experimental setup of hydride generator with cryogenic trap for AAS.

around 6 since it is crucial for reaching 100% hydride generation efficiency. In collection step, iAs and methylated As forms are converted to arsines and methylated forms and retained in the cryogenic trap cooled by liquid nitrogen. The cryogenic trap is subsequently heated in volatilization step to release collected arsenic species to the atomizer stepwise according to their boiling points. The whole procedure can be automated [6].

The general aim of this work was to contribute to further improvement of the cryogenic trap system. The targets were to minimize water vapour amount entering to the cryogenic trap and subsequently to the atomizer since frozen water vapour blocks cryogenic trap and makes analysis impossible. Moreover, water vapour in atomizer increases baseline noise and causes drift as well. Nafion tube dryer is commonly used to prevent water vapour to enter the trap/atomizer system. Unfortunately, the nafion tube dryer caused losses of generated arsenic volatile compounds during drying as demonstrated in this study. Therefore another approach with potassium hydroxide as dryer was constructed and tested.

## 2. Experimental

### 2.1. Instrumentation

The detection was performed by atomic absorption spectrometer Perkin Elmer Analyst 800 (Norwalk, Mass, U.S.A.) equipped with FIAS 400 flow injection accessory (FIAS). The arsenic EDL lamp System II (Perkin Elmer) operated at 376 mA with deuterium background correction was used. The slit width was set to 0.7 nm. A multiple microflame quartz tube atomizer (multiatomizer) heated to 900 °C and supplied with 35 ml min<sup>-1</sup> of air as outer gas was employed as an atomizer.

### 2.2. Standards and Reagents

A stock solution of 1000 µg As L<sup>-1</sup> was prepared for each of arsenic species in water using following compounds: As<sub>2</sub>O<sub>3</sub>, Lachema, Czech Republic (iAs(III)); Na<sub>2</sub>CH<sub>3</sub>AsO<sub>3</sub>·6H<sub>2</sub>O, Chem. Service, West Chester, USA (MAs(V)); H(CH<sub>3</sub>)<sub>2</sub>AsO<sub>2</sub>, Strem Chemicals, Newburyport, USA (DMAs(V)); (CH<sub>3</sub>)<sub>3</sub>AsO University of British Columbia, Vancouver, Canada (TMAOs(V)). Working standards were prepared for individual species by serial dilution of the stock solutions in water. Mixed standards were prepared by mixing the solutions of individual species during the last dilution, i.e. at the ng mL<sup>-1</sup> level.

Deionized water (<0.2 µS cm<sup>-1</sup>, ULTRAPURE, Watrex) was used for preparation of all solutions. The reductant solution containing 1% NaBH<sub>4</sub> (Fluka, Buchs, Switzerland) in 0.1% (m/v) KOH (p.a., Lachema, Brno, Czech Rep.) was prepared daily. A 0.75 mol L<sup>-1</sup> tris(hydroxymethyl)aminomethane (TRIS-HCl buffer (pH = 6) was prepared from a reagent grade Trizma<sup>®</sup> hydrochloride (Sigma) and pH adjusted to 6 by NaOH (Lachner, Czech Republic). Other reagents included HCl (p.a., Merck, Darmstadt, Germany) and a biochemistry grade L-cysteine hydrochloride monohydrate (Merck).

### 2.3. Hydride Generator and Cryogenic Trap

A scheme of the hydride generator-cryogenic trap-atomic absorption spectrometer (HG-CT-AAS) system is shown in Fig. 1. All gas flows were controlled by mass flow controllers (FMA-2400 or 2600 Series, Omega Engineering, Stamford, USA). The sampling coil of 500 µl was used. The manifold was built using PTFE T-pieces, see Ref. 6 for detailed description of the manifold and cryogenic trap.

## 2.4. Atomizers

The multiatomizer for atomic absorption measurement was identical to that described previously (model MM5 in Ref. [6]).

## 2.5. Cryotrapping Procedure

Cryotrapping procedure consists of two steps: (i) collection of arsenic hydrides which are collected in the trap under the  $-190\text{ }^{\circ}\text{C}$ , and (ii) the volatilization step which is based on heating of the trap thereby arsenic hydrides are released according to their boiling points to the atomizer. The procedure is described in detail in Ref. [6].

## 2.6. Nafion Dryer

Two types of the nafion dryer tubes Tube 1: MD-110-12FP, i.d. 2.184 mm, o.d. 2.742 mm, length 310 mm (Perma Pure, Toms River, USA) and Tube 2: MD-070-24F-2, i.d. 1.524 mm, o.d. 1.829 mm, length 610 mm (Perma Pure, Toms River, USA) of nafion dryer were employed. These dryers were inserted between gas-liquid separator and cryogenic trap and compared with experiments without dryer realized only by polytetrafluorethylene tube with the same inner diameter as nafion dryers.

## 2.7. Hydroxide Dryer

The hydroxide dryer consisted of polypropylene tube (dryer tube, commercial product P-Lab, Czech Republic) 1.7 cm i.d., 10 cm in length which was simply filled either with solid sodium or potassium hydroxide of different size of hydroxide beads. Following three types of hydroxide dryers were tested: D1 – NaOH pure, Lachner, Czech Republic, o.d. 1.5 mm; D2 – NaOH p.a., Lachner, Czech Republic, o.d. 3 mm; D3 – KOH pure, Lachema, Czech Republic,  $6 \times 2.5 \times 2.5$  mm. The results with and without dryer were compared analogously as for nafion dryers.

## 3. Results and Discussion

### 3.1. Nafion Dryers

Effect of nafion tube dryers on peak areas of arsenic forms is shown in Fig. 2. Losses were observed for both nafion tubes (Tube 1 and Tube 2, see Section 2.6. for description of the tubes). Signal of DMAs(V) decreased of 19.3% and response for TMAs(V)O completely disappeared (sensitivity under detection

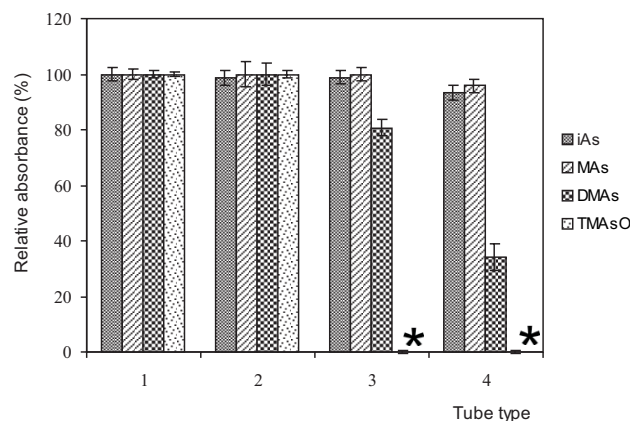


**Fig. 2.** Comparison of relative absorbance of different nafion tubes: (1) connection without tube, (2) connection with PTFE tube (length 610 mm), (3) connection with Tube 1 (length 310 mm), (4) connection with Tube 2 (length 610mm), \* < LOD.

limit) employing Tube 1. Losses were even much more pronounced using Tube 2 (see Fig. 2): 6.7% for iAs(III), 4.2% for MAs(V), 65.9% for DMAs(V) and 100% for TMAs(V)O (sensitivity under detection limit). Since no losses of any arsenic form were observed for PTFE tube of the same length as the longer dryer tube (Tube 2) it can be concluded that it is the nafion surface which is unambiguously responsible for the losses not the increased distance between the gas liquid separator and the trap.

### 3.2. Hydroxide Dryer

The different hydroxides with different outer diameters of beads were employed (see Section 2.7.). There is evidence of losses of iAs(III) (~6%) and DMAs(V) (~2%) if the D1 hydroxide dryer (1.5 mm o.d.) was used. There is no evidence of losses of any arsenic forms if the outer diameter is higher (hydroxide dryers D2 and D3). These experiments clearly demonstrate influence of hydroxide's outer diameter on arsenic losses. Moreover, the hydroxide dryer is capable to eliminate nonspecific absorption caused probably by sulfane (decomposition of L-cysteine) and water vapour (from frozen spray droplets released from cryogenic trap in volatilization step) as shown in Fig. 3 (on next page).

Peak for inorganic arsenic is higher and more symmetric when the hydroxide dryer D2 is employed as shown in Fig. 3. As a result, shorter signal integration time may be used. As a consequence, lower LOD may be reached since the fluctuation of baseline noise for blank experiments is also lower when shorter integration time is used. Moreover, the use of deuterium background correction (DBC) can be avoided because non-specific absorption disappears when using the

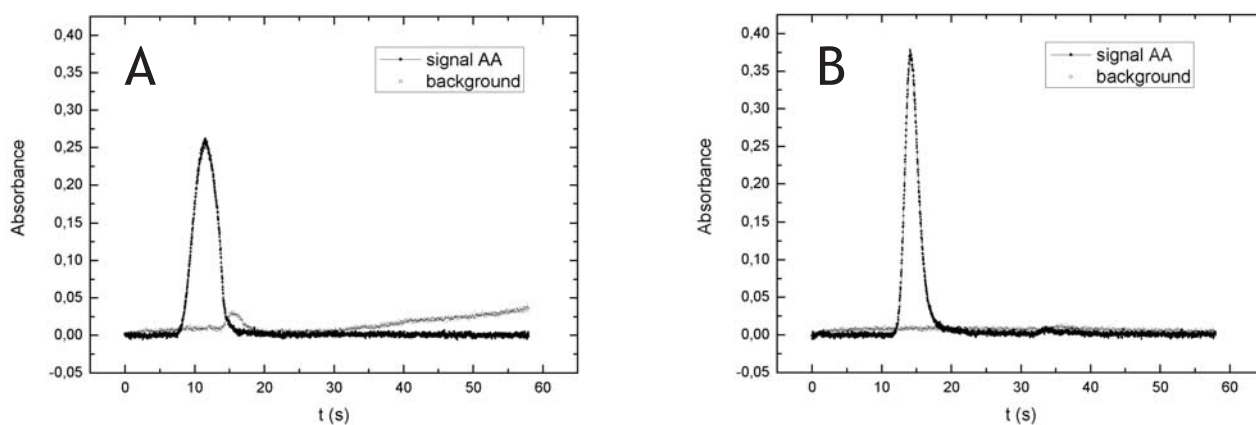


**Fig. 3.** Comparison of chromatograms (A) without and (B) with hydroxide dryer D2; the line demonstrate deuterium background correction which correct nonspecific absorption visible on the (A) chromatogram.

**Table 1**

Comparison of limits of detection [ng] without and with deuterium background correction (DBC)

arsenic specie	without DBC	with DBC
iAs(V)	23	29
MAs(V)	19	23
DMAAs(V)	21	27
TMAAs(V)O	35	38

hydroxide dryer. This enables to decrease the LOD furthermore since DBC in general causes increase of baseline noise as demonstrated in Tab. 1.

#### 4. Conclusions

First part of this study is focused on quantification of arsenic losses, especially of its methylated forms, using the nafion dryer. Trimethylarsineoxide's losses are 100% in both of nafion tubes. This is a clear proof that nafion tube dryer is not a suitable device to remove water vapour for arsenic speciation analysis.

On the other hand hydroxide dryers, especially those with hydroxide beads larger than 1.5 mm, were found to be a suitable alternative. They enable not only effective removal of water vapor from carrier gas stream without any losses of arsenic species but they also eliminate nonspecific absorption caused probably by sulphane evolved from L-cysteine decomposition. Employing hydroxide dryers deuterium background correction can be omitted. Thus, lower LOD and more accurate results can be reached compared to dryers based on nafion.

#### Acknowledgments

This work was supported by GA CR (grant No. 203/09/1783); GA UK (projects No. 133008 and No. SVV 261204); MŠMT No. MSM0021620857; Institute of Analytical Chemistry of the ASCR. v.v.i. (Institute research plan AV0Z40310501) and by a Gillings Innovation Laboratory award from the UNC Gillings School of Global Public Health (project Analytical Laboratory for Development of Biomarkers of Environmental Exposures to Arsenic).

#### References

- [1] Sundin N. G., Tyson J. F.: *Spectrochim. Acta B* **50** (1995), 369–375.
- [2] Crecelius E.A.: *Anal. Chem.* **50** (1978), 826–827.
- [3] Stýblo M., Del Razo L.M., Vega L., Germolec D.R., Le Cluyse E.L., Hamilton G.A., Reed W., Wang C., Cullen W.R., Thomas D.J.: *Arch. Toxicol.* **74** (2000), 289–299.
- [4] Francesconi K.A., Kuehnelt D.: *Analyst* **129** (2004), 373–395.
- [5] Devesa V., Del Razo L.M., Adair B., Drobná Z., Waters S.B., Hughes M.F., Stýblo M., Thomas D.J.: *J. Anal. At. Spectrom.* **19** (2004), 1460–1467.
- [6] Matoušek T., Hernández-Zavala A., Svoboda M., Langerová L., Adair B. M., Drobná Z., Thomas D. J., Stýblo M., Dědina J.: *Spectrochim. Acta B* **63** (2008), 396–406.

# Arsenic Speciation Analysis by Hydride Generation – Cryotrapping – Atomic Fluorescence Spectrometry with Flame-in-Gas-shield Atomizer

MILAN SVOBODA<sup>a, b</sup>, STANISLAV MUSIL<sup>a, b</sup>, TOMÁŠ MATOUŠEK<sup>b</sup>, PETR RYCHLOVSKÝ<sup>a</sup>, JIŘÍ DĚDINA<sup>b</sup>

<sup>a</sup> Department of Analytical Chemistry, Faculty of Science, Charles University in Prague, Albertov 6, 128 40 Prague 2, Czech Republic

<sup>b</sup> Institute of Analytical Chemistry of the Academy of Science of the Czech Republic, v.v.i., Veveří 97, 602 00 Brno, Czech Republic, ✉ svoboda750@biomed.cas.cz

## Keywords

arsenic speciation  
atomic fluorescence spectrometry  
cryogenic trapping  
hydride generation  
hydroxide dryer

## Abstract

The main target of this work was further improvement of detection limits in the method of arsenic speciation analysis of tri- and pentavalent human metabolites in complex biological matrices. The method combines selective hydride generation (based on the pre-reduction of pentavalent arsenic species by L-cysteine) with preconcentration and subsequent separation of substituted arsines in a cryogenic trap. The possibility of hyphenation of the hydride generation system with the flame-in-gas-shield atomizer and atomic fluorescence detector was investigated. The sodium hydroxide dryer was found feasible for removing water vapour from the gaseous phase and the advantages are pointed out. The performance of the system was found excellent owing to superb atomic fluorescence sensitivities and owing to the fact that sensitivities were equal for all arsenic species. The limits of detection obtained with the advanced flame-in-gas-shield atomizer were 1.0; 0.2 and 0.5 ng L<sup>-1</sup> for iAs(V), MAs(V) and DMAs(V), respectively. They are significantly better compared to those obtained with the standard atomic fluorescence atomizer (miniature diffusion flame) and much lower than those obtained with atomic absorption spectrometry detection.

## 1. Introduction

Inorganic arsenic (iAs) is a prevalent form of arsenic in the environment. Human metabolism of inorganic arsenic (iAs) consists of reduction of pentavalent arsenicals and oxidative methylation of trivalent species that yields methylated arsenicals [1]. Toxicity of arsenite (iAs(III)), arsenate (iAs(V)) and their tri- and pentavalent methylated analogues differs significantly [2]. Therefore, the method development for oxidation state specific speciation analysis of arsenic in biological matrices has become a key issue of both toxicology and analytical chemistry. Although the iAs(III)/iAs(V) analysis is very common, the reports on the oxidation state specific speciation analysis of methylated species: methylarsonite (MAs(III)), methylarsonate (MAs(V)), dimethylarsinite (DMAs(III)), dimethylarsinate (DMAs(V)) and trimethylarsine oxide (TMAs(V)O) remain very scarce [3].

One of the approaches to arsenic speciation analysis combines selective hydride generation with atomic absorption spectrometry. Whereas one aliquot is pre-reduced by L-cysteine in order to determine total arsenic as the sum of trivalent and pentavalent

arsenic forms, another sample aliquot is not treated by L-cysteine. Thus, only trivalent arsenic forms are determined in the latter aliquot and content of the pentavalent forms is calculated from the difference. TRIS buffer was found to be the most suitable reaction medium yielding the highest generation efficiency for arsenic species. The pH of the buffer must be kept around 6 since it is crucial for reaching 100% hydride generation efficiency. In collection step, iAs and methylated As forms are converted to arsines and methylated forms and retained in the cryogenic trap cooled by liquid nitrogen. The cryogenic trap is subsequently heated in volatilization step thereby the collected arsenic species are released to the atomizer stepwise according to their boiling points. The whole procedure can be automated [4].

Atomic fluorescence spectrometry (AFS) is a suitable detection technique for speciation studies [5] because of its excellent sensitivity when compared to atomic absorption spectrometry (AAS). It has been found recently that commonly used miniature diffusion flame (MDF) as the AFS atomizer can be overcome by a flame in gas shield atomizer (FIGS) regarding the sensitivity and above all the baseline noise which are the critical parameters controlling

detection limit (LOD). The principal advantage of FIGS is that a controlled flow of oxygen is delivered to hydrogen/argon mixture forming a microflame shielded by high argon flow from ambient atmosphere. As a result much smaller flame is produced compared to MDF where air from ambient atmosphere serves as source of oxygen. The baseline noise is than minimized in FIGS, for detailed description of the FIGS and its inherent advantages see Ref. [6].

The general aim of this work was to couple the hydride generator with the cryogenic trap (HG-CT) system with AFS detector, test it with the standard MDF atomizer and then to assess performance of the FIGS atomizer to reach substantially lower LOD than with the same HG-CT system interfaced to AAS detector.

## 2. Experimental

### 2.1. Instrumentation

The in-house designed research grade atomic fluorescence spectrometer equipped with arsenic EDL lamp System II (Perkin Elmer) operating at 340 mA and with a photomultiplier supplied by 1300 or 1500 V was employed [5].

### 2.2. Standards and Reagents

A 1000 mg L<sup>-1</sup> arsenic AAS standard solution (Merck, Germany) was used as iAs(V) stock standard solution. Other arsenic stock solutions of 1000 mg L<sup>-1</sup> were prepared in deionized water using following compounds: Na<sub>2</sub>CH<sub>3</sub>AsO<sub>3</sub>·6H<sub>2</sub>O (Chem. Service, West Chester, USA); (CH<sub>3</sub>)<sub>2</sub>As(O)OH (Strem. Chemicals, USA). Deionized water (<0.2 μS cm<sup>-1</sup>,

ULTRAPURE, Watrex) was used for preparation of all solutions. Mixed standards were prepared by mixing of individual species solutions during the last dilution, i.e. at the ng L<sup>-1</sup> level. The reductant solution containing 1% (m/v) NaBH<sub>4</sub> (Fluka, Switzerland) in 0.1% (m/v) KOH (p.a., Lachema, Czech Rep.) was prepared daily. A 0.75 mol L<sup>-1</sup> tris(hydroxymethyl)-aminomethane hydrochloride (TRIS.HCl) buffer was prepared from a reagent grade Trizma<sup>®</sup> hydrochloride (Sigma) and pH was adjusted to 6 by KOH. Biochemistry grade L-cysteine hydrochloride monohydrate (Merck) was employed as a pre-reductant agent.

### 2.3. Hydride Generator with Cryogenic Trap

A scheme of the HG-CT-AFS system is shown in Fig. 1. The manifold was built using PTFE tubings and PTFE T-pieces (see Ref. 4 for detailed descriptions) and the liquids were propelled by peristaltic pumps at the rate 1 mL min<sup>-1</sup>. The flow rate of carrier gas He was 90 mL min<sup>-1</sup>. The sampling loop of 500 μl was used.

### 2.4. Atomizers

The FIGS and MDF, respectively, atomizers were described in detail elsewhere [6]. For both atomizers the flow rates of carrier gas argon and hydrogen were 500 mL min<sup>-1</sup> and 300 mL min<sup>-1</sup>, respectively. In addition, the FIGS atomizer was supplied by shielded gas argon (1.5 L min<sup>-1</sup> in each channel) and by 5 mL min<sup>-1</sup> of oxygen through a quartz capillary (0.53 mm). All the gas flows were controlled by mass flow controllers (Omega Engineering, USA) or rotameters.

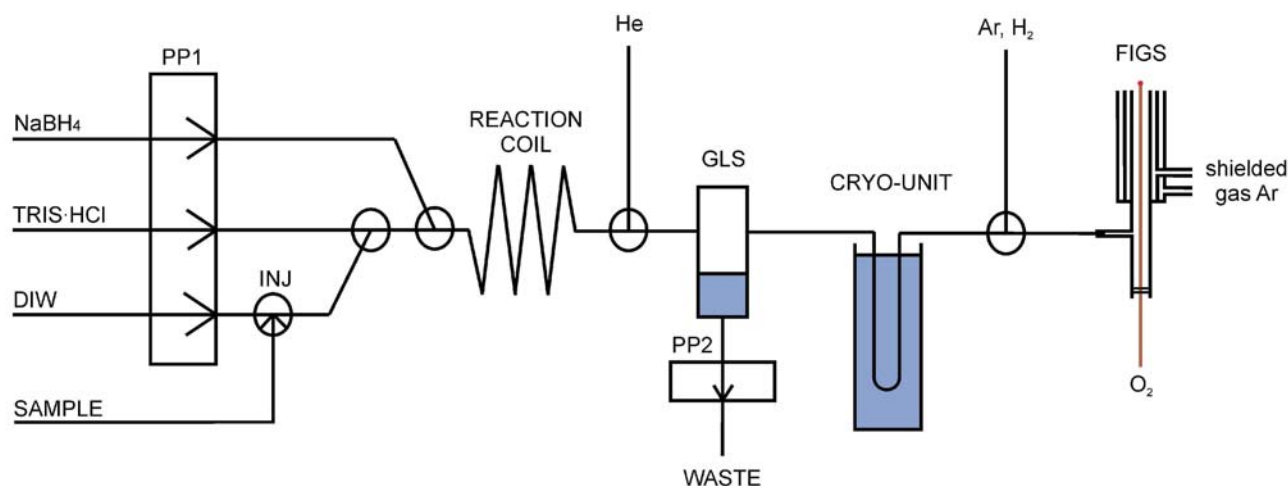


**Fig. 1.** Experimental setup of HG-CT-AFS system: INJ – injection (0.5 mL sample loop), GLS – gas liquid separator, PP1 and PP2 – peristaltic pumps, FIGS – flame in gas shield atomizer.

### 2.5. Cryotrapping Procedure

The cryotrapping procedure consists of two consecutive steps, i.e. collection of arsines and their volatization. The U-tube was immersed into the Dewar flask with liquid nitrogen during trapping step while in the release step the U-tube was gradually heated with power supply by means of current of 1.6 A (23.5 V) so that the arsines were successively released according to their boiling points to the atomizer [4].

### 2.6. Hydroxide Dryer

The hydroxide dryer consisted of a 10 cm long polypropylene tube (P-Lab, Czech Republic) of 1.7 cm i.d. which was filled with solid sodium hydroxide (p.a., Lachner, Czech Republic, pearls of 3 mm o.d.). The sufficient drying ability (removal of water vapour and L-cysteine decomposition products) was confirmed when coupled to AAS (see page 15).

## 3. Results and Discussion

The feasibility of the hydroxide dryer was tested and the peak areas were related to those measured without the dryer, i.e. the gas-liquid separator outlet was connected directly to the U-tube. The peak areas of iAs(V), MAs(V) and DMAs(V) were 30.4; 28.1 and 29.6  $\mu\text{V s}$  with relative standard deviations (RSD;  $n = 9$ ) 2.1; 2.0 and 2.7% for measurement with the hydroxide dryer. The peak areas obtained without hydroxide dryer were 29.9; 28.0 and 30.2  $\mu\text{V s}$  with RSDs ( $n = 6$ ) 1.5; 2.0 and 1.9%. Thus, the hydroxide dryer was proved to be suitable for removing the water vapour transported from the gas liquid separator without any sensitivity depression for all arsenic forms. The typical chromatogram measured with FIGS atomizer and hydroxide dryer is displayed in Fig. 2. More symmetric and higher peak was observed especially for iAs(V) peak when using the hydroxide dryer. Since the water vapour presence would result in an instability of the signal baseline and/or in U-tube

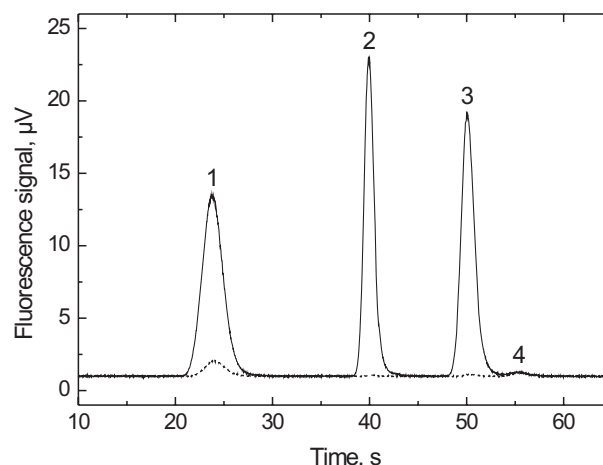


**Fig. 2.** Typical chromatogram measured with the FIGS atomizer. Solid line: 100  $\text{ng L}^{-1}$  arsenic of each species pre-reduced by L-cysteine. Dashed line: blank with L-cysteine. Peaks: (1) iAs(V), (2) MAs(V), (3) DMAs(V), (4) TMAs(V)O.

blocking by frozen water, the hydroxide dryer was found crucial component of the HG-CT-AFS setup.

Calibration graphs were obtained for pentavalent species that were treated with L-cysteine and LODs were evaluated for both tested fluorescence atomizers. As it is seen in Table 1 the superb sensitivities measured with FIGS are about 3 times better when compared to those measured with MDF. However, the main limiting factor for a further LODs improvement seems to be the blank (see also Fig. 2). The high blanks were observed mainly at iAs peak (corresponding concentration 9.2  $\text{ng L}^{-1}$ ) but even at DMAs(V) and TMAs(V)O (collective corresponding concentration 2.4  $\text{ng L}^{-1}$ ). The blank value for MAs(V) was slightly above its LOD. The peak of TMAs(V)O always accompanied the DMAs(V) peak though it had never been used for purpose of this study. Although memory effects appeared in the case of methylated forms to some extent, the contamination from reagents was the main source of high blank signals (especially for iAs) since even cleaning the generator with strong nitric or hydrochloric acid was not capable to decrease blank values satisfactorily.

**Table 1**

Slopes of calibrations, relative sensitivities and LODs for FIGS and MDF atomizers (10, 20, 50 and 100  $\text{ng L}^{-1}$  of each arsenic form for calibration graphs).

Atomizer	As species	Slope [ $\text{L ng}^{-1} \text{ s } \mu\text{V}$ ]	Relative sensitivity <sup>a</sup> [%]	LODs [ $\text{ng L}^{-1}$ ]
FIGS	iAs(V)	$0.2919 \pm 0.0034$	$100.0 \pm 1.7$	1.0
	MAs(V)	$0.2762 \pm 0.0024$	$94.6 \pm 1.4$	0.2
	DMAs(V)	$0.2895 \pm 0.0015$	$99.2 \pm 1.3$	0.5
MDF	iAs(V)	$0.0923 \pm 0.0015$	$100.0 \pm 2.3$	1.1
	MAs(V)	$0.0899 \pm 0.0003$	$97.5 \pm 1.6$	0.6
	DMAs(V)	$0.0984 \pm 0.0003$	$106.7 \pm 1.6$	1.5

<sup>a</sup> related to iAs(V) sensitivity

**Table 2**

Comparison of limits of detection [ $\text{ng L}^{-1}$ ] for AFS-FIGS and recently reached limit of detection [ $\text{ng L}^{-1}$ ] with the same HG-CT connected with AAS.

As species	AFS	AAS
iAs(V)	1.0	47
MAs(V)	0.2	39
DMAAs(V)	0.5	42

#### 4. Conclusions

The selective HG-CT and connected with new FIGS atomizer for AFS was found capable of arsenic speciation analysis at  $\text{ng L}^{-1}$  level. The reached LODs (Table 2) now enable to decrease the amount of the sample which is desirable mainly for determination of biological samples of tissues. Furthermore, the same sensitivities were measured for all arsenic species with both atomizers so that standardization by standards of single species (e.g. iAs(V)) for quantification of all other toxicologically important arsenic forms is possible.

#### Acknowledgments

This work was supported by GA CR (grant No. 203/09/1783); GA UK (projects No. 133008 and No. SVV 261204); MŠMT No. MSM0021620857; Institute of Analytical Chemistry of the ASCR, v.v.i. (Institute research plan AV0Z40310501) and by a Gillings Innovation Laboratory award from the UNC Gillings School of Global Public Health (project Analytical Laboratory for Development of Biomarkers of Environmental Exposures to Arsenic).

#### References

- [1] Stýblo M., Del Razo L.M., Vega L., Germolec D.R., Le Cluyse E.L., Hamilton G.A., Reed W., Wang C., Cullen W.R., Thomas D.J.: *Arch. Toxicol.* **74** (2000), 289–299.
- [2] Francesconi K.A., Kuehnelt D.: *Analyst* **129** (2004), 373–395.
- [3] Devesa V., Del Razo L.M., Adair B., Drobná Z., Waters S.B., Hughes M.F., Stýblo M., Thomas D.J.: *J. Anal. At. Spectrom.* **19** (2004), 1460–1467.
- [4] Matoušek T., Hernández-Zavala A., Svoboda M., Langerová L., Adair B. M., Drobná Z., Thomas D. J., Stýblo M., Dědina J.: *Spectrochim. Acta B* **63** (2008), 396–406.
- [5] Dědina J., Selecká A., Jedlinský J., Podhájecký P.: *work in preparation* (2010).
- [6] Dědina J. and D' Ulivo A.: *Spectrochim. Acta B* **52** (1997), 1737–1746.

# Sensing Strip for Biogenic Amines Using a Chromogenic (Chameleon) Probe, a Reference Dye, and RGB Optical Readout

MARK-STEVEN STEINER, AXEL DUERKOP, OTTO S. WOLFBEIS

*Institute of Analytical Chemistry, Chemo- and Biosensors, University of Regensburg, D-93040 Regensburg, Germany, ✉ mark-steven.steiner@chemie.uni-r.de*

## Keywords

biogenic amines  
RGB optical readout  
sensing strip

Biogenic amines are abundant products of animal, herbal and microbiological metabolism in a variety of food including meat, fish, vegetables and fruits. They are being generated during storage or processing of fish, meat and their products, mainly by thermal or bacterial enzymatic decarboxylation of amino acids [1, 2].

We have developed sensing strips containing an amino-reactive indicator dye and a green fluorescent (amino-insensitive) reference dye incorporated in a hydrogel matrix that is deposited on a paper strip. Such strips enable rapid and direct determination of primary amines. A color change from blue to red occurs on addition of the test strips to a slightly alkaline sample containing primary amines in a concentration range from  $1 \times 10^{-5}$  mol L<sup>-1</sup> to  $1 \times 10^{-2}$  mol L<sup>-1</sup> within 15 min, thus enabling rapid qualitative and semi-quantitative evaluation. The color shift is accompanied by a strong increase of the fluorescence intensity of the dye, with a peak at 620 nm after photo-excitation at 505 nm.

In order to enable quantitative fluorometric measurements and imaging, a reference dye displaying green fluorescence (peaking at 515 nm) was incorporated into the hydrogel. A home-built setup was used for quantitative readout of the strips which are illuminated with high-power 505-nm LEDs in a box that is impermeable to ambient light. The strips then are photographed with a conventional digital camera. The digital color information stored in the camera is then extracted via an red-green-blue (RGB) readout [3]. By referencing the red channel to the green channel, a quantitative signal is obtained that was used to create pseudo-color pictures of the sensor area and respective calibration plots.

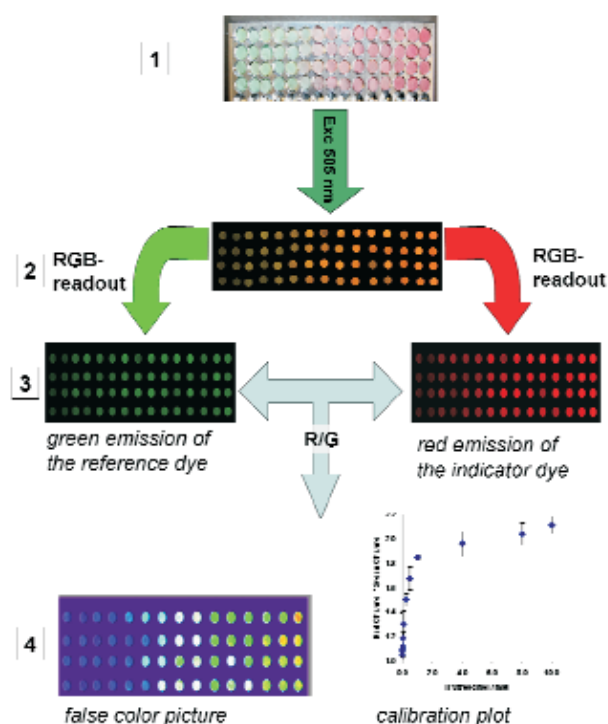


**Fig. 1.** RGB-readout scheme of test strips: (1) Photograph of a calibration measurement; left (cyan): 0 mM putrescine, right (red) 10 mM putrescine;  $n = 4$ . (2) Test strips illuminated at 505 nm. (3) RGB readout. (4) Referencing the red channel to the green channel delivers false color pictures or plots.

## References

- [1] Önal A.: *Food Chem.* **103** (2007), 1475–1486.
- [2] Steiner M.-S., Meier R. J., Spangler C., Duerkop A., Wolfbeis O. S.: *Microchim. Acta* **167** (2009), 259–266.
- [3] Wang X.-D., Meier R. J., Link M., Wolfbeis O. S.: *Angew. Chem.* **122** (2010), 5027–2029.

# Determination of Platinum Group Elements (Pt, Rh and Pd) in Biological Material by Inductively Coupled Plasma Mass Spectrometry – Solving the Problem of Interferences

KATEŘINA WRANOVÁ<sup>a, b</sup>, LUCIE KAŠPAROVÁ<sup>b</sup>, VĚRA SPĚVÁČKOVÁ<sup>b</sup>

<sup>a</sup> Department of Analytical Chemistry, Faculty of Science, Charles University in Prague, Hlavova 8, 128 43 Prague 2, Czech Republic

<sup>b</sup> National Institute of Public Health Šrobárova 48, 100 42 Prague 10, Czech Republic, ✉ wranova@szu.cz

## Abstract

Platinum Group Elements (PGEs), particularly platinum, palladium and rhodium, are nowadays increasingly emitted into the environment from automotive catalytic converters. Growing PGEs' levels in the environment, their unknown concentrations in biological material (especially human fluids) and health risks needs the development of the sensitive method for their determination. The aim of presented work was the development and validation of the method for determination of ultra trace concentration of chosen PGEs in human body fluids (blood, plasma and urine). The concentration of PGEs in samples is very low and therefore the sensitive inductively coupled plasma mass spectrometry (ICP-MS) was used because of its high sensitivity and low limit of detection. The optimal parameters of mass spectrometer were found, appropriated isotopes of analysed elements were chosen, pre-treatment of samples and using of the internal standard were studied and defined. Spectral interferences from monatomic and polyatomic ions produced from the matrix constituents and used gases were studied and corrected using elaborated mathematical correction equations based on signal ratio measurement. The validation parameters as specificity, limit of detection and limit of quantification or repeatability were estimated. The accuracy of the method was checked by analyse of certified reference material and by the successful participation in international laboratory comparison tests organised by University of Erlangen (G-EQUAS) in year 2008 and 2009 (Pt). The developed method was recently used for the determination of platinum group elements in blood of 50 professionally non-exposed women aged 50–59. Relation found among individual metals was Rh > Pt.

## Keywords

biological material  
ICP-MS  
interferences  
platinum group elements

## 1. Introduction

The concentration of platinum group elements (PGEs), particularly platinum, palladium and rhodium, in the environment has been increased during the last two decades because of their role in catalytic converters which are widely fitted to cars [1, 2]. As a result of their use in North America (since 1976) and Europe (since 1980s), automotive emission of NO<sub>x</sub>, CO and various hydrocarbons have been greatly reduced [3]. On the other hand a disadvantage of these catalysts is an abrasion and an ablation of their surface leading to emission of PGEs, mainly in the elemental state or as oxides, to the environment [2].

It is known that several PGEs and their compounds (e.g., complex salts) can cause allergy, asthma and other serious health problems [3–7]. With regard to increasing number of cars with catalysts, the

concentration of these pollutants is being also increased [1]. The presence of PGEs can affect the human health and living organisms and therefore it is necessary to monitor their levels in the environment and also in biological materials [8].

According to very low levels of PGEs in human fluids samples sensitive instrumental techniques such as electrothermal atomic absorption spectrometry (ETAAS), inductively coupled plasma optical emission spectrometry (ICP-OES), inductively coupled plasma mass spectrometry (ICP-MS) and neutron activation analysis (NAA) are required [8–12]. For the determination of these elements, the cathodic stripping voltammetry could be also used [1, 8, 13].

In this work the inductively coupled plasma mass spectrometer was used. It is one of the most attractive analytical and detection systems for element determination. To its advantage belongs e.g. an excellent

detection limit, selectivity, possibility of a multi-element capability, a wide linear dynamic range or speed of measurement [14, 15].

In spite of many advantages, ICP-MS has also some limitations. The biggest problems which have to be mentioned are interferences. Especially spectral interferences caused by atomic or molecular ions with the same mass-to-charge ratio ( $m/z$ ) as measured analytes are probably the largest class of interferences in ICP-MS. They are formed from sample matrix precursors, reagents used for preparation and plasma gases [16]. The differences between levels of PGEs and interferents which could be higher of several orders of magnitude and natural abundance of monitored isotopes are for the measurement also significant. Therefore these problems were widely studied [e.g., 1, 2, 8, 12, 16–18] and spectral interferences in ICP-MS determination were corrected using mathematical correction equations based on signal ratio measurements.

The main aim of this work was the development of sensitive method for determination of chosen PGEs in biological material by using of available sensitive method ICP-MS with solving of interferences' problem.

We were especially interested in studying following types of spectral interferences:

- i) "isobaric" interferences (e.g.,  $^{106}\text{Cd}^+ \sim ^{106}\text{Pd}^+$ ),
- ii) interferences from polyatomic ions caused by plasma (e.g.,  $^{40}\text{Ar}^{63}\text{Cu}^+ \sim ^{103}\text{Rh}^+$ ), and
- iii) interferences from polyatomic ions caused by sample matrix (e.g.,  $^{179}\text{Hf}^{60}\text{O}^+ \sim ^{195}\text{Pt}^+$ ).

## 2. Experimental

### 2.1. Instrumentation

The determination of PGEs was carried out on a Perkin Elmer ICP-MS Elan DRC-e (Perkin Elmer-SCIEX Instrument, Canada) through all the experiments. The quadrupole ICP-mass spectrometer was equipped with nickel sampler and skimmer cones, a concentric PFA teflon nebuliser (sample flow rate  $1 \text{ mL min}^{-1}$ ) and a cooled cyclonic spray chamber (Peltier, at  $5^\circ\text{C}$ ).

The conditions of the instrument were controlled daily by freshly prepared solution of  $10 \mu\text{g L}^{-1}$  Be, Mg, Co, Rh, In, Ce, Ba and Pb. The optimisation of the ICP RF Power, lens voltage and the nebuliser gas flow for PGEs' analyses was done by using of  $10 \mu\text{g L}^{-1}$  solution of individual platinum elements. The optimal operation conditions of the ICP-MS system are summarised in Table 1.

**Table 1**

Instrumental operating conditions

<i>Plasma</i>	
RF Power	1000–1250 W
Ar flow rate <sup>a</sup>	$\sim 0.82 \text{ L min}^{-1}$
T spray chamber	$5^\circ\text{C}$
Lens voltage <sup>a</sup>	$\sim 11.5 \text{ V (Pt)}$ $\sim 6.5 \text{ V (Rh)}$ $\sim 11.0 \text{ V (Pd)}$
<i>Mass Spectrometer</i>	
Sampling cone	nickel
Skimmer	nickel
Analyser vacuum	$\sim 7.0 \times 10^{-6} \text{ Torr}$
<i>Acquisition parameters</i>	
Measurement mode	peak jumping
PGEs' isotopes	$^{103}\text{Rh}$ , $^{105}\text{Pd}$ , $^{106}\text{Pd}$ , $^{194}\text{Pt}$ , $^{195}\text{Pt}$
Monitored interferents	$^{63}\text{Cu}$ , $^{65}\text{Cu}$ , $^{85}\text{Rb}$ , $^{87}\text{Sr}$ , $^{89}\text{Y}$ , $^{178}\text{Hf}$ , $^{179}\text{Hf}$ , $^{206}\text{Pb}$
Dwell time	100 ms
Internal standard	$^{115}\text{In}$ , $^{187}\text{Re}$
<sup>a</sup> Optimization of argon flow rate and lens voltage was done daily by using of a solution of $10 \mu\text{g}$ of PGE element per litre.	

Mineralization of blood samples was carried out with a microwave oven system Milestone 1200 (Milestone, Italy) in teflon vessels by nitric acid and hydrogen peroxide.

### 2.2. Reagents and reference materials

Reagents of highest purity grade were used: 65% nitric acid, 30% hydrogen peroxide (Suprapur, Merck, Germany). Stock solution of analytes, interfering species and internal standards were prepared from standard solutions  $1000 \text{ mg L}^{-1}$  Merck ICP CertiPUR (Cd, Cu, Hf, Pt, In, Pb, Rb, Re Rh, Sr, Y, Zn, Zr), and  $10 \text{ g L}^{-1}$  AAS (Pd) single element standard solutions. Working standards of individual elements were prepared from the standard solution and stabilized by 1% (v/v) nitric acid. Demineralised water ( $18.2 \text{ M}\Omega \text{ cm}^{-1}$ ) from a Milli-Q water purification system (Millipore, France) was used.

$^{115}\text{In}$  was selected as an internal standard for determination of Rh and Pd,  $^{187}\text{Re}$  was used as an internal standard for Pt. Using of internal standards help to control instrumental drift or non-spectral interferences.  $^{115}\text{In}$  and  $^{187}\text{Re}$  were chosen because of its very low abundance in samples, similar atomic mass, ionisation potential and especially similar chemical and physical behaviour to measured platinum elements [7].

The certified reference materials (CRMs) with declared levels of PGEs in biological material were not available. The accuracy of used method was checked by using of certified reference material of whole blood Seronorm Trace Elements Whole Blood

L-1 (SERO, Norway) where the concentrations of measured elements were  $< 1 \text{ ng L}^{-1}$  for Pt and  $< 10 \text{ ng L}^{-1}$  for Pd and Rh.

### 2.3. Sample collection and preparation

About fifty blood samples from non-professional exposed women of age from 50 to 59 were collected into commercial plastic tubes (Vacuette Greiner Bio One GmbH, Germany) and stored at  $-20 \text{ }^\circ\text{C}$  until analysis. The study was approved by Ethic committees and written consent was obtained from each woman.

Before analyses, samples of plasma were diluted ten times by deionised water and samples of urine were diluted five times by 1%  $\text{HNO}_3$  (v/v). Blood samples were mineralized in microwave oven with nitric acid and hydrogen peroxide. Final dilution by 1%  $\text{HNO}_3$  (v/v) was ten times.

## 3. Results and discussion

### 3.1. Preliminary study

At the beginning of the study, all PGEs were determined simultaneously in one sample solution according to [19]. Unfortunately, problems with interferences led us to revise the original method and provide a determination of Pt, Rh and Pd individually. Optimal method parameters were found for all elements and are shown in Table 1.

### 3.2. Analyte versus interfering species

The biological material is a difficult matrix with many interfering species which could affect PGEs' analytical results and could cause their positive errors. In Table 2 are shown levels of interfering species presented in CRM "Seronorm Whole blood" used for the method validation. It is well seen that some contents of interfering species are several orders of magnitude higher than that of PGEs. Therefore it is necessary to observe possible influences of interfering species on PGEs.

### 3.3. Correlation equations and chosen PGEs' isotopes

#### 3.3.1 Platinum

Platinum has six isotopes (190, 192, 194, 195 and 196). Isotopes with the highest natural abundance and with no isobaric interferences are isotope 194 (32.9%) and 195 (33.8%). Concentration of Pt in biological

**Table 2**

Content of possible interfering species in certified reference material Seronorm (trace elements, whole blood, Norway)

Monitored interferent-analyte	Certified reference material	
	L-1 [ $\mu\text{g L}^{-1}$ ]	L-2 [ $\mu\text{g L}^{-1}$ ]
copper <sup>a, b</sup>	564	666
zinc <sup>a</sup>	5 500	5 200
strontium <sup>a, b</sup>	27.8	34
rubidium	1 278 000	1 282 000
ytterbium	0.05	0.04
zirconium	0.28	0.136
cadmium <sup>b</sup>	0.74	6.0
hafnium <sup>c</sup>	0.004	0.0023
lead <sup>a</sup>	27.6	393

<sup>a</sup> interferent of rhodium  
<sup>b</sup> interferent of palladium  
<sup>c</sup> interferent of platinum

material is very low and therefore the sums of both isotopes' signals were used. The same mass to charge ratio have ions  $^{178}\text{Hf}^{16}\text{O}^+$  and  $^{179}\text{Hf}^{16}\text{O}^+$ . As the content of Hf in human blood is similar to Pt concentration (Table 2) the possible affect was studied.

The correction factors were calculated from signal ratios and the final equation for determination of corrected platinum amount was designed:

$$(^{194}\text{Pt}^+ + ^{195}\text{Pt}^+)_{\text{K}} = (^{194}\text{Pt}^+ - k_1 ^{178}\text{Hf}^+) + (^{195}\text{Pt}^+ - k_2 ^{179}\text{Hf}^+) \quad (1)$$

$$k_1 = \text{Mass } 194 / ^{178}\text{Hf}^+ \quad (2)$$

$$k_2 = \text{Mass } 195 / ^{179}\text{Hf}^+ \quad (3)$$

$k_1$  and  $k_2$  are correction factors calculated as a ratio of Mass 194 signal and intensity  $^{178}\text{Hf}^+$  and Mass 195 and  $^{179}\text{Hf}^+$  respectively, in aqueous solution of Hf with the concentration corresponding to Hf level in real sample without Pt.

#### 3.3.2 Rhodium

Rhodium is a monoisotopic element and isotope 103 was used for determination. The same  $m/z$  ratio as  $^{103}\text{Rh}^+$  has double charged  $^{206}\text{Pb}^{2+}$  and polyatomic ions  $^{40}\text{Ar}^{63}\text{Cu}^+$ ,  $^{87}\text{Sr}^{16}\text{O}^+$  and it is necessary to take them into account.  $^{87}\text{Rb}^{16}\text{O}^+$  interference had a negligible influence and was not studied.

The final equation for determination of corrected Rh concentration was obtained by calculation of signal ratio:

$$(^{103}\text{Rh}^+)_{\text{K}} = ^{103}\text{Rh}^+ - (k_1 ^{63}\text{Cu}^+ + k_2 ^{206}\text{Pb}^{2+} + k_3 (^{87}\text{Sr}^+ - k_4 ^{85}\text{Rb}^+)) \quad (4)$$

$$k_1 = \text{Mass } 103/^{63}\text{Cu}^+ \quad (5)$$

$$k_2 = \text{Mass } 103/^{206}\text{Pb}^{2+} \quad (6)$$

$$k_3 = \text{Mass } 103/^{87}\text{Sr}^+ \quad (7)$$

$$k_4 = A_{87\text{Rb}}/A_{85\text{Rb}} \quad (8)$$

Correction factors  $k_1$ ,  $k_2$  and  $k_3$  were calculated in the same way as in the case of Pt. Factor  $k_4$  is the ratio between natural abundance of Rb 87 and 85 ( $A_{87\text{Rb}}$  is 27.83 % and  $A_{85\text{Rb}}$  is 72.165%).  $^{87}\text{Rb}$  has the same  $m/z$  ratio as  $^{87}\text{Sr}$  and by using of  $k_4$  factor it is possible to correct this isobaric interference.

### 3.3.3 Palladium

Palladium has six isotopes (102, 104, 105, 106 and 108), but only isotopes 105 (22.33%) and 106 (27.33%) were suitable to analyse (higher natural abundance, less isobaric interferences). Polyatomic ions  $^{40}\text{Ar}^{65}\text{Cu}^+$ ,  $^{87}\text{Sr}^{18}\text{O}^+$ ,  $^{89}\text{Y}^{16}\text{O}^+$  and  $^{87}\text{Rb}^{18}\text{O}^+$  have the same  $m/z$  ratio as  $^{105}\text{Pd}^+$ , last two ions were not taken in account because of their small signals and influence on Pd results. In case of isotope Pd 106 there are interferences of  $^{40}\text{Ar}^{66}\text{Zn}^+$ ,  $^{90}\text{Zr}^{16}\text{O}^+$ ,  $^{106}\text{Cd}^+$  and possible  $^{88}\text{Sr}^{18}\text{O}^+$ . Finally the isotope Pd 105 was chosen for analysis. It is influenced by less interferences and brings some benefits such as decreasing of measurement time.

The final equation for determination of corrected Pd amount was created:

$$(^{105}\text{Pd}^+)_K = ^{105}\text{Pd}^+ - (k_1 ^{65}\text{Cu}^+ + k_2 (^{87}\text{Sr}^+ - k_3 ^{85}\text{Rb}^+)) \quad (9)$$

$$k_1 = \text{Mass } 105/^{65}\text{Cu}^+ \quad (10)$$

$$k_2 = \text{Mass } 105/^{87}\text{Sr}^+ \quad (11)$$

$$k_3 = A_{87\text{Rb}}/A_{85\text{Rb}} \quad (12)$$

Correction factors  $k_1$  and  $k_2$  were calculated as previously. Factor  $k_3$  was calculated as the ratio between natural abundance of Rb 87 and 85.

### 3.4. Validation of method

The described method and correlation equation correctness were checked and validated.

Method specificity and selectivity is done by the mass properties of individually isotopes. LOD and LOQ values are given in Table 3 and were calculated

**Table 4**

Certified and measured values of rhodium and platinum in certified reference material of whole blood Seronorm L-1.

Element	Certified value [ng L <sup>-1</sup> ]	Measured value [ng L <sup>-1</sup> ]
Rh	< 10	~ 7.0
Pd	< 10	contamination

**Table 3**

Instrumental limits of detection and limits of quantification.

Element	instrumental LOD [ng L <sup>-1</sup> ]	LOQ [ng L <sup>-1</sup> ]
Pt	0.7	2.5
Rh	0.5	2.0
Pd	7.5	25.0

as three times, respectively ten times, of standard deviation (ten measurements of blank sample). The linearity and repeatability (RSD < 10%) were also checked and linearity was proved in whole measured range.

There is a lack of suitable certified reference biological materials with declared value of monitored elements and therefore the control of accuracy is problematic. In case of Pt, all samples were analysed simultaneously with the analyses for the European interlaboratory comparison test organised by University of Erlangen (G-EQUAS, The German External Quality Assessment Scheme for Analyses in Biological Materials), where our results were successful. Rh and Pd were determined in CRM Seronorm and results are shown in Table 4. The measured value of Rh was in agreement with certified value. In case of Pd higher concentration was found. It could be explained by a possible contamination of samples or by influence of other interfering species which were not under control. The reason of this higher value will be the object of future study.

### 3.5. Analyse of real samples

The validated methods were used for determination of PGEs in blood samples of 50 professionally non-exposed women in age 50–59.

Concentrations of Pd were on  $\mu\text{g L}^{-1}$  level (median 2.42; min 0.59; max 11.26), the possibility of samples contamination or influence of other interfering species have to be taken into account. For Rh, the maximum measured signal corresponded to the concentration of  $0.2 \mu\text{g L}^{-1}$ , other Rh results were lower. The results majority for Pt was under detection limit ( $0.007 \mu\text{g L}^{-1}$ ).

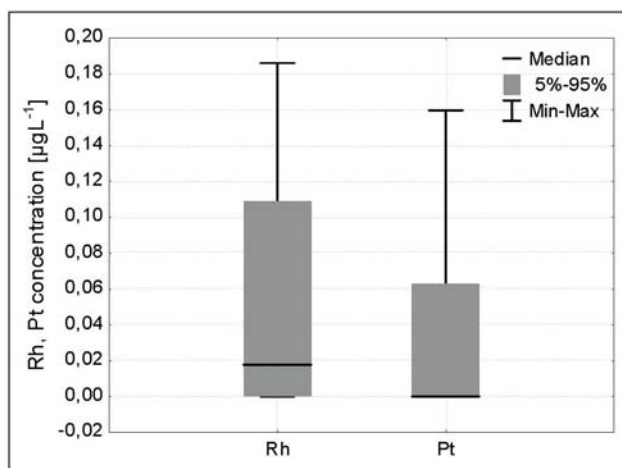


Fig. 1. Rhodium and platinum concentration in blood samples

Rh and Pt concentrations in samples determined in this study are shown in Figure 1. Our results correspond to the results published in the literature [e. g., 20], where  $Pd \gg Rh > Pt$ .

#### 4. Conclusion

The described method ICP-MS was used for determination of Pt, Pd and Rh in biological material.

The problem of spectral interferences had been solved. The affect of possible interfering species such as Cu, Hf, Pb, Rb and Sr have to be under control. The correlation equations were proposed and calculated and their validity was checked by measurement of available CRMs. Levels found for Pt and Rh was in good agreement with declared values. Higher value of Pd could be caused by a possible contamination of sample or affected of other interferences. The solution of this problem will be an object of future study.

The method was used for the determination of PGEs in fifty samples of professionally non-exposed women. The concentration values of all elements were very low and in the case of Pt their majority was under LOD.

These methods could be used for the determination of PGEs in samples of professionally exposed persons.

The method, the possibility of improvement of instrumental parameters for individually elements, pretreatment of samples and interferences will be more studied.

#### Acknowledgements

The work was supported by European project PHIME (Public health impact of long-term, low level mixed element exposure in susceptible population strata, Number FOOD-CT-2006-016253). We also thank to the Grant Agency of Charles University (project SVV 261204) for the financial support, the research project MSM0021620857 and the development program of Ministry of Education, Youth and Sports (RP 14/63 MŠMT).

#### References

- [1] Gomez M. B., Gomez M. M., Palacios M. A.: *Anal. Chim. Acta* **404** (2000), 285–294.
- [2] Simitchiev K., Stefanova V., Kmetov V., Andreev G., Sanchez A., Canals A.: *Talanta* **77** (2008), 889–896.
- [3] Petrova P., Celichkov S., Velitchova N., Haveyov I., Daskalova N.: *Spectroch. Acta Part B* **65** (2010), 130–136.
- [4] *International Programme on Chemical Safety: Platinum. Environmental Health Criteria 125*. WHO, Geneva 1991.
- [5] Bocca B., Alimonti A., Cristaudo A., Cristallini E., Petrucci F., Caroli S.: *Anal. Chim. Acta* **512** (2004), 19–25.
- [6] Farago M. et al.: *Analyst* **123** (1998), 451–454.
- [7] Bosch Ojeda C., Sánchez Rojas F., Cano Pavón J. M.: *Food Control* **17** (2006), 365–369.
- [8] Leśniewska B., Godlewska-Zytkiewicz B., Ruszczynska E., Hulanicki A.: *Anal. Chim. Acta* **564** (2006), 236–242.
- [9] Lopes C., Almeida A., Saraiva M., Lima J.: *Anal. Chim. Acta* **600** (2007), 226–232.
- [10] Seiler Hans G.: *Handbook on Metals in Clinical and Analytical Chemistry*. New York, Marcel Dekker 1994.
- [11] Cornetis R.: *Handbook of Elemental Speciation II. Species in Environment, Food, Medicine and Occupational Health*. Chichester, Wiley 2005.
- [12] Petrucci F. et al.: *Microchem. J.* **76** (2004), 131–140.
- [13] Zhefeng Fan, Zucheng Jiang, Fei Yang Bin Hu: *Anal. Chim. Acta* **510** (2004), 45–51.
- [14] Nelms S. M.: *ICP Mass Spectrometry Handbook*. Oxford, Blackwell 2005.
- [15] Szpunar J., Łobiński R.: *Hyphenated Techniques in Speciation Analysis*. London, The Royal Society of Chemistry 2003.
- [16] May T. W., Wiedmeyer R. H.: *Atomic Spectroscopy* **19** (1998), 150–155.
- [17] Higney E., Olive V., MacKenzie A. B., Pulford I. D.: *Appl. Geochem.* **17** (2002), 1123–1129.
- [18] Parent M., Vanhoe H., Moens L., Dams R.: *Talanta* **44** (1997), 221–230.
- [19] Magarini R.: *Application Note Perkin Elmer; Pt, Rh and Pd determination in whole blood by ICP-MS*.
- [20] Ek K. H. et al.: *Science of the Total Environment* **334–335** (2004), 149–159.

# Determination of Pesticide Residues in Lemon Matrices by Fast Gas Chromatography and Mass Spectrometry

MÁRIA ANDRAŠČÍKOVÁ, SVETLANA HROUZKOVÁ, ANDREA HERCEGOVÁ

*Department of Analytical Chemistry, Faculty of Chemical and Food Technology Slovak University of Technology in Bratislava, Radlinského 9, 812 37 Bratislava, The Slovak Republic, ✉ maria.andrascikova@stuba.sk*

## Abstract

Combination of fast gas chromatography (GC) with quadrupole mass detector was utilized for determination of pesticide residues causing disruption of endocrine system. The QuEChERS method was used for lemon samples preparation. Narrow-bore column (15 m × 0.15 mm i.d. × 0.15 μm film of 5% diphenyl 95% dimethylsiloxane stationary phase) and MS working with electron ionization (EI) and negative chemical ionization (NCI) modes were used for separation and detection of pesticides. Comparison of result obtained using different ionization techniques was performed. The mean recoveries of pesticides ranged between 70–120% with RSD ≤ 20% for both ionization modes. For majority of pesticides high linearity in NCI mode in the concentration range from 5 to 500 ng mL<sup>-1</sup> with coefficient of determination higher than 0.9938 except linuron is reported. Better coefficient of determination were obtained for NCI mode in comparison to EI. The developed fast GC method was applied to the determination of endocrine disrupting pesticides in real lemon samples.

## Keywords

electron ionization  
endocrine disrupting pesticides  
fast GC-MS  
lemons  
negative chemical ionization

## 1. Introduction

Pesticides are of interest in food analysis because of their widespread use in a variety of crops, such as fruits and vegetables, for field- and post-harvest protection. Pesticides and their degradation products could be of potential health hazards because of their toxicity or carcinogenicity. Consequently, strict regulation of maximum residue limits (MRLs) has been set for most food products [1]. Some pesticides in addition behave as endocrine disrupting chemicals (EDCs) and are able to cause adverse effects by interfering in some way with the body's hormones or chemical messengers and induce a broad spectrum of biochemical and toxic responses even at low environmentally relevant dose [2], often lower than MRLs set.

The analysis of pesticides poses special problems for the chemist, as the pesticides belong to different groups of chemical substances having a broad range of polarity and acidic characteristics. Most pesticides are volatile and thermally stable, and therefore are amenable to gas chromatography in combination with element-specific detectors or with mass spectrometry [3] preceded by complicated, time- and labor-consuming sample preparation.

The aim of this work was the determination of pesticide residues in lemon matrices using gas

chromatography coupled with mass spectrometry (GC-MS) in selected ion monitoring mode (SIM). The extraction was carried out using QUECHERS (Quick Easy Cheap Effective Rugged and Safe) method employing liquid extraction with acetonitrile and cleaning-up by dispersive SPE using PSA (primary-secondary amine) sorbent. The goal was to provide a direct comparison of the NCI-MS and EI-MS set-ups, both in the SIM mode when concerning the calibration data, LOD, LOQ values and recovery data.

## 2. Experimental

### 2.1. Chemicals

Pesticide standards were obtained from various sources (Bayer, Leverkusen, Germany; Dr. Ehrenstorfer, Augsburg, Germany; Cheminova, Harboore, Denmark; Ciba-Geigy, Basel, Switzerland; Shering, Kenilworth, NJ, USA; Dow AgroScience, Indianapolis, IN, USA; Agrovita, Ivanka pri Dunaji, Slovak Republic) and were of purity ≥99% except for bifenthrin (96.6%). List of pesticides is given in Table 1. Solutions of individual pesticides were prepared in toluene (Merck KGaA, Darmstadt, Germany) at a concentration of 10 mg mL<sup>-1</sup>. Stock solution of pesticide mixture at a concentration of 0.02 mg mL<sup>-1</sup> was prepared in toluene. Working standard pesticide

mixture solution with lower concentration were prepared in acetonitrile by dilution. Magnesium sulfate (clean, anhydrous) and sodium chloride (*per analysis*) were from Lachema (Brno, Czech Republic). Primary and secondary amine (PSA) sorbent – Bondesil 40  $\mu\text{m}$  – was obtained from Varian (Varian, Harbor City, USA).

### 2.2. QuEChERS sample preparation method

Lemons (not-treated with pesticides) and real samples of lemons were mixed with a Braun MX 2050 blender (Braun, Kronberg, Germany). Certain changes were made in the original QuEChERS procedure [4] according to our needs and resources [5]. The final blank lemon sample extract was used for the preparation of matrix-matched standard solutions. For the recovery studies, lemons from untreated trees were spiked with the appropriate standard pesticide mixture in acetonitrile. The spiking was performed at the concentrations of  $1 \mu\text{g kg}^{-1}$ ,  $5 \mu\text{g kg}^{-1}$ ,  $10 \mu\text{g kg}^{-1}$  and  $250 \mu\text{g kg}^{-1}$  (all in three replicates) for both GC-EI-MS and GC-NCI-MS experiments. Spiked samples were left to stand for 30 min prior to extraction in order to allow pesticide absorption onto the matrix.

### 2.3. Preparation of calibration solutions

In the NCI mode, nine concentration levels of pesticides were used for calibration: 0.1, 0.5, 1, 5, 10, 50, 100, 250 and  $500 \text{ ng mL}^{-1}$  (corresponding to 0.1, 0.5, 1, 5, 10, 50, 100, 250 and  $500 \mu\text{g kg}^{-1}$  in a sample). For calibration in EI mode, seven concentration levels of pesticides were used: 1, 5, 10, 50, 100, 250 and  $500 \text{ ng mL}^{-1}$  (corresponding to 1, 5, 10, 50, 100, 250, and  $500 \mu\text{g kg}^{-1}$  in a sample). Calibration standards for each concentration level were measured six times, starting with the lowest concentration level. Matrix-matched calibration solutions were prepared as follows:  $975 \mu\text{L}$  blank lemon sample extract +  $25 \mu\text{L}$  working standard solutions of pesticides in acetonitrile at various concentrations. These matrix-matched calibration solutions were used for the evaluation of linear range, instrument LODs and LOQs and repeatability.

### 2.4. GC-MS instrumentation

GC-MS measurements were performed on an Agilent 6890N GC system coupled to an Agilent 5975 mass-selective detector (Agilent, Avondale, PA, USA). The PTV was operated in the solvent vent mode under temperature programmed conditions. The flow through the split-valve was  $50 \text{ mL min}^{-1}$ . Chromato-

graphic separation was performed using the following temperature program:  $60 \text{ }^\circ\text{C}$  (hold 1.75 min),  $60 \text{ }^\circ\text{C min}^{-1}$  to  $150 \text{ }^\circ\text{C}$ ,  $23.8 \text{ }^\circ\text{C min}^{-1}$  to  $300 \text{ }^\circ\text{C}$  (hold 1.90 min). The total analysis time was 11.45 min. The injection volume was  $2 \mu\text{L}$ . Helium with purity 5.0 was used as a carrier gas in a constant flow mode at  $1.2 \text{ mL min}^{-1}$ . Narrow-bore chromatographic column CP-Sil 8 CB (Varian, Middelburg, The Netherlands) with 5% diphenyl 95% dimethylsiloxane stationary phase  $15 \text{ m} \times 0.15 \text{ mm i.d.} \times 0.15 \mu\text{m}$  utilized connected to a nonpolar deactivated precolumn ( $1 \text{ m} \times 0.32 \text{ mm i.d.}$ ) was utilized. The MS with NCI mode using methane with purity 4.5 as the reagent gas and EI mode (70 eV) was operated in SIM mode.

## 3. Results and discussion

The selection of pesticides was performed according to their importance in agriculture. Thirty five pesticides that belong to different chemical classes were selected to fulfill the multiresidual character of the analysis. All the selected pesticides are considered being endocrine disruptors or they are suspected or tested for potential endocrine disrupting behaviour. Twenty nine pesticides were active also in NCI-MS mode. For both analytical methods (fast GC-EI-MS and fast GC-NCI-MS) the matrix-matched standard solutions were used to determine the selected validation parameters, the linearity range, LOD, LOQs and recovery rates.

### 3.1. Calibration

Linearity defines the ability of the method to obtain test results proportional to the concentration of analyte. To evaluate linearity, calibration curves were constructed for both analytical methods (fast GC-NCI-MS and fast GC-EI-MS). Matrix-matched standards were used to compensate for matrix effects. Nine concentration levels were used in the NCI mode ( $0.1\text{--}500 \text{ ng mL}^{-1}$  corresponding to the range of  $0.1\text{--}500 \mu\text{g kg}^{-1}$  in a real sample) and seven concentration levels in the EI mode ( $1\text{--}500 \text{ ng mL}^{-1}$  corresponding to the range of  $1\text{--}500 \mu\text{g kg}^{-1}$  in real sample). A list of studied pesticides, their retention times, SIM acquisition table for both NCI and EI mode and coefficients of determination ( $R^2$  squared correlation coefficient) for the investigated concentration range are given in Tables 1a and 1b. The ions monitored were divided into groups, with 3 to 15 ions in each group. Linearity of calibration curves constructed from absolute peak areas, expressed as  $R^2$ , was in the range of 0.9938–0.9999 except prochloraz in the NCI mode and 0.9711–0.9991 in the EI mode except

**Table 1a**

List of pesticides measured in EI mode, retention times, monitored ions, SIM group start times, data acquisition rate, and determination coefficients ( $R^2$ ) for matrix-matched calibration standards.

Pesticide	Retention time [min]	Monitored ions <sup>a</sup>	SIM group start time [min]	data acquisition rate [scans s <sup>-1</sup> ]	$R^2$
1 o-Phenylphenol	5.12	<b>170</b>	141	8.47	0.9972
2 Trifluralin	5.14	<b>306</b>	307		0.9983
3 Hexachlorobenzene	5.43	<b>284</b>	286	6.44	0.9991
4 Dimethoate	–	<b>87</b>	93	125	–
5 Atrazine	5.77	<b>200</b>	215	202	0.9813
6 Lindane	5.75	<b>181</b>	183	109	0.9500
7 Acetochlor	6.11	<b>146</b>	162	223	0.9875
8 Chlorpyrifos-methyl	6.13	<b>386</b>	288	125	0.9976
9 Vinclozolin	6.20	<b>212</b>	187	124	0.9965
10 Parathion-methyl	6.20	<b>263</b>	125	109	0.9896
11 Metribuzin	6.25	<b>198</b>	199	103	0.9907
12 Fenitrothion	6.42	<b>277</b>	125	260	0.9951
12 Linuron	6.47	<b>248</b>	160	61	0.9982
14 Malathion	6.41	<b>173</b>	127	93	0.9959
15 Chlorpyrifos	6.47	<b>197</b>	314	199	0.9999
16 Triadimefon	6.65	<b>208</b>	181	128	0.9999
17 Dicofof	6.68	<b>139</b>	251	253	0.9906
18 Fipronil	7.05	<b>367</b>	368	369	0.9749
19 Procymidone	7.00	<b>96</b>	283	285	0.9972
20 Triadimenol	7.05	<b>112</b>	168	128	0.8175
21 Folpet	–	<b>260</b>	104	262	–
22 Endosulfan-alfa	7.11	<b>241</b>	239	195	0.9711
23 Imazalil	7.54	<b>215</b>	173	217	0.9933
24 Myclobutanil	7.54	<b>179</b>	245	288	0.9972
25 Endosulfan-beta	7.59	<b>241</b>	239	195	0.9954
26 Chlordecone	7.70	<b>272</b>	274	270	0.9967
27 Tebuconazole	8.23	<b>250</b>	125	127	0.9970
28 Iprodione	8.39	<b>314</b>	316	187	0.9843
29 Bifenthrin	8.29	<b>181</b>	165	166	0.9888
30 Fenoxycarb	8.42	<b>116</b>	255	186	0.9849
31 Mirex	8.73	<b>272</b>	274	270	0.9987
32 Fenarimol	–	<b>139</b>	107	219	–
33 Prochloraz	9.31	<b>308</b>	310	266	0.9839
34 Cypermethrin	9.47	<b>163</b>	165	181	0.9790
35 Deltamethrin	10.23	<b>181</b>	253	251	0.9783

<sup>a</sup>Target ions are marked in bold.

**Table 1b**

List of pesticides measured in NCI mode, retention times, monitored ions, SIM group start times, data acquisition rate, and determination coefficients ( $R^2$ ) for matrix-matched calibration standards.

Pesticide	Retention time [min]	Monitored ions <sup>a</sup>	SIM group start time [min]	data acquisition rate [scans s <sup>-1</sup> ]	$R^2$
1 Trifluralin	4.98	<b>335</b>	336	6.65	0.9961
2 Hexachlorobenzene	5.18	<b>284</b>	286	282	0.9996
3 Dimethoate	5.41	<b>157</b>	158	159	0.9974
4 Lindane	5.44	<b>255</b>	257	253	0.9991
5 Chlorpyrifos-methyl	5.88	<b>212</b>	214	285	0.9996
6 Metribuzin	5.94	<b>198</b>	184	199	0.9983
7 Vinclozolin	5.91	<b>241</b>	243	245	0.9994
8 Parathion-methyl	5.95	<b>263</b>	154	264	0.9986
9 Fenitrothion	6.14	<b>277</b>	168	278	0.9983
10 Linuron	6.22	<b>157</b>	158	159	0.9986
11 Malathion	6.22	<b>248</b>	250	217	0.9885
12 Chlorpyrifos	6.23	<b>313</b>	315	214	0.9999
13 Triadimefon	6.38	<b>127</b>	166	129	0.9996
14 Dicofof	6.38	<b>250</b>	252	251	0.9938
15 Fipronil	6.61	<b>384</b>	366	331	0.9990
16 Procymidone	6.69	<b>283</b>	284	285	0.9985
17 Folpet	6.74	<b>146</b>	147	148	0.9991
18 Endosulfan-alfa	6.88	<b>406</b>	408	372	0.9997
19 Chlordecone	7.10	<b>383</b>	385	387	0.9996
20 Myclobutanil	7.14	<b>288</b>	290	289	0.9998
21 Endosulfan-beta	7.37	<b>406</b>	408	372	0.9998
22 Iprodione	7.99	<b>329</b>	331	301	0.9999
23 Bifenthrin	8.00	<b>386</b>	241	205	0.9999
24 Mirex	8.14	<b>368</b>	370	372	0.9910
25 Fenarimol	8.57	<b>276</b>	294	278	0.9996
26 Prochloraz	8.92	<b>377</b>	375	379	0.9687
27 Cypermethrin	9.18	<b>207</b>	209	171	0.9998
28 Deltamethrin	9.76	<b>297</b>	299	79	0.9999

<sup>a</sup>Target ions are marked in bold.

**Table 2**

Lowest calibration level (LCL), repeatability measurement (based on peaks areas,  $n = 6$ ) expressed as RSD, instrumental limit of detection (LOD, calculated as 3:1 S/N ratio from calibration measurements) and limit of quantification (LOQ, calculated as 10:1 S/N

No. Pesticide	EI mode				NCI mode			
	LCL [ng mL <sup>-1</sup> ]	RSD [%]	LOD [ng mL <sup>-1</sup> ]	LOQ [ng mL <sup>-1</sup> ]	LCL [ng mL <sup>-1</sup> ]	RSD [%]	LOD [ng mL <sup>-1</sup> ]	LOQ [ng mL <sup>-1</sup> ]
1 <i>o</i> -Phenylphenol <sup>a</sup>	1	8.3	0.196	0.654	–	–	–	–
2 Trifluralin	1	6.5	0.148	0.493	0.1	12	0.057	0.189
3 Hexachlorbenzene	1	11	0.411	1.370	0.1	12	0.028	0.093
4 Dimethoate	– <sup>b</sup>	–	–	–	0.1	9.3	0.046	0.154
5 Atrazine <sup>a</sup>	1	7.7	0.214	0.714	–	–	–	–
6 Lindane	1	4.8	0.286	0.952	5	4.0	0.010	1.650
7 Acetochlor <sup>a</sup>	5	12.1	2.778	9.259	–	–	–	–
8 Chlorpyrifos-methyl	1	17.1	0.469	1.563	5	5.1	0.016	2.618
9 Metribuzin	1	15	0.066	0.218	5	5.5	0.020	3.356
10 Vinclozolin	1	19	0.199	0.662	0.1	16	0.056	0.185
11 Parathion-methyl	1	10.8	0.252	0.840	5	6.2	0.004	0.708
12 Fenitrothion	5	15.9	1.056	3.521	5	1.0	0.003	0.495
13 Linuron	1	17.5	2.419	8.065	0.1	7.8	0.017	0.058
14 Malathion	1	5.2	0.224	0.746	0.1	8.8	0.008	0.028
15 Chlorpyrifos	1	5.1	0.144	0.481	0.1	12	0.029	0.095
16 Triadimefon	50	14	14.29	47.61	0.1	19	0.058	0.192
17 Dicofof	1	8.7	1.364	4.546	1	16	0.011	0.356
18 Fipronil	5	7.0	2.679	8.929	0.1	17	0.079	0.263
19 Procymidone	1	12	1.765	5.882	10	17	0.018	5.952
20 Triadimenol <sup>a</sup>	1	18	0.395	1.316	–	–	–	–
21 Folpet	– <sup>b</sup>	–	–	–	1	17	0.079	2.632
22 Edosulfan-alfa	1	11	0.025	0.084	0.1	13	0.094	0.313
23 Imazalil <sup>a</sup>	1	3.8	0.055	0.183	–	–	–	–
24 Myclobutanil	1	8.0	0.811	2.703	0.5	18	0.150	2.500
25 Endosulfan-beta	5	17	0.195	0.650	0.5	9.5	0.097	1.613
26 Chlordecone	1	13	0.144	0.479	50	19	0.035	58.82
27 Tebuconazole <sup>a</sup>	1	5.9	0.047	0.156	–	–	–	–
28 Iprodione	1	8.6	0.210	0.699	0.5	11	0.071	1.190
29 Bifenthrin	5	15	4.546	15.15	0.5	7.7	0.081	1.351
30 Fenoxycarb <sup>a</sup>	1	6.4	0.411	1.370	–	–	–	–
31 Mirex	1	12	0.682	2.273	10	11	0.004	1.337
32 Fenarimol	– <sup>b</sup>	–	–	–	0.01	8.7	0.019	0.010
33 Prochloraz	1	18	1.250	4.167	10	9.4	0.107	35.71
34 Cypermethrin	50	13	34.88	116.3	1	14	0.064	2.128
35 Deltamethrin	1	4.4	0.330	1.099	10	12	0.022	7.353

<sup>a</sup> Not detected in NCI.

<sup>b</sup> Not detectable.

triadimenol. Both ionization methods have a satisfactory linear range however, NCI is more sensitive. For the majority of EDC pesticides the LCLs were 0.1 ng mL<sup>-1</sup> (0.1 µg kg<sup>-1</sup>) for fast GC-NCI-MS and 1 ng mL<sup>-1</sup> (1 µg kg<sup>-1</sup>) for fast GC-EI-MS.

### 3.2. Limits of detection and limits of determinations

Instrument LODs and LOQs listed in Table 2 were calculated by the MS software from the signal to noise ratio (S/N) measured at the LCL (six replicates). Signal to noise ratio values of 3 and 10 were used for the calculation of LOD and LOQ, respectively. In the NCI mode, LODs were in the range from 0.003 to 0.150 ng mL<sup>-1</sup> (0.003–0.150 µg kg<sup>-1</sup> in real sample)

and LOQs were in the range of 0.010–35 ng mL<sup>-1</sup> (0.01–35.74 µg kg<sup>-1</sup> in real sample) for the majority of analytes under study. The repeatability of calculated LODs, LOQs, expressed as RSDs, was ≤20% in both EI and NCI mode. For some analytes the calculated LODs and LOQs are significantly lower than the LCLs used to construct the calibration curve. The obtained LOQs are well below the required MRLs and/or method LOQs determined as the lowest tested concentration at which recovery is in the range of 70–120% [6]. The values of  $R^2$ , LODs, LOQs and RSDs in the NCI mode are generally better compared to the EI mode. This is due to higher selectivity and sensitivity of NCI approach. The coupling with fast GC provided rapid analysis of pesticide residues at ultratrace concentration levels.

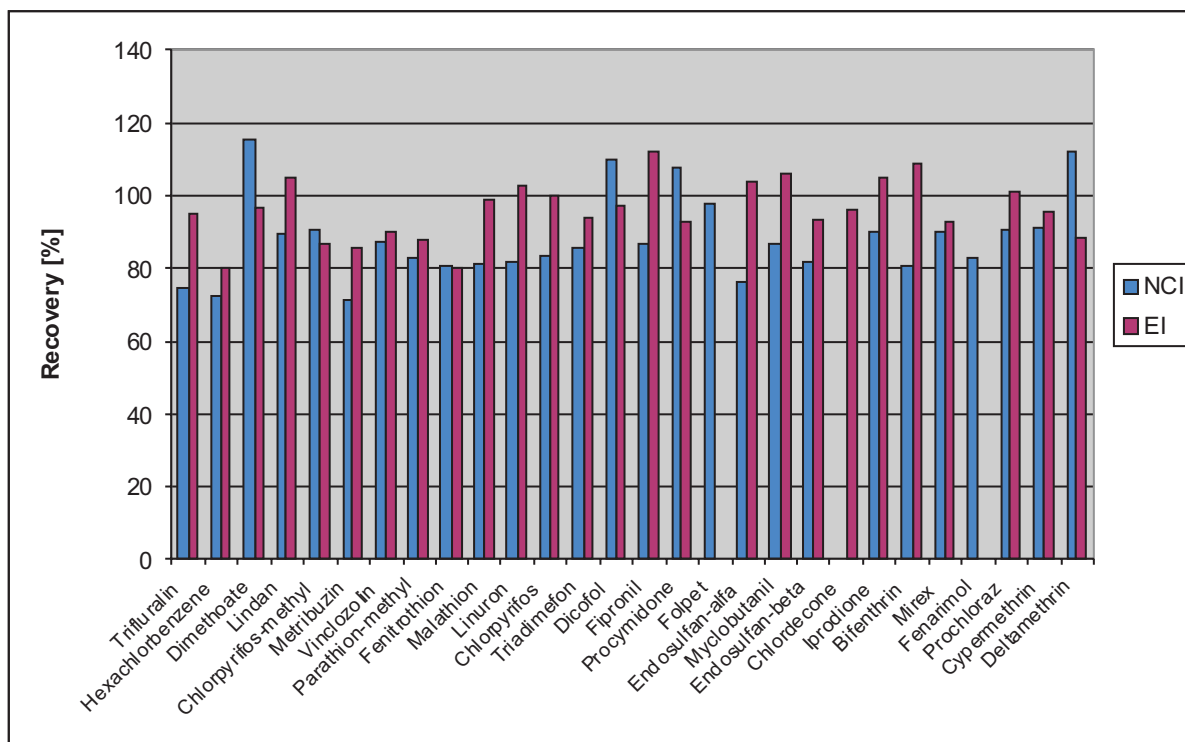


Fig. 1. Recovery of pesticides from spiked lemon sample at the concentration level of 10 µg kg<sup>-1</sup> in both EI and NCI mode.

3.3. Recovery

Trueness of the analytical method was evaluated in terms of recovery by spiking blank lemon matrix. Recovery rates were evaluated at 1, 5, 10 and 250 µg kg<sup>-1</sup> concentration levels in both EI and NCI experiments. Recoveries ranged from 70% to 120% with RSDs values ≤20% for the tested compounds at the concentration levels which are higher or equal to the LCLs, except for folpet, fenarimol in EI mode. The EU criterion [6] concerning recovery rates was fulfilled at studied concentration levels. For illustration, comparison of recovery at the selected concentration

level of 10µg kg<sup>-1</sup> is shown in Figure 1 for both ionization modes.

3.4. Real sample analysis

To demonstrate the applicability of the fast GC-MS method the analysis of real sample with high acid content was performed. Three pesticides were determined: *o*-phenylphenol (1.16 mg kg<sup>-1</sup>), imazalil (8.05 mg kg<sup>-1</sup>) and prochloraz (0.046 mg kg<sup>-1</sup>). Chromatogram of real sample analysis is presented in Figure 2. Determined concentration of *o*-phenylphenol and prochloraz were under EU MRL values

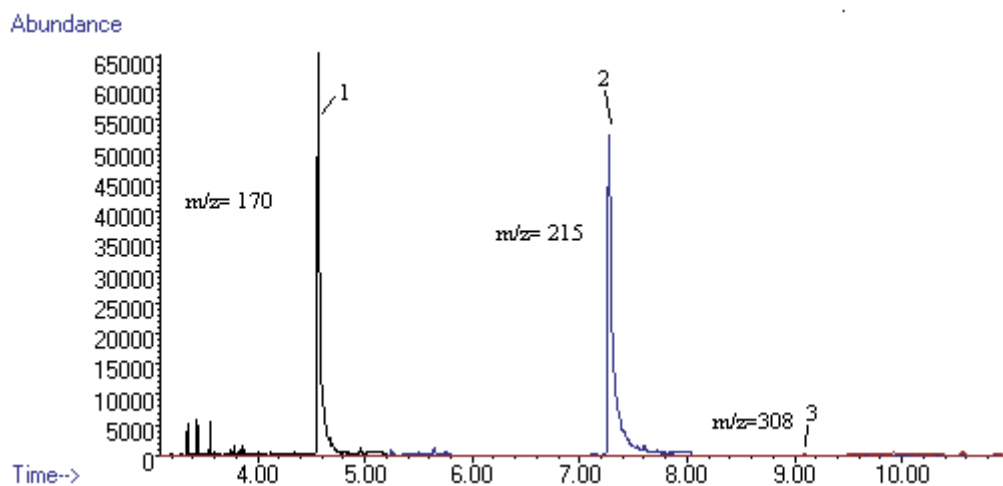


Fig. 2. Selected ion monitoring mode chromatogram of separation of the pesticides from a lemon real sample in NCI mode: (1) *o*-phenylphenol, (2) imazalil, (3) prochloraz.

(MRL for *o*-phenylphenol was 12 mg kg<sup>-1</sup> and for prochloraz was 10 mg kg<sup>-1</sup> in citrus matrices). In the case of imazalil the EU MRL value (5 mg kg<sup>-1</sup>) was exceeded. To prove the exceeded value, the sample analysis with standard addition of imazalil was performed.

#### 4. Conclusions

Fast GC-MS in EI and NCI mode were used for determination of ultra trace levels of endocrine disrupting pesticide residues in lemon matrices. The NCI mode has provided high values of coefficient of determination for calibration measurements of matrix-matched standard, significantly higher selectivity and sensitivity compared to EI mode owing to less interferences of background. Recovery rates and further validation parameters at different concentration level were determined. GC-MS in NCI mode was applied to the analysis of pesticide residues in real lemon samples, even three different pesticides exhibiting endocrine disrupting activity were determined.

#### Acknowledgement

This work was supported by the Slovak Grant Agency (project VEGA No. 1/0390/09).

#### References

- [1] [http://europa.eu/legislation\\_summaries/other/113007-c\\_en.htm](http://europa.eu/legislation_summaries/other/113007-c_en.htm)
- [2] *The Background and the Need for Change*. <http://www.pesticides.gov.uk/environment.asp?id=1523>. The Pesticides Safety Directorate. York. United Kingdom.
- [3] Careri M., Bianchi F., Corradini C.: *J. Chromatogr. A* **970** (2002), 364.
- [4] Anastassiades M., Lehotay S. J., Štajnbaher D., Schenck F. J.: *J. AOAC Int.* **86** (2003), 421–431.
- [5] Kirchner M., Hůšková R., Matisová E., Mocák J.: *J. Chromatogr. A* **1186** (2008), 271–280.
- [6] *Method Validation and Quality Control Procedures for Pesticide Residues Analysis in Food and Feed*. European Commission document SANCO/2007/3131. Brussels, 2007.

# Acrylamide Analysis in Various Matrices Employing HPLC-MS/MS and UHPLC-TOF MS

VERONIKA BARTACKOVA, ONDREJ LACINA, KATERINA VALENZOVA, KATERINA RIDDELLOVA, JANA HAJŠLOVA

Department of Food Chemistry and Analysis, Institute of Chemical Technology Prague, Technická 3, 166 28 Prague 6-Dejvice, Czech Republic, ✉ veronika.bartackova@vscht.cz

## Abstract

Occurrence of acrylamide in heat processed foodstuffs represents an issue of health concern. To monitor levels of this processing contaminant in various matrices (potato or cereal based products, coffee, etc.), reliable analytical methods are needed. Currently, the most routinely used technique for acrylamide determination is high performance liquid chromatography coupled to tandem in space mass spectrometry (HPLC-MS/MS). Typically, relatively laborious sample preparation procedure employing two-step solid phase extraction is used prior to instrumental analysis.

Our significantly simplified sample preparation procedure based on QuEChERS approach employs (i) addition of acetonitrile to primary aqueous extract, and (ii) induction of phase separation by addition of salts. Isotope dilution technique ( $^{13}\text{C}_3$ -acrylamide as an internal standard) is employed to compensate both potential losses of analyte and matrix-induced chromatographic response enhancement. The QuEChERS approach was compared to a typical analytical procedure consisting of the clean-up step employing solid-phase extraction (SPE). As it will be shown in the results section, in the case of complicated matrices (beer), the SPE clean-up is a necessary step for acrylamide determination.

Two alternative MS systems were tested in our study. In addition to a well established HPLC-MS/MS method, acrylamide analyses were also performed using an UHPLC-TOF MS system. Comparable or even better results (LOQs, repeatability) were obtained by the later approach.

## Keywords

acrylamide  
HPLC-MS/MS  
UHPLC-TOF MS

## 1. Introduction

Acrylamide, classified as a probable human carcinogen (IARC, 1994) [1], is mainly formed during Maillard reaction in starch-rich foods. The occurrence of this hazardous chemical in human diet was for the first time reported by Swedish scientists in 2002 when, consequently, a worldwide research has been started to study this substance. [2]. The findings resulted in a need for the development of an analytical procedure that can be routinely use in control of the levels of this processing contaminant in a wide range of various food matrices. Currently, acrylamide is monitored in the European Union member's states according to the European Commission Recommendation from the 3rd of May, 2007 (2007/331/EC), this recommendation will be soon replaced by a new version from the 2nd of June 2010 (2010/307/EU) [3, 4].

Nowadays trend in most of laboratories [5, 6] is to employ liquid chromatography mass spectrometry (LC-MS) for the analysis of underivatized acrylamide in food samples. To obtain acceptable LODs of these LC based techniques, it is essential to use a tandem-in-space mass analyzer (MS/MS) for the determinative

step, typically a triple quadrupole instrument [7–13]. The use of tandem MS also overcomes the fact that the molecular ion ( $m/z = 72$ ) formed during ionization in LC-MS does not allow a selective detection. The required clean-up steps for LC-MS based techniques often employ solid-phase extraction (SPE). In majority cases, combination of two or three SPE cartridges (e.g., Oasis HLB, Isolute MM, MAX, MCX, ENV+) has to be employed for purification of crude extracts prior to the determinative step [7, 11, 14]. Another approach uses a modified sample preparation procedure, known from the analysis of pesticide residues in produce samples, which is called QuEChERS (quick, easy, cheap, effective, rugged, and safe) [15].

The aim of our study was to develop a method employing modified QuEChERS sample preparation procedure with an UHPLC-TOF MS determinative step, and its comparison to a well established, routinely used HPLC-MS/MS instrumental analysis. Further simplification of acrylamide analysis was the main objective of our work. Use of UHPLC chromatographic separation entails both, better resolution within a shorter time and higher analytical selectivity. When coupled to a TOF MS detector

(time-of-flight mass spectrometer), an UHPLC chromatographic system represents a simple (no derivatization required) and rapid analytical approach with high sample throughput.

## 2. Experimental

### 2.1. Chemicals and Materials

Acrylamide (CAS 79-06-1, purity 99.5%) and magnesium sulphate (p.a., purity  $\geq 98\%$ ) were from Sigma-Aldrich (Germany).  $^{13}\text{C}_3$ -Acrylamide (isotopic purity  $\geq 99\%$ ) was purchased from CIL (USA). Sodium chloride was from Penta (Czech Republic). Aluminium oxide (basic) was from Merck (Germany). Acetonitrile and *n*-hexane were of HPLC grade quality and were supplied by Sigma-Aldrich (Germany) and Merck (Germany), resp. Demineralized water was obtained from a Millipore apparatus (Billerica, MA, USA). Isolute Multimode<sup>®</sup> and Isolute ENV+<sup>®</sup> SPE cartridges were purchased from IST (UK).

Calibration standard solutions in concentration range 1–250 ng mL<sup>-1</sup> with fixed amount of  $^{13}\text{C}_3$ -acrylamide (100 ng mL<sup>-1</sup>) were prepared in water by dilution of acrylamide stock standard solution.

### 2.2. Optimized Sample Preparation Procedure

Various food matrices: The key step of the method used is the transfer of acrylamide from the primary aqueous extract into acetonitrile forced by added salts (MgSO<sub>4</sub> and NaCl); separation of aqueous and organic phase is thus induced [3]. Most matrix interferences are then removed from organic phase by dispersive SPE (MgSO<sub>4</sub> and basic Al<sub>2</sub>O<sub>3</sub> are used for this purpose). Acetonitrile is evaporated under a gentle stream of nitrogen and solvent is exchanged to water.

Beer samples: After decarbonisation (sonication), the beer sample undergoes a two-step clean-up using two SPE cartridges. Final extract is in 60% methanol in water (v/v solution), from which methanol is evaporated by a gentle stream of nitrogen [4].

### 2.3. Instrumentation

#### 2.3.1. HPLC-MS/MS

Alliance 2695 LC system (Waters, USA) coupled to Mass spectrometer Quattro Premier XE (Waters/Micromass, USA/UK) were used for experiments.

Chromatographic separation was carried out using Atlantis<sup>®</sup> T3 analytical column (150 mm × 3 mm;

3 μm). Isocratic elution of acrylamide was achieved with mobile phase composed of acetonitrile and water (2 : 98, v/v), flow rate 0.3 mL min<sup>-1</sup>.

The mass spectrometer, equipped with electrospray interface (ESI), was operated in positive ionisation mode. Two transitions at unit resolution were monitored for acrylamide:  $m/z$  72 → 55 and  $m/z$  72 → 54 and one transition for  $^{13}\text{C}_3$ -acrylamide (internal standard):  $m/z$  75 → 58.

#### 2.3.2. UHPLC-TOF MS

Acquity<sup>™</sup> UPLC (Waters, USA) coupled to LCT Premier XE time-of-flight Mass spectrometer (Waters/Micromass, USA/UK) were used for experiments.

Chromatographic separation was carried out using Acquity<sup>™</sup> UPLC HSS T3 analytical column (100 × 2.1 mm; 1.8 μm). Isocratic elution of acrylamide was achieved with mobile phase composed of acetonitrile and water (2:98, v/v), flow rate 0.3 mL min<sup>-1</sup>.

UHPLC system was connected to an orthogonal accelerated time-of-flight mass spectrometer operated in positive (ESI+) electrospray ionisation mode. Raw mass spectra were acquired in the  $m/z$  range from 50 to 600.

## 3. Results and Discussion

### 3.1. Developed Methods

Both developed analytical methods were evaluated within a validation study involving following matrices: potato chips, crispbread, gingerbread, biscuits, chocolate, baby food, breakfast cereals, muesli and spice. The results of the study are described in paragraph 3.2 and summarised in Tab. 1. Examples of chromatographic records are shown in Fig. 1.

Since transfer of acrylamide from raw material (malt) into beer may occur, we also analysed beer samples. When using extraction technique QuEChERS for beer or lyophilised beer, it was not possible to detect any acrylamide due to chemical noise. In the next step, we involved double SPE clean-up step to remove matrix impurities more efficiently. Under these conditions acrylamide could be conveniently detected and the method fully validated. Chromatogram of beer sample is shown in Fig. 2.

### 3.2. Performance Characteristics

The tested concentration range of calibration standards (1–250 ng mL<sup>-1</sup>) corresponds to acrylamide

**Table 1**

Performance characteristics of HPLC-MS/MS and UHPLC-TOF MS methods, various food matrices.

Matrix	AA ( $\mu\text{g kg}^{-1}$ ) / RSD (%)		Recovery (%)	
	$n = 6$		$100 \mu\text{g kg}^{-1} / 1000 \mu\text{g kg}^{-1}$ $n = 4$	
	HPLC-MS/MS	UHPLC-TOF MS	HPLC-MS/MS	UHPLC-TOF MS
Biscuits	14/4	24/4	105/104	94/94
Chocolate	<LOD/ <i>n.a.</i>	<LOD/ <i>n.a.</i>	101/101	100/99
Baby food	44/5	52/5	101/101	95/95
Breakfast cereals	131/5	133/4	100/100	97/97
Potato chips	759/3	717/2	108/109	91/98
Muesli	53/7	55/3	110/106	97/97
Gingerbread	269/6	251/5	108/102	100/99
Spice paprika	571/7	538/7	<i>n.a.</i> /96	<i>n.a.</i> /93
Spice pepper	527/6	488/5	<i>n.a.</i> /104	<i>n.a.</i> /103
Crisp bread	188/6	185/1	<i>n.a.</i> /97	<i>n.a.</i> /95

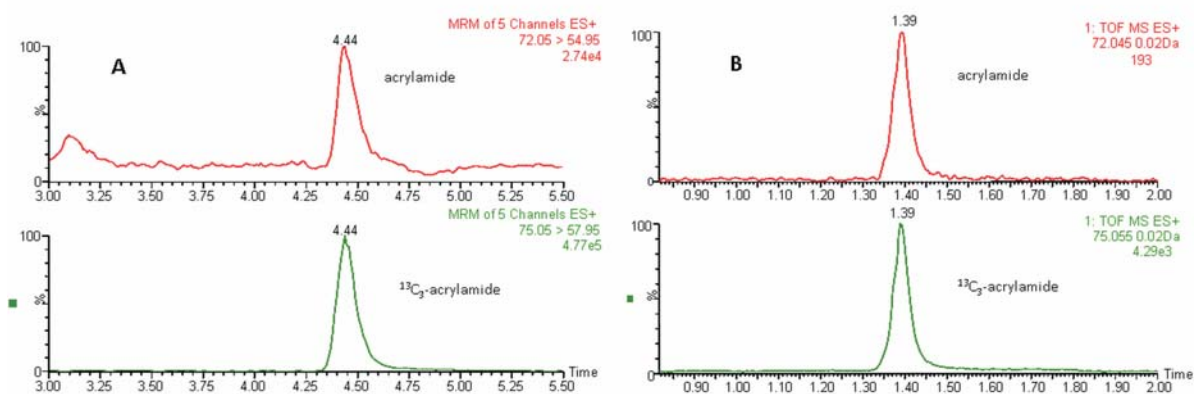


**Fig. 1.** Analysis of acrylamide in baby food: (A) HPLC-MS/MS, acrylamide level  $53 \mu\text{g kg}^{-1}$  monitored transitions  $72 \rightarrow 55$ ,  $75 \rightarrow 58$ , (B) UHPLC-TOF MS, acrylamide level  $55 \mu\text{g kg}^{-1}$ , under conditions of 0.02 Da mass window settings for extraction of target ions.

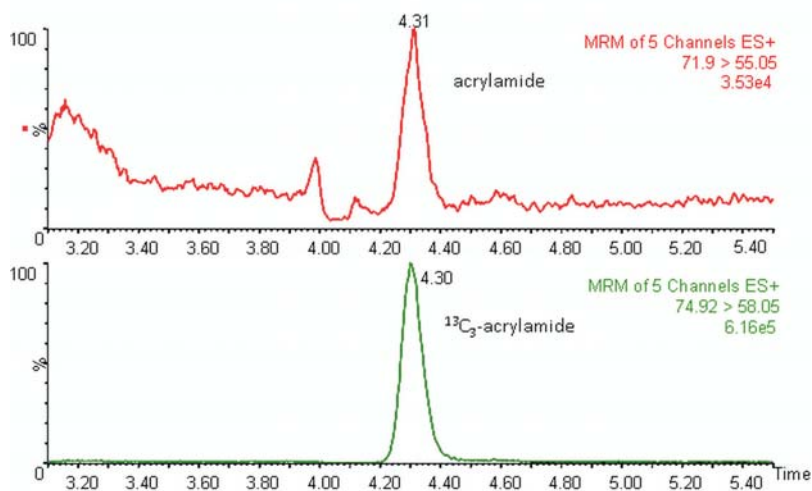


**Fig. 2.** HPLC-MS/MS analysis of acrylamide in dark beer ( $10 \mu\text{g L}^{-1}$ ), monitored transitions, unit resolution.

**Table 2**

Performance characteristics of HPLC-MS/MS and UHPLC-TOF MS methods, beer samples

Matrix	AA ( $\mu\text{g L}^{-1}$ ) / RSD (%)		Recovery (%)	
	$n = 6$		$10 \mu\text{g L}^{-1} / 20 \mu\text{g L}^{-1}$ $n = 6$	
	HPLC-MS/MS	UHPLC-TOF MS	HPLC-MS/MS	UHPLC-TOF MS
Beer	10/4	12/4	106/98	100/94

**Table 3**External quality control of data generated by both instrumental techniques: results of acrylamide analysis obtained in FAPAS<sup>®</sup> proficiency tests.

Matrix	Assigned value ( $\mu\text{g kg}^{-1}$ )	HPLC-MS/MS value ( $\mu\text{g kg}^{-1}$ )	UHPLC-TOF MS value ( $\mu\text{g kg}^{-1}$ )	HPLC-MS/MS z-score	UHPLC-TOF MS z-score
Breakfast cereals	65.8	71.0	66.4	0.4	0.0
Crisp bread	1179	1457	939	1.5	-1.3
Crisp bread	101	114	89	0.6	-0.5
Crisp bread	862	846	684	-0.1	-1.3

levels from 10 to 2500 g per kg of sample. The relative response of acrylamide to internal standard is linear within this range, with typical correlation coefficient  $R^2 = 0.9999$  for both techniques.

Precision of the methods was characterized as relative standard deviation (RSD), which was calculated from six repetitive analyses of tested samples. The obtained results, which are presented in Tab. 1 and 2, ranged between 1–7 %, depending on food matrix and extraction technique.

Isotopically labelled internal standard ( $^{13}\text{C}_3$ -acrylamide) effectively compensates for variability in acrylamide partitioning (100 % relative recovery) and signal suppression in LC-MS analysis. The trueness was firstly characterized as the recovery of acrylamide, which was calculated from four repetitive analyses of samples containing acrylamide. These samples were further spiked with acrylamide to reach a level of 100 and 1000  $\mu\text{g kg}^{-1}$ . Achieved recoveries of acrylamide were between 91–110% (see Tab. 1 and 2) depending on the examined food matrix, extraction technique and spiking level. Secondly, the trueness was characterized by the analyses of reference materials with known acrylamide levels (samples from interlaboratory tests FAPAS<sup>®</sup>, Food Analysis Performance Assessment Scheme). The results of analyses of these samples are shown in Tab. 3. All measured values would meet the desired  $Z$ -score  $\leq |2|$ .

The estimations of the limit of quantifications (LOQs) in all tested matrices were approximately 30  $\mu\text{g kg}^{-1}$  for the QuEChERS extraction. The limit of quantification of the validated method for acrylamide determination in beer (two-step SPE clean-up) was 5  $\mu\text{g L}^{-1}$ . It is necessary to emphasize that LOD and

LOQ are dependent on the actual instrument condition, the values here presented thus are approximate only.

#### 4. Conclusions

Modified QuEChERS method employing basic  $\text{Al}_2\text{O}_3$  for dispersive solid phase extraction has been demonstrated as an efficient clean-up strategy in acrylamide analysis in various matrices. The determination of acrylamide in such complicated matrix as beer represents the only exception. In this case it is necessary to use a two-step SPE clean-up to obtain satisfactory results.

Simplification and acceleration of acrylamide analysis was the main objective of our study. A progressive analytical approach using UHPLC-TOF MS determinative step has been developed and compared to an HPLC-MS/MS based method. Comparable or even better results (LOQs, repeatability) were obtained with the new instrumental approach. Besides of that, the main advantage of the UHPLC-TOF MS method is higher sample throughput compared to the commonly used HPLC-MS/MS method.

#### Acknowledgements

This study was carried out with the support from The Ministry of Education, Youth and Sports, Czech Republic: (i) project MSM 6046137305; (ii) project NPV II. n. 2B06168.

#### References

- [1] IARC Acrylamide. In: *Monographs on the evaluation of carcinogenic risks to humans – Some industrial chemicals*, IARC, Lyon, 1994, 60, 389–433.
- [2] *Acrylamide in food – Mechanisms of formation and influencing factors during heating of foods*. Report from Swedish Scientific Expert Committee, 2002.

- [3] European Commission Recommendation from the 3rd of May, 2007 (on the monitoring of acrylamide levels in food; 2007/331/EC).
- [4] European Commission Recommendation from the 2nd of June 2010 (on the monitoring of acrylamide levels in food; 2010/307/EU).
- [5] Zhang Y., Zhang G., Zhang Y.: *J. Chromatogr. A* **1075** (2005), 1–21.
- [6] Wenzl T., De La Calle M. B., Anklam E.: *Food Addit. Contam.* **20** (2003), 885–902.
- [7] Rosén J., Hellenäs K. E.: *Analyst* **127** (2002), 880–882.
- [8] Roach J.A.G., Andrzejewski D., Gay M.L., Nortrup D., Musser S.M.: *J. Agric. Food Chem.* **51** (2003), 7547–7554.
- [9] Riediker S., Stadler R.H.: *J. Chromatogr. A* **1020** (2003), 121–130.
- [10] Becalski A., Lau B.P.Y, Lewis D., Seaman S.W.: *J. Agric. Food Chem.* **51** (2003), 802–808.
- [11] Tareke E., Rydberg P., Karlsson P., Eriksson S., Törnqvist M.: *J. Agric. Food Chem.* **50** (2002), 4998–5006.
- [12] Hoenicke K., Gatermann R., Harder W., Hartig L.: *Anal. Chim. Acta* **520** (2004), 207–215.
- [13] Ono H., Chuda Y., Ohnishi-Kameyama M., Yada H., Ishizaka M., Kobayashi H., Yoshida M.: *Food Addit. Contam.* **20** (2003), 215–220.
- [14] Gökmen V., Şenyuva H.Z., Acar J., Sarioğlu K.: *J. Chromatogr. A* **1088** (2005), 193–199.
- [15] Mastovska K., Lehotay S.J.: *J. Agric. Food Chem.* **54** (2006), 7001–7008.

# Combination of Microchip Electrophoresis, Contactless Conductivity Detection and Headspace Single Drop Microextraction for the Determination of Aliphatic Amines in Seafood Samples

JONAS BLOEDT, A. KUMAR, FRANK-MICHAEL MATYSIK

*Institute of Analytical Chemistry, Chemo- and Biosensors, University of Regensburg, D-93040 Regensburg, Germany, ✉ jonas.bloedt@chemie.uni-r.de*

## Keywords

aliphatic amines  
contactless conductivity detection  
microchip electrophoresis  
microextraction  
seafood

Various volatile aliphatic amines are the reason for the typical fishy odor developing upon biodegradation of seafood tissue and are often responsible for toxic symptoms associated with fish or shrimp consumption [1]. The monitoring of this process can prove to be important in the quality control of seafood. Efficient control of amine levels in remote places requires simple, portable, fast and reliable analytical methods [2]. We have developed a method for the separation and determination of volatile aliphatic amines in complex sample matrices using a combination of headspace single drop microextraction (HS-SDME), microchip electrophoresis and capacitively coupled contactless conductivity detection ( $C^4D$ ). The separations are carried out with PMMA chips with integrated gold  $C^4D$  electrodes for contactless conductivity detection. The chip is inserted into a portable and compact device (ChipGenie) which contains all relevant components, like high voltage power supply or detection electronics, needed for the determination of charged analytes.

The device can be connected via USB to a personal computer and the data are analyzed with the corresponding LabView software. To avoid interferences by complex sample matrices, the ultrasound-assisted headspace single drop microextraction (HS-SDME) is used. Ultrasonic radiation is applied to the sample solutions (alkaline conditions) and the volatile amines are transferred from the solution into a 5  $\mu$ L drop of separation buffer (His/MES, pH 6) which is exposed at the end of a microlitre syringe (head space). The pre-concentrated samples are transferred into the chip sample reservoir, diluted and inserted with the chip into the ChipGenie system. By this means, five

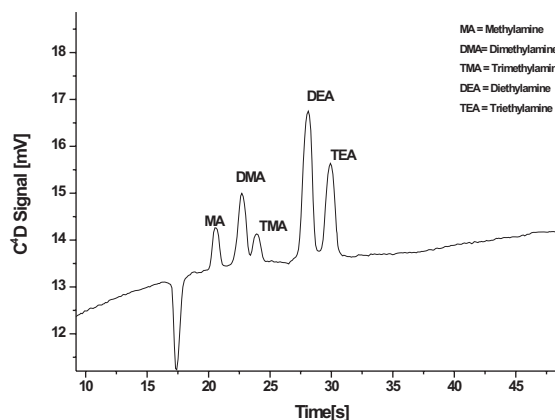


**Fig. 1.** Representative electropherogram for the separation of five volatile aliphatic amines (concentration: 3 ppm) using a PMMA microchip with  $C^4D$  detection. The determination was carried out at a separation voltage of 3.8 kV and was achieved in less than 35 second.

volatile amines (methylamine, dimethylamine, trimethylamine, diethylamine and triethylamine) are separated in less than 35 seconds at a separation voltage of 3.8 kV. In the course of the studies all relevant parameters, like separation voltage, buffer pH, detection voltage, extraction time, were optimized and applied to the real samples. Finally, the development of volatile amines resulting from improper storage of fish or shrimp samples could be studied.

## References

- [1] Wootton M., Jansen S., Wills R. B.: *J. Sci. Food. Agric.* **49** (1989), 503–506.
- [2] Vandaveer W. R., Pasas-Farmer S., Fischer D. J., Lunte S. M.: *Electrophoresis* **25** (2004), 3528–3549.

# Development and Optimization of New Microextraction Technique for Determination of Environmental Pollutants by Gas Chromatography

MIROSLAVA BURSOVÁ, RADOMÍR ČABALA

Department of Analytical Chemistry, Faculty of Science, Charles University in Prague,  
Albertov 6, 128 43 Prague 2, Czech Republic, ✉ bursova.mirka@seznam.cz

## Abstract

A new microextraction technique was developed as an alternative method for preconcentration and determination of some environmental pollutants in aqueous samples. The microextraction technique was off-line coupled with fast gas chromatography with flame ionization detector (fast GC-FID). The effects of different experimental parameters on the extraction efficiency were studied simultaneously using the collection of statistical methods called response surface methodology. The selected analytes cover a broad polarity range: toluene, ethylbenzene, mesitylene, phenol, nitrobenzene, *n*-octanol, naphthalene, dimethylphthalate and methylhexadecanoate. The variables of interest in the microextraction process were volume of extraction solvent (heptane), effect of salt addition, stirring rate, diameter of extraction vial and extraction time. A Plackett-Burman design was used for screening of variables in order to determine the significant variables that affect extraction efficiency and the obtained significant factors were optimized by using a central composite design. The quadratic model (equation) was built for the used system to include the possible curvature of the response surface and the mutual interactions among the experimental parameters. The optimum experimental conditions were determined as: extraction time 16 min, volume of extraction solvent (heptane) 115  $\mu$ l, stirring rate 850 rpm, diameter of extraction vial 1.9 cm and addition of 1.24 g of sodium chloride. The experimentally measured response under optimized conditions reached 102% of the predicted one which fact demonstrates very good agreement between the proposed model and real system and the validity of selected model presumptions.

## Keywords

fast GC  
liquid-liquid microextraction  
response surface methodology

## 1. Introduction

The term optimization has been commonly used in analytical chemistry as a means of discovering conditions at which to apply a procedure that produced the best possible response [1]. In order to improve the optimization of analytical procedures multivariate statistical techniques has been carried out, namely, response surface methodology. Response surface methodology is a collection of mathematical and statistical techniques based on the fit of a polynomial equation to the experimental data, which must describe the behavior of a data set with the objective of making statistical prevision [2].

The main step in the successful utilization of microextraction is selection of experimental conditions that can provide acceptable response at low analyte concentration. The following points are considered essential in the conduct of simple chemometric optimization [2].

### 1) Definition of the problem and selection of the appropriate variables and responses.

The selected experimental parameters are listed in the abstract. As the analytical response, either the peak areas of single analytes or the sum of peak areas of all analytes measured are used.

### 2) Screening studies

Reduced factorial designs are commonly recommended for the screening to limit the large number of experimental parameters to be optimized. The Plackett-Burman design was used which assume that the interactions among the parameters can be completely ignored at this stage, so, the main effects on the analytical response are evaluated with a reduced number of experiments [3, 4].

### 3) Choice of design of experiment

The choice of design of experiment (plan of experiments) is quite difficult step because there are several possibilities (Box-Behnken design, Doehlert design,

full three-level factorial design or central composite design) [2–4]. As the most suitable the central composite design (CCD) was chosen because it involves three mostly used ones: two-level full factorial, fractional factorial and star design [2, 5].

#### 4) *Mathematical model fitting*

In this step coefficients of polynomial equation which describes the dependence of the selected response on the experimental parameters are evaluated. In contrast to the screening step, possible interactions among the main parameters and squares of experimental parameters are included owing to possible curvature of the response surface of the mathematical model.

#### 5) *Model adequacy checking*

#### 6) *Analysis of model and effect estimates*

Commonly, points 5 and 6 are implemented within the statistical software used.

#### 7) *Allocation of the optimum*

The Derringer method (desirability function) was used for allocation of the optimal conditions and compromise between variables of the microextraction [2].

#### 8) *Robustness checking* [5]

## 2. Experimental

### 2.1. *Chemicals and Solvents*

Ethylbenzene, nitrobenzene, n-octanol and dimethylphthalate (all 99%) were purchased from Aldrich (Steinheim, Germany). Toluene and phenol (both p.a.) were purchased from Lachema (Neratovice, CZ) and mesitylene (99 %) was obtained from Fluka (Denmark, Germany). The internal standard in extraction solvent (methylhexadecanoate) was provided by Theta (USA). NaCl (p.a.) was obtained from Lach-Ner (Neratovice, CZ). Methanol (p.a., Lachema) and heptane (99.5%, Fluka) were used as solvents. Water was purified using a Mille-Q Plus (Millipore, Billerica, MA, USA).

### 2.2. *Stock Solutions*

The stock solution (10 ml) of mixture of analytes was prepared in methanol at concentration 1 mg mL<sup>-1</sup> of each analyte. Heptane and methylhexadecanoate (100.2 µg mL<sup>-1</sup>) were used as the extraction solvent and as the internal standard, respectively. All stock solutions were stored at 4 °C.

### 2.3. *GC Instrumentation*

Analyses were performed on a GC-2010 gas chromatograph (Shimadzu) with FID. Separation was performed on a 9.7 m × 0.15 mm i.d. Chromacol CP-Sil 5CB capillary column coated with 5% diphenyl-95 % dimethyl-polysiloxane (0.12 µm).

The fast-GC temperature program was: 40 °C (1 min), at 50 °C min<sup>-1</sup> to 100 °C, at 100 °C min<sup>-1</sup> to 250 °C (1 min).

The carrier gas (hydrogen, 4.0, Linde, CZ) flow rate was in constant flow mode at 70 cm s<sup>-1</sup>. The temperature of detector and injector was 300 °C. Nitrogen (5.0) and synthetic air for GC were from Linde, Czech Republic.

The GC Solutions program (Shimadzu), ver. 2.30. was used for acquisition and data evaluation. The program Microcal Origin (OriginLab, USA) was used for graphical presentation of measured data.

The new microextraction technique is being applied for the patent therefore no details could be presented at the moment.

### 2.4. *Statistical Software*

The data and experimental design were processed by statistical program NCSS 2004 (Number Cruncher Statistical Systems, Kaysville, Utah, USA), Design Expert (ver. 8.0.10., Stat-ease, Inc., Minneapolis, USA) and Minitab 16 (Minitab Inc., State College PA, USA).

## 3. Results and Discussion

### 3.1. *Screening Design*

Five experimental parameters, extraction time, volume of extraction solvent, stirring rate, diameter of extraction vial and addition of salt, were selected in order to obtain the optimum conditions for the microextraction procedure and their low and high values are listed in Table 1. The Plackett-Burman design was used for screening of these variables. The overall design matrix contained eight runs in duplicate

**Table 1**

The experimental variables and their levels in the Plackett-Burman design.

Factor	Low (-1)	High (+1)
1 Stirring rate [rpm]	500	850
2 Extraction volume (heptane) [µL]	100	300
3 Weight of sodium chloride [g]	0	2
4 Extraction time [min]	5	20
5 Dummy 1	-1	+1
6 Diameter of vial [cm]	1.9	2.7
7 Dummy 2	-1	+1

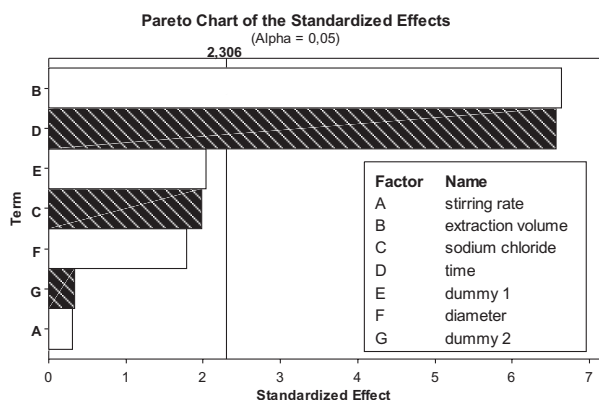


**Fig. 1.** Standardized main effect Pareto chart for the Plackett-Burman design. Vertical line in the chart defines 95% confidence level.

which are carried out randomly to nullify the effect of extraneous or nuisance factors. The analysis of variance was used to evaluate the data and statistically significant effects are determined using *t*-test (95% probability) [5] and the normalized results are reviewed in Pareto chart (Fig. 1) [5]. According to Fig. 1, the volume of heptane was the most significant variable having the highest effect on the extraction efficiency of all analytes, followed by the extraction time. The salt effect showed non-significant effect on overall extraction efficiency, but it showed significant effect for some separate analytes and therefore it was added to the following procedure. Stirring rate, diameter of vial had no significant effects on the extraction efficiency. The stirring rate of 850 rpm and the extraction vial with diameter 1.9 cm were held constant.

Based on first screening study three variables (extraction time, extraction volume of solvent and salt effect) were used for next part of response surface methodology.

### 3.2. Central Composite Design

The resulting significant variables were used in the central composite design (CCD) for investigation of their interaction and their examined levels are listed in Table 2. This design permitted the response to be modeled by fitting a second-order polynomial equation. The design consists of a factorial design with star points located at  $+α$  and  $-α$  from the center

**Table 2**

The experimental variables, their levels and star points in the central composite design.

Factor	$-α (-1.68)$	-1	0	+1	$+α (+1.68)$
Extraction time [min]	16	20	25	30	34
Extraction volume (heptane) [μl]	115	150	200	250	285
Weight of sodium chloride [g]	0.07	0.8	1.8	2.8	3.53

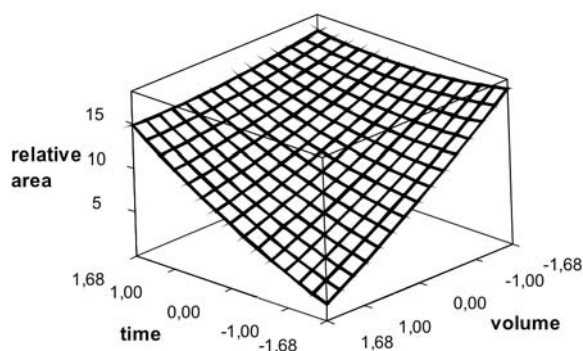


**Fig. 2.** Response surface plot for the extraction solvent volume versus the extraction time for the total relative area (the addition of sodium chloride was 1.8 g).

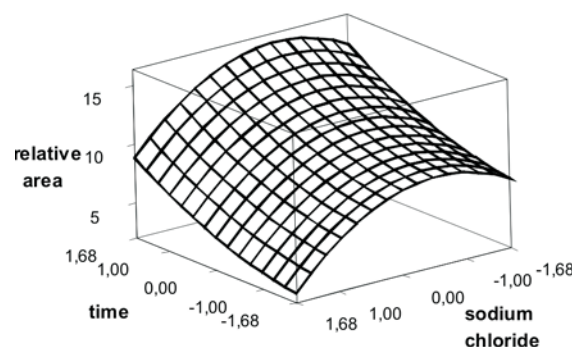


**Fig. 3.** Response surface plot for the extraction time versus the salt effect for the total relative area (the extraction volume was 200 μL).

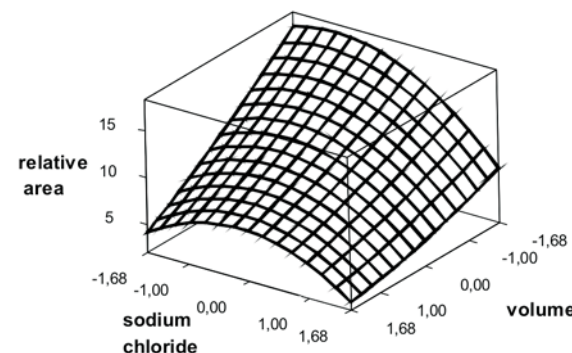


**Fig. 4.** Response surface plot for the solvent extraction volume versus the salt effect for the total relative area (the extraction time was 25 min).

of the experimental domain in order to fulfill the rotatability condition of the CCD [3–6]. The overall design matrix consists of 20 runs (8-factorials, 6-central and 6-star experiments). The results of experiments were evaluated by ANOVA test and

**Table 3**

The parameters of second-order polynomial equation from the central composite design.

Parameter		Value
Intercept	$\beta$	11.62
Time	$x_1$	1.79
	$x_1^2$	— <sup>a</sup>
Volume	$x_2$	−2.62
	$x_2^2$	— <sup>a</sup>
Salt	$x_3$	−1.52
	$x_3^2$	−1.41
Time × volume	$x_1 \times x_2$	1.22
Time × salt	$x_1 \times x_3$	— <sup>a</sup>
Volume × salt	$x_2 \times x_3$	— <sup>a</sup>
Coefficient of determination	$R^2$	0.8807

<sup>a</sup> Not significant.

a second-order polynomial regression model (Table 3) was used to calculate the response surface for each variable separately (Figs. 2–4). Figure 2 shows the response surface obtained by plotting the extraction solvent volume (heptane) versus the extraction time with the weight of salt fixed at 1.8 g whereas Fig. 3 shows the response surface plot of the salt addition versus the extraction time with the extraction solvent volume fixed at 200  $\mu\text{L}$ . Figure 4 shows the response surface chart with interaction between the salt addition and the extraction solvent volume during 25 minutes long extraction.

### 3.3. Allocation of the Optima

The second order polynomial model was used to fit the optimal conditions. Applying the desirability function, Design Expert software located the optimal condition as follows: the extraction time was 16 min, the volume of heptane 115  $\mu\text{L}$  and the addition of NaCl was 1.24 g. At these conditions, the system

experimental response reached value 17.08 (sum of relative peak areas), whereas the predicted response value was 16.86. This agreement demonstrates the applicability and validity of the optimization procedure applied.

## 4. Conclusion

New liquid-liquid microextraction technique was optimized for determination of selected environmental pollutants by GC-FID. The Plackett-Burman design and the central composite design were used within the framework of response surface methodology to evaluate the optimal experimental parameters with the minimum number of experiments. Under selected optimal conditions, the microextraction technique was tested for several environmental pollutants present in aqueous samples.

### Acknowledgment

Financial support from the Grant Agency of Charles University in Prague (GA UK-21210) is gratefully acknowledged.

### References

- [1] Araújo P. W., Brereton R. G.: *Trends Anal. Chem.* **15** (1996), 63–70.
- [2] Bezerra M. A., Santelli R. E., Oliveira E. P., Villar L. S., Escalera L. A.: *Talanta* **76** (2008), 965–977.
- [3] Mason R. L., Gunst R. F., Hess J. L.: *Statistical Design and Analysis of Experiments. With Applications to Engineering and Science*. 2nd ed. New Jersey, Wiley 2003.
- [4] Myers R. H., Montgomery D. C.: *Response Surface Methodology. Process and Product Optimization using Designed Experiments*. 2nd ed. New York, Wiley 2002.
- [5] Stalikas C., Fiamegos Y., Sakkas V., Albanis T.: *J. Chromatogr. A* **1216** (2009), 175–189.
- [6] Ebrahimzadeh H., Yamini Y., Kamarei F.: *Talanta* **79** (2009), 1472–1477.

# A New, Effective Method for Determination of Polycyclic Aromatic Hydrocarbons in Tea

LUCIE DRABOVA, JANA PULKRABOVA, KAMILA KALACHOVA, VLADIMIR KOCOUREK, JANA HAJLSLOVA✉

*Department of Food Chemistry and Analysis, Faculty of Food and Biochemical Technology, Institute of Chemical Technology, Technická 3, 166 28 Prague 6, Czech Republic, ✉ jana.hajslova@vscht.cz*

## Abstract

In this study, a new and efficient method for analysis of 16 polycyclic aromatic hydrocarbons (16 EU PAHs) which are classified as a priority for various food groups by the Scientific Committee on Food (SCF) in different types of tea samples (black, green, white) is described. The sample preparation procedure included ethyl acetate extraction followed by a solid phase extraction (SPE) using a molecularly imprinted polymers (MIPs) column for a selective isolation of target compounds was optimized and validated. For the final identification/quantitation of target 16 EU PAHs a two-dimensional gas chromatography coupled with a time-of-flight mass spectrometry (GC×GC-TOF MS) was used. Performance characteristics of this new procedure including repeatability (2–9%), limit of quantitations (LOQs = 0.15–0.30 µg kg<sup>-1</sup>) and recovery (73–103 %) were assessed.

## Keywords

GC×GC-TOF MS  
MIP  
PAH  
tea

## 1. Introduction

Tea is an old, worldwide popular commodity. It is valued for its specific aroma and flavour, as well as for health-promoting properties. However, under certain conditions tea leaves may contain some contaminants such as pesticides originated from pre/post and harvest treatment or polycyclic aromatic hydrocarbons (PAHs), which may indicate improper process of tea leaves drying. Recently, an increasing public concern and a scientific investigation have been focused on the occurrence of PAHs and their control in herbal products of plant teas to assess the potential health hazards more thoroughly [1].

Polycyclic aromatic hydrocarbons, a group of organic pollutants that consists of two or more fused aromatic rings, are a well-known class of carcinogenic compounds found in various foods, and they have been intensively studied over the last decade. Gaseous and particle-bound PAHs can be transported over long distances before deposition on vegetation. This could cause human exposure to PAHs through contaminated food consumption and, thus, might pose a human health risk. Tea leaves with high surface area may accumulate PAHs, especially from air. As another source of PAHs may be considered production process itself if tea leaves are dried using combustion gases generated by burning wood, oil or coal. PAHs are invariably present in the combustion gases, and can be absorbed by tea product when they come in contact [2].

Considering a number of papers dealing with the

occurrence of PAHs in tea, the high levels of PAH in this commodity have been widely proved [1–7]. However, no data on levels of genotoxic 16 EU PAHs which are classified as a priority for different food groups by Scientific Committee on Food (SCF) have been reported until now [8].

Most of analytical methods used for the determination of PAHs in different types of tea samples involve various types of extraction and clean-up procedures. Pressurized liquid extraction (PLE) [5], saponification [6] and soxhlet extraction [3, 9] are possible extraction techniques. Solid phase extraction (SPE) [4, 9] and gel permeation extraction (GPC) [5] can be used as the following clean-up step. For the detection and quantitation of PAHs in tea samples, a high performance liquid chromatography with photometric or fluorimetric detection [2, 10–12] and/or a gas chromatography with flame ionization detector [6] or mass spectrometric detector [6, 13] were typically used.

The aim of the presented study was to optimize and validate a fast and simple sample preparation procedure for the determination of 16 EU PAHs, in tea samples.

## 2. Experimental

### 2.1. Method Test Material

A sample of black tea (originated from China) obtained at the Czech retail market was used for a method development and validation. Before

experiments, tea sample was homogenized using GRINDOMIX GM 200 (Retsch, Germany) and stored at the room temperature.

## 2.2. Chemicals

*n*-hexane, cyclohexane, toluene ethyl acetate and dichloromethane (Merck, Germany) and acetonitrile (HPLC gradient grade, J. T. Baker), were used as supplied. Magnesium sulphate and sodium chloride were delivered from Sigma Aldrich (Germany) and Lach-Ner (Czech Republic), respectively. Styrene-divinylbenzene gel (Bio-Beads® S-X3, 200–400 mesh) was purchased from Bio-Rad (USA). SupelMIP™ SPE-PAH was purchased from Supelco (USA).

Individual standard solutions of 16 priority PAHs dissolved in cyclohexane were supplied by Dr. Ehrenstorfer GmbH (Germany). Purity of individual standards was not less than 95%. Certified standard solution of labelled PAHs in nonane, was supplied by Cambridge Isotope Laboratories Inc. (USA).

## 2.3. Analytical Method

### 2.3.1. Isolation

In the first step, 3 different extraction solvents: (i) acetonitrile (MeCN), (ii) ethyl acetate (EtOAc) and (iii) hexane (Hex) were tested for the extraction of 16 target PAHs. 2.5 g of homogenized tea (with surrogate <sup>13</sup>C-PAH 20 ng absolutely) was mixed with 10 mL of water and 10 mL of respective extraction solvent in polypropylene tube and then shaken vigorously for 1 min. Subsequently, 4 g of MgSO<sub>4</sub> and 1 g of NaCl were added. The tube was shaken for 1 min once again, than centrifuged for 5 min (11 000 min<sup>-1</sup>) and finally an aliquot of 5 mL from the upper layer was taken from the tube and evaporated.

### 2.3.2. Clean-up

To evaluate the efficiency of this new extraction step, a routinely used GPC technique was firstly employed for a clean-up. Afterwards, when the isolation of PAHs was fully optimized, a GPC was replaced by SupelMIP™ SPE-PAH column.

*Clean-up by GPC followed by SPE on silicagel mini columns:* For the GPC clean-up, Bio-Beads® S-X3 gel as a stationary phase and chloroform as a mobile phase was used. The fraction corresponding to the elution volume of 16–32 mL was collected. After evaporation, the residue was dissolved in 1 mL of *n*-hexane and was cleaned-up using 1 g silica gel SPE

mini column and hexane:dichloromethane (3:1, v/v) as the elution solvent. Eluate was evaporated and dissolved in 0.25 mL toluene

*Clean-up on SupelMIP™ SPE-PAH column:* The SPE MIPs column was conditioned with 1 mL of cyclohexane and 2.5 mL of sample in cyclohexane were loaded. After that the column was washed with 3 mL of cyclohexane. For the elution of PAHs 6 mL of dichloromethane were used. Eluate was evaporated and dissolved in 0.25 mL toluene.

## 2.4. GC × GC-TOF MS Analysis

All experiments were performed using an Agilent 6890N GC system (Agilent, USA) coupled to a Pegasus III (LECO Corp, USA) high-speed time-of-flight mass spectrometer (GC-TOF MS) operated in electron ionization mode (EI). Target analytes were separated on BPX-50 capillary column (30 m × 0.25 mm i.d.; 0.25 μm film thickness) and BPX-5 capillary column (1 m × 0.1 mm i.d.; 0.1 μm film thickness). The GC conditions were as follows. Oven temperature programme: 1st column BPX-50: 80 °C (4.3 min), 30 °C min<sup>-1</sup> to 240 °C, 2 °C min<sup>-1</sup> to 270 °C, 5 °C min<sup>-1</sup> to 320 °C, 40 °C min<sup>-1</sup> to 360 °C (12 min); 2nd column BPX-5: 90 °C (4.3 min), 30 °C min<sup>-1</sup> to 250 °C, 2 °C min<sup>-1</sup> to 280 °C, 5 °C min<sup>-1</sup> to 330 °C, 40 °C min<sup>-1</sup> to 360 °C (12 min). Carrier gas helium with flow 1.3 mL min<sup>-1</sup>; PTV injection: solvent vent; 1 × 8 μL; initial temperature: 50 °C (2.3 min); inlet rating velocity: 400 °C; final inlet temperature: 300 °C.

The TOFMS detector was operated under the following conditions: mass range: *m/z* = 45–750; ion source temperature: 250 °C; transfer line temperature: 280 °C; acquisition speed: 100 spectra s<sup>-1</sup>. The modulation period was 4.5 s. The ChromaTOF 4.24 software (LECO Corp, USA) was used for data processing.

## 3. Results and Discussion

At the beginning of our study, an efficiency of extraction procedure for isolation of PAHs from tea samples was optimized. Within the conducted experiments, following parameters were tested:

- extraction solvent (Hex, MeCN, EtOAc),
- addition of amount of NaCl in the partition step, and
- two different cleans-up techniques.

Subsequently, the optimized extraction procedure was fully validated by analysis of black tea sample fortified with target analytes at two concentration levels (0.5 and 5 μg kg<sup>-1</sup>).

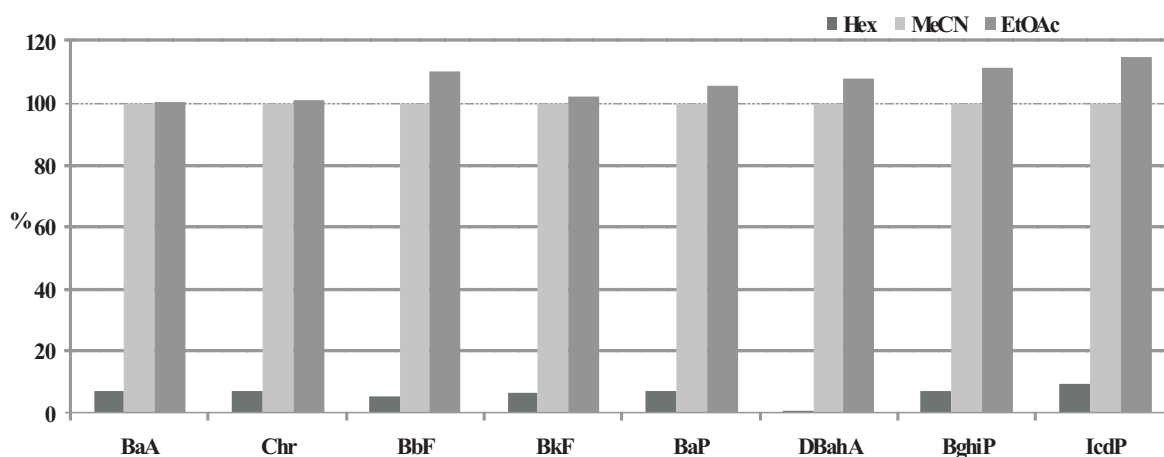


**Fig. 1.** Extraction efficiency of eight most important representatives of PAHs. Using three extraction solvent for the isolation. The extraction with acetonitrile and 1 g of NaCl was set as 100 %.

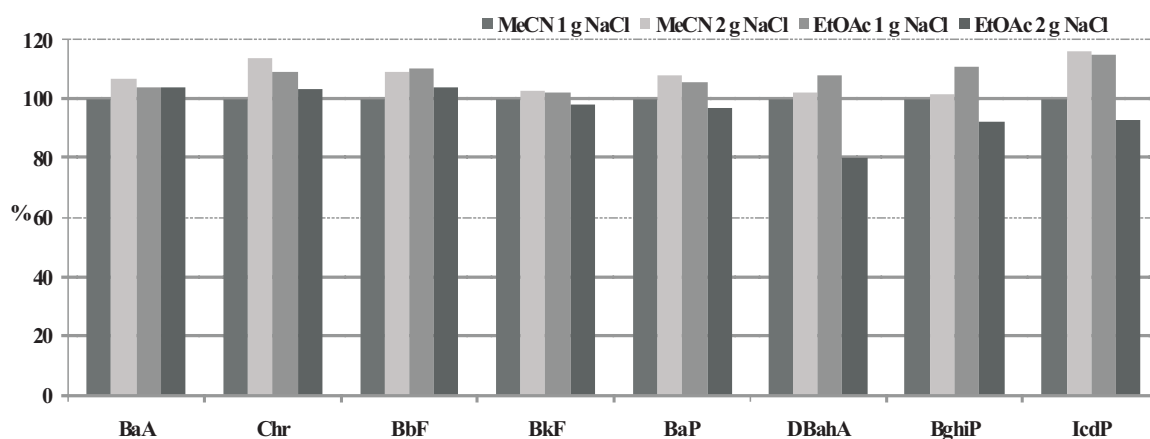


**Fig. 2.** Extraction efficiency of PAHs when two solvent (acetonitrile and ethylacetate) was used with NaCl addition 1 and 2 g. The extraction by acetonitrile and 1 g NaCl addition was set as 100 %.

### 3.1. Optimization of Extraction Step

#### 3.1.1. Selection of Extraction Solvent

As already mentioned before, three solvents were evaluated for their extraction efficiency. The results obtained in this study are shown in Figure 1. Very low recoveries were obtained when using non-polar hexane (although PAHs are highly hydrophobic), on the other hand, comparable extraction efficiency of ethylacetate and acetonitrile was achieved. Therefore, the later two solvents were selected for optimization follow up experiments.

#### 3.1.2. Optimization of NaCl Addition

One of the most important parts of the method optimisation was the selection of NaCl amount (1 or 2 g) added within partition step (see Figure 2). The best results were achieved when 1 g of NaCl was added into the sample and ethyl acetate was used as

extraction solvent. The results obtained when the amount of NaCl was 2 g and extraction solvent was acetonitrile, were almost comparable. The choice of ethyl acetate is not based only economically (lower cost) but also due to lower toxicity and time needed for evaporation.

#### 3.1.3. Comparison of Clean-up Techniques

Tea matrix (black, green tea) contains a high amount of polyphenols, methyl xanthines such as caffeine, purines and also different phenolic acids [4]. The main aim of clean-up step optimisation was to remove those co-extracts as much as possible using different procedures. The most commonly used techniques for clean-up are (GPC) on Bio Beads S-X3 and SPE [6, 7, 9–12], which are also compared here (i) GPC followed by SPE and (ii) SupelcoMIPs SPE. As shown in Figure 3 and 4, both of the tested clean-up techniques are suitable for clean-up of tea samples before GC×GC-TOF MS analyses, but comparing

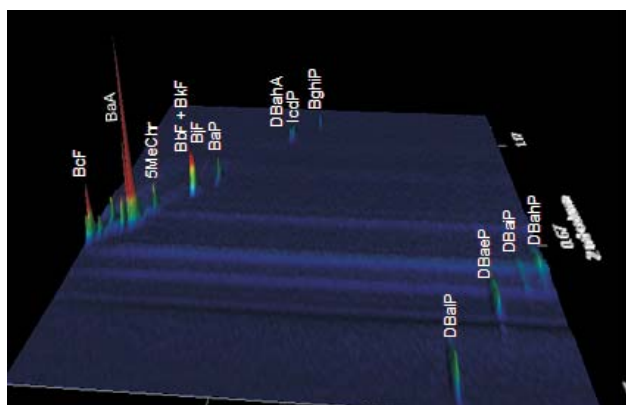


**Fig. 3.** Illustrative chromatogram of black tea sample spiked with PAHs ( $0.5 \mu\text{g kg}^{-1}$ , GC×GC-TOF MS) clean-up using GPC followed by SPE. Injected equivalent of matrix: 20 mg.

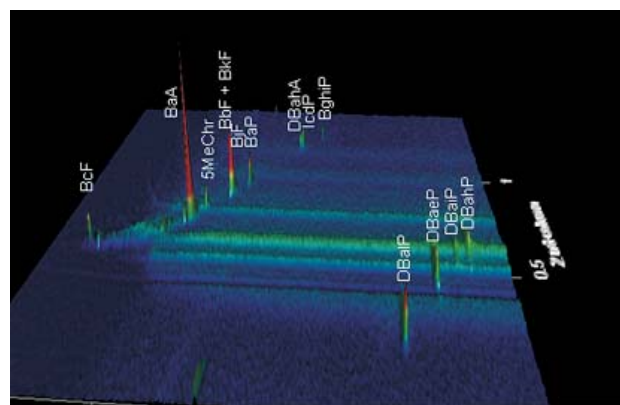


**Fig. 4.** Illustrative chromatogram of black tea sample spiked with PAHs ( $0.5 \mu\text{g kg}^{-1}$ , GC×GC-TOF MS) clean-up using Supelco-MIP PAHs. Injected equivalent of matrix: 20 mg.

time consumption, the latter one is much more advantageous.

### 3.2. Method Validation

In order to verify the accuracy of the optimized sample preparation procedure (extraction solvent ethyl acetate, 1 g NaCl, 10 mL H<sub>2</sub>O added from partition, followed by MIPS SPE clean-up), recovery and repeatability experiments were carried out at levels 0.5 and  $5 \mu\text{g kg}^{-1}$ . Within the validation study, spiked samples of dry black tea were used. Six replicates were performed for both spiking levels. With each six samples, the procedural blank was prepared. The recoveries (%) and repeatabilities, expressed as RSD (%), calculated from these six replicates are shown in Table 1. Limits of quantitations (LOQs) for all 16 EU target PAHs of the optimised method are between 0.15 and  $0.30 \mu\text{g kg}^{-1}$ .

## 4. Conclusions

The new, simple and rapid analytical method for the determination of 16 EU PAHs in tea samples was developed and validated within this study. The performance characteristics for all target analytes are as follows: (i) recoveries 73–103 %, (ii) repeatabilities 2–9 % and (iii) LOQs, 0.15– $0.3 \mu\text{g kg}^{-1}$ . The optimized ethyl acetate extraction with subsequent purification on MIPS SPE columns and final determination on GC×GC-TOF MS represents a very rapid method for analysis of 16 EU PAHs in teas.

The extraction procedure enabled satisfactory results and is less time-consuming (12 samples in 1 hour) compared to saponification, Soxhlet extraction or even PLE which are at present most commonly used techniques in routine laboratories. In the follow up project, the set of 90 tea samples originated from various Asian countries will be

**Table 1**

Recovery and repeatability (RSD) of all sixteen target PAHs calculated from six replicates of spiked tea at two levels.

	Level I ( $0.5 \mu\text{g kg}^{-1}$ )		Level II ( $5 \mu\text{g kg}^{-1}$ )		LOQ [ $\mu\text{g kg}^{-1}$ ]
	Recovery [%]	Repeatability [%]	Recovery [%]	Repeatability [%]	
BcFln	73	4	82	4	0.3
BaA	86	4	84	5	0.15
Chr	88	3	89	3	0.15
CPcdP	84	6	84	5	0.15
5-MeChr	85	2	90	3	0.3
BbF	98	2	103	2	0.15
BkF	93	3	88	2	0.15
BjF	87	5	95	6	0.15
BaP	88	3	92	5	0.15
DBahA	88	4	84	7	0.15
IcdP	86	4	92	4	0.15
BghiP	76	2	81	3	0.15
DBalP	85	5	84	5	0.3
DBaeP	75	3	82	4	0.3
DBaiP	77	6	82	8	0.3
DBahP	79	5	84	6	0.3

examined using this method.

#### Acknowledgment

*This study was carried out with support from the Ministry of Education, Youth and Sports, Czech Republic – partly from the project MSM 6046137305.*

#### References

- [1] Lin D.H., Tu Y., Zhu L.: *Food Chem. Toxicol.* **43** (2005), 41–48.
- [2] Ziegenhals K, Jira W, Speer K.: *Eur. Food Res. Technol.* **228** (2008), 83–91.
- [3] Lin D.H., Zhu L.Z.: *J. Agric. Food Chem.* **52** (2004), 8268–8271.
- [4] Kayadi-Sayadi M.N., Rubio-Barrosa S., Cuesta-Jimenez M.P., Polo-Diez L.M.: *Analyst* **123** (1998), 2145–2148.
- [5] Kamangar F., Schantz M.M., Abnet Ch.C., Fagundes R.B., Dawsey S.M.: *Cancer Epidemiology, Biomarkers and Prevention* **5** (2008), 1262–1268.
- [6] Fiedler H., Cheung C.K., Wong M.H.: *Chemosphere* **46** (2002), 1429–1433.
- [7] Danyi S., Brose F., Brasseur C., Schneider Y.J., Larondelle Y., Pussemier L., Robbens J., Saeger S., Maghuin-Rogister G., Louise Scippo M.: *Anal. Chim. Acta* **633** (2009), 293–299.
- [8] Commission Recommendation of 4 February 2005 (2005/108/EC). *Off. J. Eur. Union* **L34** (2005), 43–45.
- [9] Shatta A.A.: *Adv. Food Sci.* **21** (1999), 170–176.
- [10] Jacques R.A., Dariva C., Oliveira J.V., Caramao E.B.: *Anal. Chim. Acta* **625** (2008), 70–76.
- [11] Fontcuberta M., Arques J.F., Martinez M., Suarez A.: *J. Food Protect.* **69** (2006), 2024–2028.
- [12] Stijve T., Hischenhuber C.: *Deutsche Lebensmittel-Rundschau* **83** (1987), 276–282.
- [13] Ciemiak A.: *Bromatologia i Chemia Toksykologiczna* **37** (2004), 25–29.

# The Stationary Phase Bed Compaction during the Slurry Packing of Capillary Columns

MARTIN FRANČ<sup>a</sup>, PAVEL COUFAL<sup>a</sup>, ZUZANA BOŠÁKOVÁ<sup>a</sup>, EVA TESAŘOVÁ<sup>b</sup>

<sup>a</sup>Department of Analytical Chemistry, <sup>b</sup>Department of Physical and Macromolecular Chemistry, Faculty of Science, Charles University in Prague, Albertov 2030, 128 43 Prague, Czech Republic, ✉ martinfrancx@gmail.com

## Abstract

A slurry packing technique was employed to pack fused silica capillaries with Nucleosil C18 stationary phase. In attempt to improve the packing process, the influence of sonication and length of the bed compaction phase on the separation efficiency and the kinetic performance were studied. Selected columns were tested again after a few months of storage in order to determine the stability of the stationary phase bed. Neither the separation efficiency nor the kinetic performance was influenced by the length of the bed compaction phase. A major difference in the stationary phase bed density was observed between the sonicated and non-sonicated columns. The denser beds of the sonicated columns resulted in lower kinetic performance. On the other hand, the bed stability was increased and therefore, the performance of the sonicated columns did not deteriorate with time.

## Keywords

capillary liquid chromatography  
separation impedance  
slurry packing  
van Deemter curve

## 1. Introduction

Micro-separation methods are widely used these days as they are environmentally friendly and require only a small amount of sample. A very attractive way of acquiring a capillary column is packing of one's own. Packing process is quite simple, cheap and such a column can be customized to meet the desired requirements. The easiest packing method is called slurry packing [1–4]. Stationary phase slurry is pushed into an empty column by a solvent under pressure. The stationary phase particles are retained inside by the column's outlet frit. When the column is filled, the obtained stationary phase bed is compacted by rinsing with a suitable solvent.

There is a number of conditions in the packing process that could influence the resulting column performance. Some of these conditions have already been studied, for instance solvents used [5, 6], connection between the column and the slurry reservoir [1, 7] and slurry concentration [8–10]. The influence of others is yet uncertain and they are usually selected by trial and error. The stationary phase bed is usually compacted for 20–30 minutes [9, 11, 12], although a longer time was also used (1 hour [5], 12 hours [13]). Sonication was sometimes employed to produce more compact stationary phase beds [4, 12, 14] but the exact effect is unclear, as no problems were reported when the sonication was not used during the packing [13, 15].

## 2. Experimental

Polyimide coated fused silica capillaries were purchased from Supelco (Bellefonte, USA). Nucleosil C18 stationary phase with 5- $\mu\text{m}$  particles was from Macherey-Nagel (Düren, Germany). Acetonitrile, HPLC grade, and toluene, pure, were purchased from Merck (Darmstadt, Germany). Thiourea, pure, was from Sigma-Aldrich (St. Louis, USA). Phenol, p.a. was from Penta (Prague, Czech Republic). Deionized water was purified with Milli-Q Water Purification System (Millipore, USA). Isocratic pump LCP 4000 (Ecom, Prague, Czech Republic) and ultrasound bath Elmasonic S15H (P-Lab, Prague, Czech Republic) were used to pack the capillaries. The chromatographic system consisted of syringe pump 100DM (Isco, Lincoln, USA), 100 nl valve injector (Valco Instrument, Schenkon, Switzerland) and UVIS-205 spectrophotometric detector (Linear Instruments, San Jose, USA).

The packing process was based on earlier works [3, 5, 8]. To prepare an empty column, a piece of glass wool was first pushed into one end of a 320  $\mu\text{m}$  i.d. capillary to serve as an outlet frit. A short 75  $\mu\text{m}$  i.d./280  $\mu\text{m}$  o.d. capillary was then cemented into the 320  $\mu\text{m}$  i.d. capillary to secure the glass wool inside. The column was connected to a slurry reservoir made from an empty stainless steel HPLC column with an approximate volume of 1.5  $\text{cm}^3$ . Slurry concentration was 0.05  $\text{g cm}^{-3}$  in 100% acetonitrile and it was sonicated for 10 minutes prior to transfer

**Table 1**

Summary of the packing conditions, three columns were prepared under each condition.

Total compaction time (min)	Sonication time (min)
30	25
30	–
15	10
15	–
5	–

into the reservoir. 65% acetonitrile was used as the packing solvent. The initial flow was set to  $0.3 \text{ mL min}^{-1}$  and lowered once the pressure reached 30 MPa in order to maintain the pressure. After the column was filled, the pressure was increased to 33 MPa and held for 5, 15 or 30 minutes to compact the stationary phase bed. The columns packed using ultrasound were sonicated for 10 or 25 minutes and then compacted for another 5 minutes without sonication. The packing conditions are summarized in Table 1.

The test sample consisted of  $1 \text{ mg cm}^{-3}$  thiourea,  $10 \text{ mg cm}^{-3}$  phenol and  $10 \text{ mg cm}^{-3}$  toluene. Flow cell diameter was  $100 \text{ }\mu\text{m}$ , detector was set to the wavelength of 214 nm. Mobile phase was 65% acetonitrile. The chromatograms were recorded and analyzed with Clarity 2.4.4.105 (Data Apex, Prague, Czech Republic). Origin 6.0 (OriginLab, Northampton, USA) was used to fit the van Deemter plots to the obtained data.

### 3. Results and Discussion

The results in Table 2 show that the average theoretical plate height ( $H$ ) values of all the columns were similar regardless of the packing conditions. The highest and the lowest values differ by 4.4 and  $2.8 \text{ }\mu\text{m}$  for the test compounds phenol and toluene, resp. This difference represents reduced plate height values of approximately 1 and 0.5 particle diameter only. Moreover, all the packing conditions resulted in

a good reproducibility of packing, except for the 15-minute bed compaction with 10-minute sonication. A high deviation of their  $H$  values shows that the sonication introduces a random effect into the packing process. Therefore, the sonication has to be used for a time long enough to balance this random effect. 25 minutes of sonication proved to be sufficient. While no substantial difference in column permeability exists among the columns compacted for different times, there is an apparent influence of sonication. The sonicated columns exhibited significantly lower column permeability values. Therefore, the kinetic performance of the 30-minute sonicated columns is slightly worse compared to the 30-minute non-sonicated columns, in spite of the better separation efficiency (compare the values of 30-minute columns in Table 2).

The lower column permeability means a better stationary phase bed compaction, a higher density and consequently a higher bed stability. This fact was proven by testing selected columns again after nine months of storage. The  $H$  values of all the tested columns after the storage were lower by approximately  $2 \text{ }\mu\text{m}$  for the test compound phenol and  $1 \text{ }\mu\text{m}$  for the test compound toluene, regardless of the packing conditions. The column permeability values of the non-sonicated columns decreased by around  $1 \times 10^{-14} \text{ m}^2$ , therefore their kinetic performance deteriorated during the storage. On the other hand, the column permeability values of the sonicated columns decreased only by around  $0.2 \times 10^{-14} \text{ m}^2$ . Hence, their kinetic performance remained unchanged.

### 4. Conclusion

When no sonication is used during the packing process, the length of the bed compaction phase has no influence on both the separation efficiency and the kinetic performance. Such columns have less stable beds and their performance deteriorates with time. As they can be prepared quickly and easily, they are ideal

**Table 2**

Performance of the slurry-packed columns.  $H$  – average theoretical plate height, RSD – relative standard deviation of theoretical plate height,  $E$  – average separation impedance,  $K$  – average column permeability.

Bed Compaction Time	$H$ (phenol) [ $\mu\text{m}$ ]	$H$ (toluene) [ $\mu\text{m}$ ]	RSD (phenol) [%]	RSD (toluene) [%]	$E$ (phenol)	$E$ (toluene)	$K$ [ $10^{-14} \text{ m}^2$ ]
5 min	18.6	16.3	4.6	4.4	9900	5400	4.83
15 min	21.3	17.5	1.3	1.2	13500	6500	4.44
15 min <sup>a</sup>	22.5	17.6	17.5	14.2	18500	9800	3.61
30 min	19.3	17.0	2.5	1.3	10300	6200	4.80
30 min <sup>a</sup>	18.1	14.8	1.5	1.7	11200	5800	3.82

<sup>a</sup> Columns packed with the aid of ultrasound.

for testing of new stationary phases or harsh separation conditions. The sonicated columns have highly stable beds and their separation efficiency is slightly better, provided that the sonication was used for a sufficient length of time to balance its random effects. Their performance remains the same during several months at least.

#### Acknowledgements

The projects SVV 261204 and 78808 of the Grant Agency of the Charles University in Prague and Research Projects MSM 0021620857 and RP 14/63 of the Ministry of Education, Youth and Sports of the Czech Republic are acknowledged for the financial support.

#### References

- [1] Keller H. P., Erni F., Linder H. R., Frei R. W.: *Anal. Chem.* **49** (1977), 1958–1963.
- [2] Bristow P. A., Brittain P. N., Riley C. M., Williamson B. F.: *J. Chrom.* **131** (1977), 57–64.
- [3] Borra C., Han S. M., Novotny M.: *J. Chrom.* **385** (1987), 75–85.
- [4] Ehlert S., Rösler T., Talarek U.: *J. Sep. Sci.* **31** (2008), 1719–1728.
- [5] Vissers J. P. C., Claessens H. A., Laven J., Cramers C. A.: *Anal. Chem.* **67** (1995), 2103–2109.
- [6] Zimina T., Smith R. M., Highfield J. C., Myers P., King B. W.: *J. Chrom. A* **728** (1996), 33–45.
- [7] Meyer R. F., Hartwick R. A.: *Anal. Chem.* **56** (1984), 2211–2214.
- [8] Gluckman J. C., Hirose A., McGuffin V. L., Novotny, M.: *Chromatographia* **17** (1983), 303–309.
- [9] Cortes H. J., Pfeiffer C. D.: *Anal. Chem.* **65** (1993), 1476–1480.
- [10] Kennedy R. T., Jorgensson J. W.: *Anal. Chem.* **61** (1989), 1128–1135.
- [11] Andreolini F., Borra C., Novotny M.: *Anal. Chem.* **59** (1987), 2428–2432.
- [12] Shen Y., Yang Y. J., Lee M. L.: *Anal. Chem.* **69** (1997), 628–635.
- [13] Karlsson K. E., Novotny M.: *Anal. Chem.* **60** (1988), 1662–1665.
- [14] Roulin S., Dmoch R., Carney R., Bartle K. D., Myers P., Euerby M. R., Johnson C.: *J. Chrom. A* **887** (2000), 307–312.
- [15] Wong V., Shalliker R. A., Guiochon G.: *Anal. Chem.* **76** (2004), 2601–2608.

# Analysis of Perfluorinated Compounds: Method Validation According to the Commission Decision 2002/657/EC

PETRA HRÁDKOVÁ, JAN POUSTKA, JANA PULKRABOVÁ, ONDŘEJ LACINA, JANA HAJŠLOVÁ

*Department of Food Chemistry and Analysis, Institute of Chemical Technology, Prague, Technická 3, CZ-16628 Prague 6, Czech Republic, ✉ petra.hradkova@vscht.cz*

## Abstract

Perfluorinated compounds (PFCs), a wide group of food and environmental contaminants, have been found until now in various types of both abiotic and biotic matrices including human samples, such as plasma, blood and/or breast milk. To assess health risks associated with a dietary intake of these compounds European Food Safety Authority (EFSA) recommended to member states to monitor major representatives of these persistent organic compounds (POPs) – perfluorooctane sulfonate (PFOS), perfluorooctanoic acid (PFOA), and perfluorooctane sulfonamide (FOSA) –, which is precursor of PFOS, in various types of food stuff.

Within the experiments of this study a simple, fast and cheap sample preparation procedure including extraction and clean-up for PFOS, PFOA and FOSA in fish fillets was validated, in accordance with the Commission Decision 2002/657/EC. The novel analytical approach of crude methanol extract clean-up using carbon powder (activated charcoal) combined with liquid chromatography tandem mass spectrometry (LC-MS/MS) was applied. In comparison with other traditionally used methods for PFCs which are rather time consuming and laborious, a sample preparation procedure developed within this study needs only cca 60 minutes for 10 samples.

## Keywords

CC<sub>α</sub>  
CC<sub>β</sub>  
method validation  
perfluorinated compounds  
2002/657/EC

## 1. Introduction

The interest in perfluorinated compounds (PFCs) has exponentially increased since the end of 20th century. With regard to a wide range of applications, such as e.g. surface treatment agents, polymerization aids and in fire-fighting foams and their exceptional stability in the environment, PFCs have “emerged” as a global pollution problem [1–3].

Perfluorooctane sulfonate (PFOS) and perfluorooctanoic acid (PFOA) together with a major PFOS precursor, perfluorooctane sulfonamide (FOSA), are the most investigated representatives of these POPs [4–7]. Contrary to polychlorinated biphenyls (PCBs) or polybrominated diphenyl ethers (PBDEs) which can be accumulated in lipid-rich tissue, PFCs bind to blood proteins and thus accumulate in liver. For this reason, analytical methods for determination of “classic” hydrophobic POPs are not applicable for PFCs analysis. Recently, the review focusing on extraction and clean up strategies employed for the PFCs analysis in environmental and human matrices has been published [8]. Most of older studies of the biota samples applied ion-pair extraction (IPE) introduced by Hansen [9]. Unfortunately, this procedure is a very time-consuming, laborious and, moreover,

some lipids and other less polar matrix components are co-isolated and may interfere (strong matrix effects) within an instrumental determinative step, therefore simple isolation/clean-up approaches were developed [10]. For instance, polar solvents such as methanol, acetonitrile, or aqueous solutions of formic and acetic acid or its salts have been employed for isolation of PFCs from biological samples. For removing of matrix components from crude extracts, solid-phase extraction (SPE) on HLB or WAX cartridges was used [11–13]. In some studies, alkaline digestion was carried out prior to SPE step [14, 15]. Alternatively, dispersive Envi-Carb<sup>®</sup> sorbent can be employed [14, 16].

The European Food Safety Authority (EFSA), based on CONTAM (Scientific Panel on Contaminants in the Food Chain) recommendation, established the tolerable daily intake (TDI) 150 ng kg<sup>-1</sup> b.w. for PFOS and 1500 ng kg<sup>-1</sup> b.w. for PFOA, from July 2008 [17]. In May 2009, PFOS and its salts, together with other eight halogenated POPs, was listed on the Stockholm convention on persistent organic pollutants [18]. In March 2010, the European Commission (EC) recommended to member states to monitor presence of perfluoroalkylated substances including PFOS, PFOA, their precursors such as FOSA,

*N*-EtFOSE, 8:2 FTOH and other similar compound with different chain length (C4–C15) and also polyfluoroalkyl phosphate surfactants (PAPS) in order to estimate the relevance of their presence in food. The used analytical methods have been proven to generate reliable results; ideally the recovery rates should be in the 70–120% range with limit of quantifications (LOQs) of  $1 \mu\text{g kg}^{-1}$  [19].

The aim of the presented study was to develop and validate a simple, fast analytical procedure with LOQs below  $1 \mu\text{g kg}^{-1}$  applicable for accurate analysis of PFOS, PFOA and FOSA in fish tissues. To achieve this objective, a charcoal-based clean-up step was employed together with liquid chromatography (LC) coupled with mass spectrometric detection (MS/MS).

## 2. Experimental

### 2.1. Sample Preparation

2 g of representative fish sample were transferred to plastic homogenizing (PP) tube and internal standards were added (corresponds to concentration  $3 \mu\text{g kg}^{-1}$ ). The sample was extracted with 6 mL of methanol using Ultra Turrax homogenizer. Activated charcoal was added to purify the suspension. Sample was shaken 1 min on minishaker and centrifuged at 10 000 rpm for 5 min. The supernatant was filtered through  $0.2 \mu\text{m}$  centrifugal filter and approximately 500  $\mu\text{L}$  transferred into vial for the following HPLC-MS/MS analysis.

### 2.2. HPLC-MS/MS Analysis

**Table 1**

Ion transitions of target analytes used in MRM analysis in LC-MS/MS (masses in bold are those used for quantification).

Compound	$t_R$ (min)	Transition
PFOA	6.2	<b>413</b> → <b>369</b> 413 → 169
PFOS	6.6	<b>499</b> → <b>99</b> 499 → 80
FOSA	8.3	<b>498</b> → <b>78</b>
$^{13}\text{C}_4$ -PFOA	6.2	<b>417</b> → <b>369</b> 417 → 169
$^{13}\text{C}_4$ -PFOS	6.6	<b>503</b> → <b>99</b> 503 → 80
$^{13}\text{C}_8$ -FOSA	8.3	<b>506</b> → <b>78</b>

A HPLC Alliance 2695 module (Waters, USA) coupled to a Quattro Premier XE mass spectrometer (Waters, USA) was used for the determination of target analytes. All separations were carried out using a separation column Atlantis T3 ( $50 \times 2.1 \text{ mm}$ ,  $3 \mu\text{m}$ ), maintained at  $30^\circ\text{C}$ . The mobile phase was water containing  $2 \text{ mmol L}^{-1}$  ammonium acetate and methanol; at a flow rate of  $0.3 \text{ mL min}^{-1}$ . The total analysis time was 13 min, see Figure 1. Identification or detection was performed with a tandem-quadrupole mass spectrometer. The instrument was operated in negative electrospray ionization multiple reaction monitoring (MRM) mode. Retention times, monitored transitions together with MS-settings are listed in Table 1.

### 2.3. Validation and Quality Control

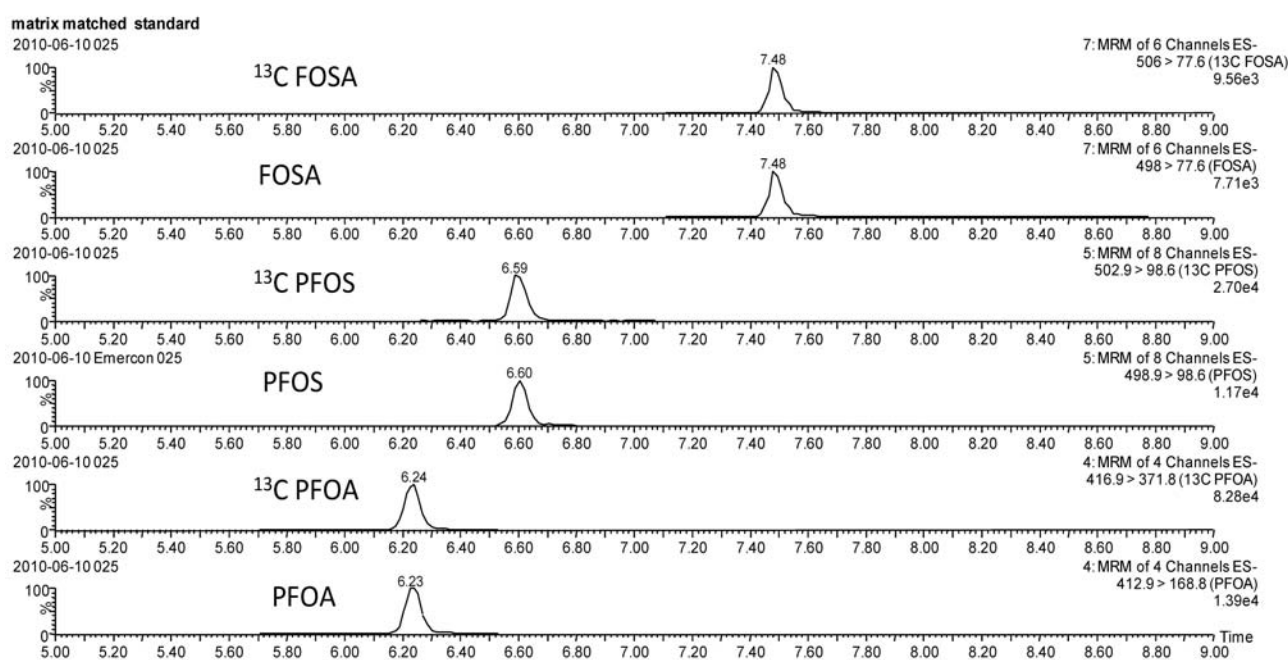


**Fig. 1.** Chromatographic record of matrix matched standard at level  $1 \mu\text{g kg}^{-1}$ .

The method was validated according the Commission Decision 2002/657/EC using fish fillets of trout (*Salmo trutta*). In the first part of the work, six replicates of blank material was fortified at levels 0.25, 0.5, 1, 1.5 and 2  $\mu\text{g kg}^{-1}$  with a standard mixture of analytes including  $^{13}\text{C}$  labelled analogues for each target compound and extracted as described before in the section Sample preparation. Subsequently, the experiment was repeated after 1 and 2 weeks to assess the within-reproducibility variance. Validation included determination of the specificity, the calibration curves, the recovery (trueness), the accuracy (repeatability and reproducibility), the robustness, decision limit ( $\text{CC}_\alpha$ ) and detection limits ( $\text{CC}_\beta$ ).

The specificity – in order to prevent misidentification of analytes due to interferences, retention time was checked for each analyte. Additionally, two transitions from a single precursor ion were monitored to complete identification insurance. These transitions were chosen for each target analyte as the most abundant ions produced from precursor.

Two types of blanks were included in the analysis: (i) instrumental blanks represented by methanol was injected after every 20 samples to monitor contamination leaching from the HPLC-MS/MS system, and (ii) procedural blanks (matrix free samples) analyzed with each set of samples were used for checking possible laboratory contamination.

### 3. Results and Discussion

As mentioned in Introduction, sample preparation procedures conducted within procedures frequently published for determination of PFCs and related compounds are very laborious and time-consuming. To overcome these problems, an alternative clean-up strategy was investigated in our study. Searching for compromise allowing simplification of sample handling procedure, we decided to test a dispersive solid phase extraction (dSPE) approach.

One of the most important issues/problems in PFCs analysis is an instrument background. So it is really necessary to involve instrumental and procedure blanks in each sample sequence. While PFOS was detected neither in instrumental nor in procedural blanks, PFOA and FOSA signals were present in both blanks. Their responses were very low, we assume that the main source of intralaboratory contamination originates from the polytetrafluorethylene parts of the instrument.

Recoveries, repeatability and reproducibility of the overall method were obtained by six replicates of fortified samples at five concentration levels. Recovery was calculated as the ratio between levels

measured and spiked amount and ranged from 85% to 110%, what is in agreement with 2002/657/EC where 70 to 120% is required. Repeatability was expressed as relative standard deviations (RSD) and ranged from 2% to 15%. Reproducibility was performed on three distinct days at one week interval in order to calculate the method repeatability as the relative standard deviation (RSD) of the recovery mean. It was evaluated similarly with minor changes, such as with different operators, different environment, different solvent batches, etc.

Decision limits ( $\text{CC}_\alpha$ ) and detection limits ( $\text{CC}_\beta$ ) were two important performance characteristics of the method for substances. Decision limits calculation was carried out in this study in accordance with the Commission Decision which defines a methodology. The method refers to the international standard ISO 11843-2, based on a linear regression model analysing fortified material at different concentration levels.

### 4. Conclusions

The simple and fast analytical procedure, consists of methanol extraction followed by clean-up of a crude extract using activated charcoal, allows to process ten samples in one hour, for determination of PFOS, PFOA and FOSA was developed and validated. The HPLC-MS/MS technique was employed for the separation and detection of target analytes. In agreement with the EC recommendation 2002/657/EC which requires recoveries from 70% to 120%, recoveries at five levels ranged from 85% to 110%. Repeatabilities expressed as relative standard deviation (RSD) ranged from 2% to 15%.

#### Acknowledgement

This research was supported by grant from the 7FP EU research project CONFIDENCE "Contaminants in food and feed: Inexpensive detection for control of exposure" (n. 211326), and by the Research Support Fund of the National Training Fund within the project EMERCON no. A/CZ0046/2/0026.

#### References

- [1] Kissa E.: *Fluorinated Surfactants and Repellents*. 2nd edition. New York, Marcel Dekker 2001.
- [2] *3M.US Public Docket AR-226-0550*. US Environmental Protection Agency, Washington 1999.
- [3] Moody C. A., Field J. A.: *Environ. Sci. Technol.* **34** (2000), 3864–3870.
- [4] Giesy J. P., Kannan K.: *Environ. Sci. Technol.* **35** (2001), 1339–1342.
- [5] Loos R., Wollgast J., Huber T., Hanke G.: *Anal. Bioanal. Chem.* **387** (2007), 1469–1478.
- [6] Kannan K., Corsolini S., Falandysz J., Oehme G., Focardi S., Giesy J. P.: *Environ. Sci. Technol.* **36** (2002), 3210–3216.
- [7] Kannan K., Corsolini S., Falandysz J., Fillmann G., Kumar K. S., Loganathan B. G., Mohd M. A., Olivero J., Van Wouwe N., Yang J. H., Aldous K. M.: *Environ. Sci. Technol.*

- 38 (2004), 4489–4495.
- [8] Leeuwen van S. P. J., Boer J.: *J. Chrom. A* **1153** (2007), 172–185.
- [9] Hansen K. J., Clemen L. A., Ellefson M. E., Johnson H. O.: *Environ. Sci. Technol.* **35** (2001), 766–770.
- [10] Arsenaault G., Chittim B., McAlees A., McCrindle R., Potter D., Tashiro C., Yeo B.: *Rapid Commun. Mass. Spectrom.* **21** (2007), 929–936.
- [11] Kuklenyik Z., Reich J. A., Tully J. S., Needhem L. L., Calafat A. M.: *Environ. Sci. Technol.* **38** (2004), 3698–3704.
- [12] Leeuwen van S. P. J., Kärman A., Bavel van B., Boer de J., Lindström G.: *Environ. Sci. Technol.* **40** (2006), 7854–7860.
- [13] Taniyasu S., Kannan K., So M. K., Gulkowska A., Sinclair E., Okazawa T., Yamashita N.: *J. Chrom. A* **1093** (2005), 89–97.
- [14] Gulkowska A., Juany Q., So M. K., Taniyasu S., Lam P. K. S., Yamashita N.: *Environ. Sci. Technol.* **40** (2006), 3736–3741.
- [15] So M. K., Taniyasu S., Lam P. K. S., Zheng G. J., Giesy J. P., Yamashita N.: *Arch. Environ. Contam. Toxicol.* **50** (2006), 240–248.
- [16] Powley C. R., George S. W., Russell M. H., Hoke R. A., Buck R. C.: *Chemosphere* **70** (2007), 664–672.
- [17] Opinion of the Scientific Panel on Contaminants in the Food chain on Perfluorooctane sulfonate (PFOS), perfluorooctanoic acid (PFOA) and their salts. *EFSA Journal* **653** (2008), 1–131.
- [18] *Stockholm Convention on persistent organic pollutants (POPs)*. <http://chm.pops.int/default.aspx> (9.4.2010).
- [19] *Commission recommendation on the monitoring of perfluoroalkylated substances in food*. 17/3/2010 (2010/161/EU) (25/05/2010)

# Comparison of DART-TOF MS, DART-Orbitrap MS and LC-MS/MS Techniques for Determination of Cyanogenic Glucosides in Flaxseed

ANNA HURAJOVÁ, VĚRA SCHULZOVÁ, JANA HAJŠLOVÁ

Department of Food Chemistry and Analysis, Institute of Chemical Technology in Prague  
Technická 3, 166 28 Prague 6-Dejvice, Czech Republic, ✉ [anna.hurajova@vscht.cz](mailto:anna.hurajova@vscht.cz)

## Keywords

DART-TOF MS  
DART-Orbitrap MS  
cyanogenic glucosides  
LC-MS/MS

## Abstract

Cyanogenic glucosides constitute a group of plant secondary metabolites, which release toxic hydrogen cyanide upon tissue disruption. Considerable dietary source of cyanogenic glucosides is flaxseed, with linustatin and neolinustatin as major representatives of this group and linamarin and lotaustralin as minor components. In this study, three different analytical techniques for determination of cyanogenic glucosides in flaxseed have been tested and compared. Flaxseed extracts were examined using LC-MS/MS, achieved results were compared with outcomes acquired by two alternative approaches consisting of unique ion source Direct Analysis in Real Time coupled with (i) time-of-flight mass spectrometer and (ii) Exactive™ benchtop Orbitrap mass spectrometer.

## 1. Introduction

Cyanogenic glucosides (CGs) are classified as phytoanticipins and chemically are characterised as  $\beta$ -glucosides of  $\alpha$ -hydroxynitriles derived from amino acids [1]. Upon disruption of plant tissue containing CGs, they are degraded by enzymes resulting in release of toxic hydrogen cyanide [2]. Hydrogen cyanide is extremely toxic to a wide range of organisms, due to its ability of linking with metals ( $\text{Fe}^{2+}$ ,  $\text{Mn}^{2+}$ ,  $\text{Cu}^{2+}$ ) that are functional groups of many enzymes inhibiting processes like the reduction of oxygen [3].

Flax (*Linum usitatissimum* L.) is one of the world oldest oilseed crop of which consumption has increased in the recent years [4]. Flaxseeds contain biologically-active compounds with putative beneficial health effects, but also belong to the group of species that produce CGs. The major CGs in flaxseeds have been identified as diglucosides linustatin and neolinustatin and minor components as monoglucosides linamarin and lotaustralin (Figure 1) [5].

A broad range of analytical methods has been applied in analysis of CGs in various commodities. The content of CGs can be determined by gas chromatography coupled to mass spectrometry detection [6] or by employing liquid chromatography (LC) with ultraviolet detection [7]. For sensitive analysis of CGs, liquid chromatography coupled to mass spectrometry detection (LC-MS) can be applied [8].

Recently developed ambient desorption ionization technique, Direct Analysis in Real Time (DART) [9]

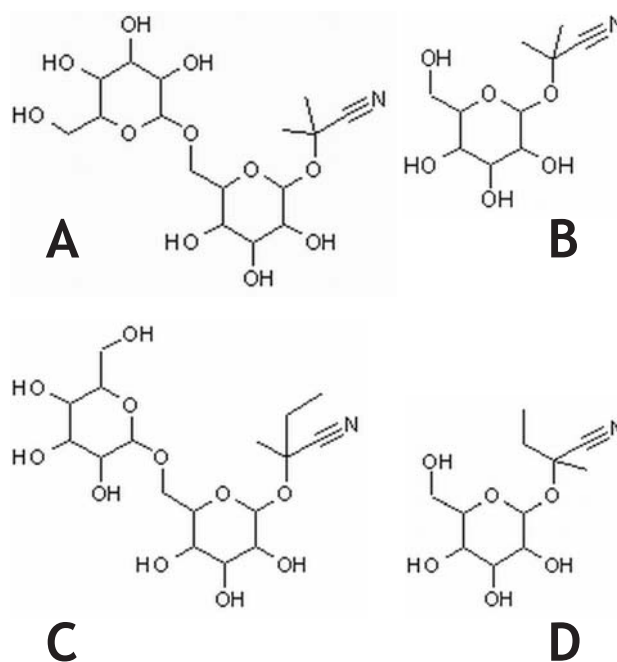


**Fig. 1.** Chemical structures of commonly occurring cyanogenic glucosides in flaxseed: (A) linustatin, (B) linamarin, (C) neolinustatin, and (D) lotaustralin.

has been demonstrated to be a useful tool for small molecules analysis such as analysis of pharmaceuticals, pesticides and several other interesting applications [10, 11]. Ionization of analytes using DART begins with an electric discharge in a stream of nitrogen or helium gas that produces a plasma of electrons, ions, and metastable species [10]. DART ion source can produce positive molecular ions,

protonated molecules and positive-charge adduct ions such as ammoniated ions and negative-charge ions [12].

The aim of present study was to compare three different approaches for analysis of CGs in flaxseed. Performance characteristics and results obtained by validated DART-TOFMS and DART-OrbitrapMS methods were confronted with conventional LC-MS/MS attitude.

## 2. Experimental

### 2.1. Standards and Chemicals

The standards of cyanogenic glucosides, linustatin ( $\geq 91.7\%$ ) and neolinustatin ( $\geq 93.7\%$ ) were purchased from ChromaDex (USA). Standards of linamarin ( $\geq 98\%$ ) and amygdalin ( $\geq 99\%$ ) were obtained from Sigma-Aldrich (Germany). Standard of lotaustralin ( $>98\%$ ) was purchased from Molekula (Germany). Methanol of HPLC grade, and sodium acetate were purchased from Sigma-Aldrich (Germany). The deionised water was prepared using Milli-Q water system (Millipore, USA).

### 2.2. Samples, Sample Preparation

Flaxseed samples were obtained from Agritec Plant Research Ltd. (Šumperk, Czech Republic). The levels of CGs were monitored in oil flax cultivars: Amon, Oural, and Recital, and fibre flax cultivar: Venica. Homogenized flaxseeds were extracted with methanol:water (60:40, v/v) under ultrasonic bath.

### 2.3. Instrumentation

HPLC analysis were performed on an Alliance chromatography separation Module 2695 (Waters, USA). Analytes were separated on Synergi HydroRP column (Phenomenex, Germany) (150 mm  $\times$  3.0 mm i. d., 4  $\mu$ m) with gradient elution of mobile phase consisted of 0.5% 50 $\mu$ M sodium acetate and methanol. Detection was performed with a Quattro Premier XE (Waters, UK) employing an electrospray ionization source operating in positive mode. The total run time for each sample was 20 min.

DART-TOFMS system consisted of a DART ion source (IonSense, USA) and AccuTOF LP time-of-flight mass spectrometer (JEOL Europe, France). Flaxseed extracts were introduced by the Dip-it tips (IonSense, USA), which were immersed into the extract and then were placed in the gas stream between the DART ion source and the AccuTOF atmospheric pressure interface. At the end of each run, mass

spectrum of polyethylen glycol (PEG) solution was acquired to perform mass drift compensation. DART ion source was operated in a positive ionization mode. The resolving power of TOF mass analyzer was 3.500 FWHM (full width at half maximum). The total run for each sample was 1 min.

DART ion source (IonSense, Saugus, USA) coupled to Exactive<sup>TM</sup> benchtop Orbitrap mass spectrometer was employed. Samples extracts were introduced by Dip-tips into the gas beam. The resolving power of Exactive<sup>TM</sup> benchtop Orbitrap mass spectrometer was 50.000 FWHM. The total run for each sample was 1 min.

### 2.4. Methods Validation

Quantification:

- LC-MS/MS: Analytes were quantified by external solvent standards calibration containing from 2 to 1000 ng mL<sup>-1</sup> of target analytes.
- DART-TOFMS and DART-OrbitrapMS: Analytes were quantified by the standard addition method. The crude flaxseed extracts were spiked with standard solution of analytes to increase the analytical signal by a factor of 1.5 to 3.

Limit of detection (LOD) was determined based on signal-to-noise ratios (S/N) of 3:1.

Repeatability (expressed as a relative standard deviation, RSD) was determined by repetitive ( $n = 6$ ) analysis.

## 3. Results and Discussion

### 3.1. Optimization of Extraction and LC-MS/MS Analysis

LC-MS/MS analysis of CGs were performed with aqueous methanolic extracts of flaxseeds. CGs were not easily ionized themselves therefore to support Na<sup>+</sup> adduct formation, sodium acetate was added to the mobile phase. In positive electrospray ionization mode, sodium adducts [M+Na]<sup>+</sup> were achieved as a parent masses. Monitored ion transitions and retention times for each compound are summarized in Table 1. The separation was carried out with Synergi HydroRP (150  $\times$  3 mm i.d., 4  $\mu$ m) column, chromatogram of CGs of real flaxseed sample is shown in Figure 2.

### 3.2. Optimization of DART-TOF MS Analysis

Qualitative analysis. The operational parameters of DART-TOF MS system were optimized within the initial experiments carried out with solvent standards

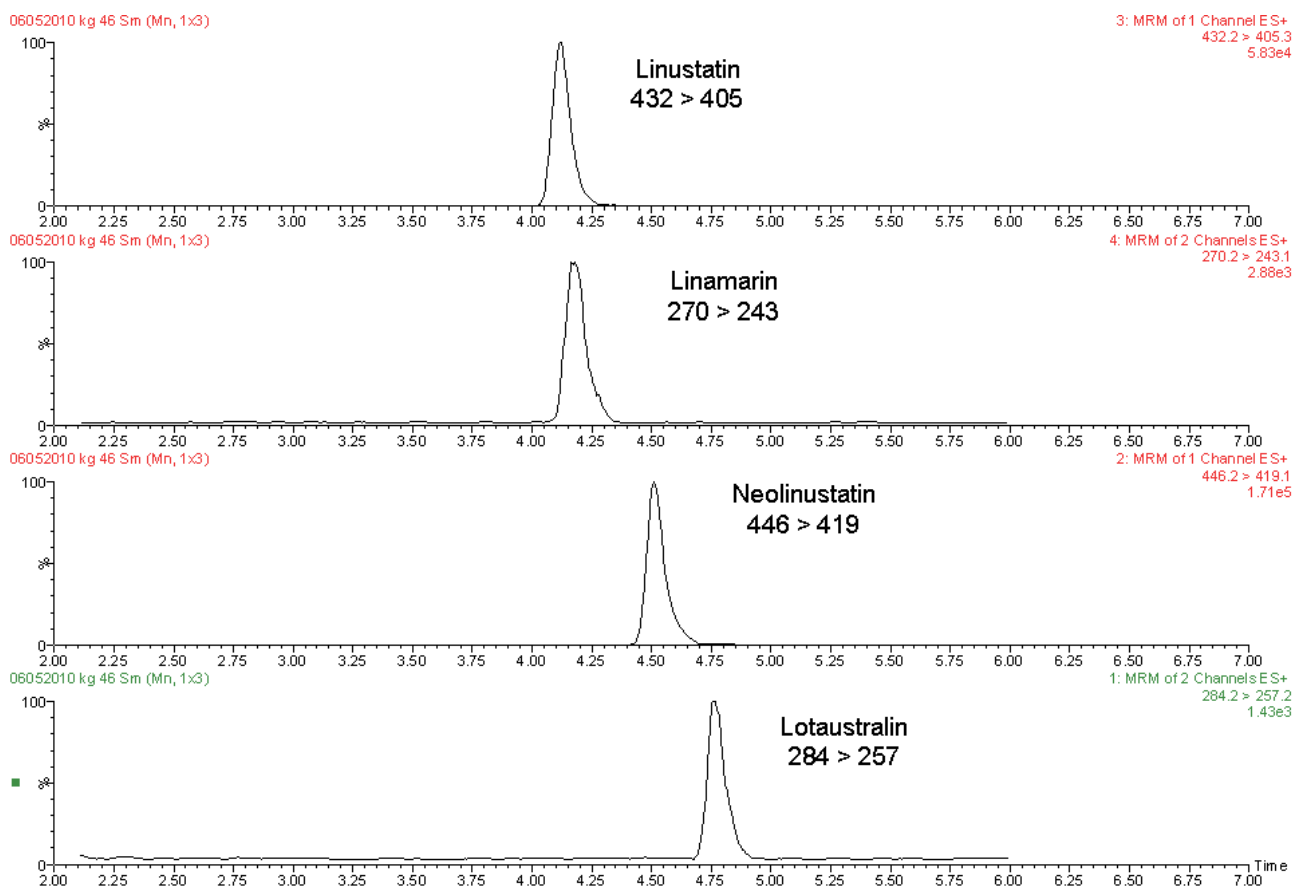


**Fig. 2.** LC-MS/MS chromatogram of real sample Recital containing linustatin at concentration 1582 mg kg<sup>-1</sup>, linamarin 50 mg kg<sup>-1</sup>, neolinustatin 468 mg kg<sup>-1</sup> and lotaustralin 32 mg kg<sup>-1</sup>.

**Table 1**

Monitored transitions and retention times of cyanogenic glucosides in LC-MS/MS.

Compound	Monitored transition [m/z]	Retention time [min]
linustatin	432 > 405	4.04
linamarin	270 > 243	4.13
neolinustatin	446 > 419	4.44
lotaustralin	284 > 257	4.73

of CGs. DART ion source operated in positive ionisation mode provided spectra with the most abundant ions corresponded to molecular adducts  $[M+NH_4]^+$  of CGs. For detection, internal mass drift correction was carried out using solution of PEG. In the samples extracts, major analytes, linustatin and

neolinustatin, were reliably identified, whilst minor CGs, linamarin and lotaustralin, which in samples occurred in low concentrations (25 times lower than major CGs) were identified with insufficient mass accuracy. Theoretical exact masses corresponded to monitored  $[M+NH_4]^+$  adducts are summarized in Table 2. Mass spectrum of real sample obtained by DART-TOF MS analysis is shown in Figure 3.

*Quantitative analysis.* Sample preparation for DART-TOF MS (as well for DART-Orbitrap MS) analysis resulted from the extraction method validated for LC-MS/MS. For quantitative analysis employing DART ion source it was necessary to use an internal standard to compensate relatively high variation of ions intensities in repeated analysis. In our case amygdaline was used.

**Table 2**

Elemental composition and theoretical exact masses of monitored cyanogenic glucosides.

cyanogenic glucosides	analyte	elemental composition of $[M+NH_4]^+$ adduct	theoretical mass $[m/z]$ $[M+NH_4]^+$
major	linustatin	C <sub>16</sub> H <sub>31</sub> N <sub>2</sub> O <sub>11</sub>	427.1928
	neolinustatin	C <sub>17</sub> H <sub>33</sub> N <sub>2</sub> O <sub>11</sub>	441.2084
minor	linamarin	C <sub>10</sub> H <sub>21</sub> N <sub>2</sub> O <sub>6</sub>	265.1399
	lotaustralin	C <sub>11</sub> H <sub>23</sub> N <sub>2</sub> O <sub>6</sub>	279.1556

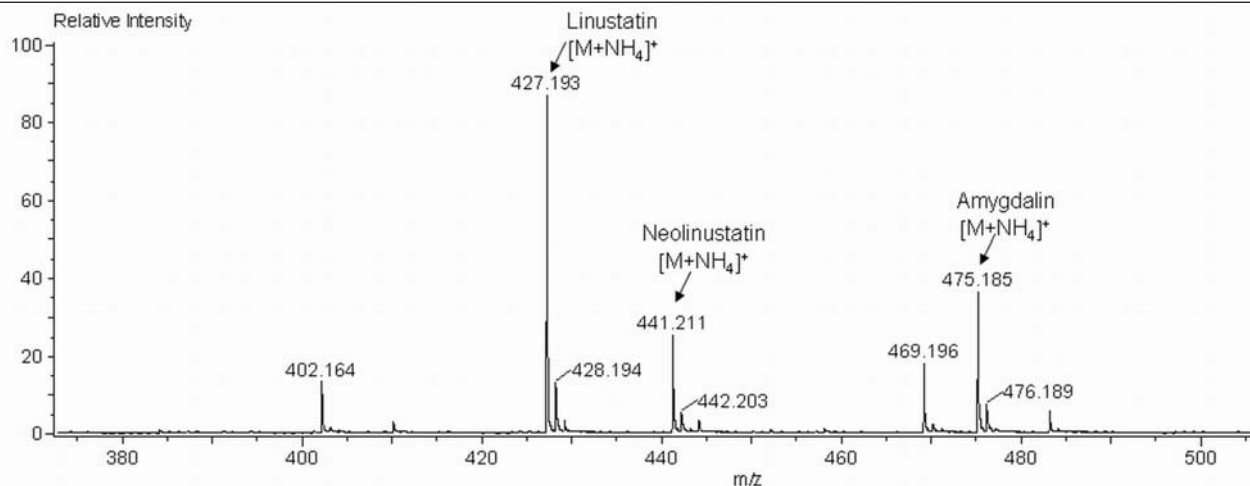


**Fig. 3.** DART-TOFMS mass spectrum (positive ionisation) of real sample Recital, identification of linustatin, neolinustatin and internal standard amygdalin.

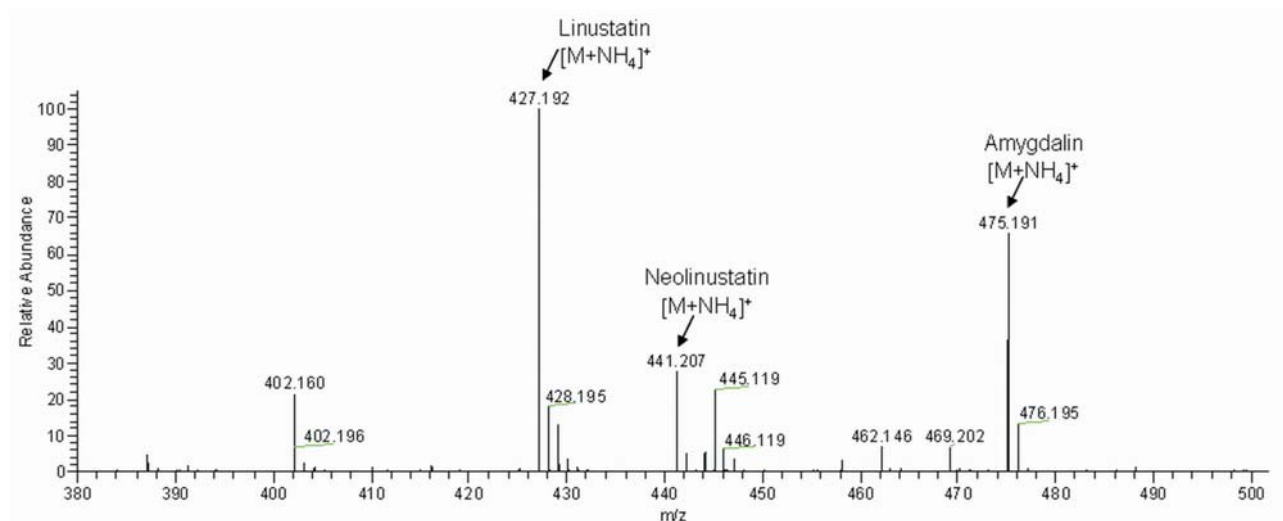


**Fig. 4.** DART-OrbitrapMS spectrum (positive ionisation) of flaxseed sample Recital, identification of linustatin, neolinustatin and internal standard amygdalin.

### 3.3. Optimization of DART-Orbitrap MS Analysis

DART-Orbitrap MS analysis were carried out with identical flaxseed extracts as were used for DART-TOF MS analysis. The operational parameters of the system were adjusted using solvent standards of CGs. Molecular adducts  $[M+NH_4]^+$  of target analytes were detected with high resolving power corresponded to 50 000 FWHM. Both major and minor CGs were reliably identified, but only linustatin and neolinustatin were quantified. High variation of ion intensities of linamarin and lotaustralin did not allow to quantify this group of CGs. DART-Orbitrap MS mass spectrum of real sample is shown in Figure 4.

### 3.4. Methods Validation

LC-MS/MS: Quantification was carried out through external calibration curves obtained by plotting the standard concentration versus the amount of the

analytes ( $ng\ mL^{-1}$ ). The stock standard mixtures were diluted to ten following concentrations: 2, 5, 10, 20, 50, 100, 200, 300, 500, 1000  $ng\ mL^{-1}$ . No matrix effects appeared during LC-MS/MS analysis. The values of LODs were 0.4  $mg\ kg^{-1}$  for major CGs and 2  $mg\ kg^{-1}$  for minor CGs. RSD ranged from 0.8 to 2.1%.

DART-TOF MS and DART-Orbitrap MS: Quantification was carried out using standard addition method, because the matrix components influenced the ionisation process. The fluctuation of ion intensities of low flaxseed concentrations of linamarin and lotaustralin did not allowed to quantify these analytes by methods DART-TOF MS and DART-Orbitrap MS. LODs of major CGs were 200  $mg\ kg^{-1}$  using DART-TOF MS and 10  $mg\ kg^{-1}$  employing DART-Orbitrap MS. Relative standard deviation for DART-TOF MS method reached to 13%, while DART-Orbitrap MS technique provided RSD about 5–7%.

### 3.5. Comparison of DART-TOF MS and DART-Orbitrap MS Results with LC-MS/MS

Four varieties of flaxseed samples were examined using LC-MS/MS, DART-TOF MS and DART-Orbitrap MS techniques. The levels of linustatin and neolinustatin in tested samples ranged from 900 to 2550 mg kg<sup>-1</sup> and from 460 to 1430 mg kg<sup>-1</sup>, resp. The outcomes were in relatively good agreement, the minor diversity (max. 15%) resulted from the different repetabilities of employed methods.

### 3.6. Comparison of LC-MS/MS, DART-TOF MS and DART-Orbitrap MS Methods for Determination of CGs in Flaxseed

LC-MS/MS technique enabled quantification of both major and minor CGs. Low concentrations of minor CGs were not quantified by DART-TOF MS and DART-Orbitrap MS, but their content constitutes only 3% of total CGs amount in flaxseeds, thus their concentrations can be considered as insignificant. Major CGs were reliably quantified by DART-Orbitrap MS and DART-TOF MS methods. DART-Orbitrap MS technique (FWHM 50.000) provided lower LODs and better repeatability in comparison with DART-TOF MS (FWHM 3.500). Employing of DART ion source enabled significant improvement in sample throughput.

## 4. Conclusions

Different approaches in analysis of CGs in flaxseed were tested. For rapid determination of major CGs, linustatin and neolinustatin, DART-TOFMS and DART-OrbitrapMS methods were optimized and validated. Achieved results corresponded well with LC-MS/MS outcomes.

## Acknowledgements

This study was carried out within the projects NPVII 2B06087 and MSM 6046137305 supported by the Ministry of Education, Youth and Sports of the Czech Republic.

## References

- [1] Zagrobelny M., Bak S., Ekstrøm C. T., Olsen C. E., Møller B. L.: *Insect Biochem. Mol. Biol.* **37** (2007), 10–18.
- [2] Bak S., Paquette S. M., Morant M., Morant A. V., Saito S., Bjarnholt N., Zagrobelny M., Jørgensen K., Osmani S., Simonsen H. T., Pérez R. S., van Heeswijck T. B., Jørgensen B., Møller B. L.: *Phytochem. Rev.* **5** (2006), 309–329.
- [3] White W. L. B., Arias-Garzon D. I., McMahon J. M., Sayre R. T.: *Plant Physiol.* **116** (1998), 1219–1225.
- [4] Wanasundara P. K. J. P. D., Shahidi F., Brosnan M. E.: *Food Chem.* **65** (1999), 289–295.
- [5] Oomah B. D., Mazza G., Kenaschuk E. O.: *J. Agric. Food Chem.* **40** (1992), 1346–1348.
- [6] Chassagne D., Crouzet J. C., Bayonove C. L., Baumes R. L.: *J. Agric. Food Chem.* **44** (1996), 3817–3820.
- [7] Mazza G., Cottrell T.: *J. Food Comp. Anal.* **21** (2008), 249–254.
- [8] Bjarnholt N., Rook F., Motawia M. S., Cornett C., Jørgensen Ch., Olsen C. E., Jaroszewski J. W., Bak S., Møller B. L.: *Phytochem.* **69** (2008), 1507–1516.
- [9] Cody R. B., Laramée J. A., Durst H. D.: *Anal. Chem.* **77** (2005), 2297–2302.
- [10] Petucci Ch., Diffendal J., Kaufman D., Mekonnen B., Terefenko G., Musselman B.: *Anal. Chem.* **79** (2007), 5064–5070.
- [11] Haeflinger O. P., Jeckelmann N.: *Rapid Commun. Mass Spectrom.* **21** (2007), 1361–1366.
- [12] Curtis M. E., Jones P. R., Sparkman O. D., Cody R. B.: *J. Am. Soc. Mass. Spectrom.* **20** (2009), 2082–2086.

# Chiral Separation of Binaphthyl Catalysts Using New Chiral Stationary Phases Based on Derivatized Cyclofructans

LUCIE JANEČKOVÁ<sup>a</sup>, KVĚTA KALÍKOVÁ<sup>b</sup>, ZUZANA BOSÁKOVÁ<sup>a</sup>, EVA TESAŘOVÁ<sup>b</sup>

<sup>a</sup>Department of Analytical Chemistry, <sup>b</sup>Department of Physical and Macromolecular Chemistry, Faculty of Science, Charles University in Prague, Albertov 6/2030, 128 43 Prague, Czech Republic, ✉ janecko2@natur.cuni.cz

## Abstract

Cyclofructans as a completely new and promising class of chiral selectors have been introduced last year for application in separation techniques such as liquid chromatography and capillary electrophoresis. Mainly derivatives of cyclofructans perform interesting separation possibilities for a variety of compounds. The aromatic derivatized cyclofructans composed of six D-fructofuranose units (CF6) have exhibited the most interesting properties and unique enantioselectivity.

In this work, two derivatized cyclofructan-based chiral stationary phases, RN-CF6 (*R*-naphthylethyl carbamate CF6) and DMP-CF7 (dimethylphenyl carbamate CF7) were used for enantioseparation of substituted binaphthyl catalysts, widely used to control asymmetric processes. Normal separation mode, i.e. mobile phase composed of hexane and propane-2-ol in different ratios was applied and the enantioselectivity of the employed stationary phases was compared.

## Keywords

chiral stationary phase  
cyclofructans  
enantioseparation  
HPLC  
substituted binaphthyls

## 1. Introduction

Chiral separations have been given great attention over the past few decades due to their wide range of applications in pharmaceutical and food industry or agriculture. High performance liquid chromatography (HPLC) employing chiral stationary phases (CSPs) has become one of the most common and powerful techniques in enantioselective separations at both analytical and preparative scales. Variety of CSPs, usually bonded to silica gel, with complex interaction mechanisms have been reported [1]. Some classes of chiral selectors dominate the enantiomeric separations, i.e. cyclodextrins (CDs), polysaccharides and their derivatives or macrocyclic antibiotics such as vancomycin, teicoplanin or ristocetin A. Many applications of these chiral selectors have been published [1–4].

A unique class of CSPs based on cyclofructan has been introduced last year with the expectation of great separation potential both for HPLC [5] and CZE [6]. Cyclofructans (CFs) belong to a group of macrocyclic oligosaccharides with a crown ether skeleton. They consist of six or more  $\beta$ -(2 $\rightarrow$ 1) linked D-fructofuranose units (see Figure 1) and each fructofuranose unit contains four stereogenic centers and three hydroxyl groups, which can be mostly derivatized. The abbreviations such as CF6, CF7, CF8 etc. indicate

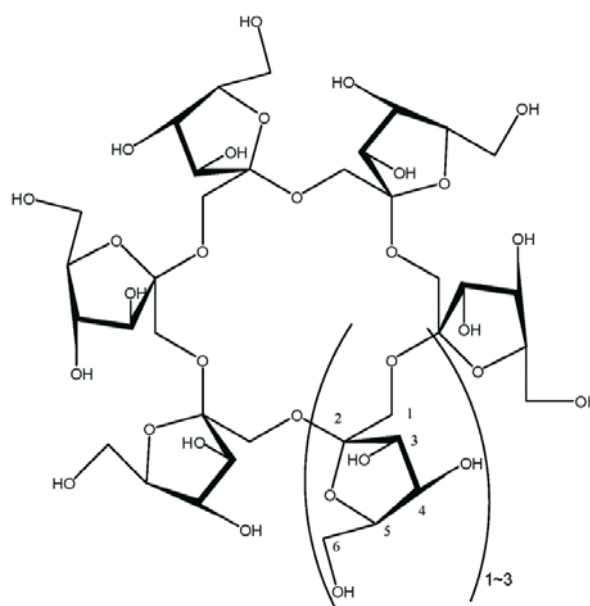
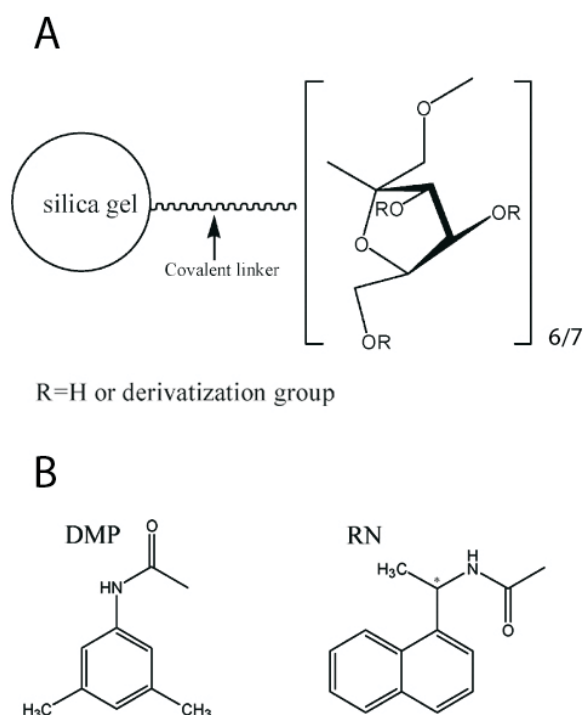


Fig. 1. Molecular structure of cyclofructan (CF6, CF7 and CF8).

the number of fructose units in the macrocyclic ring. CF6 has been largely studied due to its highly defined geometry and availability in pure form [5].

Native CFs perform rather limited enantioselectivity but their derivatized (aliphatic or aromatic functionalized) forms show improved and unique separation possibilities over a wide range of analytes.



**Fig. 2.** Scheme of (A) chemically-bonded CF6/CF7 stationary phase, and (B) chemical structures of the derivatizing groups.

Figure 2 shows two CF derivatives studied in this work. RN-CF6 utilizes *R*-naphthylethyl-functionalized CF6 as the chiral selector. It proves excellent enantioselectivity toward various types of analytes including acids, secondary and tertiary amines, alcohols, and many neutral compounds. As the chiral selector is covalently bonded to the silica gel carrier this CSP is compatible with all common organic solvents creating a wide range of compound types that can be separated [7]. DMP-CF7 was developed as a 3,5-dimethylphenyl functionalized CF7. This column also provides chiral recognition toward a broad variety of compounds. In addition, it demonstrates complementary enantioselectivity when compared to RN-CF6 [7]. Both CSPs can operate in all three separation modes (normal-, reversed-phase and polar-organic) but mostly higher selectivity can be obtained in normal-phase mode.

Binaphthyl derivatives have been extensively used to control asymmetric processes and have demonstrated excellent chiral discrimination properties, due to their unique features derived from their chirality, spatial arrangement and rigidity. The chirality of these molecules is caused by restricted rotation around the single bond in the binaphthyl skeleton [8]. Although the basic structures of the binaphthyl derivatives are similar, the substituents and their position significantly affect their properties.

Most papers on binaphthyls derivatives deal with their synthesis. Enantioselective HPLC has been used

to control the enantiomeric purity or the yield of individual final products. Just a few studies of enantioselective interactions of these compounds with CSPs can be found in the literature [9–11]. That is why we included these analytes into a set of testing compounds for the evaluation of the enantio-separation abilities of the newly developed cyclofructan-based CSPs. We worked in the normal-phase separation system with hexane and propane-2-ol as mobile phase constituents. The effect of the solvents ratio and addition of trifluoroacetic acid (TFA) was studied. We show here just our preliminary results as the work is currently in progress.

## 2. Experimental

Organic solvents of HPLC grade, *n*-hexane (HEX) and propane-2-ol (IPA), were purchased from Sigma Aldrich (St. Louis, USA). Trifluoroacetic acid (TFA), 98% purity, was from Fluka Chemie (Buchs, Germany).

The studied analytes have been synthesized as racemates at the Department of Organic and Nuclear Chemistry, Faculty of Science, Charles University in Prague. The synthesis procedure has been described in detail in Ref. [10]. The chromatographic behavior of nine compounds, i.e. binaphthol, analyte **1**, **4**, **5**, **6**, **7**, **9**, **12**, **13**, was studied in this work. Figure 3 (on next page) shows the structures of these analytes.

The chromatographic measurements were carried out on two HPLC systems (Waters, Milford, USA): Waters HPLC Breeze System (consisting of HPLC Gradient Pump 1525, an autosampler 717Plus, a column heater Jetstream 2 Plus and a UV-Vis dual absorbance detector 2487; Breeze software) and Waters Alliance System (Waters 2695 Separation Module, Waters 2996 Photodiode Array Detector, an autosampler 717Plus and a Waters Alliance Series column heater; Empower software). Chromatographic columns RN-CF6 and DMP-CF7 (column size 250 × 4.6 mm) with silica gel (particle size 5 μm) as a carrier of the CSPs were used. The chiral selectors bonded to the support were naphthyl ethyl substituted cyclofructan with 6 D-fructose units for RN-CF6 column and dimethyl phenyl derivatized cyclofructan with 7 D-fructose units for DMP-CF7 CSP. These columns have been prepared at the Department of Chemistry and Biochemistry, University of Texas at Arlington, Arlington, Texas.

Normal-phase mode was applied, i.e. mobile phase was composed of HEX/IPA in various volume ratios, the addition of TFA was also tested. The flow rate was 1 mL min<sup>-1</sup>, the temperature was 25 °C and the detection wavelength was 254 nm.

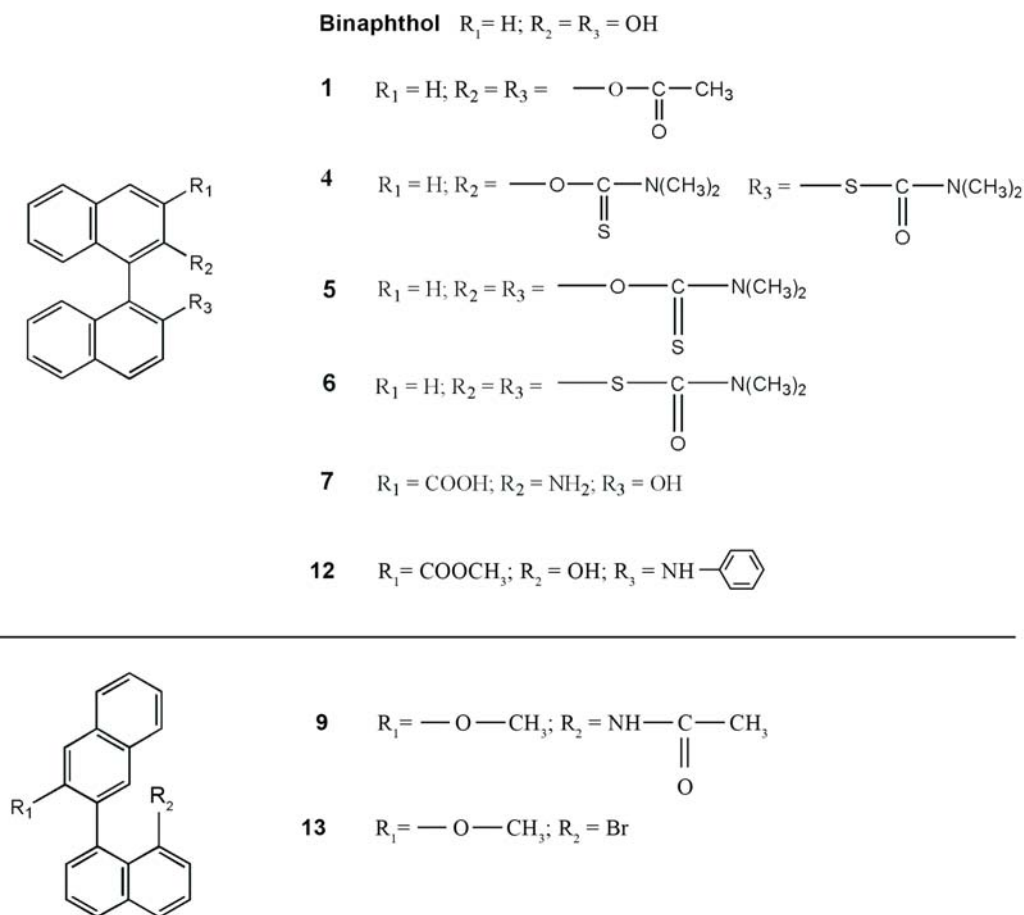


Fig. 3. Structures of the binaphthyl derivatives, studied in this work.

### 3. Results and Discussion

Two novel CSPs based on cyclofructans working in normal-phase mode were tested and successful enantioseparations of some binaphthyl derivatives were achieved so far. Other testing compounds (e.g. blockers, profens and other chiral pharmaceuticals of diverse structures) were also used to evaluate the separation properties of these CSPs. These experiments are not finished and thus we deal only with binaphthyls in this paper.

RN-CF6 column was evaluated using seven mobile phases differing in volume ratios of HEX/IPA and/or the addition of TFA. Enantioseparation of binaphthol, analyte **1** and analyte **4** was achieved in all the mobile phases but the resolution did not exceed 1.5. Sample **5** performed the best enantioseparation in HEX/IPA, 90/10 (v/v), and its enantioresolution was sufficient in all the mobile phases studied. Other analytes (**6**, **9**, **12** and **13**) were not separated in the tested systems. The addition of TFA to the mobile phase did not have significant impact on retention and resolution of the enantiomers with the exception of analyte **7** that has accessible ionizable groups. The

addition of TFA significantly improved its enantio-resolution, due to enhanced efficiency of the TFA modified separation system, which is obvious from Figure 4.

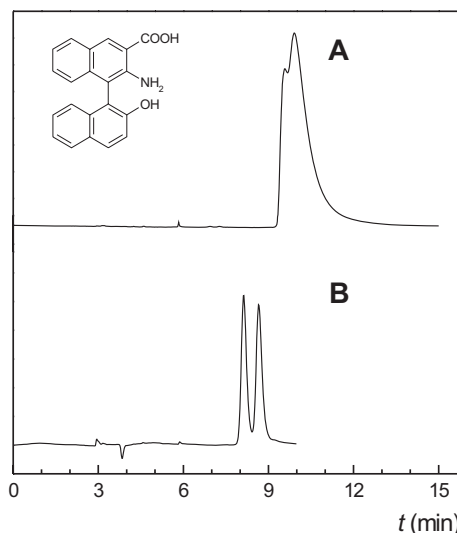
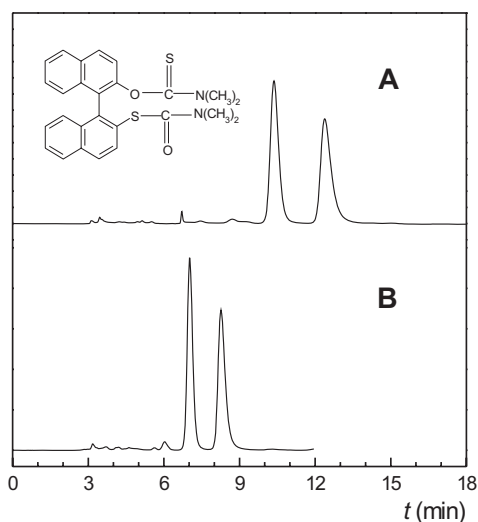


Fig. 4. Separation of analyte **7**; column RN-CF6; mobile phase: (A) HEX/IPA, 80/20 (v/v), (B) HEX/IPA/TFA, 80/20/0.5 (v/v/v); temperature: 25 °C, flow rate: 1 mL min<sup>-1</sup>, UV detection: 254 nm.



**Fig. 5.** Separation of analyte **4**; column DMP-CF7; mobile phase: (A) HEX/IPA, 80/20 (v/v), (B) HEX/IPA, 60/40 (v/v); temperature: 25 °C, flow rate: 1 mL min<sup>-1</sup>, UV detection: 254 nm

DMP-CF7 column was tested using two mobile phases, based on the results obtained with RN-CF6 CSP. The mobile phases were composed of HEX/IPA, 80/20 (v/v) and HEX/IPA, 60/40 (v/v). In these two systems enantioseparations with excellent resolution values were achieved for binaphthol, analyte **4** and analyte **5**. Figure 5 illustrates excellent separation of analyte **4** in the studied mobile phases. Samples **1** and **12** performed partial separation. Four other compounds studied (analyte **6**, **7**, **9** and **13**) did not show any enantioseparation in the mobile phases studied as on RN-CF6 column. Increased amount of IPA in the mobile phase slightly decreased the retention of the analytes and improved enantioresolution. The addition of TFA is being currently tested, hence the results cannot be shown here. Figure 5 illustrates excellent separation of analyte **4** in the studied mobile phases.

## 4. Conclusion

Novel CSPs based on derivatized cyclofructan were tested for enantioseparation of binaphthyl derivatives, which are widely employed as catalysts of asymmetric processes. The experiments showed good separation abilities of the both cyclofructan-based CSPs in normal chromatographic mode. DMP-CF7 column offered much higher enantioresolution of some binaphthyl derivatives than did RN-CF6. The enantioselectivity of the employed CSPs seems to be slightly different, because of their different structures. The addition of TFA can help to improve the resolution.

## Acknowledgments

The Grant Agency of the Charles University in Prague, project SVV 261204 and the Ministry of Education, Youth and Sports of the Czech Republic, projects RP 14/63 and MSM0021620857 are gratefully acknowledged for the financial support. We also gratefully acknowledge prof. Daniel W. Armstrong for donating the columns.

## References

- [1] Ward T. J., Baker B. A.: *Anal. Chem.* **80** (2008), 4363–4372.
- [2] Gübitz G., Schmid M. G.: *Mol. Biotechnol.* **32** (2006), 159–179.
- [3] Gübitz G., Schmid M. G.: *Chiral Separations. Methods and Protocols. (Methods in Molecular Biology, Vol. 243.)* Humana Press, Totowa 2004.
- [4] Liu Y., Berthod A., Mitchell C. R., Xiao T. L., Zhang B., Armstrong D. W.: *J. Chromatogr. A* **978** (2002), 185–204.
- [5] Sun P., Wang Ch., Breitbach Z. S., Zhang Y., Armstrong D. W.: *Anal. Chem.* **81** (2009), 10215–10226.
- [6] Jiang C., Tong M. Y., Breitbach Z. S., Armstrong D. W.: *Electrophoresis* **30** (2009), 3897–3909.
- [7] <http://azypusa.com/index-2.html> (cited 10.8.2010).
- [8] Pu L.: *Chem. Rev.* **8** (1998), 2405–2494.
- [9] Loukotková L., Tesařová E., Bosáková Z., Repko P., Armstrong D. W.: *J. Sep. Sci.* **33** (2010), 1244–1254.
- [10] Loukotková L., Rambousková M., Bosáková Z., Tesařová E.: *Chirality* **20** (2008), 900–909.
- [11] Han X., Berthod A., Wang C., Huang K., Armstrong D. W.: *Chromatographia* **65** (2007), 381–400.

# Comparison of Two Methods of Calculation LSER Descriptor $L$ on Retention Data of Octenes

ŠTĚPÁN JIRKAL, JIŘÍ G. K. ŠEVČÍK

Department of Analytical Chemistry, Faculty of Science, Charles University in Prague, Albertov 6, 128 43 Prague 2, Czech Republic, ✉ [maus@natur.cuni.cz](mailto:maus@natur.cuni.cz)

## Keywords

alkenes  
calculation of descriptors  
gas chromatography  
LSER  
prediction retention

## Abstract

Linear Solvation Energy Relationships (LSER) is a method used for description of separation process in chromatography. Descriptor  $L$  is an important parameter influencing partition of analytes in gas chromatography. Two access of calculation  $L$  based on a sum of contribution have been used, method Havelec-Ševčík (HS) and method Platts-Butina (PB). The values  $L$  together with a calculated descriptor  $E$  have been applied for prediction of retention 93 acyclic octenes on stationary phase squalan and polydimethylsiloxan. The description of retention behaviour was more suitable in case of application the descriptor  $L_{PB}$ . While using only one variable to predict the retention, estimation with the descriptor  $L_{HS}$  was more convenient. In both cases, LSER method provided good description of the separation process.

## 1. Introduction

Knowledge of separation mechanism in gas chromatography can be important in selection of experimental procedure. Linear Solvation Energy Relationships (LSER) is a method for description of retention, which can evaluate selective types of interaction [1]

$$SP = lL + eE + sS + aA + bB + c \quad (1)$$

where  $SP$  is solute property, i.e. retention characteristic as  $\log k$  or retention index ( $RI$ );  $L$ ,  $E$ ,  $S$ ,  $A$ ,  $B$  are solute descriptors (selective properties of separated solute);  $l$ ,  $e$ ,  $s$ ,  $a$ ,  $b$  are regression coefficients (properties of stationary phase). The  $L$  is descriptor of partition coefficient between gas and hexadecane (known as  $\log L^{16}$ ). The  $E$  is excess molar refraction (known as  $R_2$ ). The  $S$  is descriptor of dipolarity or polarisability (known as  $\pi_2^H$ ). The  $A$  is descriptor of acidity (known as  $\Sigma\alpha_2^H$ ). The  $B$  is descriptor of basicity (known as  $\Sigma\beta_2^H$ ). The  $c$  is constant (without specific chemical meaning).

Descriptors are known for more than 5000 compounds. It is possible to calculate them for other substances by variety methods of estimation, but the accuracy is limited [2, 3].

The aim of this work is to compare two methods of calculation the descriptor  $L$  applied on prediction retention of octenes. The database of known substances contains only a small group of octenes. In this work, the retention data include all acyclic 93 octenes. It is necessary to calculate the descriptors for these

compounds. Then, it is possible to estimate the retention of studied analytes. Calculated values of retention can be compared with the experimental and ability of prediction can be evaluated. Based on chemometrics, it is possible to assess, which model is more suitable to describe the retention.

## 2. Experimental

### 2.1. Methods

Octenes, generally all alkenes, create limited types of interactions with the stationary phase. Therefore, just two terms of LSER equation (1) are significant,  $lL$  and  $eE$ . The descriptors  $S$  and  $B$  have a constant value for all alkenes and the descriptor  $A$  is equal to zero. Hence, there is a specific form of LSER equation for prediction of retention octenes:

$$RI = lL + eE + c \quad (2)$$

where  $RI$  denotes retention index and other parameters are the same as in equation (1). Descriptor  $L$  can be experimentally determined as a logarithm of partition coefficient gas/hexadecane ( $\log L^{16}$ ), ref. [4]. Two access of calculation  $L$  are applied in this work, based on a sum of particular contributions of the molecule, method Havelec-Ševčík (HS) [5] and method Platts-Butina (PB) [6]. It can be seen in Table 1 that the standard deviation of *cis* contribution is rather large than the others.

Descriptor  $E$  is defined as a difference of molar refraction of compound and refraction of hypothetical

**Table 1**

Table of specific value of contribution for calculation of descriptor  $L$  by method Havelec-Ševčík and method Platts-Butina. The standard deviation of the contribution is marked as *s.d.*; alkyl interaction means contribution of two neighboring alkyles bonded on main carbon chain.

Group	Havelec-Ševčík		Platts-Butina	
	value	<i>s.d.</i>	value	<i>s.d.</i>
-CH <sub>3</sub>	0.340	0.006	0.321	0.009
-CH <sub>2</sub> -	0.502	0.001	0.499	0.002
-CH<	0.467	0.012	0.449	0.011
>C<	0.443	0.021	0.443	0.025
=CH <sub>2</sub>	0.249	0.016	0.244	0.021
=CH-	0.504	0.013	0.469	0.004
=C<	0.658	0.020	0.624	0.008
<i>cis</i> isomer	0.112	0.040	-	-
alkyl interaction	0.119	0.013	-	-
intercept	-	-	0.130	0.025

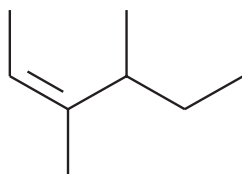
alkanes with the same molar volume as the compound [2, 3]. This descriptor can be easily calculated from refractive index and McGowan's volume ( $V_x$ ) of the molecule [7].

## 2.2. Calculation of Descriptors and Correlation with Experimental Retention

Retention data of 93 octenes were taken from work Soják and Kubinec [8]. Experimental data include all isomers of C8 acyclic alkenes with a double bond. These compounds were measured by gas chromatography with mass spectrometry detection (GC-MS) on stationary phase squalan and polydimethylsiloxan (PDMS).

The descriptor  $L$  has been calculated for all analytes, by the method HS and PB. Value of  $L$  for a compound has been obtained as a sum of contribution fragments listed in Table 1.

The descriptor  $E$  has been calculated based on methods as was mentioned (2.1 methods).



$$\begin{aligned}
 L_{\text{HS}} &= 4 \times (-\text{CH}_3) + (= \text{CH}-) + (= \text{C} <) + (-\text{CH} <) + (-\text{CH}_2-) + \\
 &+ (\textit{cis} \text{ isomer}) + (\text{alkyl interaction}) = \\
 &= 4 \times 0.34 + 0.504 + 0.658 + 0.467 + 0.502 + 0.112 + \\
 &+ 0.119 = \mathbf{3.722}
 \end{aligned}$$

$$\begin{aligned}
 L_{\text{PB}} &= 4 \times (-\text{CH}_3) + (= \text{CH}-) + (= \text{C} <) + (-\text{CH} <) + (-\text{CH}_2-) + \\
 &+ (\text{intercept}) = \\
 &= 4 \times 0.321 + 0.469 + 0.624 + 0.449 + 0.499 + 0.13 = \mathbf{3.455}
 \end{aligned}$$

**Fig. 1.** Example of calculation descriptor  $L$  for 3,4-dimethyl-Z-2-hexene.

Calculated values of  $L$  and  $E$  have been statistically processed using multiple linear regression analysis to set a dependence with the experimental retention. This procedure resulted in regression coefficients of equation (2) and statistical parameters. All calculations were done on computer with Microsoft Excell 2002.

## 3. Results and Discussion

Values of the descriptor  $L$  have been calculated by both methods, HS and PB. Further, values of the descriptor  $E$  have been obtained for 82 compounds. Due to inaccessibility of refractive index for 11 octenes, it has been impossible to calculate  $E$  for all compounds.

In case of descriptor  $L_{\text{HS}}$ , a contribution for *cis* interaction was omitted because of better fit to experimental data. It can be seen in Table 1 that the standard deviation of *cis* contribution is rather high. A correlation analysis between  $L$  and  $E$  has been carried out. There was not find any significant relationship. Experimental retention of octenes on Squalan and PDMS has been processed by multiple linear regression analysis with the descriptors  $L_{\text{HS}}$ ,  $E$  and  $L_{\text{PB}}$ ,  $E$ . Four sets of data have been provided this way. Here are regression equations for prediction of retention:

$$\begin{aligned}
 RI &= 135.33 (\pm 11.01) L_{\text{HS}} + 81.23 (\pm 48.44) E + \\
 &+ 266.40 (\pm 34.91) \\
 \text{Squalan-HS: } R^2 &= 0.784, F = 144, \text{AAE}(RI) = 10.48, n = 82
 \end{aligned} \quad (3)$$

$$\begin{aligned}
 RI &= 114.40 (\pm 7.61) L_{\text{PB}} + 225.30 (\pm 36.35) E + \\
 &+ 325.88 (\pm 24.69) \\
 \text{Squalan-PB: } R^2 &= 0.837, F = 203, \text{AAE}(RI) = 8.99, n = 82
 \end{aligned} \quad (4)$$

$$\begin{aligned}
 RI &= 143.40 (\pm 9.7) L_{\text{HS}} + 78.97 (\pm 42.69) E + \\
 &+ 248.86 (\pm 30.77) \\
 \text{PDMS-HS: } R^2 &= 0.838, F = 205, \text{AAE}(RI) = 9.41, n = 82
 \end{aligned} \quad (5)$$

$$\begin{aligned}
 RI &= 119.82 (\pm 6.54) L_{\text{PB}} + 234.33 (\pm 31.23) E + \\
 &+ 316.34 (\pm 21.21) \\
 \text{PDMS-PB: } R^2 &= 0.884, F = 301, \text{AAE}(RI) = 7.89, n = 82
 \end{aligned} \quad (6)$$

The value in parenthesis is the standard error of estimation the coefficient. On the second line, there is a notation of data set and statistical parameters of the regression:  $R^2$  is the coefficient of determination,  $F$  is the Fischer statistic,  $\text{AAE}(RI)$  is the absolute average error, and  $n$  is the number of compounds.

Description of retention by using two variables fits better for the model PB (with descriptor  $L_{\text{PB}}$ ). It is obvious from higher value of the  $F$ -statistics, the coefficient of determination and lower the absolute average error in equations (4) and (6). Based on results of the equations (3)–(6), prediction of retention is

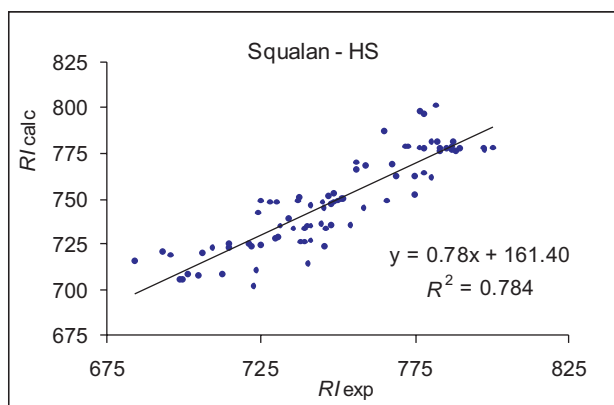


**Fig. 2.** Comparison of experimental retention ( $RI_{exp}$ ) and calculated retention ( $RI_{calc}$ ) of 82 octenes on stationary phase Squalan, based on the two descriptor model Havelec-Ševčík, equation (3).

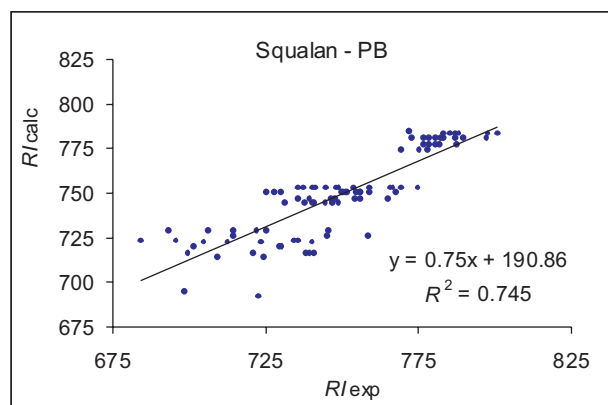


**Fig. 4.** Comparison of experimental retention ( $RI_{exp}$ ) and calculated retention ( $RI_{calc}$ ) of 93 octenes on stationary phase Squalan, based on the one descriptor model Platts-Butina, equation (8).

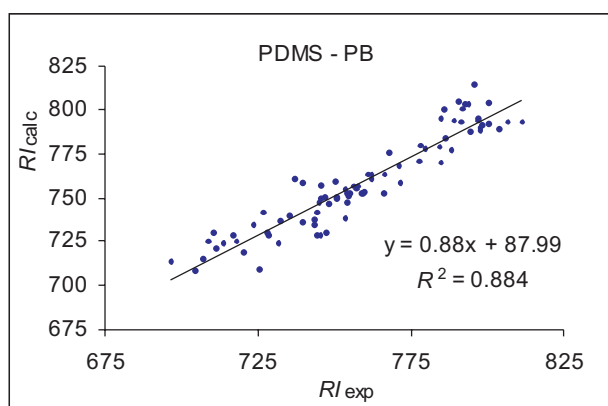


**Fig. 3.** Comparison of experimental retention ( $RI_{exp}$ ) and calculated retention ( $RI_{calc}$ ) of 82 octenes on stationary phase PDMS, based on the two descriptor model Platts-Butina, equation (6).

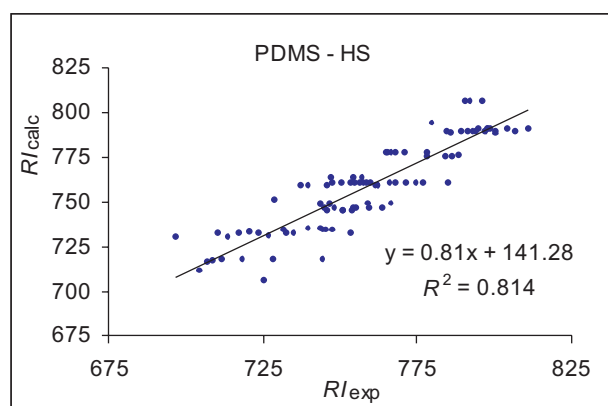


**Fig. 5.** Comparison of experimental retention ( $RI_{exp}$ ) and calculated retention ( $RI_{calc}$ ) of 93 octenes on stationary phase PDMS, based on the one descriptor model Havelec-Ševčík, equation (9).

better on stationary phase PDMS than squalane (Figures 2 and 3).

Next, the linear regression has been processed only with one parameter, the descriptor  $L$ . Knowledge of  $L$  for all 93 octenes is convenient, unlike the previous model with incomplete set of the descriptor  $E$ . Here the predictive ability of the descriptor  $L$  is more evident:

$$RI = 144.70 (\pm 8.66) L_{HS} + 244.27 (\pm 30.22) \quad (7)$$

Squalan-HS:  $R^2 = 0.754$ ,  $F = 279$ ,  $AAE(RI) = 10.75$ ,  $n = 93$

$$RI = 132.60 (\pm 8.13) L_{PB} + 292.48 (\pm 28.01) \quad (8)$$

Squalan-PB:  $R^2 = 0.745$ ,  $F = 266$ ,  $AAE(RI) = 11.10$ ,  $n = 93$

$$RI = 152.65 (\pm 7.65) L_{HS} + 226.86 (\pm 26.71) \quad (9)$$

PDMS-HS:  $R^2 = 0.814$ ,  $F = 398$ ,  $AAE(RI) = 9.61$ ,  $n = 93$

$$RI = 138.68 (\pm 7.49) L_{PB} + 281.87 (\pm 25.8) \quad (10)$$

PDMS-PB:  $R^2 = 0.790$ ,  $F = 343$ ,  $AAE(RI) = 10.22$ ,  $n = 93$

Meaning of symbols is the same as in the previous equations (3)–(6). Both models provided similar results of agreement between experimental and calculated data. Based on statistics parameters ( $R^2$ ,  $F$ ,  $AAE$ ) of equations (7)–(10), it is clear that description of retention by using one parameter is a bit more advantage in application of the descriptor  $L_{HS}$ . Regression coefficient  $l_{HS}$  is higher in equations (7) and (9) than in case of  $l_{PB}$  in equations (8) and (10). It can be said, the term  $l L_{HS}$  more contributes to retention and more affects selectivity of separation unlike the  $l L_{PB}$  (Figures 4 and 5).

Comparing of equation (3)–(10), it is evident, the retention of octenes is better predicted with two parameters equation, the descriptors  $L$  and  $E$ . For this purpose, it is better to use the model PB. Only in situation with knowledge just the descriptor  $L$ , there is more convenient to predict retention with the model HS.

Prediction of retention by LSER method provides only limited accuracy of estimation. On the present, methods based on topological indices are able to predict retention in GC much more accurately. Evaluation of separation process in term of selective interactions is main advantage of LSER.

#### 4. Conclusion

Two methods of calculation the descriptor  $L$  have been used for prediction of retention octenes. Parameter  $L$  has been estimated using by two access, Havelec-Ševčík (HS) and Platts-Butina (PB), based on sum of fragments of molecule. Values  $L_{HS}$  and  $L_{PB}$  have been applied together with the descriptor  $E$  for description of retention. Experimental data of octenes on stationary phase Squalan and Polydimethylsiloxan (PDMS) have been processed by multiple linear regression analysis to find a relationship with the calculated descriptors. Prediction by parameter  $L_{PB}$  provided better fit between experimental and calculated retention. Next, linear regression just with the descriptor  $L$  has been treated. In this case of one

parameter equation, the model HS turned out to be more suitable. Generally, description of retention was better on stationary phase PDMS. LSER method provided satisfactory evaluation of separation process.

#### Acknowledgement

*This work was supported by the Ministry of Education, Youth and Sports of Czech Republic (project No. MSM 113100002).*

#### References

- [1] Carr P.W., Vitha M.: *J. Chromatogr. A* **1126** (2006), 143–194.
- [2] Poole C.F., Atapattu S.N., Poole S.K.: *Anal. Chim. Acta* **652** (2009), 32–53.
- [3] Abraham M.H., Ibrahim A., Zissimos A.M.: *J. Chromatogr. A* **1037** (2004), 29–47.
- [4] Abraham M.H.: *Chem. Soc. Rev.* **22** (1993), 73–83.
- [5] Havelec P., Ševčík J. G. K.: *J. Phys. Chem. Ref. Data* **25** (1996), 1483–1493.
- [6] Platts J.A., Butina D., Abraham M.H., Hersey A.: *J. Chem. Inf. Comput. Sci.* **39** (1999), 835–845.
- [7] Abraham M. H., McGowan J. C.: *Chromatographia* **23** (1987), 243–246.
- [8] Soják L., Addová G., Kubinec R.: *J. Chromatogr. A* **1025** (2004), 237–253.

# Implementation of GC×GC-TOF MS for the Simultaneous Determination of PCBs, PBDEs and PAHs in Environmental Samples

KAMILA KALACHOVÁ, JANA PULKRABOVÁ, TOMÁŠ ČAJKA, LUCIE DRÁBOVÁ, JANA HAJŠLOVÁ ✉

Department of Food Chemistry and Analysis, Faculty of Food and Biochemical Technology, Institute of Chemical Technology, Technická 3, 166 28 Prague 6, Czech Republic, ✉ jana.hajslova@vscht.cz

## Abstract

In this study, comprehensive two-dimensional gas chromatography coupled to time-of-flight mass spectrometry (GC×GC-TOFMS) for the simultaneous determination of eighteen polychlorinated biphenyls (PCBs), seven polybrominated diphenyl ethers (PBDEs) and sixteen polycyclic aromatic hydrocarbons (PAHs) was optimized to obtain the best chromatographic resolution and quantification limits (LOQs) of target analytes. Two injection techniques, pulsed splitless and large volume programmable temperature vaporization (LV-PTV), and several capillary column systems were tested within the experiments (BPX-5 and BPX-50 in the 1st dimension and BPX-50, Rt-LC35 and HT-8 in 2nd dimension). All tested combinations of columns were able to separate all target PCBs and PBDEs. Selection of the column system was therefore mainly influenced by its ability to separate the critical groups of PAHs (1st group: B[a]A, CP[ca]P, and Chr; 2nd group: B[*l*]F, B[*k*]F, and B[*b*]F; 3rd group: DB[*ah*]A, I[*1,2,3-cd*]P, and B[*ghi*]P). Although none of the column combinations evaluated in the present study allowed a complete separation of all target PAHs, a combination of BPX-50 × HT-8 columns showed the best ability to separate the 2nd group of PAHs. Application of PTV injection technique decreased LOQs of almost all target analytes approximately by one order of magnitude. The LOQs achieved using LV-PTV-GC×GC were as follows: PCBs 0.1–0.25 µg kg<sup>-1</sup>, PBDEs 0.5–2.5 µg kg<sup>-1</sup>, PAHs 0.05–0.25 µg kg<sup>-1</sup>.

## Keywords

fish  
GC×GC-TOF MS  
PAH  
PBDE  
PCB  
PTV

## 1. Introduction

To protect consumers' health against undesirable effects originating from food contaminants, several legislative steps have been accepted until now [1]. However, considering the lack of reliable information in some areas, the European Food Safety Authority (EFSA) continually announces the calls to collect information on the occurrence of selected persistent organic pollutants (POPs) in food to assess their potential human exposure [2]. Regarding these requirements, quick, inexpensive and high throughput analytical approaches have to be developed.

Comprehensive two-dimensional gas chromatography (GC×GC) coupled to time-of-flight mass spectrometry (TOF MS) represents a powerful tool for the simultaneous determination of different types of contaminants that considerably increase the separation efficiency of GC analysis [3, 4]. Since the whole system comprises two capillary columns with different polarities, the total peak capacity for GC×GC is the outcome of the individual column

capacities [5]. Moreover, focusing effects allows achieving lower limits of detection needed for the residue analysis as compared with one-dimensional GC [5]. Until now, various applications of GC×GC coupled to TOFMS in food and environmental analyses have been reported [3, 6–11], but according to the authors' best knowledge simultaneous determination of PCBs, PBDEs and PAHs within a single run has never been presented until now.

The main aim of this study was to develop and optimize the GC×GC-TOFMS method for the simultaneous determination of PCBs, PBDEs and PAHs to obtain the best chromatographic resolution and detection limits for all target analytes. Therefore, several chromatographic capillary column combinations were tested. In the subsequent experiments, the large volume programmable temperature vaporization (LV-PTV) injection technique was optimized. To confirm the application of this newly developed method, several real-life contaminated fish samples were analyzed.

## 2. Experimental

### 2.1. Test Material

Since fish contamination by halogenated pollutants such as PCBs and PBDEs has different sources from PAHs, which originate mainly from incomplete combustion or heat-induced decomposition of organic matter, it is very difficult to obtain fish contaminated with all these groups of contaminants. Because of that, two different naturally contaminated fish and one blank fish sample were used for the experiments. Trout (blank sample) previously tested for the absence of PCBs, PBDEs and PAHs obtained from the Czech retail market was used for QA/QC experiments. All samples were kept at  $-18^{\circ}\text{C}$  after pooling and homogenization.

### 2.2. GC×GC-TOF MS Analysis

All experiments were performed using an Agilent 6890N GC system (Agilent, Palo Alto, USA) coupled to a Pegasus III (LECO Corp, USA) high-speed time-of-flight mass spectrometer (GC-TOF MS) operated in electron ionization mode (EI). Target analytes were separated using several chromatographic capillary column combinations with different polarities (see Table 1). All columns except for Rt-LC35 (Restek, USA) were purchased from SGE Analytical Science (Australia). Columns used in the 1st and 2nd dimension were of following parameters:  $30\text{ m} \times 0.25\text{ mm i.d.} \times 0.25\text{ }\mu\text{m}$  film thickness and  $1\text{ m} \times 0.1\text{ mm i.d.} \times 0.1\text{ }\mu\text{m}$  film thickness, respectively. Different first/second-dimension oven temperature programmes depending on the column used were tested. Pulsed splitless (injected volume  $1\text{ }\mu\text{L}$ ) and LV-PTV injection in solvent vent mode (injected volume  $1 \times 5\text{ }\mu\text{L}$ ,  $1 \times 8\text{ }\mu\text{L}$  and  $1 \times 10\text{ }\mu\text{L}$ ) were tested. Carrier gas helium flow was  $1.3\text{ mL min}^{-1}$  during all experiments. The TOFMS detector was operated under the following conditions: mass range:  $m/z = 45\text{--}750$ ; ion source temperature:  $250^{\circ}\text{C}$ ; transfer line temperature:  $280^{\circ}\text{C}$ ; acquisition speed:  $100\text{ spectra s}^{-1}$ . The modulation period was dependant on the column system (see Table 1). The ChromaTOF

**Table 1**

The GC column set-ups tested within the experiments.

Column system	1st dimension	2nd dimension	Modulation period [s]
1	BPX-5	BPX-50	4.0
2	BPX-5	Rt-LC35	2.0
3	BPX-5	HT-8	3.5
4	BPX-50	BPX-5	2.5
5	BPX-50	HT-8	4.5

**Table 2**

Large volume programmable temperature vaporization inlet parameters within the method optimization.

Injection volume [ $\mu\text{L}$ ]	Purge time [s]	Solvent vent time [s]
5	190	70
8	260	140
	300	180
10	320	200
	370	250

4.24 software (LECO Corp, USA) was used for data processing.

## 3. Results and Discussion

### 3.1. Optimization of Injection Technique

In the initial part of our experiments, hot splitless injection ( $1\text{ }\mu\text{L}$ ) was used mainly due to its ease of operation. Unfortunately, the obtained LOQs were too high to meet the goal of the study; therefore, LV-PTV injection in solvent vent mode (up to  $10\text{ }\mu\text{L}$ ) was optimized. Using this approach desired LOQs were achieved. As an additional benefit, discrimination of certain analytes was reduced as compared to hot splitless injection.

However, LV-PTV requires more operating parameters to be optimized as compared to hot splitless injection [7]. Firstly, different injection volume ( $5$ ,  $8$  and  $10\text{ }\mu\text{L}$ ) was tested. An  $8\text{-}\mu\text{L}$  injection was seen as optimal since it allowed to achieve the lowest LOQs; the higher injection tested provided worse performance, probably due to its lower capacity. Simultaneously with the injection volume, purge time and solvent vent time were optimized (for more details see Table 2). Secondly, the influence of an injection speed ( $10$  and  $30\text{ }\mu\text{L s}^{-1}$ ) was tested and the best results were obtained by injecting the sample at a speed of  $10\text{ }\mu\text{L s}^{-1}$ . Better results using slower injection rate are in accordance with results of Gómez-Ruiz *et al.* who deals with optimization of PTV injection in PAHs analysis [7]. The initial inlet temperature  $50^{\circ}\text{C}$  was set on the basis of previous experiments and data reported in literature [7]. The comparison of LOQs obtained by  $1$  and  $8\text{ }\mu\text{L}$  injection volume in one dimensional system is summarized in Table 3 (see on next page).

Further decrease of LOQs was achieved using GC×GC thanks to the modulator focusing effect (Table 3) [5].

**Table 3**

Limits of quantification using one-dimension GC (1D-GC) and GC×GC obtained by the optimized methods.

Analytes		LOQ [ $\mu\text{g kg}^{-1}$ ]		
		1D-GC		GC×GC
		1 $\mu\text{L}^a$	8 $\mu\text{L}^b$	8 $\mu\text{L}^b$
Mono-ortho PCBs	PCB 105	2.5	0.25	0.1
	PCB 114	2.5	0.25	0.1
	PCB 118	2.5	0.25	0.1
	PCB 123	2.5	0.25	0.1
	PCB 156	5	0.5	0.25
	PCB 157	5	0.5	0.25
	PCB 167	5	0.5	0.25
	PCB 189	5	1	0.5
Major PCBs	PCB 28	2.5	0.1	0.1
	PCB 52	2.5	0.25	0.1
	PCB 101	2.5	0.25	0.1
	PCB 138	2.5	0.5	0.1
	PCB 153	2.5	0.5	0.1
	PCB 180	5	1	0.25
Non-ortho PCBs	PCB 77	2.5	0.25	0.1
	PCB 81	2.5	0.25	0.1
	PCB 126	2.5	0.5	0.1
	PCB 169	5	0.5	0.25
PBDEs	PBDE 28	10	2.5	0.5
	PBDE47	10	1	0.5
	PBDE 99	10	1	0.5
	PBDE 100	10	1	0.5
	PBDE 153	>10	1	0.5
	PBDE 154	>10	1	0.5
	PBDE 183	>10	2.5	2.5
EU PAHs	B[a]A	1	0.1	0.05
	B[a]P	1	0.1	0.05
	B[b]F	1	0.1	0.05
	B[c]Fln	1	0.1	0.05
	B[j]F	1	0.1	0.05
	B[k]F	1	0.1	0.05
	B[ghi]P	1	0.25	0.25
	Chr	1	0.1	0.05
	CP[cd]P	1	0.1	0.05
	DB[ah]A	1	0.25	0.25
	DB[ae]P	2.5	0.5	0.5
	DB[ah]P	2.5	0.5	0.5
	DB[ai]P	2.5	0.5	0.5
	DB[al]P	2.5	0.5	0.5
	I[cd]P	1	0.25	0.25
5MeChr	1	0.25	0.05	

<sup>a</sup> Hot splitless injection.

<sup>b</sup> Large volume programmable temperature vaporization.

### 3.2. Selection of GC×GC Capillary Column Combination

The column combinations included in the presented study were selected on the basis of data previously reported in the literature and on the orthogonal requirements of GC×GC system. Since the PAHs with a high molecular weight were involved in these experiments, only columns with a high upper

temperature limit (more than 360 °C) could be chosen. During GC×GC optimization, two capillary columns with different polarities were used for the first-dimension separation: (i) non-polar BPX-5 (5% phenyl polysilphenylene-siloxane) and (ii) medium-polar BPX-50 (50% phenyl polysilphenylene-siloxane). (Note: Different elution order of PCB 114 and 153 and of CP[cd]P with B[a]A and Chr using these two columns in one dimensional setting was observed.)

In the second dimension, following capillary columns with different stationary phases were tested: (i) BPX-50 (50% phenyl polysilphenylene-siloxane), (ii) Rt-LC35 (dimethyl (50% liquid crystal) polysiloxane), (iii) BPX-5 (5% phenyl polysilphenylene-siloxane) and (iv) HT-8 (8% phenylpolysiloxane-carbonare). All column set-ups tested within the experiments were able to separate all target PCBs and PBDEs. Figure 1 (on next page) shows an example of the chromatogram of PCBs and PBDEs using BPX-50 × HT-8 column set-up. Therefore, selection of “best” column combination was mainly influenced by its ability to separate the critical groups of PAHs (1st group: B[a]A, CP[cd]P, and Chr; 2nd group: B[f]F, B[k]F, and B[b]F; 3rd group: DB[ah]A, I[1,2,3-cd]P, and B[ghi]P). Unfortunately, none of the column set-ups tested within this study was able to separate the 1st and 3rd critical group. The best separation of the 2nd critical group formed by three isomers of benzofluoranthene was achieved using BPX-50 × HT-8 column set-up (Figure 2; see on next page).

### 3.3. QA/QC

All experiments were performed in an accredited laboratory (No. 1316.2) in the Czech Republic; currently operating in compliance with EN ISO/IEC 17025. Recoveries (%) and repeatabilities (expressed as RSD, %) of all target analytes calculated from six replicates were as follows: PCBs 82–118% (RSD 3–15%), PBDEs 79–118% (RSD 5–14%), and PAHs 83–102% (RSD 3–9%). The LOQs are summarized in Table 3.

## 4. Conclusions

GC×GC-TOF MS employing EI represents a powerful tool for the simultaneous identification and quantification of various groups of chemicals including PCBs, PBDEs and PAHs as well as for a potential non-target screening. All target PCB and PBDE congeners were separated on all tested column combinations. Therefore selection of the column system was mainly influenced by its ability to separate the critical



**Fig. 1.** An example of GCxGC chromatogram of PCBs and PBDEs (200 pg injected) using BPX-50xHT-8 capillary column system;  $m/z = 256, 290, 324, 358, 390, 404, 484, 564, 644$  (yellow mono-ortho PCBs, green non-ortho PCBs, white major PCBs, red PBDEs).

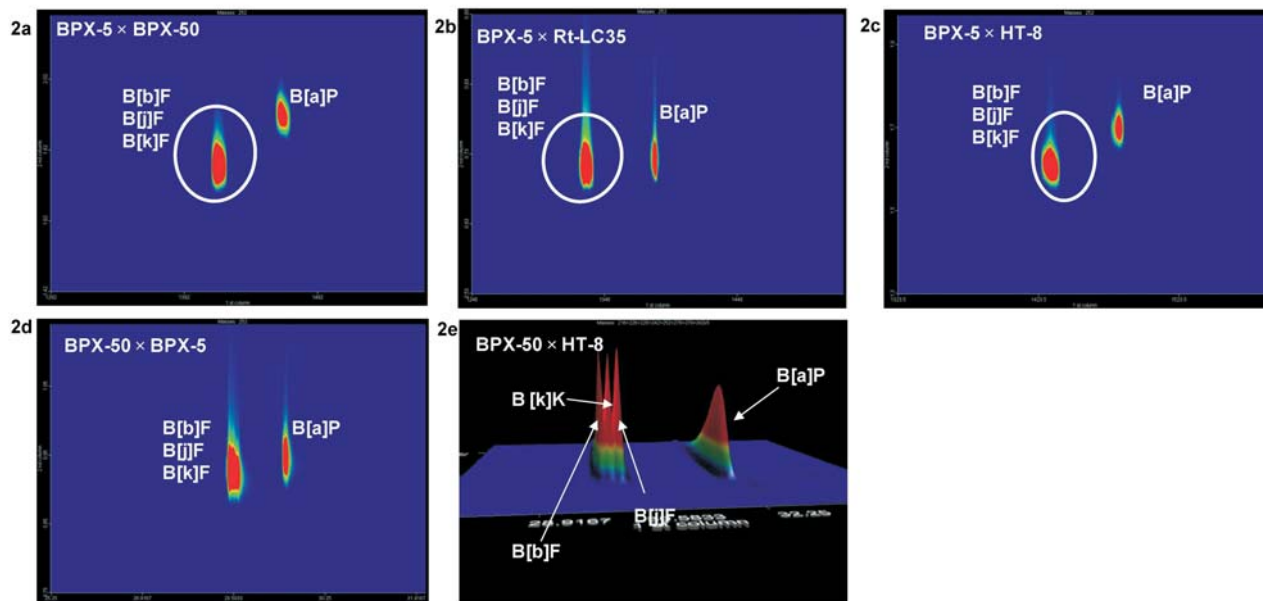


**Fig. 2.** Separation of B[b]F, B[j]F, B[k]F and B[a]P;  $m/z = 252$  (200 pg injected) using different capillary column systems.

groups of PAHs (1st group: B[a]A, CP[cd]P, and Chr; 2nd group B[j]F, B[k]F, and B[b]F; 3rd group: DB[ah]A, I[1,2,3-cd]P, and B[ghi]P). Although none of the column combination evaluated in the presented study allowed a complete separation of all target PAHs, BPX-50 x HT-8 column set-up showed the ability to separate the 2nd group of PAHs. Other two groups remained still unseparated. To achieve desired LOQs, the LV-PTV injection (8  $\mu$ L) was implemented

allowing to obtain LOQs for almost all target analytes by approximately one order of magnitude lower as compared to hot splitless injection (1  $\mu$ L).

**Acknowledgements**

The financial support by the European Commission through the 7th Framework Programme (contract no FP7-211326-CP – CONFIDENCE) and the Ministry of Education, Youth and Sports of the Czech Republic (MSM6046137305) is gratefully acknowledged.

**References**

- [1] Directive 2003/11/EC of 6 February 2003 amending for the 24th time Council Directive 76/769/EEC relating to restrictions on the marketing and use of certain dangerous substances and preparations (pentabromodiphenyl ether, octabromodiphenyl ether).
- [2] Request for data on Brominated Flame Retardants Levels in Foodstuffs, European Food Safety Authority <http://www.efsa.europa.eu/en/data/call/datex091215.htm> (23.3.2010).
- [3] Borajandi L. R., Ramos J. J., Sanz J., González M. J., Ramos L.: *J. Chromatogr. A* **1186** (2008), 312–324.
- [4] Korytár P., Leonards P. E. G., de Boer J., Brinkman U. A. Th.: *J. Chromatogr. A* **1086** (2005), 29–44.
- [5] Marriott P. J., Haglund P., Ong R. C. Y.: *Clin. Chim. Acta* **328** (2003), 1–19.
- [6] Leeuwen S.P.J., Boer J.: *J. Chromatogr. A* **1186** (2008), 161–182.
- [7] Gómez-Ruiz J. A., Cordeiro F., López P, Wenzl T.: *Talanta* **80** (2009), 643–650.
- [8] Adahchour M., Beens J., Vreuls R. J. J., Brinkman U. A. Th.: *Trend Anal. Chem.* **25** (2006), 726–740.
- [9] Adahchour M., Beens J., Vreuls R. J. J., Brinkman U. A. Th.: *Trend Anal. Chem.* **25** (2006), 821–840.
- [10] Korytár P., Haglung P., Boer J., Brinkamn U. A. Th.: *Trend Anal. Chem.* **25** (2006), 373–396.
- [11] Dasputa S., Banerjee K., Patil S. H., Ghaste M., Dhumal K. N., Adsule P. G.: *J. Chromatogr. A* **1217** (2010), 3881–3889.

# Determination of Mycotoxins in Infant and Baby Food Using UPLC-MS/MS Analytical Method

MARTA KOSTELANSKÁ, IVANA SOSNOVCOVÁ, ONDŘEJ LACINA, JANA HAJŠLOVÁ✉

Department of Food Chemistry and Analysis, Institute of Chemical Technology Prague, Technická 3, 166 28 Prague 6, Czech Republic, ✉ jana.hajslova@vscht.cz

## Keywords

baby food  
liquid chromatography  
multi-target analysis  
mycotoxins  
tandem mass spectrometry  
UPLC-MS/MS

## Abstract

A study on occurrence of a broad scope of mycotoxins in cereal-based infant and baby food was carried out. In total, 34 samples of baby's biscuits and mush were analyzed for contamination with almost fifty different mycotoxins. An ultra-high-performance liquid chromatography-tandem mass spectrometry (UPLC-MS/MS) method, enabling sensitive, reliable and fast determination of target mycotoxins was developed and validated for this purpose. Tested samples of infant and baby food were found to be positive for *Fusarium* mycotoxins (predominantly deoxynivalenol, its metabolite deoxynivalenol-3-glucoside, fumonisins and enniatins). It should be noted, that the concentrations of detected toxins did not exceeded hygienic limits established by the European Commission legislation.

## 1. Introduction

Infant and baby food, as well as other foodstuffs, can be frequently contaminated with various kinds of mycotoxins. Mycotoxins are known as secondary toxic metabolites of various fungi species, which can very easily affect raw materials, intended for food production, in both pre-harvest and storing period. To the most widely spread and most often detected mycotoxins, which can threaten health of adults, infants and small children are: aflatoxins, fumonisins, trichothecenes, altertoxins, ochratoxin A, ergot alkaloids and patulin. These contaminants can cause serious health risks connected with acute and/or chronic dietary intake of contaminated food. It was proved that the content of some mycotoxins can be decreased to some extent during the technological procedures as a result of a thermal treatment. On the other hand, some other mycotoxins, e.g. trichothecenes, are stable under the processing conditions, thus can be found in final food products.

Infants and small babies have very specific dietary demands (compared to adult population), which have to be reflected in requirements on special foods destined for these small consumers. Infants and babies are considered to be much more susceptible to intake of various toxins, due to their low body weight, higher metabolic rate and low ability to detoxify hazardous contaminants/xenobiotics, such as mycotoxins [1]. The previous studies, which were focused on determination of mycotoxins in this special group of food, clearly document the fact that most of cereal-based baby foods, usually the first solid meals given to

infants, frequently contain a wide range of mycotoxins at relatively low concentration levels [2–5]. Considering this fact, an accurate prediction of the possible health impact of mycotoxins in infant foods represents extremely difficult task, which is further complicated by the additive or synergistic effects of multiple mycotoxins present in infant food. The inevitable exposure and harmful impact of mycotoxins on consumers lead to necessity to establish their health assessment. Unfortunately, the availability of suitable analytical methods and data for baby food is rather limited. Worth to notice, that relatively strict maximum hygienic limits in baby's and infant food were already set for some mycotoxins by the European Commission (1881/2006/EC, 1126/2007/EC and 105/2010/EC) [6–8].

Latest trend in mycotoxin analysis tends to develop and implement very sensitive analytical procedures that can be used for multi-residual food monitoring analyses of mycotoxins in single short run without any time consuming sample pre-treatment. The aim of this study was to develop such an analytical method employing ultra-high-performance liquid chromatography-tandem mass spectrometry and use it for mycotoxins monitoring in baby food samples [9–11].

## 2. Experimental

### 2.1. Analytical Standards and Chemicals

Acetonitrile and methanol (both HPLC gradient grade), acetic acid, formic acid, ammonium acetate

and ammonium formate were obtained from Sigma-Aldrich (USA). All following analytical standards (purity higher than 97%) of mycotoxins were obtained from Biopure (Austria). Analytical standards of mycotoxins: aflatoxins B1, B2, G1, G2; altertoxins: altenuene, alternariol, alternariol-methylether; patulin; ochratoxin A; fusarium toxins: zearalenon,  $\alpha$ -zearalenol,  $\beta$ -zearalenol, trichothecenes B such as deoxynivalenol, deoxynivalenol-3-glucosid, nivalenol, fusarenon-X, 3-acetyldeoxynivalenol, 15-acetyldeoxynivalenol; trichothecenes A: T-2 toxin, HT-2 toxin, T-2 triol, T-2 tetraol, verrucarol, diacetoxyscirpenol, neosolaniol; fumonisins B1, B2, B3; ergot alkaloids: ergokornin, ergokristin, ergokryptin, ergosin; enniatins A, A1, B, B1; beauvericin, citrinin, deepoxy-deoxynivalenol, moniliformin, penitrem A and roquefortin C.

## 2.2. Samples

Cereal-based baby food samples were obtained from Czech retail markets at the beginning of year 2010. In total, 13 samples of children biscuits and 21 samples of cereal mush were analyzed; some of them contained dried fruits, multi-cereal components and milk.

## 2.3. Analytical Method

Tested samples were homogenized prior to extraction procedure. Representative sample (5 g) was extracted with 20 mL of mixture of acetonitrile:water:formic acid (79:20:1, v/v/v) for 60 min. An aliquot (4 mL) of crude extract was evaporated to dryness and the residue was dissolved in 1 mL of metanol:water mixture (1:1, v/v). Sample analyses were performed using UPLC-MS/MS system consisting of Ultra-Performance Liquid Chromatography (Acquity, Waters, USA) coupled to a QTRAP 5500 System (Applied Biosystems, USA). The chromatographic separation was carried out with the use of an Acquity UPLC HSS T3 column (100  $\times$  2.1 mm i.d., 1.7  $\mu$ m particle size, Acquity, Waters, USA) was used. The working parameters of analytical method were set as follows: flow rate 0.5  $\mu$ L min<sup>-1</sup>, column temperature 40 °C, injection volume 5  $\mu$ L, auto-sampler temperature 10 °C, the fast linear gradient program for separation of target compounds was used, the mobile phase 1 (for LC-MS ESI- analyses, time of method 10 min) consisted of 5 $\times$ 10<sup>-3</sup> mol L<sup>-1</sup> ammonium acetate in water (A1) and 100% methanol (B1), the mobile phase 2 (for LC-MS ESI+ analyses, time of method 13 min) consisted of 5 $\times$ 10<sup>-3</sup> mol L<sup>-1</sup>

ammonium formate in water + 0.2% formic acid (A2) and methanol + 0.2% formic acid (B2). The mass spectrometer operated in both electrospray ionization modes ESI+/- (MRM), the ion source temperature was 600 °C, ion spray voltage +/- 4500 V.

## 3. Results and Discussion

Determination of such a wide range of mycotoxins, which largely differ in physico-chemical properties, is quite a difficult analytical task, especially with regard to established low legislation limits.

The parameters of MS/MS method (declustering potential, cell exit potentials, collision energies and tuning of MRM transitions) were optimized for all analytes in positive and negative mode with both ammonium formate and acetate as mobile phase additives. At the beginning of analytes tuning, it was expected that reasonable signals for all analytes in only one mode (positive mode was expected) will be obtained. Unfortunately, some mycotoxins, e.g. trichothecenes B and patulin, did not give such a good results and their limits of detection would be higher than established legislation limits. Switching of polarities was also not possible, because of the retention times of aflatoxins, which are similar to those of trichothecenes B. On the basis of these results, it was decided to split analytes into two groups and analyse the samples in both positive and negative mode. Method validation was carried out using biscuits blank sample, which was artificially spiked by mycotoxins mixture at two different concentration levels (20 and 100 ng g<sup>-1</sup>) and that the whole procedure of extraction and sample preparation was applied. Performance characteristics of the analytical method are summarized in Table 1 (on next page), examples of analytes' chromatograms are shown in Figures 1 and 2 (on following pages).

All together, 34 cereal based samples destined for infants and babies were analyzed. The majority of positive samples contained Fusarium toxins, namely trichothecenes, fumonisins and enniatins. Approximately 67% (14/21) of cereal mush samples were contaminated. Zearalenon was positive in 14% of samples with mean contamination level 40  $\mu$ g kg<sup>-1</sup>. The markers of Fusarium contamination, deoxynivalenol (DON) as well as its conjugated form DON-3-glucoside (D3G) were positive in five of all samples. Their concentration levels ranged from 19 to 134  $\mu$ g kg<sup>-1</sup> for DON and from 10 to 81  $\mu$ g kg<sup>-1</sup> for D3G. In six cases, HT-2 toxin was detected at levels approximately 17  $\mu$ g kg<sup>-1</sup>. Two mush samples (produced from wheat flour with oat flour addition) also

**Table 1**

Precursor and product ions of analytes and performance characteristics of the method.

Analyte	tr [min]	Precursor ion [m/z]	Product ions [m/z]	Recovery (%)	RSD (%)	LOQ (ng/g)
15-ADON	2.88	356.1 [M+NH <sub>4</sub> ] <sup>+</sup>	321.0/137.1	84	6.2	15
3-ADON	2.35	397.09 [M+CH <sub>3</sub> COO] <sup>-</sup>	336.9/306.9	87	4.1	10
Aflatoxin B1	2.74	313.0 [M+H] <sup>+</sup>	285.0/241.0	95	6.8	0.5
Aflatoxin B2	2.54	315.0 [M+H] <sup>+</sup>	287.1/259.0	103	7.1	0.5
Aflatoxin G1	2.54	331.1 [M+H] <sup>+</sup>	313.0/189.0	101	6.9	0.5
Aflatoxin G2	2.54	328.96 [M+H] <sup>+</sup>	273.03/229.1	105	7.0	0.5
Altenuen	2.30	293.1 [M+H] <sup>+</sup>	275.1/257.0	101	5.6	5
Alternariol	3.78	256.98 [M-H] <sup>-</sup>	214.9/213.0	95	6.4	5
Alternariol-methylether	4.88	273.0 [M+H] <sup>+</sup>	128.0/112.0	106	6.7	5
Beauvericin	7.47	801.28 [M+NH <sub>4</sub> ] <sup>+</sup>	784.1/262.2	107	6.1	5
Citrinin	3.00	251.1 [M+H] <sup>+</sup>	233.1/205.1	79	6.0	2.5
Deepoxydeoxynivalenol	2.04	339.1 [M+CH <sub>3</sub> COO] <sup>-</sup>	248.9/59.1	83	8.3	5
Deoxynivalenol	1.80	355.1 [M+CH <sub>3</sub> COO] <sup>-</sup>	295.1/265.1	86	6.7	10
Diacetoxyscirpenol	2.97	383.99 [M+NH <sub>4</sub> ] <sup>+</sup>	307.2/105.0	87	7.1	5
DON-3-Glucoside	1.72	517.13 [M+CH <sub>3</sub> COO] <sup>-</sup>	456.9/426.9	92	4.2	5
Enniatin A	7.99	699.36 [M+NH <sub>4</sub> ] <sup>+</sup>	228.2/210.1	99	3.4	5
Enniatin A1	7.76	685.36 [M+NH <sub>4</sub> ] <sup>+</sup>	214.1/210.1	106	6.1	5
Enniatin B	7.27	657.3 [M+NH <sub>4</sub> ] <sup>+</sup>	213.9/196.1	105	3.4	5
Enniatin B1	7.53	671.24 [M+NH <sub>4</sub> ] <sup>+</sup>	228.1/214.1	102	5.7	5
Ergocormine	2.76	562.13 [M+H] <sup>+</sup>	268.2/223.2	111	8.1	5
Ergocristine	3.13	610.09 [M+H] <sup>+</sup>	223.1/208.045	104	6.4	5
Ergocryptine	3.08	576.12 [M+H] <sup>+</sup>	268.1/223.1	110	4.2	5
Ergosine	2.57	548.12 [M+H] <sup>+</sup>	223.1/208.0	112	5.1	5
Fuminisin B1	4.69	722.4 [M+H] <sup>+</sup>	352.3/334.3	89	6.4	5
Fuminisin B2	4.24	706.4 [M+H] <sup>+</sup>	336.2/318.3	85	3.8	5
Fuminisin B3	2.79	706.4 [M+H] <sup>+</sup>	336.2/318.3	91	4.5	5
Fusarenon X	1.98	413.10 [M+CH <sub>3</sub> COO] <sup>-</sup>	353.1/263.0	89	4.2	5
Gliotoxin	4.41	326.89 [M+H] <sup>+</sup>	282.0/263.1	94	8.1	5
HT-2 toxin	3.60	442.2 [M+NH <sub>4</sub> ] <sup>+</sup>	263.0/215.1	87	4.1	2.5
Moniliformin	1.25	96.9 [M-H] <sup>-</sup>	41.2	68	9.7	5
Neosolaniol	1.98	399.97 [M+NH <sub>4</sub> ] <sup>+</sup>	305.1/215.1	97	3.7	2.5
Nivalenol	1.55	401.96 [M+CH <sub>3</sub> COO] <sup>-</sup>	311.1/281	71	3.5	5
Ochratoxin A	4.63	403.9 [M+H] <sup>+</sup>	239.0/102.0	115	5.4	0.5
Ochratoxin $\alpha$	1.81	254.95 [M-H] <sup>-</sup>	211.0/166.1	87	4.9	5
Patulin	1.54	213 [M+CH <sub>3</sub> COO] <sup>-</sup>	152.9/109.0	83	5.8	10
Penitrem A	3.48	635.091 [M+H] <sup>+</sup>	616.2/558.2	107	5.8	5
Roquefortin C	1.61	390.066 [M+H] <sup>+</sup>	322.1/193.0	105	8.3	5
Sterigmatocystin	4.83	325.0 [M+H] <sup>+</sup>	310.0/281.0	96	3.9	5
T-2 tetraol	2.20	316.01 [M+NH <sub>4</sub> ] <sup>+</sup>	233.1/215.1	81	5	10
T-2 toxin	4.15	484.2 [M+NH <sub>4</sub> ] <sup>+</sup>	305.2/215.1	85	3.7	5
T-2 triol	1.98	400.004 [M+NH <sub>4</sub> ] <sup>+</sup>	233.1/215.1	80	5.3	10
Verrucarol	1.99	267.074 [M+H] <sup>+</sup>	249.1/231.2	91	8.1	10
Zearalenon	5.06	317.1 [M-H] <sup>-</sup>	175.1/131.0	91	6.5	10
$\alpha$ -Zearalenol	4.25	319.1 [M-H] <sup>-</sup>	275.0/174.0	83	2.8	5
$\beta$ -Zearalenol	4.82	319.1 [M-H] <sup>-</sup>	275.0/175.0	89	3.4	5

contained “new and emerging” mycotoxins belonging to group of enniatins. The mean concentration of these analytes was established at 8  $\mu\text{g kg}^{-1}$ .

The majority of investigated baby's biscuits was made from wheat flour and skimmed dried milk, to some of them corn, rice and oats were added. Alike in case of cereal mush samples, the main representatives of *Fusarium* mycotoxins, the markers of cereals' contamination by moulds, were the main contaminants of biscuits. Only in one sample the toxic and

dangerous ochratoxin A was detected at the level 0.43  $\mu\text{g kg}^{-1}$ . The overview of sample contaminations is shown in Figure 3. None of other tested mycotoxins were detected in tested baby food samples. Future experiments will be aimed at analytes scope enlargement and method validation for additional types of baby food.

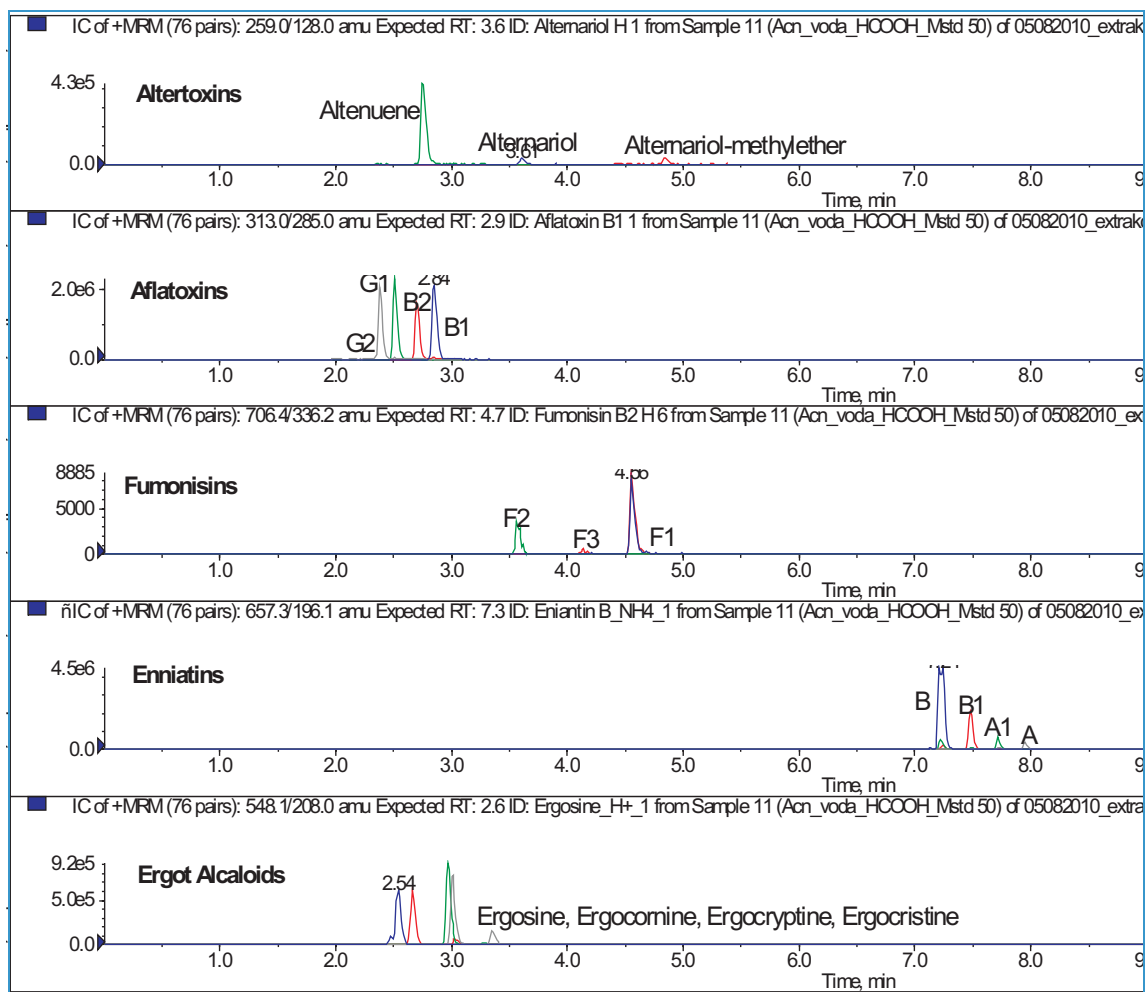


Fig. 1. UPLC/(ESI+)-MS/MS chromatograms of matrix-matched standard of representatives of analysed mycotoxins ( $50 \text{ ng mL}^{-1}$ ).

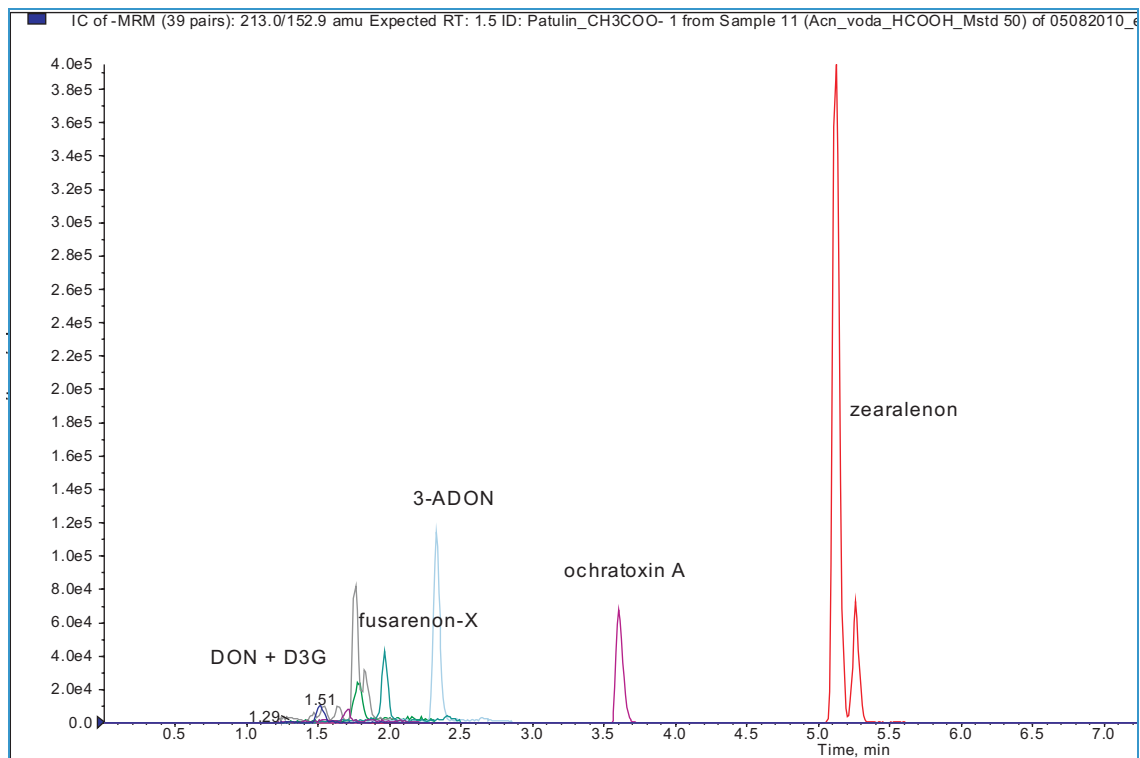
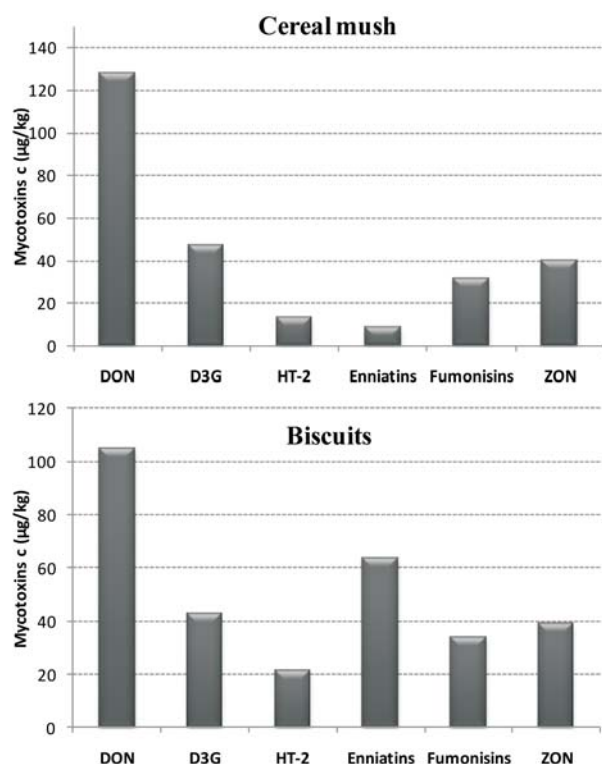


Fig. 2. UPLC/(ESI-)-MS/MS chromatograms of matrix-matched standard of representatives of analysed mycotoxins ( $50 \text{ ng mL}^{-1}$ ).



**Fig. 3.** Mean concentrations of detected mycotoxins in tested infant and baby food samples.

#### 4. Conclusions

Fast, sensitive and reliable UPLC-MS/MS method has been developed for determination of multiple mycotoxins in cereal-based infant and baby food. This new validated method has been used for monitoring of mycotoxins in 34 samples of discussed special type of food. To the most often detected mycotoxins belong fumonisins, deoxynivalenol, zearalenon and enniatins. It should be noted, that all of tested samples met the maximum hygienic limits established for some mycotoxins by European Commission and the overall contamination of tested samples is rather low.

#### Acknowledgments

This study was carried out within the scope of national projects (NPV II 2B08049, NPV II 2B06118 and MSM 6046137305), that were financially supported by Ministry of Education, Youth and Sports of the Czech Republic.

#### References

- [1] Sherif S. O., Salama E. E., Abdel-Wahhab M. A.: *Int. J. Hyg. Envir. Heal.* **4** (2009), 347–368.
- [2] Lombaert G. A., Pellaersy P., Roscoey V., Mankotiaz M., Neilz R., Scott P. M.: *Food Addit. Contam.* **20** (2003), 494–504.
- [3] Alvito P. C., Sizoo E. A., Almeida C. M. M., Egmond H. P.: *Food Anal. Method.* **3** (2010), 22–30.
- [4] D'Arco G., Fernández-Franzón M., Font G., Damiani P., Mañes J.: *J. Chromatogr. A* **1209** (2008), 188–194.
- [5] Caldas D. E., Silva A. C. S.: *J. Agr. Food Chem.* **6** (2007), 7974–7980.
- [6] Commission Regulation (EC) No 1881/2006 of 19 December 2006. *Official Journal of the European Union* (2006), 5–24.
- [7] Commission Regulation (EC) No 1126/2007 of 28 September 2007. *Official Journal of the European Union* (2007), 14–17.
- [8] Commission Regulation (EC) No 105/2010 of 5 February 2010. *Official Journal of the European Union* (2010), 7–8.
- [9] Zöllner P., Mayer-Helm B.: *J. Chromatogr. A* **1136** (2006), 123–169.
- [10] Krska R., Molinelli A.: *Anal. Bioanal. Chem.* **387** (2007), 145–148.
- [11] Sulyok M., Berthiller F., Krska R., Schuhmacher R.: *Anal. Bioanal. Chem.* **389** (2007), 1505–1523.

# The Enzyme Kinetics Study Using Capillary Electrophoresis: Determination of Chitobiose and *N*-Acetylglucosamine

TOMÁŠ KRÍŽEK<sup>a</sup>, PAVEL COUFAL<sup>a</sup>, RADOMÍR ČABALA<sup>a</sup>, HELENA RYŠLAVÁ<sup>b</sup>

<sup>a</sup>Department of Analytical Chemistry, <sup>b</sup>Department of Biochemistry, Faculty of Science, Charles University in Prague, Albertov 6/2030, 128 43 Prague, Czech Republic, ✉ krizek@natur.cuni.cz

## Keywords

capillary electrophoresis  
chitobiose  
hexosaminidase  
kinetics

## Abstract

Study of enzyme kinetics of glycosidases is inevitable for understanding their functions in complex biological systems. However, such a study cannot be performed without monitoring the concentration of products and substrates of these enzymes. For this purpose, a fast and reliable analytical method is necessary. The separation mechanism of capillary electrophoresis is well suited for separation of chitobiose and *N*-acetylglucosamine as a substrate and product of  $\beta$ -*N*-acetylhexosaminidase. Thus a reliable and sufficiently sensitive capillary electrophoresis method for their determination has been developed and successfully utilized for kinetics studies of  $\beta$ -*N*-acetylhexosaminidase. Reliability of the method was confirmed by repeatability studies and chemometric analysis of calibration data. A remarkable advantage of the method lays in no need of derivatization of analytes as well as the fact that the enzyme reaction is terminated simply by injecting the reaction mixture into the capillary.

## 1. Introduction

Glycosidases are enzymes that catalyze cleavage of poly- and oligosaccharide chains. Expression of some glycosidases is also connected with pathogenesis that takes place under stressing conditions [1].  $\beta$ -*N*-acetylhexosaminidase is a representant of glycosidases enzyme family and catalyzes for example cleavage of disaccharide chitobiose to monosaccharide *N*-acetylglucosamine.  $\beta$ -*N*-acetylhexosaminidase has several functions in the biochemistry of fungi [2–4]. The investigation of activity and kinetics of this enzyme is crucial for understanding the complex biological processes in which  $\beta$ -*N*-acetylhexosaminidase participates. The activity of enzymes is usually studied by observing the concentration of their substrates and products in the reaction mixture. Such a procedure, however, requires a fast analytical method of a sufficient sensitivity and selectivity.

In the literature, mainly separation techniques were reported for determination of saccharides [6]. Capillary electrophoresis (CE) is well established as a tool for determination of saccharides [7, 8]. However, the CE separation of saccharides is rather complicated problem as they possess electric charge only in highly alkaline solutions and this charge is negative which means that they exhibit counter-electroosmotic flow migration resulting in a long analysis time, enhanced adverse dispersion effects and a lower repeatability of

measurements. Moreover, saccharides exhibit very low UV absorbance. Both these difficulties can be solved by derivatization of analytes before analysis. Appropriate chromophore [9] or fluorophore [10] can thus be introduced into the molecule of analyte. This approach enables highly sensitive detection, especially when the fluorescence detector is used. On the other hand, the derivatization brings the risk of sample loss or contamination during the procedure as well as a prolonged sample processing. Therefore, methods using indirect UV [11] or conductivity detection [12] have been developed. Nevertheless, none of them surpassed the others remarkably. In this work, a method for separation of saccharides chitobiose and *N*-acetylglucosamine was developed. As can be seen in Figure 1, these analytes contain the UV absorbing amide bond in their structures and thus direct UV detection can be utilized with sufficient sensitivity.

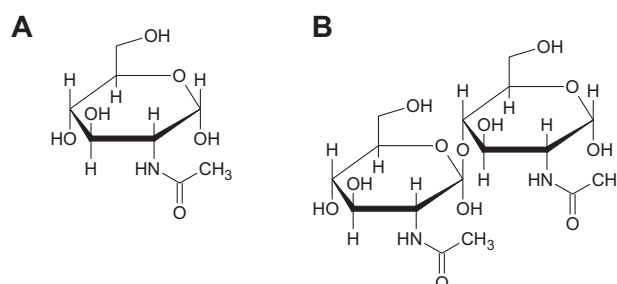


**Fig. 1.** Structures of *N*-acetyl-D-glucosamine (A) and *N,N'*-diacetylchitobiose (B).

**Table 1**

The repeatability of migration times, peak areas and peak heights in 50 and 75  $\mu\text{m}$  i.d. capillaries expressed as the relative standard deviation,  $n = 10$ . Background electrolyte: 25 mM sodium tetraborate, pH = 9.2; temperature 25  $^{\circ}\text{C}$ ; voltage 30 kV for 50  $\mu\text{m}$  and 15 kV for 75  $\mu\text{m}$  capillary; detection at 200 nm; concentration  $1 \times 10^{-3} \text{ mol L}^{-1}$ .

	relative standard deviation [%]					
	50 $\mu\text{m}$ i.d. capillary			75 $\mu\text{m}$ i.d. capillary		
	time	area	height	time	area	height
Hydrodynamic injection						
Chitobiose	0.7	14.1	11.1	1.4	8.1	5.6
<i>N</i> -Acetylglucosamine	0.8	15.2	15.5	1.4	6.5	4.5
Electrokinetic injection						
Chitobiose	0.4	11.5	9.3	1.6	3.4	4.6
<i>N</i> -Acetylglucosamine	0.4	11.8	12.5	0.8	3.4	3.5

## 2. Experimental

### 2.1. Chemicals

$\beta$ -*N*-acetylhexosaminidase was graciously donated by Prof. Karel Bezouška (Charles University in Prague, Faculty of Science, Department of Biochemistry). The enzyme was isolated from *Aspergillus oryzae* strain CCF1066 following the procedure described in cit. [13]. Sodium hydroxide, p.a., and sodium tetraborate decahydrate, p.a., were purchased from Lachema (Brno, Czech Republic). *N,N'*-diacetylchitobiose,  $\geq 96\%$ , and *N*-acetyl-D-glucosamine,  $\geq 99\%$ , were delivered by Sigma (St. Louis, MO, USA). Background electrolytes and samples were prepared using deionized water produced by a Milli-Q system, Millipore (Billerica, MA, USA).

### 2.2. Instrumentation

Experiments were carried on an Agilent CE3D 7200 instrument (Agilent Technologies, Waldbronn, Germany). Fused silica capillaries, 50 and 75  $\mu\text{m}$  i.d, were cut to the 65 cm length. Detection window was burnt by a butane flame 56.5 cm from the inlet end of the capillary. Prior to the first use, the capillary was flushed 20 min with 1 M sodium hydroxide and 10 min with water using a pressure of 100 kPa. Before each run, the capillary was flushed 2 minutes with background electrolyte. Samples were injected using either pressure of 5 kPa for 3 s or 5 kV for 5 s. A voltage of 15 kV was applied during the separation (30 kV for 50  $\mu\text{m}$  id). The capillary was thermostated at 25  $^{\circ}\text{C}$ .

## 3. Results and Discussion

Chitobiose is a dimer of *N*-acetylglucosamine as obvious from the Figure 1. Since the electrophoretic

mobility is proportional to the ratio of charge and hydrated radius of an ion, chitobiose and *N*-acetylglucosamine differ in their electrophoretic mobilities which means that, despite their similar chemical properties, they can be separated by CE. Saccharides are ionized (and migrate in electric field) only in extremely alkaline background electrolytes. However, these electrolytes possess a critically high conductivity, which makes them rather unsuitable for CE experiments. To avoid use of highly alkaline electrolytes, borate buffer was employed as the borate anions form negatively charged complexes with saccharides [14, 15]. These complexes then migrate in electric field and can be separated. As 20 mM sodium tetraborate buffer, pH = 9.2, did not provide baseline separation of the analytes, ionic strength was elevated to 25 mmol L<sup>-1</sup>. The mentioned buffer provided a complete separation and the current of 42  $\mu\text{A}$  was still acceptable with respect to Joule heat produced during the run.

The method was originally developed for 50  $\mu\text{m}$  i.d. capillary and provided separation in 5 minutes. However, for the quantification purposes, 50  $\mu\text{m}$  i.d. capillary was found to be unsuitable because the repeatability of peak area was insufficient. This can be attributed to a higher tendency of the 50  $\mu\text{m}$  i.d. capillary to clog. Due to instable hydrodynamic resistance in capillary, the efficiency of sample injection varied and the peak area became irreproducible. Thus the method was adapted to 75  $\mu\text{m}$  i.d. capillary. As the higher inner diameter brings a significantly higher electric current, the voltage had to be reduced to 15 kV so that the corresponding current of 55  $\mu\text{A}$  was kept at acceptable level. This voltage adjustment prolonged the analysis time to 9 minutes. Nevertheless, Table 1 shows that a three-fold improvement of the peak area repeatability was achieved. Electrokinetic and hydrodynamic injection modes were tested and are compared in Table 1 as well. Based on the results, the

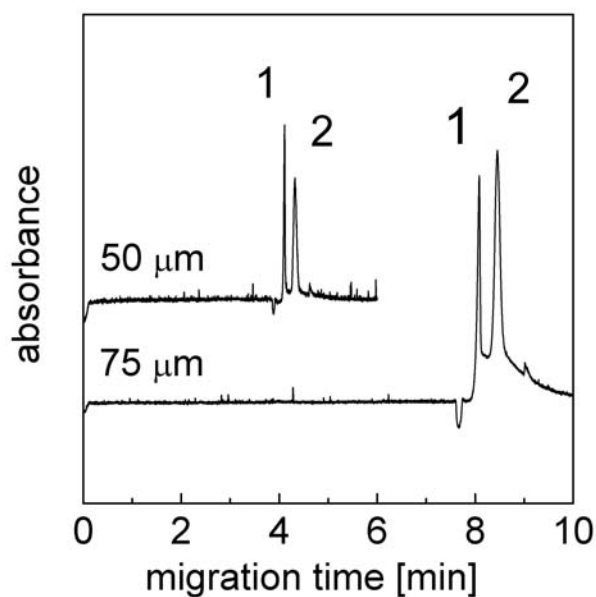


**Fig. 2.** Separations of chitobiose (1) and *N*-acetylglucosamine (2) in capillaries of the 50 and 75  $\mu\text{m}$  inner diameter. Background electrolyte: 25 mM sodium tetraborate, pH = 9.2; temperature 25  $^{\circ}\text{C}$ , voltage 30 kV for 50  $\mu\text{m}$  and 15 kV for 75  $\mu\text{m}$  capillary, detection at 200 nm, concentration  $1 \times 10^{-3} \text{ mol L}^{-1}$ .

electrokinetic injection was chosen because it provided a higher repeatability (see Table 1). Electropherograms obtained with the 50 and 75  $\mu\text{m}$  i.d. capillaries are displayed in Figure 2.

The 75  $\mu\text{m}$  i.d. capillary was used for further experiments. Calibration standards in the concentration range from 0.1 to 2.0  $\text{mmol L}^{-1}$  were measured and linear regression was performed using the least squares method. The resulting calibration curve was subjected to chemometric analysis. Parameters of the method for determination of chitobiose and *N*-acetylglucosamine are shown in Table 2. Obviously, linear regression provides a satisfactory model of response as it explains 99.7% of the response variability for both analytes (see  $R^2$  values). The deviation of linearity coefficients from ideal value,  $l = 1$ , is safely within 5% range, which means that the detector response can be considered as linear over the studied

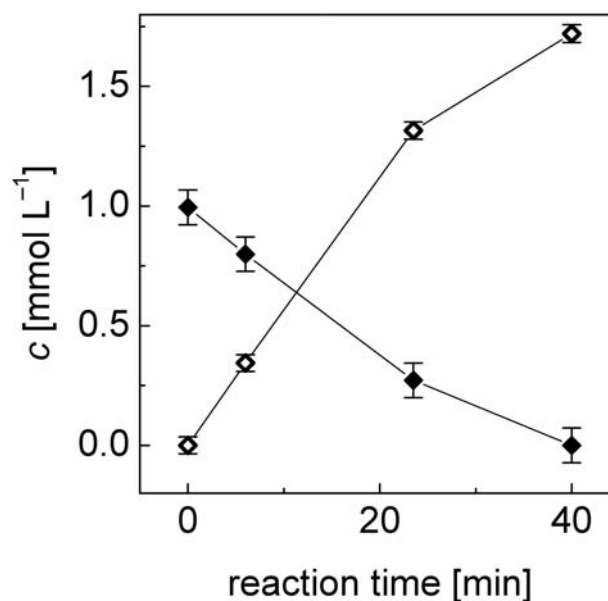


**Fig. 3.** Concentrations of chitobiose (◆) and *N*-acetylglucosamine (◇) in the reaction mixture as a function of the reaction time. The enzyme hexosaminidase diluted 1/20 000. 50 mM citrate buffer, pH=4.5.

concentration range. These results show that an elevation of the baseline after the chitobiose peak observed in electropherograms with the 75  $\mu\text{m}$  capillary has no adverse effect on quantification. The limit of detection and the limit of quantification were calculated from standard deviation of intercept; their values  $0.4 \times 10^{-4}$  and  $1.2 \times 10^{-4} \text{ mol L}^{-1}$ , respectively, show that the developed method is sufficiently sensitive for the enzyme kinetics study.

The developed method was employed to prove that chitobiose is the substrate of  $\beta$ -*N*-acetylhexosaminidase. Figure 3 shows a decrease of the chitobiose concentration and an increase of the *N*-acetylglucosamine concentration in the reaction mixture. The graph in the Figure 3 also suggests that one molecule of chitobiose is cleaved into two molecules of *N*-acetylglucosamine which is in accordance with the expected stoichiometry. The developed

**Table 2**

The calibration parameters of the capillary electrophoresis method for determination of chitobiose and *N*-acetylglucosamine.

	Chitobiose	<i>N</i> -Acetylglucosamine
Calibration range	0.1–2.0 $\text{mmol L}^{-1}$	0.1–2.0 $\text{mmol L}^{-1}$
Slope	21.05 $\text{min L mmol}^{-1}$	51.44 $\text{min L mmol}^{-1}$
Intercept	–0.2682 min	–0.4182 min
$R^2$	0.9975	0.9972
$N$	27	27
Linearity coefficient	0.9750	0.9968
Limit of detection	0.04 $\text{mmol L}^{-1}$	0.04 $\text{mmol L}^{-1}$
Limit of quantification	0.12 $\text{mmol L}^{-1}$	0.12 $\text{mmol L}^{-1}$

method is also advantageous for the kinetics study because the enzymatic reaction can be terminated simply by injection of the reaction mixture into the capillary. The enzymatic reaction stops immediately after beginning of the run because the overall charge of the enzyme is under the employed conditions positive and the enzyme and the chitobiose molecules migrate in the opposite direction.

#### 4. Conclusions

A capillary electrophoresis method for fast simultaneous determination of chitobiose and *N*-acetylglucosamine as the substrate and product of the enzyme  $\beta$ -*N*-acetylhexosaminidase has been developed. The reliability of the method was confirmed by the migration time and peak area repeatability study. Further, the evaluation of the calibration curve proved that the method is well applicable for quantification over the concentration range considered. The method was used to prove that  $\beta$ -*N*-acetylhexosaminidase catalyzes the cleavage of chitobiose into two molecules of *N*-acetylglucosamine. A study of  $\beta$ -*N*-acetylhexosaminidase kinetics is in progress and is to be followed by an enzyme kinetics study with chitotriose, which is a trimer of *N*-acetylglucosamine.

#### Acknowledgements

The financial support of the Grant Agency of Charles University in Prague, projects No. 710 and SVV 261204, the Ministry of Education, Youth and Sports of the Czech Republic, project MSM0021620857 and RP 14/63 as well as the Norwegian Financial Mechanism, project CZ0116, is gratefully acknowledged.

#### References

- [1] Ryšlavá H., Holakovská B., Trefančová J., Doubnerová V., Spoustová P., Synková H., Čeřovská N.: *FEBS Journal* **276** (2009), 24–24.
- [2] Gooday G. W., Zhu W. Y., Odonnell R. W.: *FEMS Microbiol. Lett.* **100** (1992), 387–391.
- [3] Bulawa C. E.: *Annu. Rev. Microbiol.* **47** (1993), 505–534.
- [4] Cheng Q. M., Li H. S., Merdek K., Park J. T.: *J. Microbiol.* **182** (2000), 4836–4840.
- [5] Venugopal M., Obaie O. J., Thirugnanasampanthar M., Ping T. S.: *Chromatographia* **65** (2007), 493–496.
- [6] Montero C. M., Doderio M. C. R., Sanchez D. A. G., Barosso C. G.: *Chromatographia* **59** (2004), 15–30.
- [7] El Rassi Z.: *Electrophoresis* **20** (1999), 3134–3144.
- [8] Suzuki S., Honda S.: *Electrophoresis* **19** (1998), 2539–2560.
- [9] Momenbeik F., Johns C., Breadmore M. C., Hilder E. F., Macka M., Haddad P. R.: *Electrophoresis* **27** (2006), 4039–4046.
- [10] Tseng H. M., Gattollin S., Pritchard J., Newbury H. J., Barrett D. A.: *Electrophoresis* **30** (2009), 1399–1405.
- [11] Gurel A., Hizal J., Oztekin N., Erim F. B.: *Chromatographia* **64** (2006), 321–324.
- [12] Rainelli A., Hauser P. C.: *Anal. Bioanal. Chem.* **382** (2005), 789–794.
- [13] Ettrich R. et al.: *BMC Structural Biology* **7** (2007), 32.
- [14] Foster A. B.: *Adv. Carbohydr. Chem.* **12** (1957), 81–116.
- [15] Mechref Y., Ostrander G. K., El Rassi Z.: *Electrophoresis* **16** (1995), 1499–1504.

# Monolithic Poly(styrene-divinylbenzene-methacrylic acid) Capillary Columns For Separation of Low-Molecular-Weight Compounds

ADÉLA SVOBODOVÁ<sup>a</sup>, EVA TESAŘOVÁ<sup>b</sup>, JANA SOBOTNÍKOVÁ<sup>a</sup>, PAVEL COUFAL<sup>a</sup>

<sup>a</sup> Department of Analytical Chemistry, Faculty of Science, Charles University in Prague, Albertov 6, 128 43 Prague 2, Czech Republic, ✉ adelka.svoboda@seznam.cz

<sup>b</sup> Department of Physical and Macromolecular Chemistry, Faculty of Science, Charles University in Prague, Albertov 6, 128 43 Prague 2, Czech Republic

## Abstract

In this work, we are demonstrating a very easy method for preparation of polystyrene-based monolithic columns for capillary liquid chromatography suitable for low-molecular-weight compounds. The influence of addition of methacrylic acid in the polymerization mixture on the separation selectivity and column efficiency was investigated. The preparation method is universal for both capillary liquid chromatography and capillary electrochromatography measurement. Due to the simplicity of monolith fabrication, comprehensive studies of the retention and separation behaviour of monolithic poly(styrene-divinylbenzene-methacrylic acid) columns resulted in high run-to-run and batch-to-batch repeatability.

## Keywords

capillary liquid chromatography  
low-molecular-weight compound  
methacrylic acid  
polystyrene-based monolithic column

## 1. Introduction

Monolithic columns represent powerful and cheap alternative to conventional packed columns for application in capillary techniques. The current approach is focused on preparation of universal columns suitable for separations in both, capillary liquid chromatography (CLC) and capillary electrochromatography (CEC). Polymer-based monoliths have widely been studied in recent years. Thanks to their simple preparation and no need of retaining frits, they have attracted a growing attention in separation techniques. In addition, the morphologic properties and functionality of the polymeric monolithic supports can easily be modified by either changing the composition of polymerization mixture or polymerization conditions. Polystyrene-based monoliths have been proved to be excellent stationary phases because of their high chemical stability across a wide pH range. They offer unique efficiency and fast analyses, particularly in the separation of larger molecules such as peptides, proteins and nucleic acids [1–3]. However, the number of studies applying polystyrene-based monoliths to separation of small molecules is limited. Up to now, very few reports of efficient CEC separations of neutral low-molecular-weight compounds on polystyrene-based monoliths could be found in the literature [4–6]. To adapt the stationary phase for separation of small molecules, the monolith can be modified either by changing the composition of

the monomer mixture or by post-polymerization modification [7, 8].

The influence of methacrylic acid (MAA) addition to the polymerization mixture for CLC columns was studied and compared with common monoliths based on polystyrene. The newly designed polymeric monolithic support enables highly efficient separations of typical low-molecular-weight compounds.

## 2. Experimental

### 2.1. Chemicals and Reagents

3-(trimethoxysilyl)-propyl methacrylate (99%) and ethylbenzene (p.a.) were purchased from Fluka (Buchs, Switzerland). Styrene (for synthesis), divinylbenzene (for synthesis), toluene (extra pure), methacrylic acid (for synthesis) and  $\alpha, \alpha'$ -azobisisobutyronitrile (AIBN) (98%) were obtained from Merck (Germany). Thiourea (99%), phenol (99%), aniline (98%), benzene (99%), propylbenzene (99%) and butylbenzene (98%) were purchased from Sigma Aldrich (USA). Isooctane (p.a.) and orthophosphoric acid (p.a.) were bought from Lach-Ner (Czech Republic). Sodium hydroxide (p.a.) was provided by Lachema (Czech Republic). Acetonitrile and methanol (gradient-grade for liquid chromatography) were supplied by Merck (Germany). Polyimide coated fused-silica capillaries of 320  $\mu\text{m}$  i.d. were obtained from Supelco (USA). Deionised water was

prepared using a Milli-Q water system (Millipore, Milford, USA). All samples were dissolved in mobile phases in concentrations ranging from 0.2 to 0.5 mg mL<sup>-1</sup>.

## 2.2. Apparatus

The CLC experiments were performed with an ISCO syringe pump model 100 DM (Lincoln, USA), a Valco International injection valve with a 0.10 µL internal loop (Schenk, Switzerland) and a LINEAR UVIS-205 photometric detector (USA). Clarity software (Data Apex, Czech Republic) was used for data collection and evaluation.

## 2.3. Preparation of the Monolithic Columns

Prior to the polymerization, the inner wall of a 320 µm i.d. capillary was treated according to the procedure described by Courtois *et al.* [9]. The fused-silica capillary was first flushed and filled with 1 mol L<sup>-1</sup> NaOH. Both ends of the capillary were sealed and the capillary was kept in a thermostated oven for 3 hours at 120 °C. Subsequently, the capillary was rinsed with deionized water followed by acetone, dried by nitrogen for 10 min and then left in an oven for another 1 h at 120 °C. The silanization mixture containing 10% (v/v) 3-(trimethoxysilyl)-propyl methacrylate in toluene was filled into the capillary. The capillary ends were sealed and the capillary was kept for 2 h at room temperature.

Preparation of the poly(styrene-divinylbenzene-methacrylic acid) monolith was carried out using the procedure described in [4]. This procedure was adopted in several points for preparation of styrene-based capillary monolithic columns for CLC. The polymerization mixture contained 50 µL of styrene, 100 µL of divinylbenzene and 50 µL of methacrylic acid as monomers, 300 µL of toluene and 300 µL of isooctane as the porogen mixture and AIBN as the initiator (1% (w/w) with respect to the monomers). The polymerization mixture was sonicated for 15 min until it became homogeneous, and then degassed with a stream of nitrogen for 10 min. The silanized capillary was filled with the polymerization mixture, both ends were sealed and the capillary was placed in a water bath at 60 °C for 6 h. A syringe pump was used to wash the monolithic column first with methanol then with the mobile phase.

## 3. Results and Discussion

### 3.1 Influence of the Methacrylic Acid Addition on Resolution Properties of the Monolith

Both Xiong *et al.* [10] and Jin *et al.* [4] successfully prepared negatively charged polystyrene-based monolith by a single step polymerization using MAA as a charge-bearing monomer for CEC. Surprisingly, the impact of MAA on selectivity of the monolithic columns is rarely considered in the literature. To assess the effect of incorporation of charge-bearing monomer (MAA) to the polymerization mixture, two batches of columns with and without MAA was prepared according to the modified procedure described in the literature [4]. The test mixture containing eight low-molecular-weight compounds (thiourea, phenol, aniline, benzene, toluene, ethylbenzene, propylbenzene, butylbenzene) was chosen to evaluate influence of the methacrylic acid addition on separation selectivity of the monolithic columns. When the monolithic columns were polymerized without MAA, no separation of the test compounds was observed (Fig. 1, chromatogram I). On the other hand, all the columns prepared with addition of MAA provided baseline separation of all eight test analytes with a column efficiency of about 28,000 theoretical plates m<sup>-1</sup> (Fig. 1, chromatogram II). These experimental results clearly demonstrate a meaningful impact of MAA on the chromatographic behaviour of the monolithic columns.

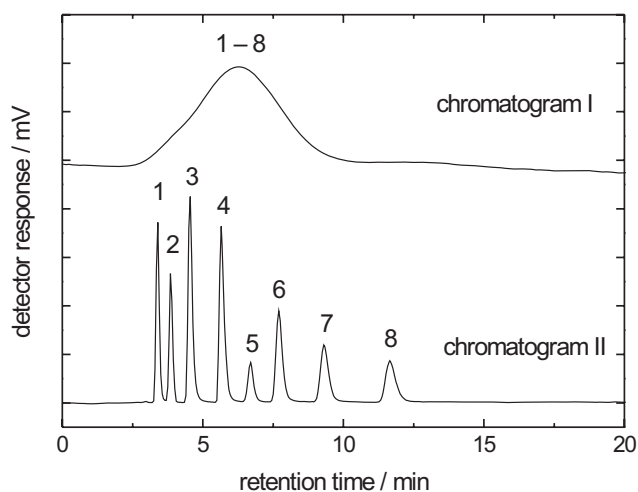


**Fig. 1.** Capillary liquid chromatography separation of small molecules on poly(styrene-co-divinylbenzene) columns without methacrylic acid (chromatogram I) and with methacrylic acid (chromatogram II). Experimental conditions: eluent acetonitrile-water (65:35, v/v), photometric detection at 214 nm; flow rate 4 µL min<sup>-1</sup>; injection volume 0.10 µL; effective column length 17 cm. Peaks: (1) thiourea, (2) phenol, (3) aniline, (4) benzene, (5) toluene, (6) ethylbenzene, (7) propylbenzene, and (8) butylbenzene.

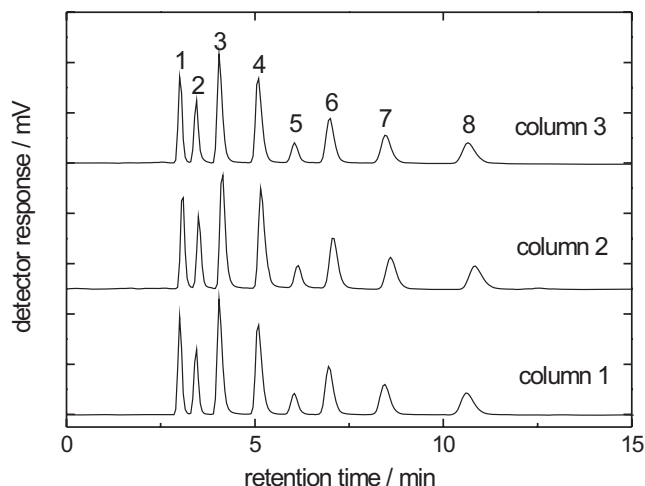


**Fig. 2.** Column-to-column repeatability of three independently prepared poly(styrene-*co*-divinylbenzene-*co*-methacrylic acid) capillary columns illustrated by separation of the test mixture. Experimental conditions: eluent acetonitrile-water (65:35, v/v), photometric detection at 214 nm; flow rate 4  $\mu\text{L min}^{-1}$ ; injection volume 0.10  $\mu\text{L}$ ; effective column length 17 cm. Peaks: (1) thiourea, (2) phenol, (3) aniline, (4) benzene, (5) toluene, (6) ethylbenzene, (7) propylbenzene, and (8) butylbenzene.

### 3.2 Repeatability of the Monolith Preparation and the Column Performance

High separation efficiency is one of the most important factors that makes separation media attractive to their users. However, repeatability is undoubtedly essential requirement, too. The preparation of monolithic columns based on organic polymers is relatively simple compared to the fabrication of common packed columns. Nevertheless, the pretreatment of the capillary, the preparation and optimization of the polymerization mixture and the polymerization process itself make each column original. Therefore, the batch-to-batch repeatability has to be assessed. The retention times and theoretical plate heights of the test compounds were used to study the batch-to-batch and the run-to-run repeatability of the prepared monoliths. Fig. 2 shows comparison of the chromatographic properties of three monolithic columns synthesized from three independent polymerization mixtures of the same composition. The retention behaviour of all investigated analytes turned out to be comparable, RSDs ranged from 1.0 to 1.5% for retention times. Furthermore, the fluctuation of separation efficiencies was found low (RSD = 1.6–5.5% for HETP). The run-to-run repeatability of poly(styrene-divinylbenzene-methacrylic acid) monolith was checked by repetitive separations of the test mixture. The investigation of repeatability of

the retention behaviour was based on fifteen runs performed on the same column. The RSD values for the retention times were found to be between 0.3–0.5%. The RSD values obtained show a high reproducibility of the preparation procedure of monolithic columns presented in this study.

## 4. Conclusions

We have shown highly efficient separations of low-molecular-weight compounds achieved with poly(styrene-*co*-divinylbenzene-*co*-methacrylic acid) monolith as stationary phase for CLC. Despite of the fact that majority of scientific papers considers MAA only as a charge-bearing agent for the generation of EOF in CEC, this work demonstrates a general notable effect of this monomer on the separation selectivity of monoliths. The comprehensive batch-to-batch and run-to-run repeatability studies revealed a high reliability of the prepared separation media.

## Acknowledgements

Projects No. 78808, 710 and SVV 261204 of the Grant Agency of the Charles University and Research Projects MSM 0021620857 and RP14/63 of the Ministry of Education, Youth and Sports are acknowledged for the financial support.

## References

- [1] Švec, F., Fréchet J. M. J.: *Anal. Chem.* **64** (1992), 820–822.
- [2] Oberacher H., Huber C.G.: *Trends Anal. Chem.* **21** (2002), 166–174.
- [3] Jandera P., Urban J., Moravcová D.: *J. Chromatogr. A* **1109** (2006), 60–73.
- [4] Jin W., Fu H., Huang X., Xiao H., Zou H.: *Electrophoresis* **24** (2003), 3172–3180.
- [5] Huang, H.-Y., Lin, H., Y., Lin, S.-P.: *Electrophoresis* **27** (2006), 4674–4681.
- [6] Zhang Y.P., Ye X.W., Tian M.K., Qu L.B., Choi S.H., Gopalan A.I., Lee K.P.: *J. Chromatogr. A* **1188** (2008), 43–49.
- [7] Kucerova Z., Szumski M., Buszewski B., Jandera P.: *J. Sep. Sci.* **30** (2007), 3018–3026.
- [8] Davankov V.A., Tsyurupa M.P., Ilyin M., Pavlova L.: *J. Chromatogr. A* **965** (2002), 65–73.
- [9] Courtois J., Szumski M., Bystrom E., Iwasiewicz A., Shchukarev A., Irgum K.: *J. Sep. Sci.* **29** (2006), 14–24.
- [10] Xiong B., Zhang L., Zhang Y., Zou H., Wang J.: *J. High Resolut. Chromatogr.* **23** (2000), 67–72.

# Micellar Electrokinetic Chromatography of Natural Organic Dyes

EVA SVOBODOVÁ, ZUZANA BOSÁKOVÁ

Department of Analytical Chemistry, Faculty of Science, Charles University in Prague, Albertov 6, 128 43 Prague 2, Czech Republic, ✉ svobod15@natur.cuni.cz

**Keywords**  
identification  
MEKC  
organic dyes

## Abstract

World of colours goes with human population since ancient time. People use natural dyes for the paints and textile dyeing or making of organic pigments and lakes. Natural organic dyes are extracted from plants and animals. They contain various organic compounds which are typical for locality and climatic conditions of their origin. Their main colouring substances are structurally very similar and thus separation methods are used for their identification. Micellar electrokinetic chromatography has a power to resolve the dye-stuffs from their complex matrix with high separation efficiency. The effects of buffer pH (6.5–10.8) and sodium dodecyl sulfate concentration (0.01–0.02 mol L<sup>-1</sup>) on the effective mobilities of the analytes and their identification were tested. Micellar electrokinetic chromatography permits separation of all the analytes within 16 min, using 0.015 mol L<sup>-1</sup> sodium dodecyl sulfate in 0.01 mol L<sup>-1</sup> tetraborate buffer, pH = 8.5, at a voltage of 20 kV. Although this technique belongs to destructive methods, it allows to identify organic dyes more accurately than any of non-destructive methods.

## 1. Introduction

Natural organic dyes are wide used to prepare organic pigments, lakes and textil dyeing. For textil dyeing the dyestuffs are extracted from plants or animal bodies (especially insects), flushed in baths and precipitated on inorganic medium. Plants and animals living at different climate and geographic ground contain particular organic and inorganic substances. Identification of these unique substances is important for restorers, as well as for verification of the authenticity of works of art. So, the development of the analytical methods is of great interest.

The natural organic dyestuffs contain so called main colouring components which are responsible for colour of each dye. The main colouring components mostly belong to derivatives of indole (blue tones), phenol (yellow tones) and quinone (red tones) [1–3]. Their chemical structures are very similar in the same group of derivatives (Fig.1). Therefore the high-efficiency methods are needed for their separation and identification.

The main scope of this paper is optimization of micellar electrokinetic chromatography (MEKC) for identification of chosen natural organic dyes, namely acaroid, brazilwood, dragon's blood, kamala, logwood, cochineal, madder and lac-dye.

The most of chosen natural organic dyes belong to group of mordant dyes. The mordant dyes constitute a class of dyes according to technique of textile dyeing.

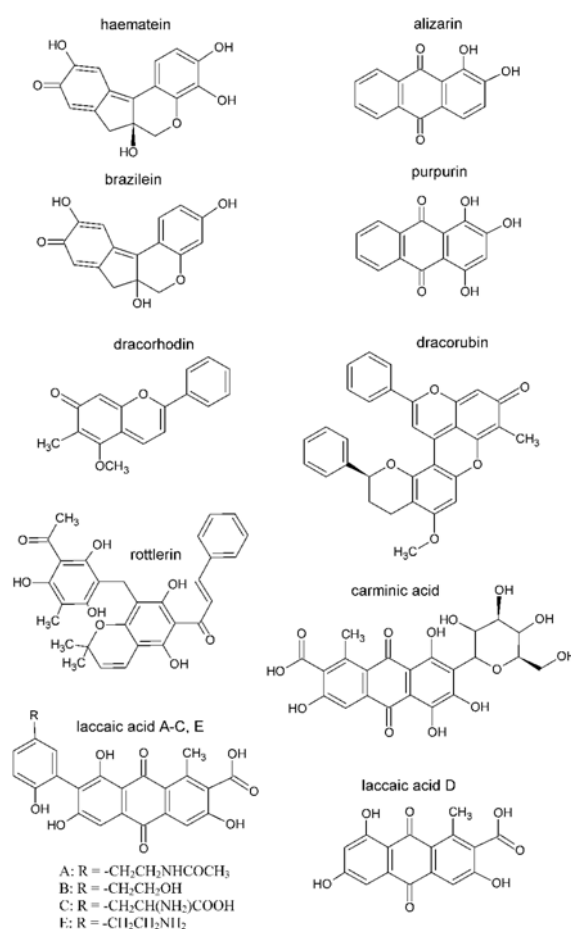


**Fig. 1.** Chemical structures of known main colouring matters of chosen organic dyes.

The textile fibres must be first mordanted by salt of multivalent ion of metal known as mordant. It is in effect an adsorption bond of metal ion into the fibre structure. After that the mordant dyes create the insoluble colourful complex with metal ion, known as lake. Acaroid and brazilwood belong to resin dyes. The main colouring component of brazilwood is brazilein. Brazilein's structural homologous is haematein which is a main colouring matter of dye logwood. The dye dragon's blood contains resins, tanstuffs and main colouring compounds which are derivatives of pyrrole dracorhodin and dracorubin. Rottlerin is a main colouring matter of dye kamala. Other quinone derivatives alizarin and purpurin are responsible for colourful tone of dye called madder or krapp. Alizarin and purpurin are homologues differing in number and position of hydroxyl groups (Fig.1). Carminic acid and laccaic acid are derivatives of anthraquinone, too and are prepared from dried bodies of insect. Carminic acid is main colouring compound of the dye cochineal. Laccaic acid contained in dye called lac-dye occurs in five forms marked as A to E (see Fig.1). The laccaic acid A is the majority form of laccaic acid. The chemical structures of main colouring compounds of chosen natural organic dyes are shown in Fig.1. [1, 4, 5].

## 2. Experimental

### 2.1. Chemicals

The analytes 1-acetyl-2,4,5,7-tetrahydroxy-9,10-anthraquinone (tetra-HA), 1-acetyl-2,4,5,7,8-penta-hydroxy-9,10-anthraquinone (penta-HA) and 1,2-dihydroxy-9,10-anthraquinone (alizarin), were isolated at the Institute of Microbiology of the Academy of Sciences of the Czech Republic with a purity > 98.0% determined by HPLC [6, 7]. 1,2,4-trihydroxy-9,10-anthraquinone (purpurin) with a purity > 95.0% were obtained from Fluka (Switzerland). The other standards of colouring main compounds of dyes, carmine, carminic acid, laccaic acid, haematein and rottlerin were obtained from Sigma-Aldrich, Germany. The dyes acaroid, kamala and madder were obtained from Kremer Pigmente (Germany). The dyes dragon's blood and cochineal (dried abdomens of *Coccus cacti*) were purchased from Sandragon (Czech Republic). Other dyes brazilwood, logwood and lac-dye were donated by Department of Chemical Technology of Monuments Conservation, ICT Prague.

For the preparation of the background electrolytes, disodium tetraborate decahydrate (p.a.), sodium dihydrogenphosphate (purity  $\geq 99.0\%$ ) and disodium hydrogenphosphate (purity  $\geq 99.0\%$ ) were supplied

by Lachema (Czech Republic), sodium dodecyl sulfate (SDS, purity  $\geq 95.0\%$ ) by Sigma-Aldrich (Germany), sodium hydroxide (p.a.) by Lach-Ner (Czech Republic) and hydrochloric acid (p.a.) by Penta (Czech Republic). Methanol (MeOH, purity  $\geq 99.9\%$ ) from Sigma-Aldrich was used to dissolve the analytes. The buffers were prepared using water purified by Rowapur and Ultrapur systems from Watrex (San Francisco, CA, USA).

### 2.2. Instrumentation

The electrophoretic measurements were carried out on HP<sup>3</sup>DCE with diode-array detector (Agilent Technologies, Germany) and PrinCE 250 auto-sampler (PrinCE Technologies B.V., Netherlands) with UV/Vis detector Spectra 100 (Therma Separation Products, USA). The fused-silica capillary from CACO (Slovak Republic) was used for experiments. The parameters of capillary were: i.d. = 75  $\mu\text{m}$  or 50  $\mu\text{m}$ , o.d. = 380  $\mu\text{m}$ , length to the detector 55.8 cm and total length of capillary 70 cm. The capillary was every morning flushed by deionized water (5 min), 1 mol L<sup>-1</sup> NaOH (10 min), deionized water again (5 min) and background electrolyte (BGE) for 10 min. During the analysis the capillary was flushed by 1 mol L<sup>-1</sup> NaOH (2 min), deionized water (3 min) and BGE (3 min). The measurements were carried out at temperature about 25 °C with hydrodynamically injection of 20–30 mbar for 5 s, at separation voltage of +20 kV and detection at wavelength of 254 nm. Each analysis was repeated three times. The PHM 220 instrument (Radiometer, Denmark) was used for measuring of the electrolyte pH. Methanolic solutions were sonicated in Ultrasonic bath LC30H (P-Lab, Czech Republic) and filtered through a polypropylene syringe filter with pore size of 0.2  $\mu\text{m}$  (Whatman, USA).

### 2.3. Standard Solutions and Buffers

The alizarin, purpurin, tetra-HA and penta-HA were dissolved in MeOH to obtain concentration of  $0.1 \times 10^{-3}$  mol L<sup>-1</sup>. Standard solutions of individual dyes acaroid, brazilwood, dragon's blood, logwood, kamala and lac-dye were prepared as saturated solutions in MeOH. Analogously haematein, rottlerin, carmine, carminic acid and laccaic acid were saturated in MeOH. The solutions of analytes were sonicated for 60 mins and then filtered through a 0.2  $\mu\text{m}$  disc polypropylene filter prior to the analysis. The standard solutions were diluted with MeOH to an appropriate concentration before use. The BGEs were 0.01 mol L<sup>-1</sup> phosphate buffers of pH = 7.6 and 6.6,

and 0.01 mol L<sup>-1</sup> tetraborate buffers of various pH values ranging from 8.5 to 10.8 with addition of SDS to obtain 0.010, 0.015 and 0.020 mol L<sup>-1</sup> concentrations.

### 3. Results and Discussion

Micellar electrokinetic chromatography (MEKC) serves first of all to separation of charged and uncharged molecules, as well. The separation of these hydrophobic molecules is based on different distribution coefficients between water and pseudo-stationary phase. This phase is created by micelles. According to the chemical structures of analytes, the BGE of alkaline pH values are needed. At this high pH value, the separated analytes are dissociated and carry a negative charge. However natural organic dyestuffs contain a lot of hydrophobic uncharged substances and are often insoluble in aqueous buffers. Due to this fact, the addition of sodium dodecyl sulphate (SDS) into BGEs could increase the solubility of analytes in BGE and improve the separation of uncharged molecules.

The four homologous derivatives of anthraquinone alizarin, purpurin, tetra-HA and penta-HA were chosen to obtain optimized conditions of MEKC separation. The effects of pH values of 0.01 mol L<sup>-1</sup> phosphate buffer and 0.01 mol L<sup>-1</sup> tetraborate buffer in a range of 6.5–10.8 and sodium dodecyl sulfate concentration (0.01–0.02 mol L<sup>-1</sup>) on speed and efficiency of separation were tested. The obtained pseudoeffective mobilities are presented in the Table 1.

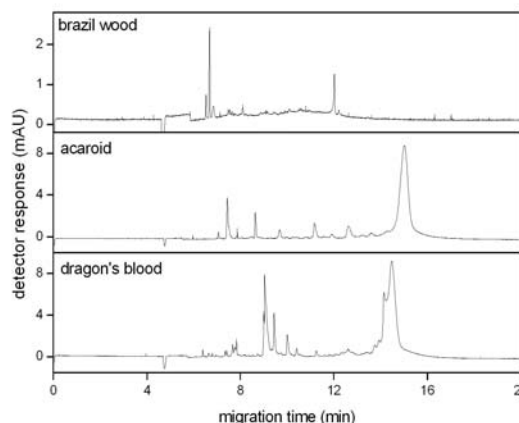


**Fig. 2.** The electrophoreograms of dyes brazilwood, acaroid and dragon's blood under optimized conditions: 0.01 mol L<sup>-1</sup> tetraborate buffer, pH = 8.5 and addition of 0.015 mol L<sup>-1</sup> SDS, hydrodynamically injection 20 mbar (in case of dragon's blood 30 mbar) for 5 s, voltage 20 kV and detection at 254 nm.

According to speed of analysis, high separation efficiency and resolution of studied analytes, the 0.010 mol L<sup>-1</sup> tetraborate buffer with pH = 8.5 and addition of 0.015 mol L<sup>-1</sup> SDS was chosen as the optimized BGE. These optimized conditions with hydrodynamic injection 20 or 30 mbar for 5 s, voltage 20 kV and detection at 254 nm were applied on separation and the electrophoretic behaviour of chosen natural organic dyes. At the same conditions, the electrophoreograms of commercially available main colouring compounds were obtained to identify and verify the majority peaks in the electrophoreograms of each dye. In the Fig. 2, there

**Table 1**

The overall electrophoretic mobilities of analytes obtained in MEKC at different pH values and different concentrations of SDS. Background electrolyte: 0.01 mol L<sup>-1</sup> tetraborate buffer (pH = 8.5–10.8) or 0.01 mol L<sup>-1</sup> phosphate buffer (pH = 6.5–7.5).

$c(\text{SDS})$ [mol L <sup>-1</sup> ]	pH	$\mu_{\text{eff}} (10^{-9} \text{ m}^2 \text{ V}^{-1} \text{ s}^{-1})$			
		alizarin	purpurin	tetra-HA	penta-HA
0.020	10.8	-25.10	-35.43	-34.95	-34.84
	9.5	-23.39	-32.21	-33.30	-33.95
	8.5	-23.17	-29.10	-39.57	-38.91
	7.5	-39.73	-29.77	-34.49	-35.43
	6.5	-42.25	-37.89	-39.43	-38.60
0.015	10.8	-25.28	-35.31	-35.08	-34.48
	9.5	-23.32	-30.10	-34.95	-34.05
	8.5	-22.77	-26.97	-38.41	-37.92
	7.5	-35.79	-31.63	-30.50	-34.86
	6.5	-41.23	-35.07	-37.28	-34.35
0.010	10.8	-24.15	-33.94	-34.57	-34.62
	9.5	-23.24	-30.17	-33.54	-34.22
	8.5	-23.13	-28.90	-37.00	-38.23
	7.5	-30.71	-27.80	-33.81	-35.26
	6.5	-34.81	-30.53	-31.01	-31.43

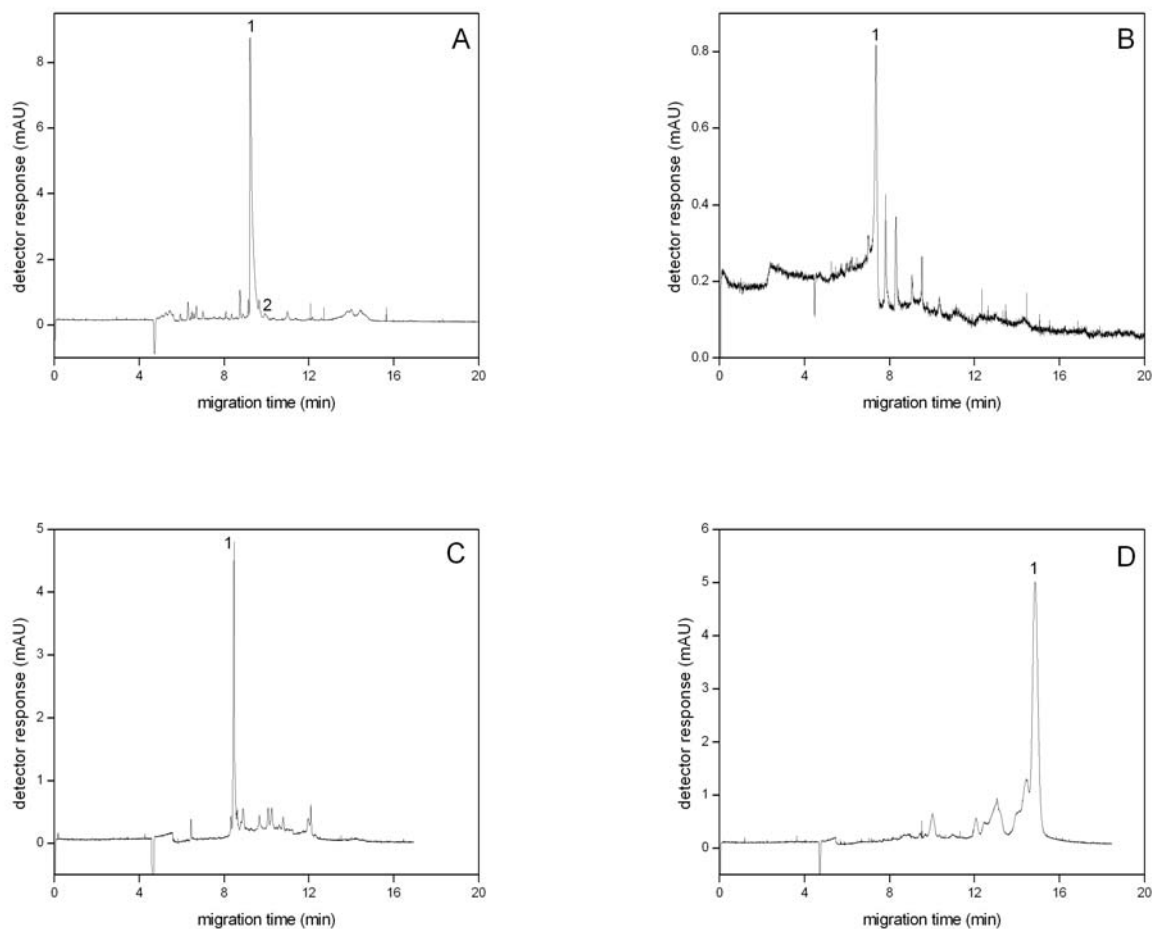


**Fig. 3.** The electrophoreograms of four dyes: (A) cochineal with main colouring compounds carminic acid (1) and carmine (2); (B) madder with main colouring compound alizarin (1); (C) logwood with main colouring compound haematein (1); and (D) kamala with rottlerin (1) as its main colouring compound. The separation conditions were  $0.01 \text{ mol L}^{-1}$  tetraborate buffer,  $\text{pH} = 8.5$  and addition of  $0.015 \text{ mol L}^{-1}$  SDS, hydrodynamically injection 20 mbar for 5 s, voltage 20 kV and detection at 254 nm.

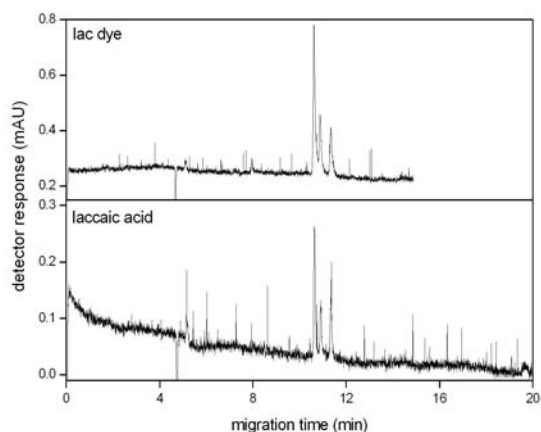


**Fig. 4.** The electrophoreogram of the dye lac-dye and its main colouring component laccic acid which coexists in up to five forms A–E. The separation conditions were  $0.01 \text{ mol L}^{-1}$  tetraborate buffer,  $\text{pH} = 8.5$  and addition of  $0.015 \text{ mol L}^{-1}$  SDS, hydrodynamically injection 20 mbar for 5 s, voltage 20 kV and detection at 254 nm.

are presented resins dyes acaroid and dragon's blood which are very similar and almost undistinguishable by infrared spectroscopy and TLC analysis. Their standards are not available, similarly to main colouring matter of brazilwood (Fig.2).

For other remaining dyes, i.e. kamala, logwood, lac-dye, madder and cochineal, the standards of main colouring components were available. Therefore, the majority peaks in electrophoreograms of each dye were verified by measurement of single main colouring component and its addition into solution of related dye, as well. In Fig. 3, MEKC analysis of dyes kamala, logwood, cochineal and madder are shown. The dye lac-dye contains three intensive peaks in its electrophoreo-gram which correspond to three peaks shown in MEKC analysis of commercially obtained standard laccic acid (Fig. 4). To identify the three laccic acids forms, a combination with the mass spectroscopy is necessary.

#### 4. Conclusions

The MEKC method is useful for reliable identification of all studied natural organic dyes at concentrations higher than  $0.1 \text{ mg mL}^{-1}$ . The optimized conditions of separation of alizarin, purpurin, tetra-HA and penta-HA were found and applied to separate of natural organic dyes. The optimized separation conditions are  $0.010 \text{ mol L}^{-1}$  tetraborate buffer,  $\text{pH} = 8.5$  with  $0.015 \text{ mol L}^{-1}$  SDS, hydrodynamical injection of 20 mbar for 5 s, separation voltage 20 kV and detection at wavelength 254 nm. There are some disadvantages of MEKC method, i.e. low solubility of studied dyes in MeOH and aqueous buffers, or destruction of sample. Therefore, non-destructive spectroscopic methods are often used. In contrary to them, MEKC makes possible to distinguish the resin dyes acaroid and dragon's blood due to the MEKC high separation efficiency. And moreover, there is a possibility of mass spectroscopy detection needed to determine a structure form of laccaic acid.

#### Acknowledgements

*This work was financially supported by the Grant Agency of Charles University (project SVV 261204) and by the Ministry of Education, Youth and Sports of the Czech Republic (projects MSM 0021620857 and RP 14/63).*

#### References

- [1] Čopíková J., Uher M., Lapčák O., Moravcová J., Drašar P.: *Chem. Listy* **99** (2005), 802–816.
- [2] Hofenk de Graaff J. H., Roelofs W. G. T., Van Bommel M. R.: *The Colourful Past. Origins, Chemistry and Identification of Natural Dyestuffs*. Riggisberg, Abegg-Stiftung 2004.
- [3] Wyplosz N.: *Laser Desorption Mass Spectrometric Studies of Artists' Organic Pigments*. Amsterdam, MolArt 2003.
- [4] Šimůnková E., Bayerová T.: *Pigmenty*. Praha, STOP 1999.
- [5] Hřebíčková B. A.: *Recepty starých mistrů aneb Malířské postupy středověku*. Brno, Computer Press 2006.
- [6] Bosáková Z., Peršl J., Jegorov A.: *J. High Res. Chromatogr.* **23** (2000), 600–602.
- [7] Stodůlková E., Kolařík M., Křesinová Z., Kuzma M., Šulc M., Man P., Novák P., Maršík P., Landa P., Olšovská J., Chudíčková M., Pažoutová S., Černý J., Bella J., Flieger M.: *Folia Microbiol.* **54** (2009), 179–187.

# *In vitro* Incubation of the Labial Gland and Fat Body of the Bumblebee Males *Bombus terrestris* with [1,2-<sup>14</sup>C]acetate and Analysis of the Metabolites

PETR ŽÁČEK<sup>a, b</sup>, RICHARD TYKVA<sup>a</sup>, JIŘÍ KINDL<sup>a</sup>, IRENA VALTEROVÁ<sup>a</sup>

<sup>a</sup> Institute of Organic Chemistry and Biochemistry, Academy of Sciences of the Czech Republic, Flemingovo nám. 2, 166 10 Prague 6, Czech Republic, ✉ zacek@uochb.cas.cz

<sup>b</sup> Department of Analytical Chemistry, Faculty of Science, Charles University in Prague, Albertov 6, 128 40 Prague 2, Czech Republic

## Keywords

*Bombus terrestris*

comprehensive two dimensional

gas chromatography

fat body

labial gland

thin layer chromatography

## Abstract

Labial glands and fat bodies of the bumblebee males species *Bombus terrestris* were incubated in the medium with sodium [1,2-<sup>14</sup>C]acetate and [1,2-<sup>12</sup>C]acetate addition. Metabolites of the acetate substrate were identified by means of localization of β emission from compounds containing <sup>14</sup>C in their structure on thin layer chromatography plates with non destructive position sensitive radio detector and comprehensive two dimensional gas chromatography (GC×GC-MS). It was found that radioactive [1,2-<sup>14</sup>C]acetate incorporated into various kind of compounds such as terpenoids, fatty acids, hydrocarbons and triacylglycerols.

## 1. Introduction

Most of the living creatures in our planet use variety kinds of compounds for communication. Pheromones belong to the group of infochemicals which are used for intra-species communication. Pheromone communication is the most important especially for insect – particularly for the social insect (ants, termites, bees, wasps, etc.). It influences all aspects of their life like mating, food source finding, identification of the colony members and others. Identification of the compounds involved in the communication and study of their biosynthesis is important for people for many reasons like using species-specific and non-toxic defence against pest (termites, ants, fruit flies, bark-beetle, etc.) or supporting development of the colonies of the “friendly” species (pollinators).

Majority of bumblebee species exhibit a patrolling behaviour. They fly around the nest tents of meters away from it and mark prominent objects in their territories (stones, leafs) with a pheromone secretion (marking pheromone) from the cephalic part of the labial gland [1–4]. The marked places attract conspecific virgin queens for mating [5]. The composition of the secretion is species-specific [1]. Labial gland of *Bombus terrestris* males contains mixture of terpenoid and aliphatic compounds [2] where 2,3-dihydrofarnesol and ethyl dodecanoate are the most abundant. This is different from for example

*Bombus lucorum* species which is closely related to the *B. terrestris* in the behavioural and habitat. *B. lucorum* males produces aliphatic compounds only. The most abundant is ethyl-(*Z*)-tetradec-9-enoate (53%) [2].

There are two potential pathways which could deliver these compounds: biosynthesis from common lipids in the fat body [6] or *de novo* from acetate units in the labial [7]. This work is focused on *de novo* biosynthesis study using method of *in vitro* incubation of the labial gland and fat body with radioactive [1,2-<sup>14</sup>C]acetate and analysis of the metabolites.

## 2. Experimental

### 2.1. Insects

The bumblebee males of both species were obtained from laboratory colonies from cooperating laboratory in Faculty of Science of Masaryk University in Brno. The tissues used in the incubations (cephalic part of the labial gland and fat bodies) were obtained from 2 days old bumblebee males.

### 2.2. Chemical

Water solution of sodium [1,2-<sup>14</sup>C]acetate was prepared from commercially available ethanol solution of specific activity 3.7 kBq uL<sup>-1</sup> (PerkinElmer, USA).

For our purposes the ethanol was evaporated by argon flow and the radioactive salt diluted in the same amount of distilled water, so the specific activity remained the same.

### 2.3. Incubation conditions

The final incubations were carried out in filtration columns (Zymo-Spin™ IIN, USA) in a medium which consisted of 1:1 mixture of Schneider's and Minimum essential Medium Eagle (Lonza, USA), 20 mM HEPES (Sigma, USA), 1% BSA (Sigma, USA), 5% sucrose (Sigma, USA), 20 mM concentration of non-active sodium [1,2-<sup>12</sup>C]acetate in a pH = 6.9 for 16 hours. The incubation columns were immersed in a water bath of temperature 35 °C. The medium was prefiltered through 0.22 μm membranes before use. Each tissue (fat body and cephalic part of the labial gland) were incubated separately in five parallels. Incubation process was started by addition of 5 μL of the water solution of sodium [1,2-<sup>14</sup>C]acetate of the specific activity 3.7 kBq uL<sup>-1</sup>. There were also prepared incubations without the radioactive acetate addition. These samples were used for GC×GC-MS analysis.

### 2.4. Samples preparation for analysis

Incubation process was finished by separation of the medium from the tissue by centrifugation (2000 g, 20 s for labial gland; 4000 g, 20 s for fat body). Incubation medium was entrapped to a collection tube and used for radioactivity measurement. The tissue stayed on the filter in the filtration column was washed three times by 300 μL of the incubation medium without sodium acetate addition. The same centrifugation parameters were used to remove the medium after each of the three washing procedures.

After that both types of the incubated tissues were removed from the filtration columns and put to the vial with 400 μL of chloroform. The vials were sank into the liquid nitrogen until the content frozen. After the vials defrosted they were sonified in a water bath for 15 minutes. This procedure was repeated once again. Each vial with the tissue and chloroform extract was centrifuged for 3 minutes before the chloroform phase was removed for next measurement.

### 2.5. Liquid scintillator analysis

For the extract radioactivity measurement 50 μL of the extract was mixed with 5 mL of the liquid scintillation cocktail (Ultima Gold, PerkinElmer, USA) and the equipment Tri-Carb 2900TR (PerkinElmer, USA) was used.

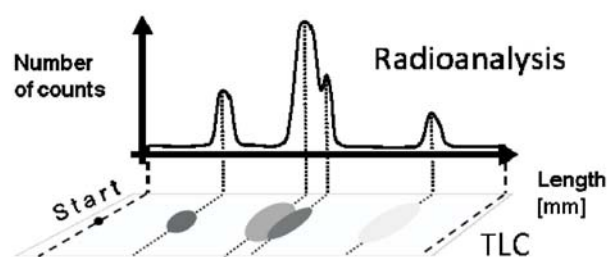


Fig. 1. Schema of the visualization of the bands on the TLC plate by the radioactivity detector.

### 2.6. TLC analysis

Thin layer chromatography separation of the components of the extract was performed on TLC silica gel plates (10×20 cm) 60 F254 with concentrating zone (2.5 cm) (Merck, USA). There were three separation lanes on one plate. The left side was used for separation of the group of the compounds expected in the tissue extracts. Extract of the gland incubated in the medium with radioactive acetate was fractionized in the middle part. Right side was used for separation of the extracts made of the tissue incubated without radioactivity. Volume of 75 μL or 100 μL of extract was applied. Mobile phase composition was optimized. The mobile phase used for sample made of labial gland consisted of hexan:ethylacetate:formic acid (70:30:1). For fat body samples a mobile phase of this composition hexan:ethylacetate:formic acid (90:10:1) was used. The middle part was analyzed by means of the non-destructive detection of <sup>14</sup>C-distribution by position sensitive detector (Raytest, model Rita star, USA); see Fig. 1.

### 2.7. GC/MS analysis

The bands on the right lane of the plates used for GC-MS analysis were localized by means of the positions of the same bands found by the radioactivity distribution detector on the middle lane. Gaseous iodine was used to determine the possible abnormalities in the chromatography separation for better localization of the bands of the same compounds among in all separation lanes on the plate. Iodine evaporated from the plate within 1 hour. Then the silica gel from the determined spot was removed from the plate and extracted in the filtration column by means of ether (2 × 150 μL). Subsequently the ether phase was removed using argon flow. Then 50 μL of hexane and 1 μL of 1-bromodecane standard (1.9 mg mL<sup>-1</sup>) were added. Spots containing fatty acids (according standards) were methylated by diazomethane and analyzed in a form of methyl esters.

The solution was analyzed by means of the comprehensive two dimensional gas chromatography with mass detection (GC×GC-MS) (Pegasus 4D from LECO, Co. (USA)). This system consists of gas chromatograph Agilent 6890N with split/splitless injector and mass analyser Time Of Fly (TOF). Separation parameters: splitless; constant He column flow 1 mL min<sup>-1</sup>; inlet temperature 250 °C; injection volume 1 µL; modulation time: 4 s (hot pulse 0.5 s); modulation temperature offset: 30 °C. First dimension column: length 30 m; 250 µm i.d.; film thickness 0.25 µm; phase DB-5 (J & W Scientific, USA); temperature gradient was applied: 50 °C (1 min), then 1 °C min<sup>-1</sup> to 320°C (1 min). Second dimension column: length 1.86 m; 100 µm i.d.; film thickness 0.1 µm, phase BPX-50 (SGE, Australia); temperature gradient was applied: 60 °C (1 min), then 10 °C min<sup>-1</sup> to 330 °C (1 min).

### 3. Results and Discussion

Biological aspect of this study the will not be discussed in this paper.

#### 3.1. Analytical problems

Analytical tools must have been chosen carefully and modified fully with respect to the biochemical requirements. Parameter which complicated the analysis most was high concentration of the non-active [1,2-<sup>12</sup>C]sodium acetate in the incubation solution which diluted the labeled acetate. This aspect greatly influenced the sensitivity of the TLC radio-analysis. This fact was connected with necessity to apply as much of the extract as possible which led to overdosing of the plates and deterioration in quality of the chromatography and next identification.

#### 3.2. Metabolites found in the fat body

The radioanalysis showed four signals in the TLC plate with fractionized fat body extract (Fig. 2). The peak (1) belongs probably to the very polar organic compounds like glycolipids, phospholipids and others. These compounds are out of our interest because there are not assumed to be straightly connected with pheromone biosynthesis process. The peak (2) belongs to the fatty acids analyzed as methyl-esters. The most abundant in the extract were triacylglycerols. They were identified by means of triacylglycerols standards. The peak (4) contains hydrocarbons.

#### 3.3. Metabolites found in the labial gland

Similarly to the chromatogram of the fractionized fat body there were also four signals found in the labial gland (Fig. 3). First peak likely belongs to the same group of compounds as in the fat body. The peak (3) presumably originate from two TLC bands whereas higher contribution of the signal appertain to the band with lover retardation factor ( $R_f = 0.51$ ; area A in Fig. 3). The GC×GC-MS analysis showed presence of the 2,3-dihydrofarnesol and a little amount of hexadecanol (Fig. 4A). Whereas in the band with  $R_f = 0.55$  hexadecanol, higher aliphatic alcohols and geranyl-citronellol were the most abundant. According the retardation factors of the standards presence of the fatty acids in the peak (4),  $R_f = 0.60$ , was expected. This part of the TLC was analysed after methylation by diazomethane (Fig. 3, area B). There were aliphatic methylesters with various length of the carbon chain found (Fig. 4B). The peak (4) clearly belongs to the higher aliphatic and terpenic (squalen) hydrocarbons.

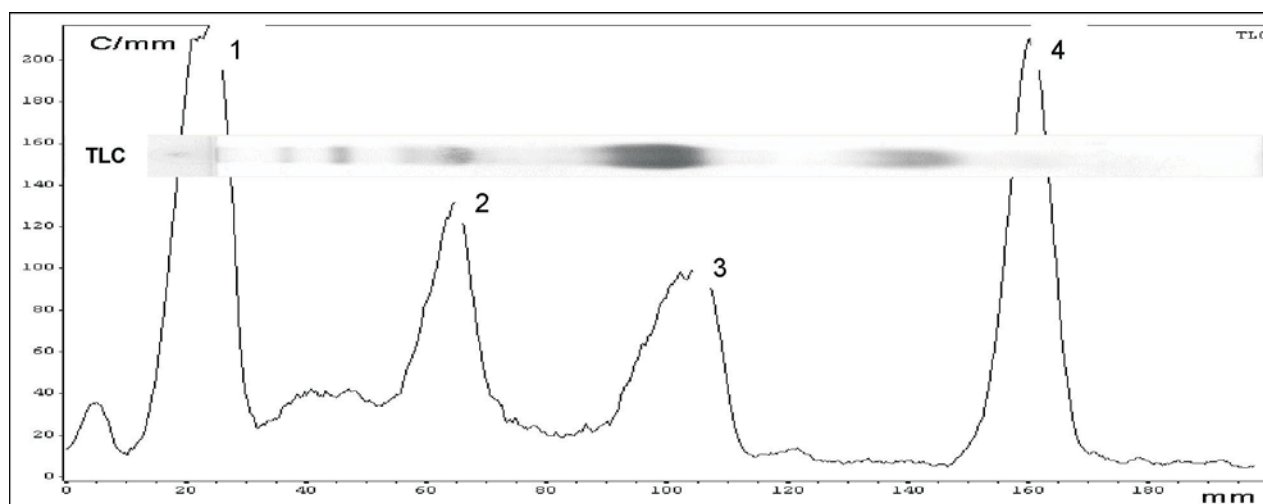
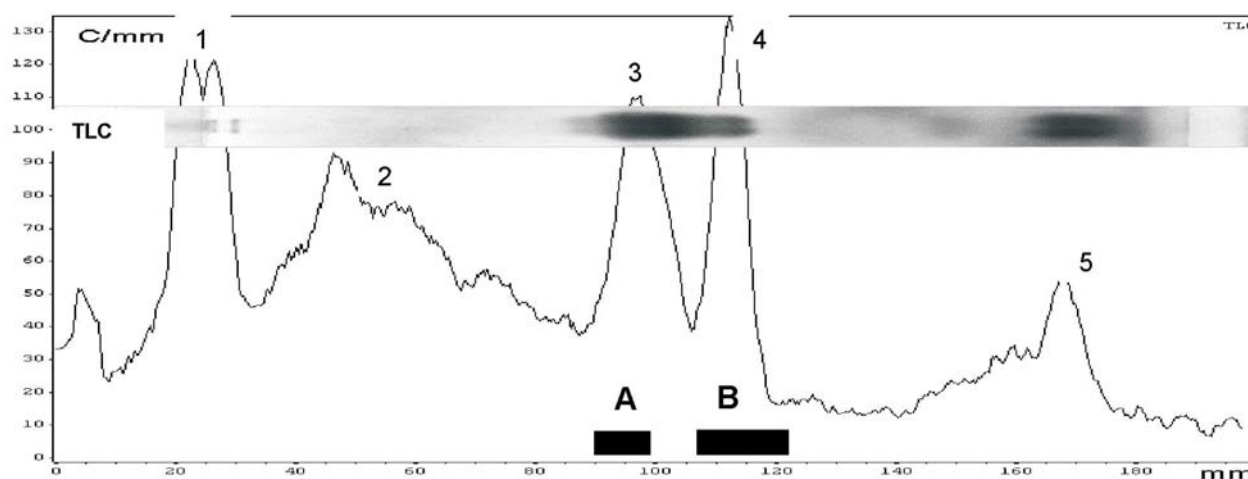
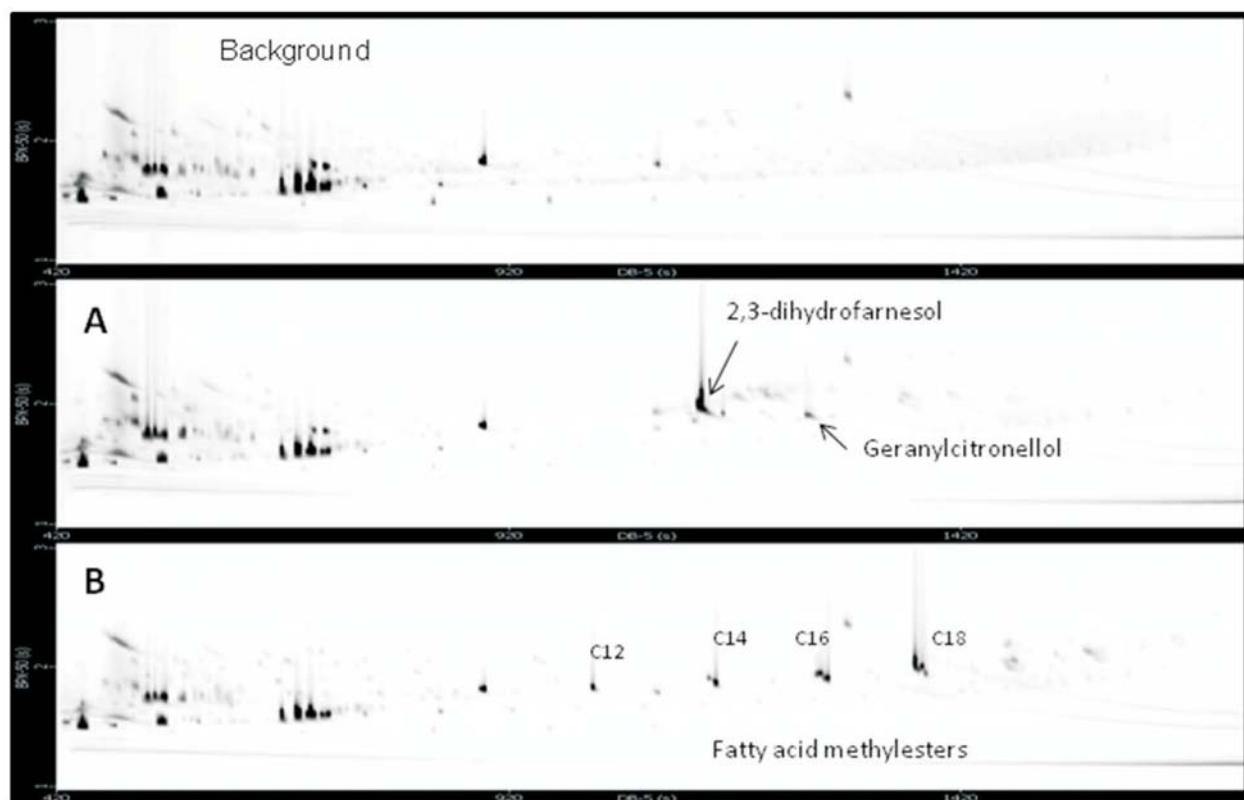


Fig. 2. TLC exposed to the concentrated sulphuric acid and visualization of the <sup>14</sup>C containing compounds in the fat body: (1) polar lipids (?), (2) fatty acids, (3) triacylglycerols, (4) hydrocarbons.



**Fig. 3.** TLC exposed to the concentrated sulphuric acid and visualization of the  $^{14}\text{C}$  containing compounds in the labial gland; (1) polar lipids (?), (2) background, (3) terpenic alcohols, (4) fatty acids, (5) hydrocarbons, A, B – areas with displayed 2D chromatogram in Fig. 4 from GC $\times$ GC-MS analysis.



**Fig. 4.** Two-dimensional chromatograms of the analysis from the two areas sampled from TLC of the labial gland extract.

#### 4. Conclusions

Compounds or group of compounds in the TLC areas containing radioactivity were identified. It is highly probable that certain percentage of these compounds were synthesised during the incubation process from acetate units.

These results suggest possibility of the *de novo* biosynthesis of the main component of the marking pheromone in labial gland.

#### Acknowledgements

The authors thank to Dr. Josef Holík from the Institute of Experimental Botany, Academy of Science of the Czech Republic, for making possible the radioanalysis, and Czech Science Foundation (#203/09/1446) for financial support.

#### References

- [1] ergström G., Svensson B. G., Appelgren M., Groth I.: Complexity of bumble bee marking pheromones. Biochemical, ecological and systematical interpretations. In: *Biosystematics of Social Insects. Vol. 19.* London, Academic Press 1981, p. 175.

- [2] Kullenberg B., Bergström G., Ställberg-Stenhagen S.: *Acta Chem. Scand.* **24** (1970), 1481–1483.
- [3] Morse D. H.: *Social Insect. Vol. III.* H. R. Hermann (Ed.). New York, Academic Press 1982, p. 245.
- [4] Bergström G.: *Zoon Suppl.* **1** (1973), 31–42.
- [5] Kullenberg B., Bergström G., Bringer B., Calberg B., Cederberg B.: *Zoon Suppl.* **1** (1973), 23–25.
- [6] Luxová A., Valterová I., Stránský K., Hovorka O., Svatoš A.: *Chemoecology* **13** (2003), 81–87.
- [7] Mann J.: *Chemical Aspects of Biosynthesis.* Oxford, Oxford University Press 1994.

# Polymers As a Construction Part of Electrochemical Nucleic Acid Biosensors

KATARÍNA BENÍKOVÁ, ADRIANA FERANCOVÁ, JÁN LABUDA

*Institute of Analytical Chemistry, Faculty of Chemical and Food Technology, Slovak Technical University in Bratislava, Radlinského 9, 812 37 Bratislava, Slovak Republic, ✉ katarina.benikova@stuba.sk*

## Keywords

biosensor  
electrochemical transducer  
nucleic acid  
polymers

## Abstract

During the last twenty years polymers became essential part in construction of biosensors. Wide variety of accessible types with specific advantages and functions enabled the enhancement in the field of biosensing. This article deals with the state of art in polymers used for construction of nucleic acid biosensors within the last years.

The use of polymers as an interface material for transducers modification increased sharply in recent years. Properties of the polymer-modified electrodes differ from those of the unmodified ones. By using polymeric layers, fairly thick films containing more active sites than a monolayer can be formed on the electrode.

Polymers in nucleic acid biosensors can provide many different functions, they can act as biorecognition element immobilization matrices, matrices for selective analyte binding and preconcentration, separation agents for analytes and interfering species, agents for reducing background adsorption of proteins or simply as electron transfer media. A large group of polymers used as biosensors represent electroactive polymers which are characterized by a response to external potential stimuli. They are used as sensors, actuators, highly sensitive membranes and energy storage. Besides synthetic polymers, this group of materials includes also natural polymers which offer a certain degree of functionality not available in most synthetic polymers. On the other hand, some applications are limited because of their special mechanical properties and doping feasibility. Electroactive polymers can be further divided in to electro conductive polymers such as poly-*p*-phenylene (PPP), polyphenylene sulphide (PPS), polythiophene (PT) polyaniline (PANI), and polypyrrole (PPY). The second class of electroactive polymers are non-conductive polymers (polyethyleneimine (PEI) and chitosan (CHIT)) doped with electrochemically active ions. The third class consist of polymeric redox mediators of the electron transfer like poly(vinylferrocene) or coordinating polymers like poly(4-vinylpyridine) which contain groups that can coordinate to metal ions and integrate them into the polymer matrix. Polymers may also be utilized or further modified as *co*-polymer composites, polymer composites with nanomaterials as polymer nanotube composite films or polymer

nanofibers, functionalized polymers or polymer-oligonucleotide (ODN) probes.

Most of the polymeric film properties and functions depend on its preparation. The mostly used methods are solvent casting, spin coating and electropolymerization. In solvent casting is a very simple method approach unfortunately two disadvantages have to be considered, uniformity of the polymeric film and reproducibility of its preparation. This method is usually used for the preparation of redox active or non-conducting polymers [1] and coatings of composites of nanomaterials with polymers [2]. Problems with uniformity and reproducibility can be avoided using spin coating method this method was successfully used for the preparation of the film of poly(3,4-ethylenedioxythiophene) (PEDOT) doped with poly(styrene sulfonic acid) (PSS) at the surface of indium tin oxide electrodes [3] and for the preparation of immunosensor based on conjugated poly(phenylene vinylene) derivative of defined thickness [4]. Another method often used for the preparation of conducting polymers, such as polypyrrole, polyaniline, polythiophene, and their derivatives is deposition by electropolymerization in the electrolyte contained monomers. This method can be used for the polymerization of compounds which possess a relatively low anodic oxidation potential and are susceptible to electrophilic substitution reaction. The advantage of this method is that the rate of film deposition can be controlled by varying the potential of the working electrode in the system [5]. Functionalization of polymers to modify properties of the polymeric film can be easily performed by two methods. First, the functional groups are attached to the monomers through covalent bonds and then electropolymerization is provided. Disadvantage of this method is loosing of polymer conductivity, steric hindrance and cross-linking effects. Another often

used method is an incorporation of dopand into the polymeric network electrostatically during the process of electropolymerization [6].

Next problem to be solved in nucleic acid biosensors is the immobilization of nucleic acid according to polymers. Polymer assisted immobilization of biomolecules, including nucleic acids, is widely reviewed [7]. Nucleic acid can be either immobilized at the surface of polymer modified electrode or can be incorporated in the polymer layer. In the second case, the method of electropolymerization is mostly used. Immobilization of DNA onto polymer modified electrode surface where nucleic acid can be attached to the polymer modified electrode surface using several methods: simple adsorption [8], covalent bonds [9] (first appropriate functional groups are introduced to the polymer, then DNA is covalently attached) or via affinity binding (avidin-biotin). Immobilization of DNA within a polymeric matrix by electropolymerization is another, widely used method. Negatively charged biomolecules, such as DNA and oligonucleotides, can be advantageously employed as dopands of positively charged polymeric structure [10]. The control of the current density at galvanostatic method or potential at potentiostatic method during the electropolymerization process is very important to avoid the loosing of bioactivity or decomposition of entrapped biomolecules.

As to describe the state of art of using polymers in construction of electrochemical nucleic acid biosensors the latest papers were chosen. Polypyrroles are group of polymers with excellent properties which can be advantageously used in enzyme (transducing the analytical signal generated by redox enzyme reactions) as well as affinity biosensors (DNA biosensors, immunosensors). Polypyrroles are used as an electrostatic adsorption matrix for immobilization of DNA onto porous silicon substrate without using covalent bonds [11]. Polypyrroles are reported as convenient matrix for the immobilization of nanomaterials at the surface of electrode [12]. In this case the combination of unique properties of conducting polymers in combination with those of nanomaterials exhibits the synergic effect which positively affects the stability, electron transfer and improved performance of final biosensors. Polypyrrole film possessed the uniform surface for the immobilization of Au-Pt hybrid nanoparticles [13].

Polyaniline is widely used for the preparation of the electrochemical enzyme biosensors and immunosensors [14]. However, several applications in DNA biosensors can also be found. Polyaniline can be prepared by electropolymerization using galvanostatic method, potentiostatic method leading to

a polymer adhered weakly at the electrode surface or potential cycling which produces polymer well adhered at the electrode surface [15].

Polythiophenes and their derivatives are also widely used for the preparation of DNA biosensors. The disadvantage of this polymers is in difficult electropolymerization of polymers with functional groups suitable for the immobilization of biomolecules (amino- or carboxylic groups) [16]. Electropolymerized poly(4-hydroxyphenyl thiophene-3-carboxylate) as cationic polymer was advantageously used for the electrostatic binding of polyanionic ODN [17]. Moreover, interaction between PEDOT and specific ODN was studied using electrophoresis and spectroscopic methods [18]. It was shown that together with non-specific electrostatic interactions specific hydrogen binding interactions between polymer and methylated ODN appeared and stable complexes were formed. PEDOT was first prepared by electropolymerization at the surface of glassy carbon electrode and then DNA solution was spread over the polymer modified electrode [19]. DNA was available for the electrostatic binding of Nile blue as redox indicator.

Quinone containing polymers, namely poly(5-hydroxy-1,4-naphtoquinone-co-5-hydroxy-3-thioacetic acid-1,4-naphtoquinone), known as poly(JUG-co-JUGA), are also popular for the preparation of DNA biosensors. In contrast to classical conducting polymers, such as polypyrrole or polyaniline where signal transduction is performed via redox process of the polymer exchanging anion, in the case of poly(JUG-co-JUGA) the signal is transduced by quinine group in the polymer [20]. Electropolymerized polyquinone film was successfully derivatized with glutathione [21]. Glutathione was used as a precursor for subsequent biomolecule linkage via carboxylic groups.

Poly(vinylferrocene) is soluble polymer which can be easily deposited at the surface of platinum [22] or graphite working electrode [23] by its electrooxidation resulting in a less soluble polymer poly(vinylferrocenium). Such electrode can be then advantageously used for the immobilization of negatively charged DNA. Low non-specific immobilization of DNA on this polymer was reported [23]. Electrochemical signal of such polymer can be used for the detection of hybridization event [22].

Polyethyleneimine and chitosan are cationic polymers with good biocompatibility and high positive charge density which allows an easy electrostatic DNA immobilization. Study of interaction between DNA molecule and polyethyleneimine-copper(II) complexes showed that together with electrostatic interaction, van der Waals

interactions and hydrogen binding is also employed probably due to the presence of multiple copper(II) complex molecular units and free amine groups of the polymer [24]. It was shown that the surface of modified electrodes was homogeneous and electron transfer was slower when polyethyleneimine formed an external layer [25].

The range of polymers conducting, non-conducting, doped or modified that can be used to prepare nucleic acid biosensor is widening markedly. New composites, *co*-polymers are reported in order to present their synergic effects.

#### Acknowledgement

This work was supported by the Scientific Grant Agency VEGA (Project No. 1/0852/08)

#### References

- [1] Chang Z., Fan H., Zhao K., Chen M., He P., Fang Y.: *Electroanalysis* **20** (2008), 131.
- [2] Rivas G. A., Rubianes M. D., Rodríguez M. C., Ferreyra N. F., Luque G. L., Pedano M. L., Miscoria S. A., Parrado C.: *Talanta* **74** (2007), 291.
- [3] Manesh K. M., Santhosh P., Gopalan A., Lee K. P.: *Talanta* **75** (2008), 1307.
- [4] Cooreman P., Thoelen R., Manca J., Vande Ven M., Vermeeren V., Michiels L., Ameloot M., Wagner P.: *Biosens. Bioelectron.* **20** (2005), 2151.
- [5] Vidal J. C., Garcia-Ruiz E., Castillo J. R.: *Microchim. Acta* **143** (2003), 93.
- [6] Raouf J. B., Ojani R., Rashid-Nadimi S.: *Electrochim. Acta* **49** (2004), 271.
- [7] Teles F. R. R., Fonseca L. P.: *Mater. Sci. Eng. C.* **28** (2008), 1530.
- [8] Zhang Y., Zhang K., Ma H.: *Anal. Biochem.* **387** (2009), 13.
- [9] Prabhakar N., Dingh H., Malhotra B. D.: *Electrochem. Commun.* **10** (2008), 821.
- [10] Xu H., Wu H., Fan C., Li W., Zhang Z., He L.: *Chin. Sci. Bull.* **49** (2004), 2227.
- [11] Jin J. H., Alocilja E. C., Grooms D. L.: *J. Porous Mater.* **17** (2010), 169.
- [12] Tiwari I., Singh K. P., Singh M.: *Russ. J. Gen. Chem.* **79** (2009), 2685.
- [13] Che X., Yuan R., Chai Y., Ma L., Li W., Li J.: *Microchim. Acta* **167** (2009), 159.
- [14] Di Wei, Ivaska A.: *Chem. Anal.* **51** (2006), 839.
- [15] Bhadra S., Khastgir D., Singha N. K., Lee J. H.: *Progress Polymer. Sci.* **34** (2009), 783.
- [16] Peng H., Zhang L., Soeller C., Travas-Sejdic J.: *Bio-materials* **30** (2009), 2132.
- [17] Uygun A.: *Talanta* **79** (2009), 194.
- [18] Aleman C., Teixeira-Dias B., Zanuy D., Estrany F., Armelin E., del Valle L. J.: *Polymer* **50** (2009), 1965.
- [19] Chen Z. W., Balamurugan A., Chen S. M.: *Bioelectrochem.* **75** (2009), 13.
- [20] Reisberg S., Piro B., Noel V., Nguyen T. D., Nielsen P. E., Pham M. C.: *Electrochim. Acta* **54** (2008), 346.
- [21] Reisberg S., Acevedo D. C., Korovitch A., Piro B., Noel V., Buchet I., Tran L. D., Barbero C. A., Pham M. C.: *Talanta* **80** (2010), 1318.
- [22] Kuralay F., Erdem A., Abaci S., Özyörük H., Yildiz A.: *Anal. Chim. Acta* **643** (2009), 83.
- [23] Kuralay F., Erdem A., Abaci S., Özyörük H., Yildiz A.: *Electrochem. Commun.* **11** (2009), 1242.
- [24] Kumar R. S., Sasikala K., Arunachalam S.: *J. Inorg. Biochem.* **102** (2008), 234.
- [25] Ferreyra N. F., Bollo S., Rivas G. A.: *J. Electroanal. Chem.* **638** (2009), 262.

# New Types of Silver Amalgam Electrodes and Their Applications

ALEŠ DAÑHEL<sup>a</sup>, JIŘÍ BAREK<sup>a</sup>, BOGDAN YOSYPCHUK<sup>b</sup>

<sup>a</sup> Charles University in Prague, Faculty of Science, Department of Analytical Chemistry, UNESCO Laboratory of Environmental Electrochemistry, Albertov 6, 128 43 Prague 2, The Czech Republic, ✉ danhel@natur.cuni.cz

<sup>b</sup> Academy of Sciences of the Czech Republic, Jaroslav Heyrovský Institute of Physical Chemistry, Dolejškova 3, 182 23 Prague, The Czech Republic

## Keywords

amperometry  
nitrophenols  
silver amalgam  
voltammetry

Silver amalgam electrodes offer wide range of application possibilities for determination of inorganic and organic electrochemically reducible compounds [1, 2]. Some new possibilities of this electrode material used for construction of working electrodes utilized in modern voltammetric and amperometric methods are presented in this work.

A silver solid amalgam paste electrode combines the advantages of silver solid amalgam electrodes (mainly wide applicable potential window) and carbon paste electrodes (easily renewable electrode surface). The silver solid amalgam paste electrodes can be easily prepared by mixing of silver amalgam fine powder and a proper pasting liquid. Easily renewable electrode surface eliminating the problem of passivation, sufficiently wide potential window in negative range of applied potentials and good signal reproducibility and sensitivity are the main advantages of the electrode in modern voltammetry. Its electrode properties were tested by voltammetric methods using 4-nitrophenol as a model compound [3].

Well known polished silver solid amalgam electrodes (p-AgSAE) can be among others applications used for amperometric detection in connection with preliminary separation techniques. A common “pen type” p-AgSAE in wall-jet arrangement and specially prepared p-AgSAE for commercially available thin-layer detector (BAS, USA) were used for amperometric detection of nitrophenol mixture after their separation using HPLC. It was found that the thin-layer arrangement utilizing p-AgSAE offers more stable baseline signal, lower background current and higher value of signal/noise ratio than wall-jet arrangement [4].

Newly developed working electrodes based on single crystal of the silver amalgam were prepared and

used for voltammetric and amperometric detection. Prepared microcylindrical electrodes were used for voltammetric determination of 4-nitrophenol and could be used in microvolume analysis. Single crystal silver amalgam was also successfully used for construction of cylindrical flow cell utilized in amperometric detection of nitrophenol mixture. However, the single crystal silver amalgam electrodes are fragile and they have relatively short lifetime. On the other hand, they offer potential window comparable with hanging mercury drop electrode, good reproducibility and high sensitivity in voltammetry and also low background current in amperometry in comparison with the solid amalgam electrodes.

There is no doubt that the mercury electrodes are the best sensors for detection of reducible compounds but the “non-toxic” silver amalgam electrodes became their suitable alternatives in voltammetry and offer numerous application possibilities in amperometry.

## Acknowledgments

Financial support from Ministry of Education, Youth and Sports of the Czech Republic (LC 06035, RP 14/63 and MSM 0021620857) and Grant Agency of Charles University (SVV 261204 and 89710/2010/B-Ch/PrF) is gratefully acknowledged.

## References

- [1] Yosypchuk B., Barek J.: *Crit. Rev. Anal. Chem.* **39** (2009), 189–203.
- [2] Yosypchuk B., Navratil T., Barek J., Peckova K., Fischer J.: Amalgam electrodes as sensors in the analysis of aquatic systems. In: *Progress on Drinking Water Research*. LeFebvre M.H., Roux M.M. (eds.), New York, Nova Science Publishers 2008, p. 143–169.
- [3] Barek J., Danhel A., Kadlcikova A., Kotkova Z., Obsil T., Silhan J.: *Chem. Listy* **103** (2009), 331.
- [4] Danhel A., Shiu K.K., Yosypchuk B., Barek J., Peckova K., Vyskocil V.: *Electroanalysis* **21** (2009), 303–308.

# Voltammetric Determination of 2-Amino-6-Nitrobenzothiazole at Different Amalgam Electrodes

DANA DEÝLOVÁ, JIŘÍ BAREK

Charles University in Prague, Faculty of Science, Department of Analytical Chemistry, UNESCO Laboratory of Environmental Electrochemistry, Albertov 6, 128 43 Prague 2, The Czech Republic, ✉ barek@natur.cuni.cz

## Keywords

amalgam electrodes  
2-amino-6-nitrobenzothiazole  
differential pulse voltammetry  
direct current voltammetry

## Abstract

Optimal conditions have been found for the determination of 2-amino-6-nitrobenzothiazole using direct current voltammetry and differential pulse voltammetry at a polished silver solid amalgam electrode in the concentration range  $1 \times 10^{-6}$  to  $1 \times 10^{-4}$  mol L<sup>-1</sup> and at a mercury meniscus modified silver solid amalgam electrode in the concentration range  $1 \times 10^{-7}$  to  $1 \times 10^{-4}$  mol L<sup>-1</sup>.

## 1. Introduction

2-Amino-6-nitrobenzothiazole (ANBT, see Fig. 1) is frequently used as a base in dyes production by diazotation [1]. Colours of thus prepared dyes are mainly red and violet [2]. This substance is a chromophore for the photoconductive measurements [3] and it is used as a high glass transition chromophore in nonlinear optical applications [4]. In the past, the polarographic and voltammetric behavior of ANBT has been investigated using polarography, oscillopolarography [5], cyclic voltammetry and coulometric techniques [6] at mercury electrodes. The first wave/peak of its electrochemical reduction corresponded to a four-electron reduction of nitro group to the hydroxyamino group and the second wave/peak to the reduction of hydroxyamino group to amino group involving two-electron electrode reaction [6].

It is obvious that mercury is the best electrode material for these determinations. However, because of fears of mercury toxicity, there is a tendency to substitute mercury with other non-toxic materials. Therefore, we pay attention to practically non-toxic polished silver solid amalgam electrode (p-AgSAE) and mercury meniscus modified silver solid amalgam electrode (m-AgSAE), which have a good mechanical stability, simple handling and regeneration including an electrochemical pre-treatment of its surface [7].

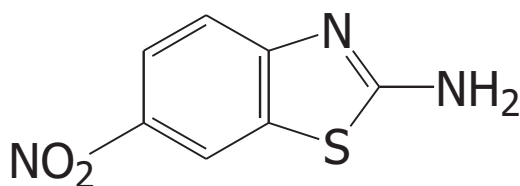


Fig. 1. Structural formula of 2-amino-6-nitrobenzothiazole

These electrodes were found suitable for the determination of submicromolar concentrations of selected nitrated polycyclic aromates, which are typical representatives of polarographically active environmental carcinogens [8].

## 2. Experimental

### 2.1. Reagents

2-Amino-6-nitrobenzothiazole ( $\geq 97\%$ , CAS Registry number: 6285-57-0) was supplied by Sigma Aldrich. A stock solution of  $1 \times 10^{-3}$  mol L<sup>-1</sup> was prepared by dissolving an exactly weighed amount of the substance in methanol. Diluted solutions were prepared by exact dilution of the stock solution with methanol. The solutions were stored in refrigerator. The diluted solutions were prepared fresh every day. Britton-Robinson (BR) buffer solutions were prepared in a usual way by mixing a  $0.04$  mol L<sup>-1</sup> solution of phosphoric acid, acetic acid and boric acid with an appropriate amount of  $0.2$  mol L<sup>-1</sup> sodium hydroxide (all of analytical-reagent grade, all obtained from Merck). Deionized water was produced by Milli-Qplus system, Millipore.

### 2.2. Apparatus

Voltammetric measurements were carried out using an Eco-Tribo Polarograph driven by Polar Pro 2.0 software (both Polaro-Sensors, Prague, Czech Republic). The software worked under the operational system Microsoft Windows 98 Plus (Microsoft Corporation). All measurements were carried out in a three-electrode system using platinum electrode PPE (Monokrystalý, Turnov, Czech Republic) as an

auxiliary electrode and silver/silver chloride electrode RAE 113 ( $3 \text{ mol L}^{-1}$  KCl, Monokrystal, Turnov, Czech Republic) as a reference electrode. A polished silver solid amalgam electrode (p-AgSAE) and a mercury meniscus modified silver solid amalgam electrode (m-AgSAE) were used as working electrodes. The preparation pencil electrodes is simple [9] and working dimensions are in square micrometers range. Scan rate,  $20 \text{ mV s}^{-1}$ , was used for both direct current voltammetry (DCV) and differential pulse voltammetry (DPV), pulse amplitude,  $-50 \text{ mV}$ , and pulse width,  $100 \text{ ms}$ , were used for DPV.

### 2.3. Procedures

For voltammetric measurements, an appropriate amount of ANBT stock solution in methanol was measured into a voltammetric vessel, methanol was added to a total volume of  $1.0 \text{ mL}$  and filled up to  $10.0 \text{ mL}$  with BR-buffer of appropriate pH. Oxygen was removed from the measured solutions by bubbling with nitrogen for five minutes. All curves were measured 3 times.

At the beginning, p-AgSAE was polished on the alumina with particle size  $1.1 \mu\text{m}$ . The m-AgSAE was prepared by the modification of p-AgSAE by dipping on  $15 \text{ s}$  to the mercury. Before starting the work, as well as in the case of electrode passivation, the electrochemical activation of electrodes was carried out in  $0.2 \text{ mol L}^{-1}$  KCl at  $-2200 \text{ mV}$  under stirring of the solution for  $300 \text{ seconds}$  followed by rinsing with distilled water. The regeneration was carried out by periodical switching every  $0.1 \text{ s}$  between regeneration potentials ( $E_{1, \text{reg}}$  and  $E_{2, \text{reg}}$ ) during  $30 \text{ seconds}$ . First regeneration potential was about  $50$  to  $100 \text{ mV}$  more negative than the potential of the anodic dissolution of the electrode, second regeneration potential was about  $50$  to  $100 \text{ mV}$  more positive than the potential of the hydrogen evolution in the given supporting electrolyte. Regeneration always ended at a more negative potential.

The parameters of calibration curves (e.g., slope, intercept, limit of determination) were calculated using statistic software Adstat, which used confidence bands ( $\alpha = 0.05$ ) for calculation of the limit of determination (LOQ). It corresponds to the lowest signal for what relative standard deviation is equal  $0.1$  [10].

## 3. Results and Discussion

The influence of pH on voltammetric behavior of ANBT was investigated in a BR buffer:methanol (9:1) media in the range of  $\text{pH} = 2.0$ – $12.0$ . It can be seen from Fig. 2 that ANBT gives one well-developed peak at  $\text{pH} = 2.0$ – $5.0$ , the second peak can be observed at

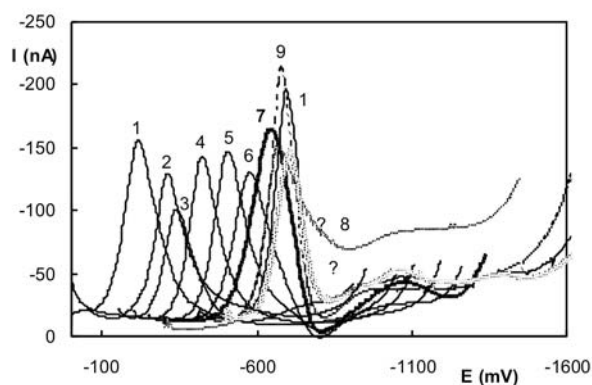


**Fig. 2.** DP voltammograms of 2-amino-6-nitrobenzothiazole ( $c = 1 \times 10^{-4} \text{ mol L}^{-1}$ ) at p-AgSAE in the BR-buffer:methanol (9:1) medium; the BR-buffer pH: 2.0 (1), 3.0 (2), 4.0 (3), 5.0 (4), 6.0 (5), 7.0 (6), 8.0 (7), 9.0 (8), 10.0 (9), 11.0 (10), 12.0 (11); polarization rate,  $20 \text{ mV s}^{-1}$ .

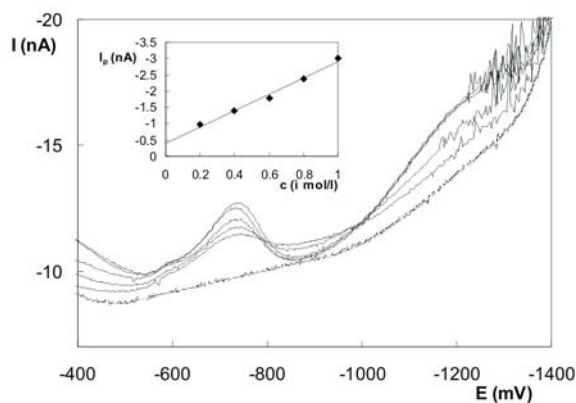


**Fig. 3.** DP voltammograms of 2-amino-6-nitrobenzothiazole ( $c = (2\text{--}10) \times 10^{-7} \text{ mol L}^{-1}$ ) at m-AgSAE in the BR-buffer ( $\text{pH} = 10.0$ ):methanol (9:1) medium (dotted line is the basic electrolyte); regeneration potentials,  $E_{1, \text{reg}} = -400 \text{ mV}$ ,  $E_{2, \text{reg}} = 900 \text{ mV}$ ; polarization rate,  $20 \text{ mV s}^{-1}$ ; the corresponding calibration straight line is given in the inset.

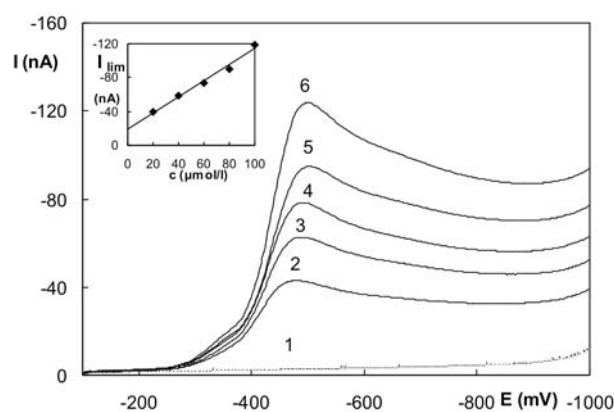


**Fig. 4.** DP voltammograms of 2-amino-6-nitrobenzothiazole at p-AgSAE in the BR-buffer ( $\text{pH} = 4.0$ ):methanol (9:1) medium concentrations measured:  $0$  (1),  $20$  (2),  $40$  (3),  $60$  (4),  $80$  (5) and  $100$  (6)  $\mu\text{mol L}^{-1}$ ; regeneration potentials,  $E_{1, \text{reg}} = -200 \text{ mV}$ ,  $E_{2, \text{reg}} = 600 \text{ mV}$ ; polarization rate,  $20 \text{ mV s}^{-1}$ ; the corresponding calibration straight line is given in the inset.

**Table 1**

Parameters of the calibration straight lines for the determination of 2-amino-6-nitrobenzothiazole measured in the lowest attainable concentration ranges

Electrode	Method	BR buffer	Concentration mol L <sup>-1</sup>	Slope 10 <sup>6</sup> nA mol L <sup>-1</sup>	Intercept nA	Correlation coefficient	LOQ mol L <sup>-1</sup>
p-AgSAE	DCV	pH = 4	(2–10)×10 <sup>-6</sup>	1.21	-13.1	0.9987	3.2×10 <sup>-6</sup>
	DPV	pH = 3	(2–10)×10 <sup>-6</sup>	1.25	-1.5	0.9961	2.6×10 <sup>-6</sup>
	DCV	pH = 10	(2–10)×10 <sup>-6</sup>	2.85	-16.3	0.9918	3.1×10 <sup>-6</sup>
	DPV	pH = 10	(2–10)×10 <sup>-6</sup>	1.38	11.6	0.9957	2.2×10 <sup>-6</sup>
m-AgSAE	DCV	pH = 4	(2–10)×10 <sup>-7</sup>	1.42	0.1	0.9880	6.8×10 <sup>-7</sup>
	DPV	pH = 3	(2–10)×10 <sup>-7</sup>	1.58	0.3	0.9932	4.5×10 <sup>-7</sup>
	DCV	pH = 10	(2–10)×10 <sup>-6</sup>	6.25	0.4	0.9895	2.7×10 <sup>-6</sup>
	DPV	pH = 10	(2–10)×10 <sup>-7</sup>	2.51	-0.4	0.9944	3.9×10 <sup>-7</sup>

more negative potentials. The peak potentials are shifted towards negative values with increasing pH which can be explained by a preceding protonation of nitro group in ANBT. This trend was observed on both electrodes using both DCV and DPV.

The best developed peak was obtained in BR-buffer (pH = 10):methanol (9:1) medium. This pH was further used for measuring the calibration curves (Fig. 3). For the sake of comparison, conditions representing acid medium, BR-buffer of pH 3.0 (for DPV) and 4.0 (for DCV) (see Fig. 4) were tested as well for both electrodes used. Parameters of calibration curves are summarized in Table 1.

The limits of determination attained using DCV or DPV at the p-AgSAE were higher in comparison with values attained at m-AgSAE. The same holds for intercepts of corresponding calibration straight lines.

#### 4. Conclusions

It has been shown that modern voltammetric methods at amalgam electrodes can be used for the determination of submicromolar concentrations of 2-amino-6-nitrobenzothiazole. Lowest calibration range were (2–10)×10<sup>-6</sup> mol L<sup>-1</sup> for DCV and DPV at p-AgSAE, and DCV at m-AgSAE (BR-buffer (pH = 10.0): methanol (9:1) medium used), and (2–10)×10<sup>-7</sup> mol L<sup>-1</sup> for DCV and DPV at m-AgSAE.

#### Acknowledgments

This research was supported by the Ministry of Education, Youth and Sports of the Czech Republic (projects MSM 0021620857, LC 06035, and RP 14/63) and by the Grant Agency of Charles University in Prague (project SVV 261204).

#### References

- [1] Sokolowska-Gajda J., Freeman H.S.: *Dyes Pig.* **20** (1992), 137–145.
- [2] Towns A.D.: *Dyes Pig.* **42** (1999), 3–28.
- [3] Diduch K., Wübbenhorst M., Kucharski S.: *Synth. Met.* **139** (2003), 515–520.
- [4] Broeck K., Verbiest T., Degryse J., Beylen M., Persoons A., Samyn C.: *Polymer* **42** (2001), 3315–3322.
- [5] Gorokhovskaya V.I.: *Zh. Obsh. Khim.* **32** (1962), 3859–3864.
- [6] Saraswati K., Vijayalakshmi K., Prameela P.: *Transaction of the SAEST* **31** (1996), 96–101.
- [7] Yosypchuk B., Novotný L.: *Electroanalysis* **14** (2002), 1733–1749.
- [8] Barek J., Fischer J., Navrátil T., Pecková K., Yosypchuk B.: *Sensors* **6** (2006), 445–452.
- [9] Yosypchuk B., Barek J.: *Anal. Chem.* **39** (2009), 189–203.
- [10] Meloun M., Militký J., Forina M.: *Chemometrics for Analytical Chemistry, PC-Aided Regression and Related Methods, Vol. 2.* Chichester, Ellis Horwood 1994.

# Electrochemical Sensor: Mediator Deposition by Drop Evaporation

VĚRA MANSFELDOVÁ<sup>a, b</sup>, PAVEL JANDA<sup>a</sup>, HANA TARÁBKOVÁ<sup>a</sup>

<sup>a</sup> *J. Heyrovský Institute of Physical Chemistry of ASCR, v. v. i., Dolejškova 3, 182 23 Prague 8, Czech Republic, ✉ mansfeldova@jh-inst.cas.cz*

<sup>b</sup> *Department of Analytical Chemistry, Faculty of Science, Charles University in Prague, Albertov 6, 128 40 Prague 2, Czech Republic*

## Keywords

atomic force microscopy  
carbon electrode  
cyclic voltammograms  
surface modification

## Abstract

Among many different kinds of electrode surface modification procedures, the surface coating by vaporized mediator solution is still used as a simple and effective method for preparation of sensing electrode. Surface of glassy carbon (GC) is often used as a supporting collector, but it requires polishing, rinsing and sonication prior to mediator deposition. In this paper, we present common methods of modification of highly oriented pyrolytic graphite (HOPG) and GC surface, respectively, from the point of surface nanomorphology investigated by atomic force microscopy.

## 1. Introduction

One of the simplest ways of electrode modification is the evaporation mediator solution drop. Glassy carbon (GC) represents relatively inert and mechanically resistant material which can be cleaned by polishing. The preparation of GC electrode mounted in Teflon includes polishing with emery paper and alumina, respectively, followed by ultrasonic cleaning in purified water before each experiment.

There are two, most frequent methods of surface modification:

- 1) Placing drop of solution containing studied compound on the GC surface [1]. Next step includes drying in air [2, 3], using infrared lamp [4, 5] or oven [6, 7].
- 2) Electrodeposition from solution containing studied compound and the electrolyte. The deposition is carried out by applying repetitive potential sweeps at certain rate in specific potential range [8].

Scanning probe microscopy (SPM) techniques are successfully employed to characterize the structure of electrode surfaces [9]. In contrary to atomically flat single crystal planes, glassy carbon has rough and ill-defined surface.

We employed an atomic force microscopy (AFM) to characterize morphology changes upon modification of GC and basal plane of highly oriented pyrolytic graphite (HOPG) electrodes, respectively. Electrochemical properties of modified surfaces and the ability to detect L-cysteine hydrochloride were investigated.

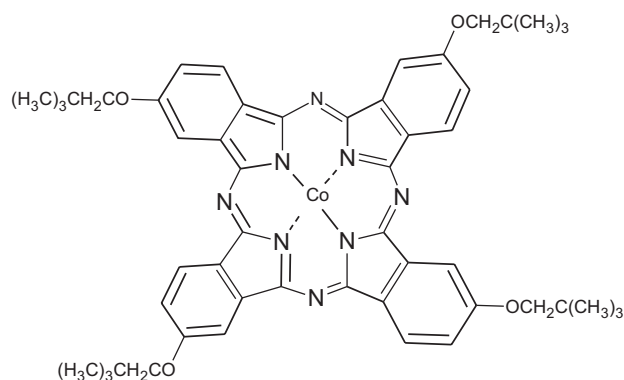


Fig. 1. Structure of cobalt tertaneopentoxy phthalocyanine.

## 2. Experimental

### 2.1. Reagents

Cobalt tetraneopentoxy phthalocyanine (CoTNPc) (Fig. 1) was synthesized in the laboratory of Tohoku University, Japan, by Kobayashi's group. Tetrabutylammonium perchlorate ( $\text{Bu}_4\text{NClO}_4$ , electrochemical grade, 98%, Fluka) and nonaqueous solvent 1,2-dichloro-benzene (*o*-DCB, 99%, Aldrich) were used as received.

The stock solution ( $c = 1 \times 10^{-2} \text{ mol L}^{-1}$ ) of L-cysteine hydrochloride (p.a., Lachema) was prepared by dissolving the exact amount of the substance in borate buffer pH = 10. The solution was prepared fresh before every measurement.

All chemicals used for borate buffer preparation were of analytical grade purity and obtained by Lachema. Purified water (Milli-Q system Gradient, Millipore, resistivity 18.2  $\text{M}\Omega\text{cm}$ ) was used for

preparation of aqueous electrolytes. Deionized water (Milipore) was used throughout.

### 2.2. Electrode Preparation and Electrochemical Measurements

Glasy carbon (Union Carbide) electrodes were prepared by polishing with diamond paste (Winter diaplast) on microcloth. The polished GC was sonicated in nanopure water for 5 min. One drop of  $1 \times 10^{-3}$  mol L<sup>-1</sup> CoTNPC solution in *o*-DCB was placed on the electrode and dried at room temperature. Basal plane of highly oriented pyrolytic graphite (HOPG) 12×12×2 mm (SPI Supplies, USA) was peeled off with an adhesive tape before each experiment. The fresh surface of HOPG was treated by two ways:

- 1) One drop of  $1 \times 10^{-3}$  mol L<sup>-1</sup> CoTNPC in *o*-DCB was placed on HOPG and dried at room temperature.
- 2) Cyclic voltammetry of  $1 \times 10^{-3}$  mol L<sup>-1</sup> CoTNPC in *o*-DCB with 0.1 mol L<sup>-1</sup> Bu<sub>4</sub>NClO<sub>4</sub> was performed on the electrode at scan rate 100 mV s<sup>-1</sup>.

The voltammetric measurements were carried out with the potentiostat/galvanostat Wenking POS 2 (Bank Elektronik, Germany) controlled by the CPC-DA software (Bank Elektronik, Germany). A three-electrode system with saturated calomel reference electrode (SCE), optional silver wire (Ag) as a quasi-reference electrode and platinum wire auxiliary electrode were used for all measurements. All experiments were performed at room temperature in solution deoxygenated by bubbling with argon for five minutes. Stock solutions were kept in glass vessels in dark at laboratory temperature. The voltammetric measurements were carried out at scan rate 10 mV s<sup>-1</sup>. The pH values were measured using pH meter (Jenway 4330, UK).

### 2.3. AFM Conditions

Surface topography was characterized by AFM (Multimode Nanoscope IIIa, Veeco, USA) in tapping and contact mode, respectively. The electrode surface was analysed by Nanoscope III Particle and Bearing Analysis Software (Nanoscope Reference Manual, version 5.12r5). The Si cantilever was oscillated at ca. 300 kHz. The surface imaging was performed with the rate 0.5 and 1.0 Hz, respectively. Images presented here are representatives of all images taken at different locations on each sample.

## 3. Results and Discussion

The influence of above mentioned procedure steps was examined by acquiring surface topography. Comparing surface images acquired without and with sonication step allowed to resolve residua of diamond paste. Figure 2 shows 10 × 10 μm topographic image of GC surface after polishing and rinsing with water (Fig. 2a, 2b) and after polishing and sonication in water (Fig. 2c, 2d), respectively. The electrode surface after simple washing is still covered by diamond polishing media, although the polishing suspension is declared as water and alcohol soluble. We have found however, that just sonication brings satisfactory results.

We have also employed rinsing with methanol after sonication as described [2, 4] but we have found that this step brings additional surface contamination by solvent impurity residua.

When the GC surface was covered by thin layer *o*-DCB and air dried for 12 hours, we were not able to acquire AFM images in tapping mode due to presence of thin layer solvent even after 20 hours of drying. We have employed dynamic force analysis in contact mode for determination the magnitude of deflection hysteresis. Figure 3 shows low values of adhesive force measured on freshly prepared clean surface of GC, while high values were found for surface where drop of *o*-DCB was deposited and dried for 12 hours. Adhesion (capillary) forces indicated residual solvent layer. The sonication in water was found to be the best way also to eliminate the residual layer of solvent.

Further, phthalocyanine CoTNPC was used as a model compound for modification of electrode surface. AFM measurements have revealed that drop deposition of CoTNPC solution in *o*-DCB (Fig. 4a) forms irregular clusters with variable height (Fig. 4b) in contrast with electrodeposition, which can create compact layer of CoTNPC up to 25 nm thick (Fig. 4d). This observation indicates that electrodeposition exhibits progressive stacking and nucleation (Fig. 4c). In case of drop deposition less compact surface were formed.

To find how preparation procedure influences electrode processes we employed detection of model analyte, L-cysteine hydrochloride, by CoTNPC-modified electrode. The difference between cyclic voltammograms acquired on the electrode prepared by electrodeposition and by drop deposition respectively is illustrated in Fig. 5. Electrodeposition formed

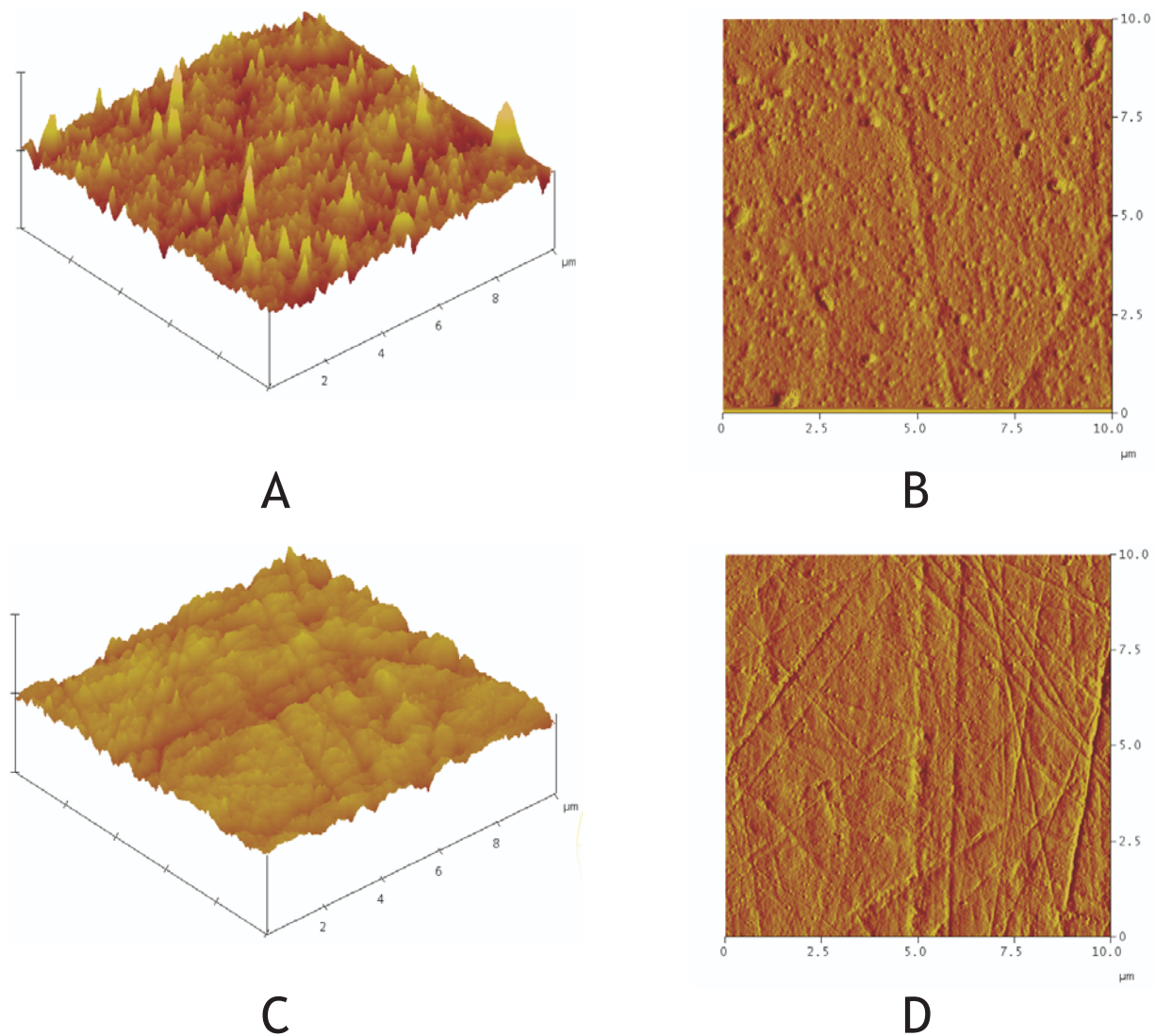


**Fig. 2.** AFM characterization of GC surface roughness: (A) Topographic ( $z$  scale = 200 nm) image  $10 \times 10 \mu\text{m}^2$  3D and (B) top view after polishing with diamond paste and rinsing with water. (C) Three dimensional topography ( $z$  scale = 200 nm) and (D) top view image after polishing with diamond paste and sonication in water.

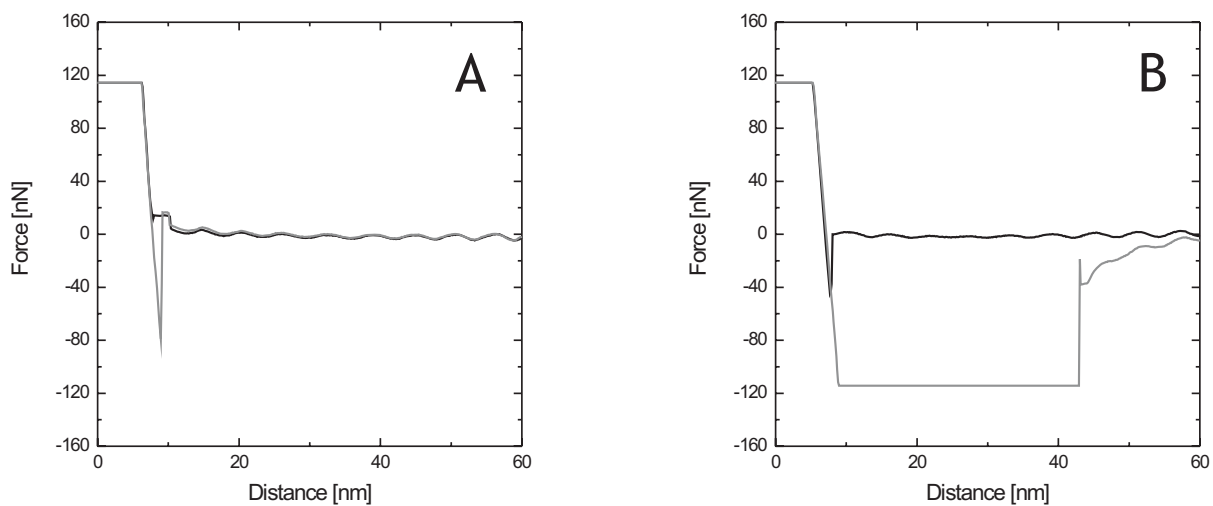


**Fig. 3.** Dynamic force versus distance curves (A) before and (B) after drop of *o*-dichlorobenzene was placed on GC surface and dried for 12 hours.

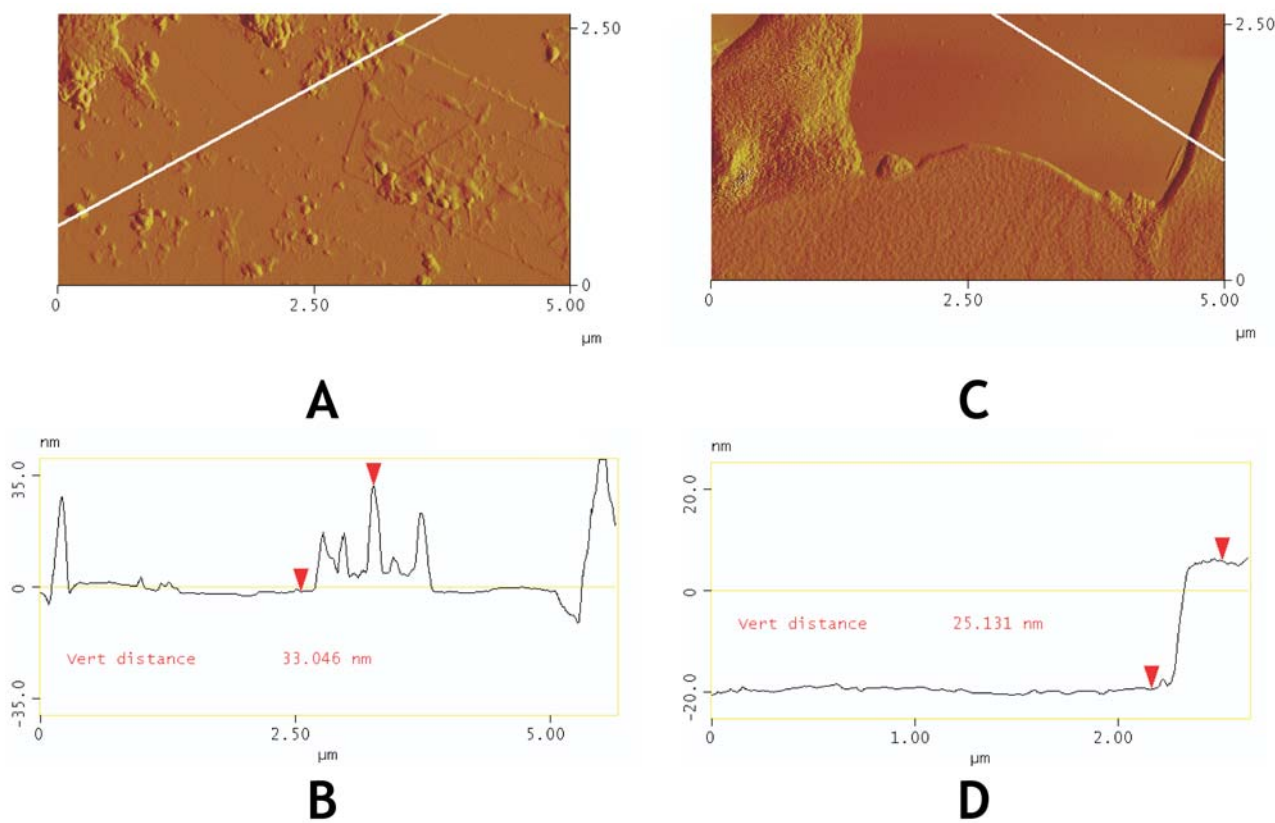


**Fig. 4.** TM-AFM images of  $5 \times 5 \mu\text{m}^2$  HOPG surface: (A) after modification by drop of  $1 \times 10^{-3} \text{ mol L}^{-1}$  CoTNPC dissolved in *o*-DCB and dried in air, (B) corresponding line analysis; (C) after cyclic voltammetry in  $1 \times 10^{-3} \text{ mol L}^{-1}$  CoTNPC and  $0.1 \text{ mol L}^{-1}$   $\text{Bu}_4\text{NClO}_4$  dissolved in *o*-DCB and dried, (D) corresponding line analysis.

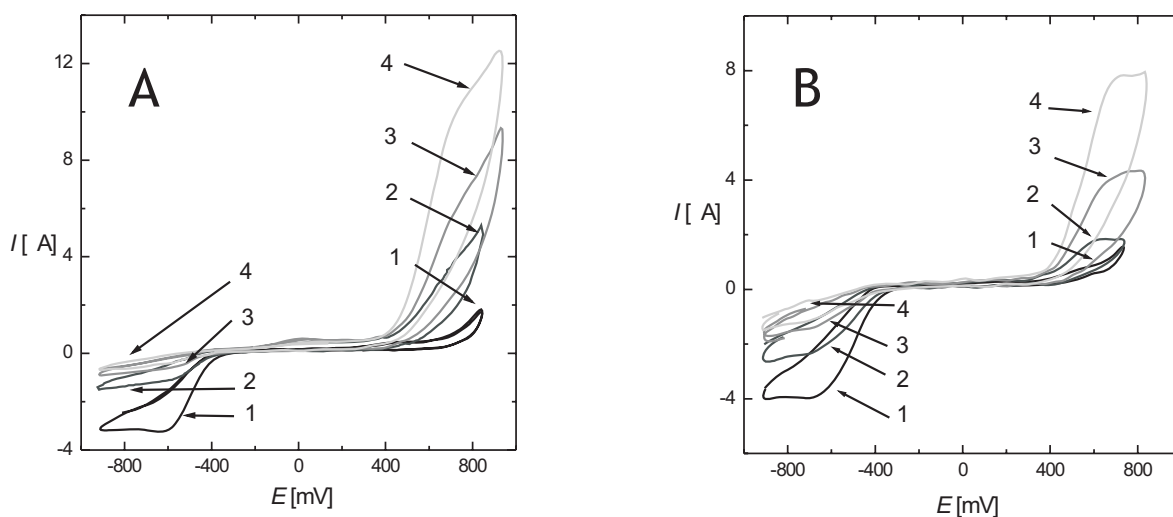


**Fig. 5.** Cyclic voltammograms of  $0.01 \text{ mol L}^{-1}$  L-cysteine hydrochloride in borate buffer  $\text{pH} = 10$ . Concentration of cysteine hydrochloride (1)  $0.0 \text{ mol L}^{-1}$ , (2)  $8.3 \times 10^{-4} \text{ mol L}^{-1}$ , (3)  $1.5 \times 10^{-3} \text{ mol L}^{-1}$ , (4),  $2.1 \times 10^{-3} \text{ mol L}^{-1}$ . Working electrode: (A) HOPG surface after modification by drop of  $1 \times 10^{-3} \text{ mol L}^{-1}$  CoTNPC dissolved in *o*-DCB and dried; (B) after cyclic voltammetry in  $1 \times 10^{-3} \text{ mol L}^{-1}$  CoTNPC and  $0.1 \text{ mol L}^{-1}$   $\text{Bu}_4\text{NClO}_4$  dissolved in *o*-DCB and dried. Reference electrode SCE, scan rate  $10 \text{ mV s}^{-1}$ .

more compact surface than drop deposition and peaks corresponding to L-cysteine reaction with Co(II)TNPC are lower. It can be explained by lower roughness of the mediator surface where lower amount of CoTNPC mediator is in contact with analyte solution.

#### 4. Conclusion

We have shown that AFM can provide valuable information on the surface nanomorphology changes after various treatment procedures. For GC electrodes, AFM indicated that after polishing and rinsing the surface is covered by abrasive particles from grinding media. Also, AFM dynamic force curve shows that *o*-DCB layer will not evaporate from the GC surface even after 24 hours. Our experiments have also shown that the best way for elimination of polishing particles and solvent residua is sonication in water. This disadvantage does not exist at HOPG which surface can be perfectly cleaned just by peeling off top layers using adhesive tape.

The HOPG electrode modification by electro-deposition from nonaqueous media opens pathways for preparation of thin layers of mediator. In comparison with modification by solution spreading and drying, electro-deposition creates more uniform layer. Unfortunately, this layer indicates lower sensitivity to L-cysteine hydrochloride than layer prepared by drop deposition.

#### Acknowledgements

We are grateful to N. Kobayashi, Tohoku University, Japan for supplying phthalocyanines used in this work. This financial support of this work by the Grant Agency of Charles University in Prague (the project SVV 261204), by the research project MSM0021620857, and by the development project RP 14/63 of the Ministry of Education Youth and Sports of the Czech Republic.

#### Literature

- [1] Obirai J. C., Nyokong T.: *J. Electroanal. Chem.* **600** (2007), 251.
- [2] Rocha J. R. C., Angnes L., Bertotti M., Araki K., Toma H. E.: *Anal. Chim. Acta* **452** (2002), 23.
- [3] Santos W. J. R., Sousa A. L., Luz R. C. S., Damos F. S., Kubota L. T., Tanaka A. A., Tanaka S. M. C. N.: *Talanta* **70** (2006), 588.
- [4] Zhu Z., Li N-Q.: *Electroanalysis* **10** (1998), 643.
- [5] Luz R., Damos F. S., Tanaka A. A., Kubota L. T.: *Sens. Actuators B* **114** (2006), 1019.
- [6] Ozoemena K. I.: *Sensors* **6** (2006), 874.
- [7] Maree S., Nyokong T.: *J. Electroanal. Chem.* **492** (2000), 120.
- [8] Guan J., Wang Z., Wang Ch., Qu Q., Yang G., Hu X.: *Int. J. Electrochem. Sci.* **2** (2007), 572.
- [9] Brülle T., Stimming U.: *J. Electroanal. Chem.* **636** (2009), 10.

# Voltammetric and HPLC Methods in the Determination of *cis*- and *trans*-Resveratrol

LENKA NĚMCOVÁ, JIŘÍ ZIMA, JIŘÍ BAREK

UNESCO Laboratory of Environmental Electrochemistry, Department of Analytical Chemistry, Charles University in Prague, Albertov 6, 128 43 Prague, Czech Republic, ✉ [nemcova.len@seznam.cz](mailto:nemcova.len@seznam.cz)

## Keywords

carbon paste electrode  
electrochemical detection  
HPLC  
polyphenols  
resveratrol  
voltammetry

## Abstract

Resveratrol is one of the numerous polyphenolic compounds found in several vegetal sources. In recent years, the interest in this molecule has increased exponentially following the major findings that resveratrol was shown to be chemopreventive, cardioprotective, antioxidative, phytoestrogenic, anti-inflammatory, neuroprotective and to have anti-aging properties. The anodic voltammetric behavior of *trans*-resveratrol was studied using differential pulse voltammetry and cyclic voltammetry. The oxidation of *trans*-resveratrol was found to be controlled by diffusion and to be irreversible. Optimum conditions involved BR buffer pH = 2 and methanol (1:1) supporting electrolyte. Both isomers of resveratrol were analyzed by HPLC with spectrophotometric (306 and 286 nm) and electrochemical ( $E = +1.2$  V) detection. The HPLC method was applied for the determination of resveratrol in seeds of common and tartary buckwheat.

## 1. Introduction

As a chemical entity, resveratrol (3,5,4'-trihydroxystilbene) is known since 1940 when it was first isolated from the roots of white hellebore (*Varatrum grandiflorum*) and later from *Polygonum cuspidatum*, a medical plant [1]. Resveratrol belongs to the group of polyphenolic phytoalexins which are produced by plants in response to exogenous stimuli like UV light, ozone exposition, mechanical damage or fungal infection [2]. Resveratrol, as a member of stilbene family, exists in two isomeric forms *trans*-resveratrol and *cis*-resveratrol (Fig. 1). The *trans*-isomer is the more stable form, *trans* to *cis* isomerisation is facilitated by UV light and high pH, the *cis* to *trans* conversion is facilitated by visible light, high temperature, or low pH. Both isomers can be present in variable amounts

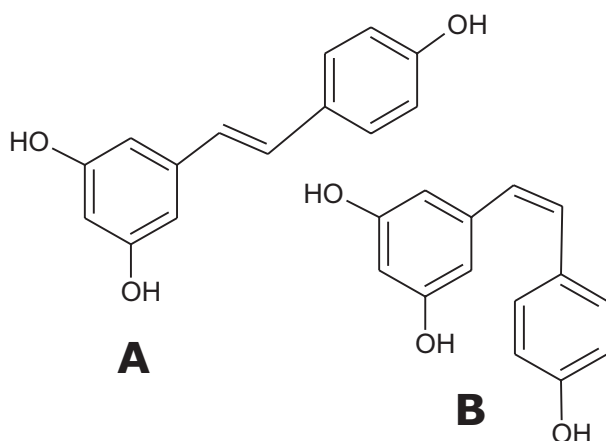


Fig. 1. Structure of *trans*-resveratrol (A) and *cis*-resveratrol (B)

in plants, but amount of *trans*-resveratrol usually predominates [3]. Numerous animal studies have demonstrated that this polyphenol holds promise against numerous age-associated diseases including cancer, diabetes, Alzheimer, cardiovascular and pulmonary disease [4, 5]. Other beneficial health effects such as antioxidative, neuroprotective, phytoestrogenic and anti-inflammatory have also been reported [6, 7]. Determination of resveratrol is mainly done by HPLC with UV/VIS [8], MS [9] and electrochemical detection [10], by GC/MS [11] or electrophoresis [12]. Resveratrol was identified in buckwheat among several other flavonoids [13]. The aim of this work was to develop voltammetric (DPV, CV) and HPLC determination with spectrophotometric detection and amperometric detection on carbon paste electrode (CPE) of trace amounts of *trans*-resveratrol and *cis*-resveratrol and to apply this methods for the determination of *trans*-resveratrol in real samples of buckwheat. Carbon paste electrodes are very useful electrochemical sensors for the determination of organic compounds that can be anodically oxidized [14–17]. They present less expensive, comparatively sensitive and more selective alternative to spectrophotometric detection.

## 2. Experimental

### 2.1. Instruments

For the voltammetric measurements, a computerized voltammetric analyzer Eco-Tribo Polarograph with

software PolarPro 4.0 (all Polaro Sensors, Czech Republic) was used. The voltammetric parameters used: scan rate  $20 \text{ mV s}^{-1}$  for differential pulse voltammetry and  $100 \text{ mV s}^{-1}$  for cyclic voltammetry, for pulse techniques the pulse amplitude of  $50 \text{ mV}$ . The surface of the working carbon paste electrode ( $2 \text{ mm}$  in diameter) was renewed mechanically by protruding the piston and smoothing the surface with a piece of wet filter paper. The reference electrode and auxiliary electrode were the same as in chromatographic method. The mixture of Britton-Robinson (BR) buffer:methanol (1:1, v/v) was used as the supporting electrolyte in batch voltammetric methods. The HPLC system consisted of high-pressure piston pump HPP 5001 (Laboratorní přístroje Praha, Czech Republic), injection valve D with  $20\text{-}\mu\text{L}$  sample loop (Ecom, Czech Republic), spectrophotometric detector Sapphire 800 UV/VIS (Ecom, Czech Republic), electrochemical detector CHI 802B (CH Instruments Electrochemical Analysis, USA) with three-electrode system consisting of reference silver/silver chloride electrode RAE 113 (Monokrystaly, Czech Republic) filled with  $3 \text{ M KCl}$ , working CPE ( $3 \text{ mm}$  in diameter) and platinum wire auxiliary electrode. Column Kromasil C-18 ( $7 \mu\text{m}$ ),  $125 \times 4 \text{ mm}$  (Prochome, India) and precolumn Gemini C-18,  $4 \times 3 \text{ mm}$  (Phenomenex, USA) were used. The amperometric detector, employing electrochemical (wall-jet) oxidation of phenolic hydroxy groups, was placed behind the UV/VIS detector operating at  $306 \text{ nm}$  (*trans*-resveratrol) or  $286 \text{ nm}$  (*cis*-resveratrol). The system was operated by Clarity 2.3.0 programme (DataApex, Czech Republic) and CHI 6.26 programme (CH Instruments, USA) working in the Windows XP system (Microsoft). The mobile phase was acetonitrile and BR buffer, 10 times diluted by deionized water (50:50 and 30:70 v/v), the flow rate was  $1 \text{ mL min}^{-1}$ . For preparation of the concentrated ethanolic samples of buckwheat seeds a vacuum evaporator Buchi B-480, R-114 (Switzerland) was used. All experiments were carried out at a laboratory temperature.

## 2.2. Materials

*Trans*-resveratrol was purchased from Sigma-Aldrich (USA). Its stock solution ( $1 \times 10^{-3} \text{ mol L}^{-1}$ ) was prepared by dissolving the accurately weighed amount of the substance in p.a. methanol (Lach-Ner, Czech Republic) and stored away from daylight at  $4 \text{ }^\circ\text{C}$  until used. Stock solution of *cis*-resveratrol was prepared from the solution ( $1 \times 10^{-4} \text{ mol L}^{-1}$ ) of *trans*-resveratrol by UV-irradiation on daylight for 48 hours (85% conversion). Britton-Robinson (BR) buffers were

prepared in a usual way, by mixing  $0.04 \text{ mol L}^{-1}$  phosphoric acid,  $0.04 \text{ mol L}^{-1}$  acetic acid and  $0.04 \text{ mol L}^{-1}$  boric acid with an appropriate amount of  $0.2 \text{ mol L}^{-1}$  sodium hydroxide. The amounts of *trans*-resveratrol were determined in six varieties of common buckwheat and two varieties of tartary buckwheat. All samples were supplied by Crop Research Institute, Department of Gene Bank (Drnovská 507, Prague 6-Ruzyně, Czech Republic). All the chemicals used were of analytical reagent grade (Lachema, Czech Republic). The mobile phase for HPLC contained acetonitrile for HPLC (Merck, Germany) and aqueous BR buffer diluted 10 times. Carbon paste contained  $250 \text{ mg}$  of spherical microparticles of glassy carbon with a diameter  $0.4\text{--}12 \mu\text{m}$  (Alpha Aesar, USA) and  $90 \mu\text{L}$  of mineral oil (Fluka Biochemica, Switzerland). All aqueous solutions were prepared using deionized water obtained from a MilliQ Plus system (Millipore, France).

## 3. Results and Discussion

### 3.1. Voltammetric study

At first, the influence of pH of the supporting electrolyte on the voltammetric behavior (DPV, CV) of *trans*-resveratrol was investigated. The effect of pH on peak current is summarized in Fig. 2. Figure 2 shows the shift of peak potential to less positive values with increasing pH thus reflecting the easier oxidation of the hydroxy group in more alkaline medium. As the optimum for measuring the anodic *trans*-resveratrol calibration dependence the medium of BR (pH = 2) and methanol (1:1) was chosen. The calibration

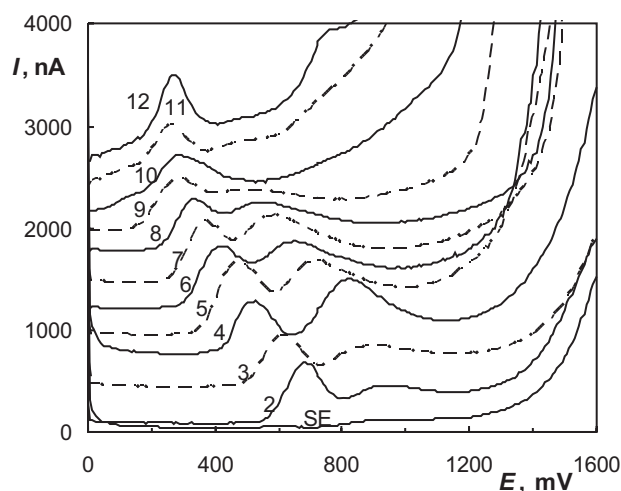


**Fig. 2.** DP voltammograms of  $1 \times 10^{-4} \text{ mol L}^{-1}$  *trans*-resveratrol in BR buffer (pH = 2–12):methanol mixture (1:1). The curve numbers correspond to pH of BR buffer before mixing with methanol (SE supporting electrolyte: BR buffer pH 2 with methanol).

**Table 1**Parameters of the calibration lines of *trans*-resveratrol and *cis*-resveratrol using CPE.

Resveratrol	Method	Optimal conditions	LOD mol L <sup>-1</sup>
<i>trans</i> -	DPV	BR buffer (pH = 2):methanol mixture (1:1)	8.9×10 <sup>-7</sup>
	CV	BR buffer (pH = 2):methanol mixture (1:1)	9.7×10 <sup>-7</sup>
	HPLC-UV/VIS	BR buffer (pH = 7):acetonitrile mixture (1:1), <i>F</i> = 1 mL min <sup>-1</sup> , injected 20 μL, λ = 306 nm	3.2×10 <sup>-8</sup>
	HPLC-ED	BR buffer (pH = 7):acetonitrile mixture (1:1), <i>F</i> = 1 mL min <sup>-1</sup> , injected 20 μL, <i>E</i> = +1.2 V	3.5×10 <sup>-8</sup>
<i>cis</i> -	HPLC-UV/VIS	BR buffer (pH = 7):acetonitrile mixture (1:1), <i>F</i> = 1 mL min <sup>-1</sup> , injected 20 μL, λ = 286 nm	6.5×10 <sup>-8</sup>
	HPLC-ED	BR buffer (pH = 7):acetonitrile mixture (1:1), <i>F</i> = 1 mL min <sup>-1</sup> , injected 20 μL, <i>E</i> = +1.2 V	1.8×10 <sup>-8</sup>

curves were measured in the concentration range from  $6 \times 10^{-7}$  to  $1 \times 10^{-4}$  mol L<sup>-1</sup> (Fig. 3, Table 1). The possibility of increasing the sensitivity of the determination by adsorptive accumulation of the analyte on the surface of CPE was investigated. The influence of accumulation potential on the peak current of  $8 \times 10^{-6}$  mol L<sup>-1</sup> *trans*-resveratrol was measured in the range from 0.0 to 0.4 V, with accumulation time from 60 s to 10 min in BR buffer (pH = 2, 7, 10 and 12), always in a mixture with methanol (95:5). The effect of the analyte accumulation was not significant. Cyclic voltammetry was used to investigate reversibility of the *trans*-resveratrol reaction on CPE. Electrochemical oxidation was studied in BR buffer (pH = 2):methanol (1:1, v/v). Cyclic voltammograms were measured with scan rates 2–1000 mV s<sup>-1</sup> (Fig. 4). It follows from the results that the oxidation is irreversible under the given condition and is controlled by diffusion.

### 3.2. HPLC study

*Trans*-resveratrol isomerizes to *cis*-resveratrol, when exposed to UV radiation, including the daylight. If we want to determine both isomers in matrices, where for its determination it is not possible to use the batch voltammetric methods without preceding separation step, HPLC with spectrophotometric or amperometric detection is one of the possibilities. The mobile phase containing BR buffer and methanol in ratio 1:1 allowed us to separate *trans*- and *cis*-resveratrol in 4.5 min. Optimum pH was determined from the hydrodynamic voltammograms (Fig. 5) from pH values compatible with the used column because the separation of *trans*-resveratrol and *cis*-resveratrol was found to be practically independent of the pH of the mobile phase within pH 3 to 7. The calibration curves were measured in the concentration range of  $4 \times 10^{-8}$  to  $1 \times 10^{-4}$  mol L<sup>-1</sup> (Table 1). The HPLC method was

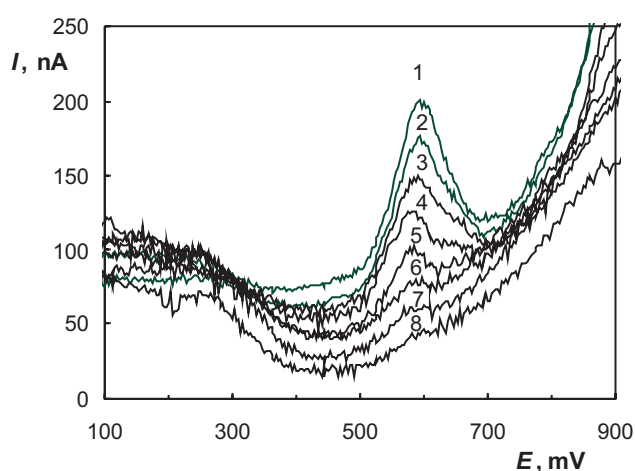


**Fig. 3.** DP voltammograms of *trans*-resveratrol of concentrations (1)  $1 \times 10^{-5}$  mol L<sup>-1</sup>, (2)  $8 \times 10^{-6}$  mol L<sup>-1</sup>, (3)  $6 \times 10^{-6}$  mol L<sup>-1</sup>, (4)  $4 \times 10^{-6}$  mol L<sup>-1</sup>, (5)  $2 \times 10^{-6}$  mol L<sup>-1</sup>, (6)  $1 \times 10^{-6}$  mol L<sup>-1</sup>, (7)  $8 \times 10^{-7}$  mol L<sup>-1</sup>, (8)  $6 \times 10^{-7}$  mol L<sup>-1</sup> in BR buffer (pH = 2):methanol mixture (1:1).

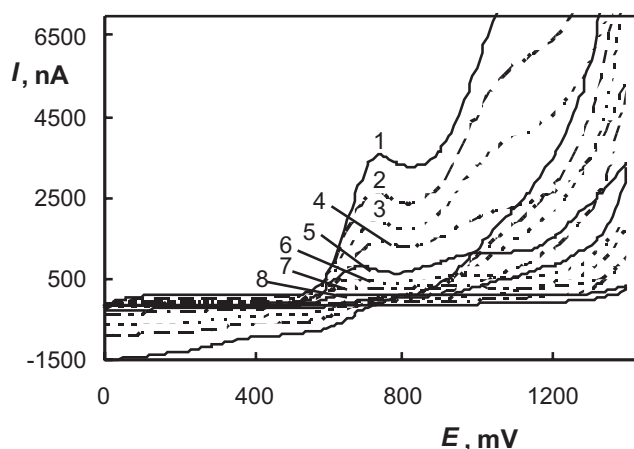


**Fig. 4.** CV voltammograms of *trans*-resveratrol ( $c = 1 \times 10^{-4}$  mol L<sup>-1</sup>) in BR buffer (pH = 2):methanol mixture (1:1), scan rate: (1) 1000 mV s<sup>-1</sup>, (2) 500 mV s<sup>-1</sup>, (3) 300 mV s<sup>-1</sup>, (4) 200 mV s<sup>-1</sup>, (5) 50 mV s<sup>-1</sup>, (6) 20 mV s<sup>-1</sup>, (7) 10 mV s<sup>-1</sup>, (8) 5 mV s<sup>-1</sup>.

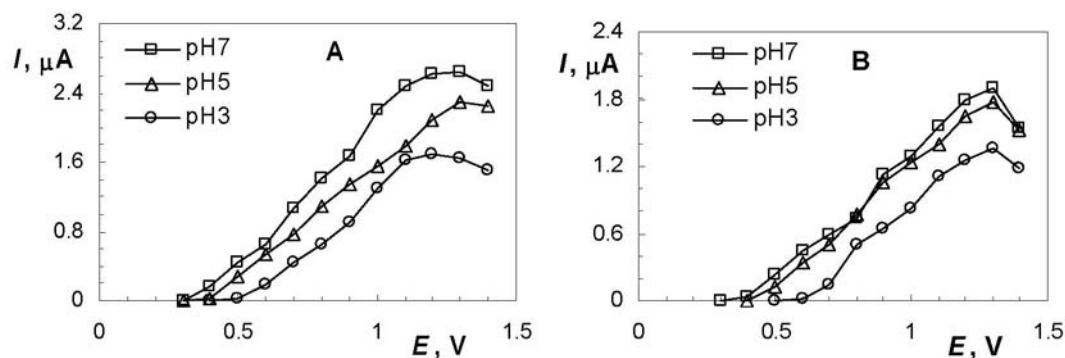


**Fig. 5.** Hydrodynamic voltammograms of *trans*-resveratrol (A) and *cis*-resveratrol (B) on CPE in the mobile phase diluted BR buffer and acetonitrile (1:1). Injected 20  $\mu\text{L}$  of  $1 \times 10^{-4} \text{ mol L}^{-1}$  resveratrol.

applied for the determination of resveratrol in samples of seeds of common and tartary buckwheat. Optimum condition for separation of *trans*- and *cis*- resveratrol in real samples were mixture BR buffer (pH = 7):acetonitrile (70:30, v/v). *Trans*-resveratrol was detected and determined in all real samples, but *cis*-resveratrol was not found in any sample. The content of *trans*-resveratrol was 3.43–3.50  $\text{mg kg}^{-1}$  of seed of tartary buckwheat and 0.98–1.68  $\text{mg kg}^{-1}$  of seeds of common buckwheat (Fig. 6).

#### 4. Conclusions

We have developed voltammetric (DPV, CV) and HPLC determination with spectrophotometric detection and amperometric detection on carbon paste electrode for the determination of trace amounts of *trans*-resveratrol and *cis*-resveratrol and successfully

applied the HPLC method for the determination of *trans*-resveratrol in real samples of buckwheat.

#### Acknowledgments

This research was supported by the Ministry of Education, Youth and Sports of the Czech Republic (project LC 06035, MSM 0021620857, RP 14/63) and by Grant Agency of Charles University (project SVV261204).

#### References

- [1] Pirola L., Fröjdo S.: *Life* **60** (2008), 323–332.
- [2] Šmidrkal J., Filip V., Melzoch K., Hanzlíková I., Buckiová D., Křisa B.: *Chem. Listy* **95** (2001), 602–609.
- [3] Trela B. C., Waterhouse A. L.: *J. Agric. Food Chem.* **44** (1996), 1253–1257.
- [4] Harikumar K. B., Aggarwal B. B.: *Cell Cycle* **7** (2008), 1020–1035.
- [5] Sharma S., Anjaneyulu M., Kulkarni S. K., Chopra K.: *Pharmacology* **76** (2006), 69–75.
- [6] López-Hernández J., Paseiro-Losada P., Sanches-Silva A. T., Lage-Yusty M. A.: *Eur. Food Res. Technol.* **225** (2007), 789–796.

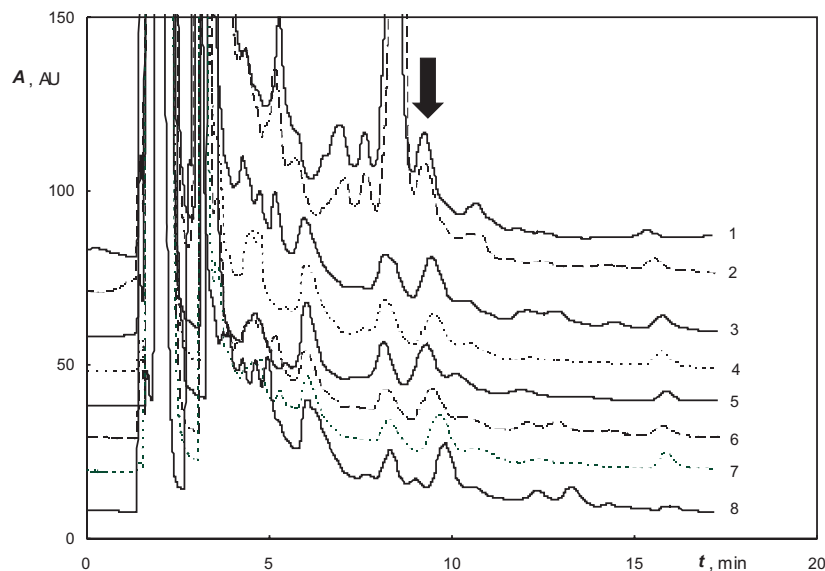


**Fig. 6.** HPLC chromatograms with spectrophotometric detection (306 nm) of concentrated ethanolic extracts of buckwheat samples of seeds. Curve numbers correspond to variety of tartary (1, 2) and common (3–8) buckwheat. Mobile phase acetonitrile and diluted BR buffer pH = 7 (30:70), flow rate  $1 \text{ mL min}^{-1}$ , injected 20  $\mu\text{L}$ , an arrow shows the peaks of *trans*-resveratrol.

- [7] Sönmez Ü., Sönmez A., Erbil G., Tekmen I., Baykara B.: *Neurosci. Lett.* **420** (2007), 133–137.
- [8] Zhu Z., Klironomos G., Vachereau A., Neirinck L., Goodman D. W.: *J. Chromatogr. B* **724** (1999), 389–392.
- [9] Stecher G., Huck Ch. W., Popp M., Bonn G. K.: *Fresenius J. Anal. Chem.* **371** (2001), 73–80.
- [10] McMurtrey K. D., Minn J., Pobanz K., Schultz T. P.: *J. Agric. Food Chem.* **42** (1994), 2077–2080.
- [11] Luan T., Li G., Zhang Z.: *Anal. Chim. Acta* **424** (2000), 19–25.
- [12] Peng Y., Zhang Y., Ye J.: *J. Agric. Food Chem.* **56** (2008), 1838–1844.
- [13] Qian J. Y., Mayer D., Kuhn M.: *Dtsch. Lebensm.-Rundsch.* **9** (1999), 343–349.
- [14] Zima J., Stoica A.I., Zítová A., Barek J.: *Electroanalysis* **18** (2005), 158–162.
- [15] Barek J., Muck A., Wang J., Zima J.: *Sensors* **4** (2004), 47–57.
- [16] Barek J., Moreira J. C., Zima J.: *Sensors* **5** (2005), 148–158.
- [17] Zima J., Švancara I., Barek J., Vytřas K.: *Crit. Rev. Anal. Chem.* **39** (2009), 204–227.

# Voltammetric Determination of Aclonifen and Fluorodifen at a Silver Solid Amalgam Electrode

VÍT NOVOTNÝ, JIŘÍ BAREK

UNESCO Laboratory of Environmental Electrochemistry, Department of Analytical Chemistry,  
Faculty of Science, Charles University in Prague  
Hlavova 8, CZ-128 43 Prague, Czech Republic, ✉ novotny1@natur.cuni.cz

## Abstract

A differential pulse voltammetric method for the determination of the herbicides Aclonifen and Fluorodifen at a silver solid amalgam electrode is developed. A mixture of Britton-Robinson buffer and methanol is used as the supporting electrolyte. The optimal conditions for the determination are investigated. The optimum pH for the determination of Aclonifen is found to be 12, the calibration dependency is linear in the concentration range  $1 \times 10^{-4}$ – $1 \times 10^{-7}$  mol L<sup>-1</sup> and the detection limit achieved is  $2 \times 10^{-7}$  mol L<sup>-1</sup>. The optimum pH for the determination of Fluorodifen is 6 and the calibration dependence is linear in the concentration range  $1 \times 10^{-4}$ – $1 \times 10^{-6}$  mol L<sup>-1</sup>.

## Keywords

herbicide  
silver solid amalgam electrode  
voltammetry

## 1. Introduction

Diphenylether herbicides (DPhEH) are an important group of agrochemicals used worldwide for the protection of important crops. It has been discovered that they pose a high risk to aquatic life. Moreover, some studies hint that they can have varied adverse effects on mammals, including teratogenesis [1], mutagenesis, cancerogenesis, interference with hormonal balance [1] and adverse effects on blood formation [2]. Considering these facts the need arises for the ability to track such substances in the environment. Although appropriate methods for the determination of DPhEH in the environment already exist, it still makes sense to develop new voltammetric methods. This is because substances of our interest do exhibit electrochemical activity [3] and electrochemical methods are convenient in many ways. Namely their cheapness, the ease with which they are performed and low detection limits [4]. Silver solid amalgam electrodes (AgSAE) are particularly suitable for the determination of many important electrochemically active compounds in trace amounts [5]. This contribution will focus on the development of similar techniques for the determination of the herbicides Aclonifen (AC) and Fluorodifen (FD). In this work we follow up with our work on the voltammetric determination of other DPhEH on AgSAE. [6]. Our goal in this work is to develop sensitive and reliable methods for the determination of AC and FD at m-AgSAE by finding the optimal conditions for the determination and testing the reliability of the method.

## 2. Materials and Methods

Aclonifen (2-Chloro-6-nitro-3-phenoxyaniline, 99.8%) was purchased from Sigma-Aldrich, Germany. The stock solution of AC ( $c = 1 \times 10^{-3}$  mol L<sup>-1</sup>) has been prepared by dissolving 0.02648 g of AC in 100 mL of methanol. Solutions of lower concentrations were prepared by precise diluting of the stock solution with methanol.

Fluorodifen (2-Nitro-1-(4-nitrophenoxy)-4-(trifluoromethyl)benzene, 99.6 %) was purchased from Sigma-Aldrich, Germany. The stock solution of FD ( $c = 1 \times 10^{-3}$  mol L<sup>-1</sup>) has been prepared by dissolving 0.03290 g of FD in 100 mL of methanol. Solutions of lower concentrations were prepared by precise diluting of the stock solution with methanol.

All the stock solutions were kept in the refrigerator. The stability of stock solutions was checked by UV-VIS spectrophotometric measurements. The stock solutions were stable for the duration of the experiments under the conditions in which they were kept. Other used chemicals: boric acid, acetic acid (99%), phosphoric acid (85%), sodium hydroxide, potassium chloride all substances p.a., Lachema Brno, Czech Republic. Methanol p.a. Merck, Germany was used. Britton-Robinson buffers of the desired pH were prepared by mixing of 0.2 mol L<sup>-1</sup> NaOH with a solution containing 0.04 mol L<sup>-1</sup> boric acid, phosphoric acid and acetic acid. Measurements of pH were performed on a Jenway 3510 (Jenway, Great Britain) pH-meter with a combined glass membrane electrode (type 924 005)

The electrode was calibrated by standard buffer solutions in water. Deionized water (Millipore, USA) was used as a solvent.

Eco-Tribo Polarograf (Polaro-Sensors, Prague, Czech Republic) and the software PolarPro version 5.1 was used for all voltammetric techniques. The software was running under the Windows XP (Microsoft) operating system. Pulses of width of 80 ms and height of  $-50$  mV were used while performing DPV. A polarization rate of  $20 \text{ mV s}^{-1}$ , and potential resolution of 3 mV were used.

All measurements were performed using a three electrode system. A silver chloride electrode ( $1 \text{ mol L}^{-1} \text{ KCl}$ ) type RAE 113, Monokrystal, Czech Republic. A platinum wire auxiliary electrode was used. A meniscus modified silver solid amalgam electrode was purchased from Polaro Sensors, Prague, Czech Republic. The electrode was activated in  $0.2 \text{ mol L}^{-1} \text{ KCl}$  solution by applying of a potential of  $-2200$  mV for 300 s. Passivation was removed by applying 300 potential pulses lasting 100 ms between potentials  $E_{in}$  and  $E_{fin}$ .

Measured solutions of AC and FD were prepared by adding an appropriate amount of the stock solution to a 10 mL volumetric flask, filling with methanol to a total volume of 5 mL and then filling the flask up to 10 mL with BR buffer of the desired pH. Values of points in calibration curves are arithmetic averages of three measurements. Error bars are derived from the same data. Detection limits are calculated according to the formula

$$LOD = 3.3 \sigma / S \quad (1)$$

where  $\sigma$  is the standard deviation of 10 measurements of the lowest concentration when the signal can still be evaluated and  $S$  is the slope of calibration curve in the vicinity of that concentration.

### 3. Results and Discussion

DP voltammograms of AC at m-AgSAE in a solution of BR buffer and methanol exhibit a single peak in the whole range of pH used. The peak height increases with an increase of pH, while the potential shifts towards more negative values. The highest peak height is obtained in the solution with BR buffer pH = 12 and so this pH was used for the calibration. The Voltammograms of AC in various pH can be found in Fig. 1. Passivation of the electrode does not take place in a 50% mixture of BR buffer pH 12 and methanol.

The calibration dependence of AC in the concentration range  $1 \times 10^{-6} - 2 \times 10^{-7} \text{ mol L}^{-1}$  can be seen in Fig. 2.

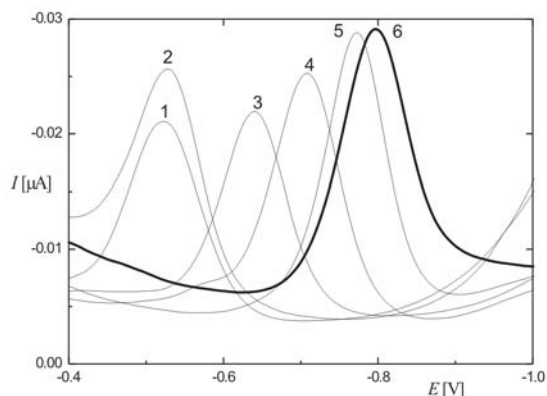


**Fig. 1.** DP voltammograms of Acclonifen ( $c = 1 \times 10^{-4} \text{ mol L}^{-1}$ ) at m-AgSAE in a solution of BR buffer of the desired pH-methanol (1:1). BR buffer: (1) pH = 2, (2) pH = 4, (3) pH = 6, (4) pH = 8, (5) pH = 10, and (6) pH = 12.

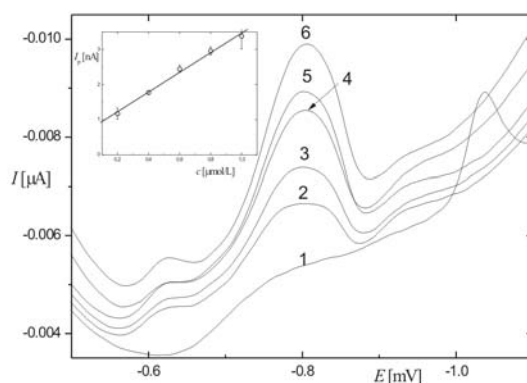


**Fig. 2.** DP voltammograms of Acclonifen at m-AgSAE in a solution of BR buffer (pH = 12)-methanol (1:1). Acclonifen concentration: (1)  $0.0 \times 10^{-6} \text{ mol L}^{-1}$ , (2)  $0.2 \times 10^{-6} \text{ mol L}^{-1}$ , (3)  $0.4 \times 10^{-6} \text{ mol L}^{-1}$ , (4)  $0.6 \times 10^{-6} \text{ mol L}^{-1}$ , (5)  $0.8 \times 10^{-6} \text{ mol L}^{-1}$ , (6)  $1.0 \times 10^{-6} \text{ mol L}^{-1}$ .

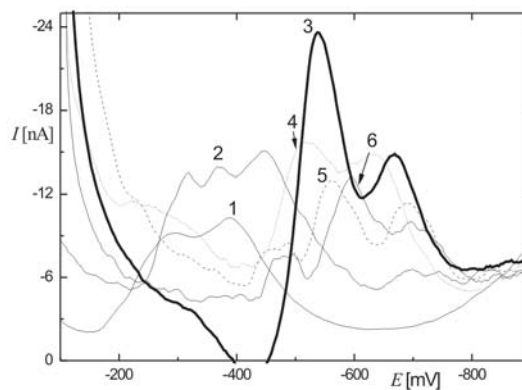


**Fig. 3.** DP voltammograms of Fluorodifen ( $c = 1 \times 10^{-4} \text{ mol L}^{-1}$ ) at m-AgSAE in a solution of BR buffer of the desired pH-methanol (1:1). BR buffer: (1) pH = 2, (2) pH = 4, (3) pH = 6, (4) pH = 8, (5) pH = 10, and (6) pH = 12.

The DP Voltammograms of FD at m-AgSAE have two peaks in the whole pH range. The peak height various pH can be seen in Fig 3.

#### 4. Conclusion

A method for the determination of AC by DPV at AgSAE has been developed. The optimum conditions for the determination are a solution of 50 % BR buffer pH 12 and methanol. The calibration dependence is linear in the concentration range from  $1 \times 10^{-4}$  mol L<sup>-1</sup> to  $1 \times 10^{-7}$  mol L<sup>-1</sup>. The detection limit reached for the determination of AC is  $2 \times 10^{-7}$  mol L<sup>-1</sup>. Electrochemical means of regenerating the surface of the electrode under the conditions described are unnecessary.

A method for the determination of FD by DPV at AgSAE has been developed. The optimum conditions for the determination are a solution of 50 % BR buffer pH 6 and methanol. The calibration dependence is linear in the concentration range from  $1 \times 10^{-4}$  mol L<sup>-1</sup> to  $1 \times 10^{-6}$  mol L<sup>-1</sup>.

#### Acknowledgments

The financial support of The Czech Ministry of Youth and Sports (project LC06035, MSM 021620857 and RP14/63) is gratefully acknowledged.

#### References

- [1] A. E. Brandsma, D. Tibboel, I. M. Vulto, J. J. M. de Vijlder, A. A. W. Ten Have-Opbroek, W. M. Wiersinga: *Biochim. Biophys. Acta* **1201** (1994), 266–270.
- [2] B. Rio, D. Parent-Massin, S. Lautraite, H. Hoellinger: *Human & Experimental Toxicology* **16** (1997), 115–122
- [3] E. B. Rupp, P. Zuman, I. Šestáková, V. Horák: *J. Agric. Food Chem.* **40** (1992), 2016–2021.
- [4] J. Barek, J. Fischer, T. Navrátil, K. Pecková, B. Yosypchuk, J. Zima: *Electroanalysis* **19** (2007), 2003–2014.
- [5] J. Zima, I. Švancara, J. Barek, K. Vytřas: *Crit. Rev. Anal. Chem.* **397** (2009), 204–227.
- [6] V. Novotný, J. Barek: *Chem. Listy* **103** (2009), 217–223.

# Modification of Gold Metal Surfaces by Thiolated Calix[4]arene and Undecanethiol: Comparative Studies

BARBORA ŠUSTROVÁ<sup>a, b</sup>, VLADIMÍR MAREČEK<sup>a</sup>, KAREL ŠTULÍK<sup>a, b</sup>

<sup>a</sup> *J. Heyrovský Institute of Physical Chemistry, Academy of Sciences of the Czech Republic, Dolejškova 3, 182 23 Prague 8, The Czech Republic, ✉ barbora.sustrova@jh-inst.cas.cz*

<sup>b</sup> *Department of Analytical Chemistry, Faculty of Science, Charles University in Prague, Hlavova 8, 128 43 Prague 2, The Czech Republic*

## Keywords

atomic force microscopy  
calix[4]arenes  
cyclic voltammetry  
gold electrode  
undecanethiol

## Abstract

This study continues our investigation of the calix[4]arene self-assembly process. In this paper we compare the electrochemical deposition of two structurally different compounds, calix[4]arene and undecanethiol, and the electrochemical behavior of a gold electrode modified by them. Undecanethiol is reduced at a higher electric potential than calix[4]arene and the optimum adsorption potentials for the two substances are also different. The adsorption processes of both the compounds satisfy the Langmuir isotherm and from the electrode charge, which is measured in the case of maximum coverage of the surface, it is possible to compute the adsorbed layer molecular width, which correlates with the software simulation. In contrast to calix[4]arene, the degree of the gold electrode surface coverage by undecanethiol greatly depends on the adsorption time.

## 1. Introduction

Surface modification of metal electrodes provides one of the most elegant approaches to optimizing many electrochemical analyses or designing ion-selective electrodes (ISE). The main aim of the modification process is directed to creating well defined, sufficiently stable and reproducible model systems, permitting electrochemical measurements on the basis of which it is possible to lower the detection limits and improve the selectivity of ISEs [1, 2].

The self-assembly technique is the most common modification technique, where amphiphilic molecules of the modifier spontaneously create a monolayer on the solid surface, which is immersed in a modifier solution [3]. Immobilization, desorption and structural behavior of the self-assembled monolayers (SAMs) could be affected by the electrode potential. The kinetics of the self-assembly process on metal electrodes varies with varying electrode potential [4].

The SAMs of alkanethiols on gold are probably most studied at present [5, 6]. The reaction may be considered formally as an oxidative addition of the S-H bond to the gold surface, followed by a reductive elimination of the hydrogen. And various factors, such as the length of the alkyl chain, temperature, the solvent, or oxygen present in the electrolyte solution can influence the SAM stability [6, 7].

In this study, the electrochemical deposition processes of two types of organothiols are compared,

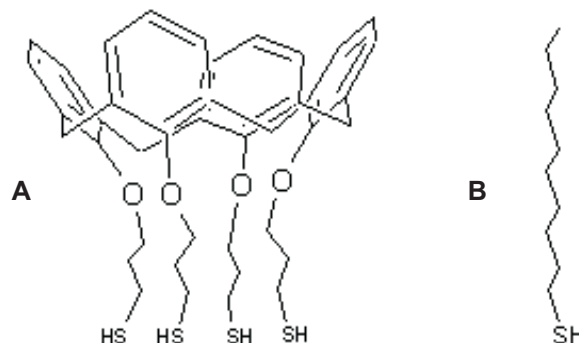


**Fig. 1.** The structures of (A) the calix[4]arene molecule substituted by four -SH functional groups on the lower rim and (B) undecanethiol.

namely, those with thiolated calix[4]arene with 4 -SH groups located on the lower rim, and linear chain undecanethiol (Fig. 1).

## 2. Experimental

The gold electrode was mechanically polished with suspensions of 1.00  $\mu\text{m}$  and then 0.05  $\mu\text{m}$  alumina particles, properly rinsed with deionized water and electrochemically activated by potential cycling in 0.1 mol L<sup>-1</sup> H<sub>2</sub>SO<sub>4</sub> within an interval from -0.6 V to +1.4 V (scan rate, 0.5 V s<sup>-1</sup>), prior to each adsorption process.

The SAM of thiolated compounds on the gold disk electrode was electrochemically prepared on

a cleaned, activated electrode from the supporting electrolyte of  $0.1 \text{ mol L}^{-1}$  NaOH dissolved in a 1:1 mixture of ethanol and water at a constant applied potential. The concentration, time, potential and scan-rate conditions were optimized from the point of view of the SAM homogeneity.

The electrochemical cell consisted of a gold disk working electrode (1 mm in diameter), a reference saturated calomel electrode (both purchased from Elektrochemické Detektory, Turnov, Czech Republic) and of a platinum wire auxiliary electrode. The electrochemical measurements were performed using an Electrochemical Workstation CHI660C (IJ Cambria Scientific, UK) with a CHI660C software. The properties of the calix[4]arene and undecanethiol modified gold electrodes were determined using cyclic voltammetry, in the supporting electrolytes of  $0.1 \text{ mol L}^{-1}$  NaOH and in the presence of a simple redox system,  $0.01 \text{ mol L}^{-1}$   $\text{K}_4[\text{Fe}(\text{CN})_6]$  in the supporting electrolyte of  $0.1 \text{ mol L}^{-1}$  HCl. Each cyclic voltammogram was recorded after 10 min of continuous stirring and degassing with nitrogen; the stirring was stopped during the measurement. The conditions of the CV measurements are specified in the appropriate paragraphs.

The SAMs on the gold platelet Gold arrandee™ / Au(111) ( $12 \times 12 \text{ mm}$ , Dr. Dirc Schroer, Germany) were imaged by atomic force microscopy (Nanoscope IIIa, Veeco, USA) in the tapping mode, using cantilevers OTESPA (Veeco, USA) with a resonant frequency of  $\sim 300 \text{ kHz}$  to minimize the tip interaction with the surface examined. The gold-coated glass platelets for AFM imaging were thermally annealed to form surface areas with prevailing 111 orientation, prior to the thiols adsorption. The SAMs of thiolated compounds on the gold platelet were prepared by

dropping  $10 \mu\text{L}$  of the calixarene or undecanethiol solution ( $5 \times 10^{-3} \text{ mol L}^{-1}$  DMF) onto the middle of the platelet; the adsorption times were 30 s for calixarene deposition, 300 s for the undecanethiol deposition. The platelet was then washed with the clean solvent (DMF), rinsed with deionized water and dried for 1 hour in the air under laboratory temperature [8].

### 3. Results and Discussion

The preliminary CV measurements of the reduction desorption processes of calix[4]arene and undecanethiol, which were electrochemically deposited on a gold electrode surfaces ( $E_{\text{dep}} = -0.8 \text{ V}$ ,  $t_{\text{dep}} = 300 \text{ s}$ , versus SCE), indicated that both the compounds desorbed in different potential ranges (Fig. 2). The calix[4]arene was reduced from the electrode surface close to  $-1.45 \text{ V}$ , in contrast to the undecanethiol reduction peak located at  $-1.30 \text{ V}$ . The peak close to a potential of  $-1.15 \text{ V}$ , which appears during the reduction scans for both the adsorbed compounds, can be attributed to lead impurities formed in alkaline solutions of hydroxy-complexes [9, 10].

First, the dependences of the reduction peak height and area on the adsorption potential were compared (Fig. 3). The optimum adsorption potential for the calix[4]arene SAM preparation was found to be  $-1.3 \text{ V}$ , that for undecanethiol equalled  $-1.0 \text{ V}$ . At lower values of adsorption potentials, below  $-1.0 \text{ V}$ , there were no peaks of impurities in the CV measurements of the reduction process.

The dependence of the calix[4]arene reduction peak area on the bulk concentration of the compound in the base electrolyte was presented in our previous study [8]. The undecanethiol concentration dependence was determined using the same procedure. The

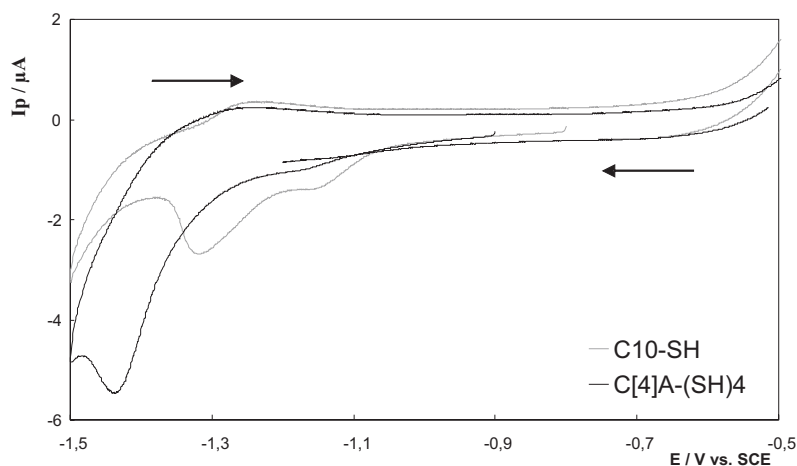


**Fig. 2.** The reduction desorption processes of electrochemically deposited calix[4]arene (thick line) and undecanethiol (thin line) from a gold electrode ( $E_{\text{in}} = -0.8 \text{ V}$ ,  $E_{\text{H}} = -0.5 \text{ V}$ ,  $E_{\text{L}} = -1.5 \text{ V}$ ; scan rate  $0.1 \text{ V} \cdot \text{s}^{-1}$ ; base electrolyte  $0.1 \text{ mol L}^{-1}$  NaOH in a 1:1 mixture of ethanol and water).

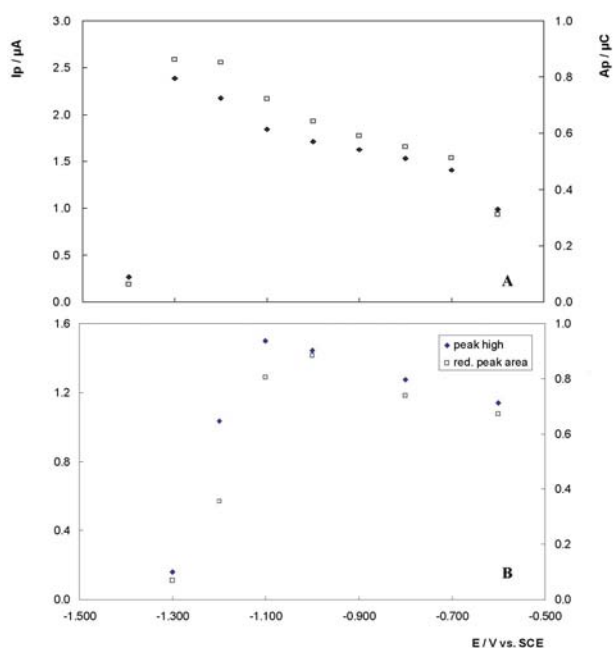


**Fig. 3.** The reduction peak height and area dependences on the adsorption potential: (A) thiolated calix[4]arene, (B) undecanethiol ( $t_{\text{dep}} = 300$  s; cyclic voltammetry:  $E_{\text{in}} = E_{\text{dep}}$ ,  $E_{\text{H}} = -0.5$  V,  $E_{\text{L}} = -1.5$  V, scan rate  $0.1$  V  $\text{s}^{-1}$ , base electrolyte  $0.1$  mol  $\text{L}^{-1}$  NaOH in a 1:1 mixture of ethanol and water).

adsorption process of both the compounds satisfies the Langmuir isotherm equation.

From the charge on the modified electrode, corresponding to the reduction peak area, the area of the gold electrode surface covered by a single calix[4]arene or undecanethiol molecule on completion of the self-assembling process was computed. The molecular widths of the layers were then computed for both the compounds (Table 1). The results correlate with the molecule simulation.

The dependence of the SAM integrity on the adsorption time was measured in the presence of a simple redox system,  $\text{K}_4[\text{Fe}(\text{CN})_6]$  in the supporting

**Table 1**

The electrode surface areas covered by a single calix[4]arene and undecanethiol molecule and molecules widths obtained for electrochemically controlled deposition.

	Surface covered by a single molecule [ $\text{nm}^2$ ]	Molecule radius [nm]
Calix[4]arene	0.58	0.43
Undecanethiol	0.17	0.20

electrolyte of  $0.1$  mol  $\text{L}^{-1}$  HCl (Fig. 4). The adsorption process of calixarene molecules on a gold surface is very fast and the amount of the adsorbed molecules practically cannot be increased by increasing the adsorption time (Fig. 4B) [8], in contrast to the adsorption process of undecanethiol, where the integrity of SAM depends on the adsorption time. After 20 min of undecanethiol adsorption, the coverage of the gold electrode surface is practically complete and, in CV measurements, the SAM on the gold surface behaves as an insulator (Fig. 4A).

Both of the compounds were adsorbed on the gold platelet Au(111). The SAMs were scanned using the AFM method. Both the compounds form mono-disperse globular aggregates on the gold surface, but some differences in the height and shape of the aggregates are observed.

#### 4. Conclusions

The adsorption processes of two different compounds, calix[4]arene and undecanethiol, on a gold surface were compared. In comparison with the SAM of calix[4]arene on gold, undecanethiol was reduced at a higher potential, the optimum adsorption potential was found to be  $-1.0$  V (compared to the value for calix[4]arene adsorption,  $-1.3$  V) and the degree of surface coverage depended on the adsorption time.

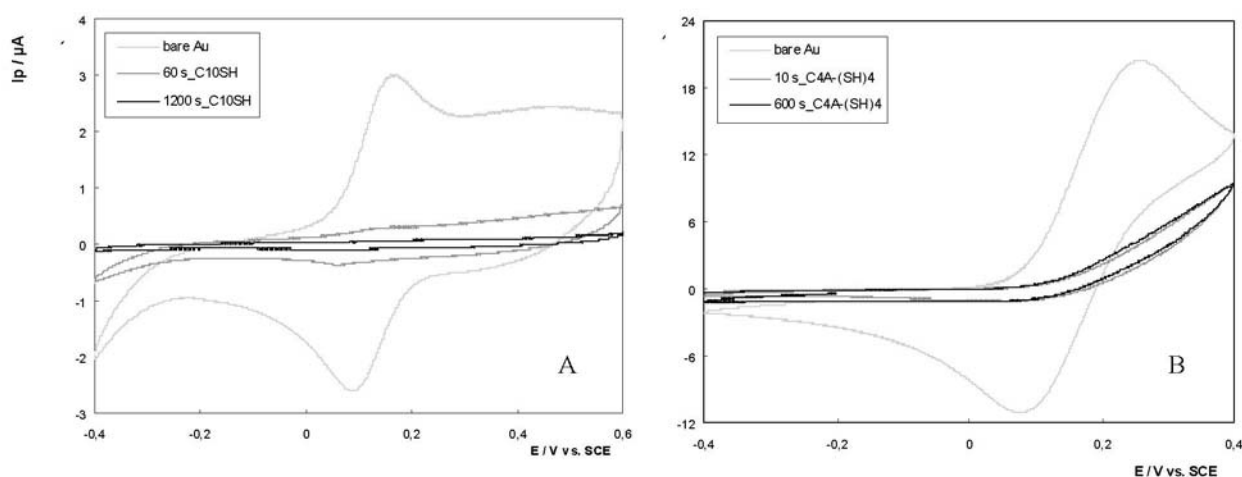


**Fig. 4.** Time dependence of the adsorption process of (A) undecanethiol and (B) calix[4]arene (cyclic voltammetry measurement in  $0.01$  mol  $\text{L}^{-1}$   $\text{K}_4[\text{Fe}(\text{CN})_6]$  in  $0.1$  mol  $\text{L}^{-1}$  HCl,  $E_{\text{in}} = -0.4$  V,  $E_{\text{H}} = 0.6$  V,  $0.4$  V respectively, scan rate  $0.1$  V  $\text{s}^{-1}$ ).

For the formation of a compact undecanethiol layer, a longer adsorption time is required. Both the adsorption processes satisfy the Langmuir isotherm and the modified electrode charges for maximum coverages of the electrode surfaces with the modifier molecules, permit the calculation of the molecular widths, which correlate with the software simulation. These results and the known properties of both the compounds will be utilized for the preparation of a specific modified gold electrode for monitoring of ion transport processes across immiscible liquid interfaces.

#### Acknowledgements

The authors gratefully acknowledge Prof. Ing. Pavel Lhoták, CSc., of the Department of Organic Chemistry, Institute of Chemical Technology (Czech Republic) for the calixarene preparation and Ing. Pavel Janda, CSc., of the Department of Electrochemical Materials, J. Heyrovský Institute of Physical Chemistry of AS CR, v.v.i. (Czech Republic) for the AFM measurement. Grant Agency of the Academy of Sciences, project No. IAA400400806, Grant Agency of Charles University, project SVV 261204, and the Ministry of Education, Youth and Sports of the Czech Republic, project No. MSM0021620857, are thanked for financial support.

#### References

- [1] Malon A., Radu A., Qin W., Qin Y., Ceresa A., Maj-Zurawska M., Bakker E., Pretsch E.: *Anal. Chem.* **75** (2003), 3865–3871.
- [2] Qin W., Zwickl T., Pretsch E.: *Anal. Chem.* **72** (2000), 3236–3240.
- [3] Mandler D., Turyan I.: *Electroanalysis* **8** (1996), 207–213.
- [4] Rohwerder M., de Weldige K., Stratmann M.: *J. Solid State Electrochem.* **2** (1998), 88–93.
- [5] Chen D., Li J. H.: *Surf. Sci. Rep.* **61** (2006), 445–463.
- [6] Ulman A.: *Chem. Rev.* **96** (1996), 1533–1554.
- [7] Everett W. R., Fritschfaules I.: *Anal. Chim. Acta* **307** (1995), 253–268.
- [8] Šustrová B., Štulík K., Mareček V., Janda P.: *Electroanalysis* **22** (2010), 2051–2057.
- [9] Nurchi V. M., Villaescusa I.: *Coord. Chem. Rev.* **252** (2008), 1178–1188.
- [10] Wagner K., Strojek J. W., Koziel K.: *Electroanalysis* **15** (2003), 392–397.

# Indexes



## Author Index

- Andraščíková M. 29  
Arslan Y. 11  
Ataman O. Y. 11  
Barek J. 100, 101, 109, 114  
Bartackova V. 35  
Benada O. 11  
Beníková K. 97  
Bloedt K. 40  
Bosáková Z. 50, 62, 87  
Bursová M. 41  
Coufal P. 50, 80, 84  
Čabala R. 41, 80  
Čajka T. 70  
Daňhel A. 100  
Dědina J. 11, 15, 19  
Deýlová D. 101  
Drábová L. 45, 70  
Dürkop A. 9, 23  
Ferancová A. 97  
Franc M. 50  
Grögel D. B. M. 9  
Hajšlová J. 35, 45, 53, 57, 70, 75  
Hercegová A. 29  
Hrádková P. 53  
Hrouzková S. 29  
Hurajová A. 57  
Janda P. 104  
Janečková L. 62  
Jirkal Š. 66  
Kalachová K. 45, 70  
Kalíková K. 62  
Kašparová L. 24  
Kindl J. 92  
Kocourek V. 45  
Kostelanská M. 75  
Kratzer J. 11  
Křížek T. 80  
Kumar A. 40  
Labuda J. 97  
Lacina O. 35, 53, 75  
Lang T. 10  
Mansfeldová V. 104  
Mareček V. 117  
Matoušek T. 11, 15, 19  
Matysik F.-M. 40  
Musil S. 11, 19  
Němcová L. 109  
Novotný V. 114  
Poustka J. 53  
Pulkrabová J. 45, 53, 70  
Riddellova K. 35  
Rychlovský P. 11, 15, 19  
Ryšlavá H. 80  
Schäferling M. 10  
Schulzová V. 57  
Sobotníková J. 84  
Sosnovcová M. 75  
Spěváčková V. 24  
Steiner M.-S. 23  
Svoboda M. 15, 19  
Svobodová A. 84  
Svobodová E. 87  
Ševčík J. G. K. 66  
Štulík K. 117  
Šustrová B. 117  
Tarábková H. 104  
Taurková P. 15  
Tesařová E. 50, 62, 84  
Tykva R. 92  
Valenzova K. 35  
Valterová I. 92  
Vobecký M. 11  
Wolfbeis O.S. 8, 23  
Wranová K. 24  
Yosypchuk B. 100  
Zima J. 109  
Žáček P. 92

## Keyword Index

- <sup>198, 199</sup>Au radiotracer 11  
2002/657/EC 53  
2-amino-6-nitrobenzothiazole 101  
acrylamide 35  
aliphatic amines 40  
alkenes 66  
amalgam electrodes 101  
amperometry 100  
arsenic speciation 15, 19  
atomic absorption spectrometry 15  
atomic fluorescence spectrometry 19  
atomic force microscopy 104, 117  
ATP 10  
baby food 75  
biogenic amines 23  
biological material 24  
biosensor 97  
*Bombus terrestris* 92  
calculation of descriptors 66  
calix[4]arenes 117  
capillary electrophoresis 80  
capillary liquid chromatography 50, 84  
carbon electrode 104  
carbon paste electrode 109  
CC<sub>α</sub> 53  
CC<sub>β</sub> 53  
comprehensive two dimensional 92  
contactless conductivity detection 40  
cryogenic trapping 15, 19  
cyanine dyes 9  
cyanogenic glucosides 57  
cyclic voltammetry 117  
cyclic voltammograms 104  
cyclofructans 62  
DART-Orbitrap MS 57  
DART-TOF MS 57  
differential pulse voltammetry 101  
direct current voltammetry 101  
electrochemical detection 109  
electrochemical transducer 97  
electron ionization 29  
enantioseparation 62  
endocrine disrupting pesticides 29  
enzyme activity 10  
fast GC 41  
fast GC-MS 29  
fat body 92  
fish 70  
gas chromatography 66, 92  
gas sensor 9  
GC×GC-TOF MS 45, 70  
generation efficiency 11  
gold electrode 117  
herbicide 114  
hexosaminidase 80  
HPLC 62, 109  
HPLC-MS/MS 35  
hydride generation 15, 19  
hydroxide dryer 15, 19  
chemical vapor generation 11  
chiral stationary phase 62  
chitobiose 80  
ICP-MS 24  
identification 87  
interferences 24  
kinetics 80  
labial gland 92  
lanthanide probe 10  
LC-MS/MS 57  
lemons 29  
liquid chromatography 75  
liquid-liquid microextraction 41  
low-molecular-weight compound 84  
LSER 66  
luminiscency 10  
MEKC 87  
methacrylic acid 84  
method validation 53  
microextraction 40  
microchip electrophoresis 40  
MIP 45  
multi-target analysis 75  
mycotoxins 75  
negative chemical ionization 29  
nitrophenols 100  
nucleic acid 97  
organic dyes 87  
PAH 45, 70  
PBDE 70  
PCB 70  
perfluorinated compounds 53  
platinum group elements 24  
polymers 97  
polyphenols 109  
polystyrene-based monolithic column 84  
prediction retention 66  
PTV 70  
response surface methodology 41  
resveratrol 109  
RGB optical readout 23  
seafood 40  
sensing strip 23  
separation impedance 50  
silver amalgam 100  
silver solid amalgam electrode 114  
slurry packing 50  
substituted binaphthyls 62  
surface modification 104  
tandem mass spectrometry 75  
tea 45  
thin layer chromatography 92  
transmission electron microscopy 11  
UHPLC-TOF MS 35  
undecanethiol 117  
UPLC-MS/MS 75  
van Deemter curve 50  
voltammetry 100, 109, 114



**Proceedings of the 6th International Students Conference "Modern Analytical Chemistry"**

Edited by Karel Nesměrák.

Published by Charles University in Prague, Faculty of Science.

Printed by Tribun EU, Brno.

Prague 2010.

1st edition – 126 pages – Number of copies: 60

ISBN 978-80-7444-005-2



ISBN 978-80-7444-005-2



9 788074 440052